TRIBHUVAN UNIVERSITY

INSTITUTE OF ENGINEERING

PULCHOWK CAMPUS

THESIS NO: 076MSEEB002

Optimization of Street Aspect Ratio for Pedestrian Comfort in Hot and Humid Climate of Nepal

by

Apekshya Ghimire

A THESIS

SUBMITTED TO THE DEPARTMENT OF ARCHITECTURE

IN PARTIAL FULFILLMENT OF THE REQUIREMENTS FOR THE DEGREE OF MASTERS OF SCIENCE IN ENERGY EFFICIENT BUILDING (MSEEB)

DEPARTMENT OF ARCHITECTURE

LALITPUR, NEPAL

OCTOBER, 2022

Copyright

Declaration

I hereby declare that the thesis entitled "Optimization of Street Aspect Ratio for Pedestrian Comfort in Hot and Humid Climate of Nepal" submitted to the Department of Architecture in partial fulfillment of the requirement for the degree of Master Science in Energy Efficient Building, is a record of an original work done under the guidance of Asso. Prof. Dr. Sanjaya Uprety, and Asso. Prof Dr. Ashim Ratna Bajracharya, Institute of Engineering, Pulchowk Campus. This thesis only contains work completed by me except for the consulted material which has been duly referenced & acknowledged.

____

Apekshya Ghimire

076MSEEB002

TRIBHUVAN UNIVERSITY

INSTITUTE OF ENGINEERING

PULCHOWK CAMPUS

DEPARTMENT OF ARCHITECTURE

The undersigned certify that they have read, and recommended to the Institute of Engineering for acceptance, a thesis entitled **"Optimization of Street Aspect Ratio for Pedestrian Comfort in Hot and Humid Climate of Nepal"** submitted by Apekshya Ghimire in partial fulfillment of the requirements for the degree of Master in Energy Efficient Building.

………………………………..

Supervisor, Dr. Sanjaya Uprety

Associate Professor

Department of Architecture

………………………………………

Supervisor, Dr. Ashim Ratna Bajracharya

Associate Professor

Department of Architecture

………………………………………

External Examiner, Parikshit Kadariya

Senior Divisional Engineer

Department of Urban Development and Building Construction, Babarmahal

………………………………………

Program Coordinator, Dr. Sanjaya Uprety
M.Sc. Energy Efficient Building

Department of Architecture

Date: 10/13/2022

Abstract

Walkable and livable cities come under the first priority of people searching for a new residential space in today's context. In order to create a comfortable walkable condition for pedestrians, more focus should be given to shading the pathway. Among many ideas, the development of an optimum aspect ratio is paramount for improving the walkability of any street. This research is focused on developing and promoting an optimum street aspect ratio in the hot and humid road section of Lumbini Sanskritik Municipality through the use of Envi-Met software. This research involves the use of temperature and humidity data to simulate 3D street layouts in order to obtain the desired results in the form of air temperature, mean radiant temperature and physiological equivalent temperature as outputs. This research concludes that for east-west oriented streets, the aspect ratio above 2 is favorable whereas for north-south oriented streets, the aspect ratio of 1.5 is the optimum result. The optimum aspect ratio obtained from the simulation reduced the ambient air temperature of the same street by more than 3.5 °C, mean radiant temperature by more than 20 °C and physiological equivalent temperature by more than 12 °C. Similarly, orientation from 30° NE/210° SW to 150 ° NW/330° SE seems better for street orientation in case of Lumbini Sanskritik Municipality.

Keywords: *Aspect Ratio, Street Canyon, Mean Radiant temperature, Physiological Equivalent Temperature*

Acknowledgment

Firstly, I am greatly indebted to my research supervisor Ass. Prof Dr. Sanjay Uprety and Ass. Prof Dr. Ashim Ratna Bajracharya (Department of Architecture) for overseeing this work and for their ongoing supervision, advice, and support throughout the completion of this thesis. I sincerely appreciate their commitment to sharing the knowledge and skills required to conduct this research.

I am extremely grateful to Philipp Heller, Customer Care assistant of ENVI-met software for providing me the student license of the software. This endeavor would not have been possible without his help and support.

Additionally, I want to thank Er. Biplav Pokhrel for his editorial assistance, suggestions, and moral support during this process. Finally, I must acknowledge my family, especially my parents, sister, and brother. Their confidence in me has sustained my enthusiasm and upbeat attitude throughout this process.

Table of Contents

List of Figures

List of Charts

List of tables

List of graphs

List of acronyms and abbreviations

PET: Physiological Equivalent Temperature

MRT: Mean Radiant Temperature

PMV: Predicted Mean Vote

GHG: Green House Gases

UHI: Urban Heat Island

UTCI :Universal Thermal Climate Index

SET: Standard Effective Temperature

ASHRAE: American Society of Heating, Refrigeration and Air Conditioning Engineers

SVF: Sky View Factor

AR: Aspect Ratio

AST: Apparent Solar Time

PSA: Passive Solar Angle

FAR: Floor Area Ratio

Kmph: Kilometers per hour

DOHM: Department of Hydrology and Meteorolgy

1. Chapter 1: Introduction

1.1. Background

Walkable and livable cities come under the first priority of people searching for a new residential space in today's context. Several researchers agree that the most effective measure to reduce greenhouse gas emissions (GHG), air pollution, and Urban Heat Island (UHI) is to promote walkability (Rodríguez-Algeciras, et al., 2018, Asarpota & Nadin, 2020). Increasing the walkability in a neighborhood is one of the approaches that can be used to create a sustainable neighborhood (Azmi & Karim, 2012). Pedestrian thermal comfort in streets influence walkability and urban livability. However, the urban planning concept often focuses more towards the vehicular accessibility and lacks the concept of thermally comfortable pedestrianized street.

Nepal is divided into three climatic regions namely Terai region, Hilly region and Himalayan region where the temperature variation between them is quite high. During the summer season the daily mean temperature ranges from 22°C to 35°C in the Terai region of Nepal (Bodach, 2014). In hot temperate regions, the use of outdoor spaces is highly influenced by warm conditions and sunlight (Nikolopoulou, et al., 2001). Lin (2009) explained that the increased value of thermal indices decreases the number of people visiting the outdoors during hot season. Hence, thermally comfortable outdoor spaces promotes walkability which in turn attract local businesses and economic activities which results in the development of the area (Nikolopoulou, et al., 2001).

Rodríguez-Algeciras, et al., (2018) states shading as one of the best urban strategies in mitigating heat stress at pedestrian level. Since, the sunlight effects the use of outdoor spaces, self- shading streets can help to improve the pedestrian thermal comfort. Self-shading streets are feasible in the form of man-made canopy that protects the building and surroundings from direct sunlight in hot and humid climate (Nikolopoulou, et al., 2001). The amount of incident and reflected sunlight radiation is influenced by the ratio of height of buildings (H) to the distance (W) between them (Johansson, 2006). The aspect ratio i.e., H/W affect the thermal performance of outdoor spaces. Several studies have found that the maximum temperature decreases with increasing H/W ratio (Johansson, 2006, Chatzidimitriou & Yannas, 2017, Ali-Toudert & Mayer, 2006).

Similar to the aspect ratio, orienting streets and buildings in the proper direction can enhance shading efficiency and improve pedestrian thermal comfort (De & Mukherjee, 2018). Thus, in order to ensure pedestrian thermal comfort, it is important to decide street orientation and aspect ratio.

Outdoor spaces are important to a sustainable city as they are the spaces that link the public with the urban built context while accommodating daily pedestrian outdoor activities. Since, the use of urban space has social, cultural and economic benefits, it is important to enhance outdoor thermal comfort. Furthermore, the appropriate design of outdoor spaces makes outdoor activities possible for most of the year in warm climate (Johansson & Emmanuel, 2006). Hence, this research aims to suggest an optimum canyon aspect ratio and street orientation.

1.2. Need of study

Urban form has a significant influence on the urban climate and, consequently, on outdoor thermal comfort at street level (Johansson & Emmanuel, 2006), hence, it is a promising area for improving the thermal comfort of outdoor environment. Comfortable and shaded streets promote walkability and sustainability. Thus, street design is an important issue in bioclimatic urban development to mitigate thermal discomfort in pedestrian level. In order to establish and sustain walkability, it is important to make urban streets comfortable as far as the ambient climate permits (Ahmed, 2003). Since, the temperature rises ranges between 22°C to 35°C in terai region of Nepal, it is difficult to carry out outdoor activities during sunny day. Johansson and Emmanuel (2006) states that increasing the height of the buildings that surround the streets brings a betterment of the pedestrian thermal conditions. According to De and Mukherjee (2018) the optimization of street geometry has significant potential to enhance pedestrian thermal comfort in hot and humid climate. Another way to cool street is to reduce the amount of radiation that it absorbs thus shading of streets can be an effective strategy for pedestrian thermal comfort (Lee, et al., 2018). Rodríguez-Algeciras, et al., (2018) confirms that street geometry has an important effect on microclimates and consequently on thermal comfort sensation in outdoor environments.

Street canyons with higher aspect ratio reduce solar access and air temperature providing 3.5°C -6°C (Kakon, et al., 2009) cooler outdoor spaces (Abdollahzadeh & Biloria, 2020). Hence, it is possible to create thermally comfortable street through proper design of street orientation and aspect ratio. However, due to the great complexity of the outdoor environment, there have been very few attempts to understand outdoor thermal conditions. In the context of Nepal, there are not many research done to prevent sunlight radiation in the street with the help of urban geometry. Hence, it is imperative to study optimization of canyon aspect ratio and street orientation to design shading for hot and humid climate of Nepal sustainably.

1.3. Importance of Study

The research aims to find out optimum street orientation and aspect ratio for hot and humid climate of Nepal and helps in prevention of sunlight radiation during hot season. Hence, this research will help urban planner, energy efficient planner, ppolicymakers designers to create thermally comfortable streets in hot and humid region of Nepal. This research will also help local authority to consider the aspect ratio for the new urban development project. Ultimately, this research aims to help the common people to walk and conduct business activities in a thermally comfortable street (Abdollahzadeh & Biloria, 2020).

1.4. Problem statement

Improving the quality of life in urban centers requires not only efficient buildings, but also climatically sensitive urban streets that can enhance and enrich urban life (Cocci grifoni, et al., 2013). A comfortable climate is important for well-being and to attract people to public spaces. Studies have shown that prolonged exposure to hot conditions can have a negative impact on human health (Lee, et al., 2018). The risk of heat-related illness increases with higher temperatures and it is an important issue especially in warm and hot cities (Johansson & Emmanuel, 2006). Furthermore, uncomfortable streets and outdoor environment makes the entire urban space unattractive and inaccessible. Studies have found that people's activities in outdoor spaces decrease in summer with an increase in air temperature (Lin et al., 2012). Thus, streets lacking shading and thermal comfort tend to be avoided and remained unused (Lenzholzer, 2012). The less interaction of people in outdoor activities has negative effect in business and economic activities (Nikolopoulou, et al., 2001). Also, unshaded street discourages people to walk and encourage them to use vehicle. The preference of people towards vehicle increases greenhouse gas emissions, air pollution and UHI effect.

Despite the problem, designers are more attracted to the impact of environmental forces on buildings, indoor climate of the buildings, design strategies, energy requirements for supporting the thermal comfort, passive solar gains (Shafaghat, et al., 2016) rather than outdoor thermal comfort. Most studies on the impact of urban layout emphasized primarily on solar and illuminance performance of buildings' fabrics (Chatzipoulka, et al., 2015) . Improving the thermal comfort of outdoor environments are generally given little importance in the planning and design processes in the context of Nepal as well. This has led to hot and uncomfortable streets especially in Terai region of Nepal which has negative effect on economic and environmental factor of the region.

Urban planning and street development are generally governed by the prevailing byelaws of individual local government. While these bylaws are very useful in proper land use and infrastructural development, it most certainly isn't all encompassing. While the architectural and structural elements are quite prominent in these byelaws, the energy efficient facet are generally ignored. Due to the lack of consideration for pedestrian thermal comfort, the prevalent street aspect ratio cannot fulfill prerequisite of optimum walkability.

1.5. Objectives of Research:

The major objective of this research is to determine optimum aspect ratio of streets for Lumbini Sanskritik Municipality.

Secondary objectives of the research are

- To prevent direct solar radiation at street level so as to promote walkability.
- To identify best orientation of streets for hot and humid climate of Nepal.

1.6. Research Validation

In the context of Nepal, very few researchers are interested to study the sector of thermal comfort under the large umbrella of Energy Efficiency and Sustainability. In addition to that, insignificant amount of attention is provided to the area of outdoor thermal comfort in the field of academia. Due to ease of observation and analysis, researchers tend to focus only on the internal thermal comfort while the larger study area that is the outdoor area is quite ignored.

So, this research aims to study the orientation and aspect ratio of the street canyons to determine whether any sort of intervention results in the change of thermal comfort to the pedestrians. This research aims to introduce a brand-new platform in the research area in the field of Energy Efficiency and thermal comfort.

1.7. Thesis Outline

Chapter one communicates the purpose and focus of the study and explains the outline of the research. The research background is briefly explained in this chapter, along with the justification for choosing the research area. In addition, the first chapter describes research frameworks and defines the study purpose and objectives.

The second chapter is a survey of the literature; therefore, it analyzes models and theoretical frameworks that have been previously presented to the field of study. This chapter defines key terminology and describes how to look for secondary data. Other writers' perspectives on the study topic in general and the research challenge in particular have been logically provided in this topic.

Chapter three addresses methodology. The chapter discusses themes related to research philosophy and outlines the research method. Additionally, the methodology chapter includes explanations of research design and the selection and use of data collection methods.

Chapter four describes the study area. The chapter covers the site's available aspect ratio as well as the structures that are currently on the street. This chapter explains the layout and a segment of the street in the chosen study region.

The examination of climatic data from various secondary sources is covered in chapter five. The results analysis from the questionnaire survey is presented in the second section of this chapter. Finally, it describes the scenarios and provides simulation results.

Chapter six addresses the discussion part. Results from several scenarios are compared, and conclusions are reached.

Chapter seven concludes the results of the thesis and provides the recommendation along with further works that can be carried out in future.

2. Chapter 2: Literature review

2.1. Outdoor thermal comfort

Thermal comfort is a difficult notion to evaluate in either an indoor or outdoor setting since it encompasses physical, physiological, and psychological factors. According to ANSHI/ASHRAE (2017), thermal comfort is the state of mind that is assessed by subjective evaluation that expresses satisfaction with the thermal environment. In another word, it is the range of climatic conditions where most people feel comfortable (Cocci Grifoni, et al., 2013). In general thermal comfort is achieved when heat gain through metabolism is dissipated to maintain thermal balance. Any further heat gain or loss causes significant discomfort. Thermal comfort has a direct influence on occupant health and productivity. According to (Lai, et al., 2020) if the occupants feel neutral, and do not desire to modify or evaluate the outside thermal environment, the outdoor area can be termed thermally comfortable.

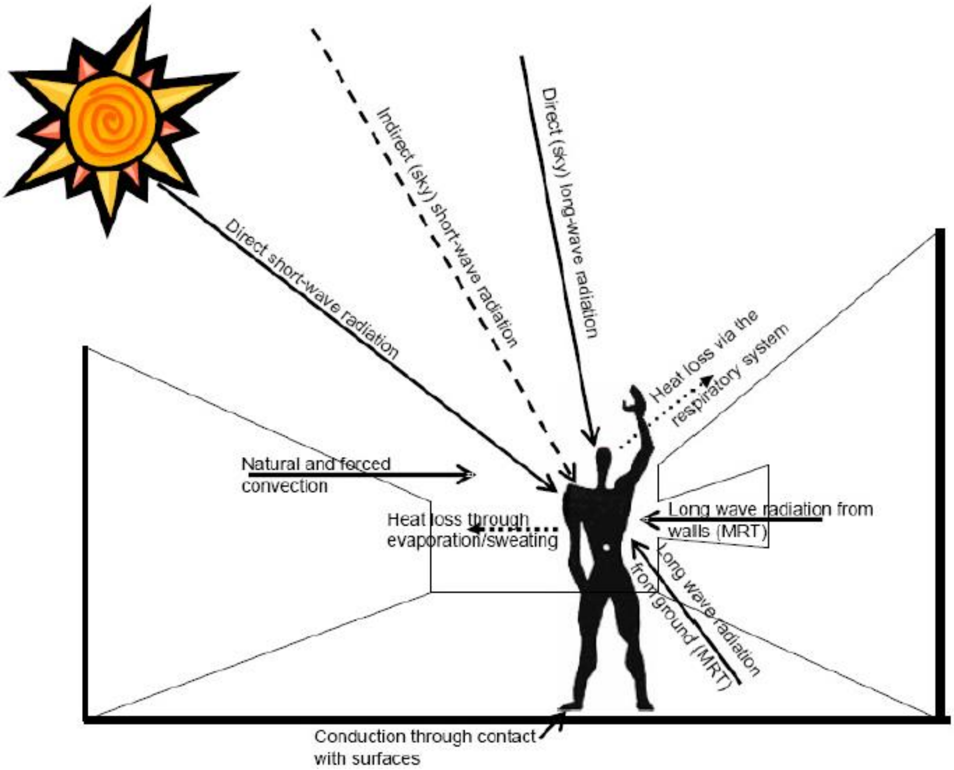

Figure 2. 1 Outdoor human energy balance
(Kenawy, et al., 2010)

As difficult as it is to measure thermal comfort in a controlled setting, it is even more difficult to comprehend outdoor thermal comfort since it cannot be described by a single component such as ambient air temperature. Physical factors like solar radiation and wind, physiological reactions including skin and core temperatures, as well as perspiration rate, psychological factors like behavior, culture, alliesthesia, etc. may also be useful indicators of outdoor thermal comfort (Lai, et al., 2020). Solar radiation and wind access are influenced by built form whereas energy balance is affected by the properties of materials used (Chatzidimitriou & Yannas, 2015). Hence, it is difficult to pick out a single factor and associate it with outdoor thermal comfort. However, the most significant factor affecting heat gain and loss is total radiation (Kenawy, et al., 2010). Bryan (2001) believes that controlling the surrounding surface temperature, also known as Mean Radiant Temperature (MRT), is a key technique for addressing thermal comfort.

The outdoor climate is influenced by various factors such as air temperature, mean radiant temperature (MRT), humidity, wind, etc. out of which air temperature and MRT are key factors along with the wind (Kenawy, et al., 2010, Bryan, 2001, Hwang & Lin, 2007). Because of the complexity of the outdoor conditions, few types of research have been carried out in the past and different types of thermal comfort indices and models have been proposed. According to Potchter et al. (2018) and his comprehensive review, out of 165 human thermal indices, only four are routinely used for outdoor thermal perception studies: Physiologically Equivalent Temperature (PET), Predicted Mean Vote (PMV), Universal Thermal Climate Index (UTCI), and Standard Effective Temperature (SET).

2.1.1. Factors affecting outdoor thermal conditions

2.1.1.1. Physical Factors

a) Ambient air temperature

The temperature of the air surrounding the occupant concerning location and time is the ambient air temperature. Air temperature is the temperature of the air that surrounds a person and is usually expressed in degrees Celsius (°C) or degrees Fahrenheit (°F) (Skilling & Munro, 2016). The convective heat exchange between the human body and the surrounding outside environment is directly determined by air temperature, while the radiative, evaporative, and respiratory heat exchanges are indirectly affected (Lai, et al., 2020). According to Liu, et al. (2016), air temperature is the most important microclimatic parameter to outdoor thermal sensation. Several studies evaluated the air temperature of streets with varied aspect ratios in order to assess the impact of urban geometry on thermal comfort (Johansson, 2006; Ali-Toudert & Mayer, 2006; Andreou & K. Axarli, 2012 and Chatzidimitriou & Yannas, 2017). It was discovered that the air temperature of a building's shadowed part is lower.

b) Mean Radiant Temperature (MRT)

Mean Radiant Temperature is a meteorological parameter that governs human energy balance and thermal comfort (Tan, et al., 2013,). The radiant temperature is related to the amount of radiant heat conveyed from a surface and is determined by the material's capacity to absorb or emit heat, also known as its emissivity. Radiations such as direct, diffuse, and reflected shortwave radiation, as well as radiations from built and natural environments, and longwave radiation tend to form mean radiant temperature (Naboni, et al., 2019).

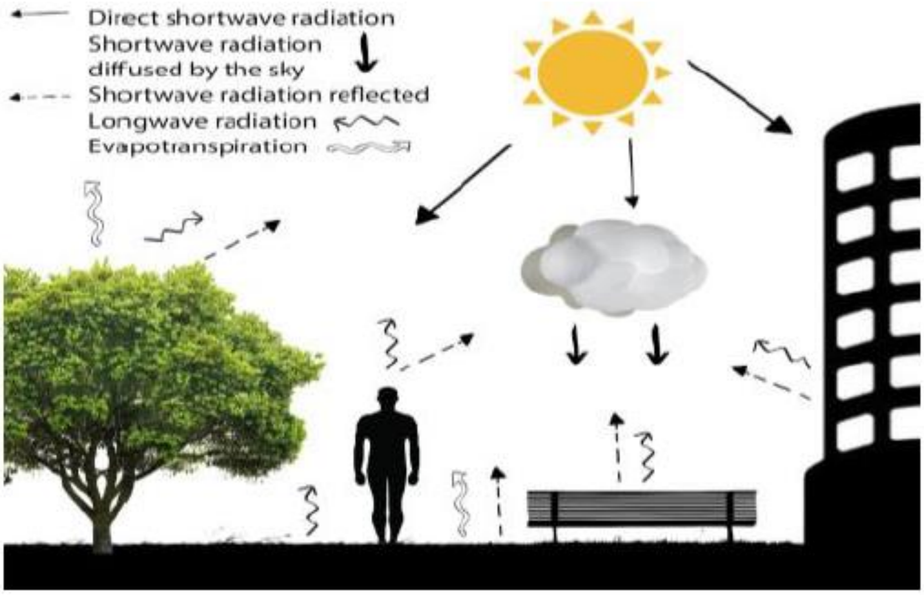

Figure 2. 2 Relevant radiation fluxes and urban entities on the determination of outdoor MRT
(Naboni, et al., 2019)

The mean radiant temperature (MRT) is based on the idea that the net exchange of radiant energy between objects is roughly proportional to their temperature difference multiplied by their heat-emitting and -absorbing abilities (emissivity) (climate adapt, n.d.). Tmrt is the most important variable in evaluating thermal sensation outdoors during daylight hours in summer (Ali-Toudert & Mayer, 2006). The difference of 8°C-11°C of MRT was observed in a sunny and shaded outdoor environment by (Middel, et al., 2017). The mean radiant temperature under the shaded region by a tree was 30K lower than the unshaded region on a summer day (Matzarakis, et al., 1999).

Calculation of Mean Radiant Temperature

MRT is calculated by determining the radiation profiles of the surrounding surfaces (temperature of all surrounding surfaces) and the visible area of the sky. Numerically it can be derived from the equation given below:

$$T_r = \left[(T_g + 273.15)^4 + \frac{1.1 \times 10^8 V_a^{0.6}}{\varepsilon D^{0.4}} \times (T_g - T_a) \right]^{0.25} - 273.15$$

Where Tg is the globe temperature, Ta is the air temperature, ε is the emissivity of the sphere, dg0.4 is the diameter of the sphere, and Va is the air velocity (Guo, et al., 2020).

The MRT can also be obtained by modeling the entire radiation field using simulation models approaches, and in response to the growing interest in outdoor thermal comfort analysis, a few modeling tools such as RayMan, ENVI-met Autodeskk CDF, Grasshopper plug-ins, Ladybug Tools, and others have been developed (Naboni, et al., 2019).

c) Humidity

The ratio between the actual amount of vapor in the air and the maximum amount of vapor that the air can hold at that air temperature is humidity and it is expressed as a percentage. The higher the relative humidity, the more difficult it is to lose heat through the evaporation of sweat. Humidity has usually been regarded as the least relevant meteorological condition influencing outdoor thermal comfort (Lai, et al., 2020). In Hong Kong, Cheng et al. (2012) regressed the outdoor thermal sensation using two linear equations, one with and one without relative humidity and discovered that the difference between the two regressed lines was minimal.

d) Wind velocity

The velocity of the air that a person is in contact with is air velocity and it is measured in m/s. The higher the velocity of wind, the exchange of heat between the person and the air is greater. (Walton, et al., 2007) discovered the significance of wind velocity as the major factor affecting outdoor thermal comfort.

2.1.1.2. Physiological Factors

The link between physiological factors and outdoor thermal comfort begins with heat exchange between the human body and the surrounding environment, which causes changes in the temperature of the human body (Lai, et al., 2020). When the external temperature conditions depart from thermal neutrality, the human body will maintain its comfort level by physiological control, such as shivering in cold weather and sweating in hot weather. Out of many physiological factors, skin temperature is the most studied in the context of outdoor thermal environments. A study showed that the mean skin temperature was statistically correlated to the sky view factor since skin temperature increased from 33.9 °C to 36.0 °C when SVF was increased from 0.082 to 0.940 (GS & MA, 2016). The study conducted by (Jeong, et al., 2016) showed the physiological effects of reducing human heat stress by comparing the skin temperature in forest and urban areas and it was found that the skin temperature in the forest area was 34°C which was 1°C less than urban area and the people visiting the forest area felts more comfortable. Hence, skin temperature is one of the factors affecting outdoor thermal comfort.

2.1.1.3. Psychological Factors

Psychological factors are associated with the influences of cognitive, social, and cultural elements, and it discusses how and to what extent habits and expectations may affect people's perceptions of the thermal environment. Because of psychological factors, an individual's degree of comfort in a particular setting may fluctuate and adapt over time. The recollection of earlier experiences may alter the subjective feeling of thermal comfort. People who live in a bad thermal environment for an extended period of time will reduce their requirements, resulting in decreased expectations. People, on the other hand, gradually increase their requirements if they live in a comfortable temperature environment for an extended period of time. On the contrary, if people are given the control over the thermal environment, they tend to feel more comfortable (Nikolopoulou & Koen Steemers, 2003).

2.1.2. Thermal comfort indices

For determining thermal comfort, several indices incorporating thermal environmental factors and the heat balance of the human body are used for e.g. predicted mean vote (PMV), standard effective temperature (SET) , OUT_SET, physiologically equivalent temperature (PET), Universal Thermal Climate Index (UTCI) etc.

a) Predicted Mean Vote Method

The PMV is an index that forecasts the mean value of votes cast by a large group of individuals using a 7-point thermal sensation scale as in table 2.1 based on human body heat balance (ISSO7330, 2005). It is the average of the votes cast by a wide group of individuals exposed to the same thermal conditions.

+ 3	Hot
+ 2	Warm
+ 1	Slightly warm
0	Neutral
− 1	Slightly cool
−2	Cool
− 3	Cold

Table 2. 1 Seven-point thermal sensation scale (ISSO 7330, 2005)

b) Physiologically Equivalent Temperature (PET)

The PET comfort index combines meteorological and thermo-physiological characteristics (clothing and activity) obtained from the human heat balance model. The PET value in the concrete scenario of the warm and bright outside settings depicted in Fig. 3 would be 43°C which indicates that an occupant of a room with an air temperature of 43°C achieves the same thermal state as if they were outside in the warm and bright conditions (Hoppe, 1999).

PET is defined as the air temperature at which the human body's heat balance (work metabolism 80 W of light activity added to basic metabolism; heat resistance of clothing 0.9 clo) is maintained in a typical indoor setting with core and skin temperatures equal to those under the conditions being assessed (Höppe, 1999).

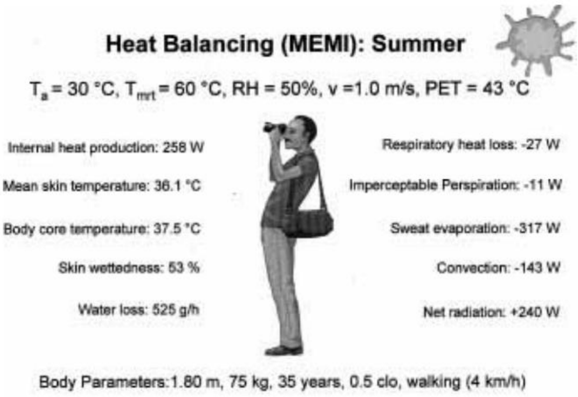

Figure 2. 3 Heat balance calculation in outdoor (Hoppe, 1999)

From the table 2.2, it can be perceived that the PET drops to 29°C from 43°C when the person moves from sunny region to shaded region. The difference between PET values in unshaded and shaded sites in Freiburg was on average, about 15 K (Matzarakis, et al., 1999). On hot summer days with direct sun irradiation, the PET value can be more than 20 K higher than the air temperature, and up to 15 K lower on a windy winter day (Hoppe, 1999).

Scenario	T_a (°C)	T_{mrt} (°C)	v (m/s)	VP (hPa)	PET (°C)
Typical room	21	21	0.1	12	**21**
Winter, sunny	–5	40	0.5	2	**10**
Winter, shade	–5	–5	5.0	2	**–13**
Summer, sunny	30	60	1.0	21	**43**
Summer, shade	30	30	1.0	21	**29**

Table 2. 2 Examples of PET for different climate scenarios (Hoppe, 1999)

Table 2.3 represents the related ranges of PMV and PET which are only valid for the assumed values of internal heat production and thermal resistance of the clothing (Matzarakis, et al., 1999). The table shows that the PET value above 41 is very hot condition which is equivalent to 3.5 scale of PMV vote.

PMV (°C)	PET	Thermal perception	Grade of physiological stress
		Very cold	Extreme cold stress
–3.5	4		
		Cold	Strong cold stress
–2.5	8		
		Cool	Moderate cold stress
–1.5	13		
		Slightly cool	Slight cold stress
–0.5	18		
		Comfortable	No thermal stress
0.5	23		
		Slightly warm	Slight heat stress
1.5	29		
		Warm	Moderate heat stress
2.5	35		
		Hot	Strong heat stress
3.5	41		
		Very hot	Extreme heat stress

Table 2. 3 Ranges of PMV and PET
(Matzarakis, et al., 1999)

PET can be calculated with the help of softwares like RayMan, Envi-met etc. which has been employed in urban built-up areas with complicated shade patterns and has produced reliable thermal environment predictions (Lin, et al., 2010). PET uses the degree Celsius (°C) as its unit of measurement, making it easier for planners to interpret for design purposes (Ali-Toudert & Mayer, 2006).

c) Universal Thermal Climate Index (UTCI)

The Universal Thermal Climate Index is defined as the air temperature of reference condition that generates the same model conditions as the actual condition (Błażejczyk, et al., 2013). It aims to measure outdoor thermal conditions in the primary disciplines of human biometeorology as a one-dimensional variable summarizing the interaction of ambient temperature, wind speed, humidity, and longwave and shortwave radiant heat fluxes (Bröde, et al., 2012). The reference condition is set as metabolic activity (≈ 135 W/m^2), wind speed (≈ 0.5 m/s 2) at 10 m height, a mean radiant temperature equal to air temperature, and humidity of 50% at a constant 20 hPa (Błażejczyk, et al., 2013).

UTCI (°C) range	Stress Category	Physiological responses
above +46	extreme heat stress	- increase in *Tre* time gradient - steep decrease in total net heat loss - averaged sweat rate >650 g/h, steep increase
+38 to +46	very strong heat stress	- core to skin temperature gradient < 1K (at 30 min) - increase in *Tre* at 30 min
+32 to +38	strong heat stress	- dynamic Thermal Sensation (DTS) at 120 min >+2 - averaged sweat rate > 200 g/h - increase in *Tre* at 120 min - latent heat loss >40 W at 30 min - instantaneous change in skin temperature > 0 K/min
+26 to +32	moderate heat stress	- change of slopes in sweat rate, *Tre* and skin temperature: mean (*Tskm*), face (*Tskfc*), hand (*Tskhn*) - occurrence of sweating at 30 min - steep increase in skin wettedness

Table 2. 4 UTCI equivalent temperature categorized in terms of thermal stress (Błażejczyk, et al., 2013)

According to table 1.4, the UTCI value ranges from +26℃ to more than +46℃. The stress category is moderate heat stress from 26-32℃ to extreme heat stress in temperatures above 46℃. It starts as increase in skin wittedness due to extreme sweating and reaches a state where the core to skin temperature gradient is very low ie less than 1k.

2.2. Shading

Shading refers to the protection of any surfaces against light and heat. The air temperature, as well as equivalent temperature, is slightly lower in shaded areas in comparison to unshaded areas thus, walking through the shaded area is more comfortable thermally. One study concluded that shaded space provided more thermally comfortable conditions than unshaded areas since the shaded areas have longer period of acceptable temperature range (Makaremi, et al., 2012,). Therefore, shading is one of the most effective ways to prevent heat exhaustion and lower outdoor temperatures, particularly in hot and humid places (Nasrollahi et al., 2020; Rodrguez-Algeciras et al., 2018). Shaded surfaces in a street, such as building facades and roofs, and seating areas in an outdoor urban setting minimize incident solar radiation, keeping the temperature down (Vartholomaios & Kalogirou, 2020). A poorly designed street is affected by incident solar radiation, which heats the surfaces around the streets and makes it uncomfortable for pedestrians to walk on. The main strategy to create thermally comfortable streets is shading as it reduces the direct solar radiation absorbed by the pedestrian which results in a reduction of radiant heat factors ultimately decreasing the mean radiant temperature (Ali Toudert, 2007).

(Lin, et al., 2010) studied the effect of shadowing on thermal comfort at university campus in Central Taiwan and found that suitable shading is required in outdoor spaces to ensure the thermal comfort either by buildings or vegetations. A study in Hongkong showed that T_{mrt} in shades was around 30° C - 34° C whereas without shading was 50° C - 60° C and suggested shading as an important feature of urban area (Ng & Cheng, 2012). (Nasrollahi, et al., 2020) also suggested shading as an effective measure to reduce mean radiant temperature and it can be done by increasing aspect ratio of urban canyon. Hence, shading is an effective parameter that restricts the direct radiation and doesn't allow the street to heat up creating comfortable streets in hot and humid climate.

a. Shading by buildings

The streets can be shaded by buildings when the height of building and the width of the street is kept in proportion. Because of the high angles during the summer, buildings must be closer together for considerable shade, so that the shadow length is to be longer than the distance between the buildings (Emmanuel, et al., 2007). For all urban orientation, the street shading fraction increases with increase in aspect ratio during summer and winter with an exception in east-west oriented streets where street shading fraction is higher in winter and lower in summer (Bourbia & Awbi, 2004).

b. Shading by trees

For the streets with lower aspect ratio, the vegetations provide shading to the street ensuring the outdoor thermal comfort for the pedestrians. In particular for E-W streets, the trees produce a 20% increase in shade percentages throughout the summer whereas for N-S streets, the shade percentages are in between 6% -10% (E. Andreou, 2014). Increasing the amount of tree cover results in cooler air temperature than uncovered regions. The surface temperature of sitting places under the dense trees has a temperature value less than 20℃ than the open space (Abdallah, et al., 2020).

2.2.1. Solar angles

a. Declination angle (δ)

The angle formed between the equator and a line drawn from the planet's center to the sun's center is known as the sun's declination. Due to the Earth's tilt on its axis of rotation and the rotation of the Earth around the sun, the declination angle, represented by the symbol, changes periodically (Honsberg & Bowden, n.d.).

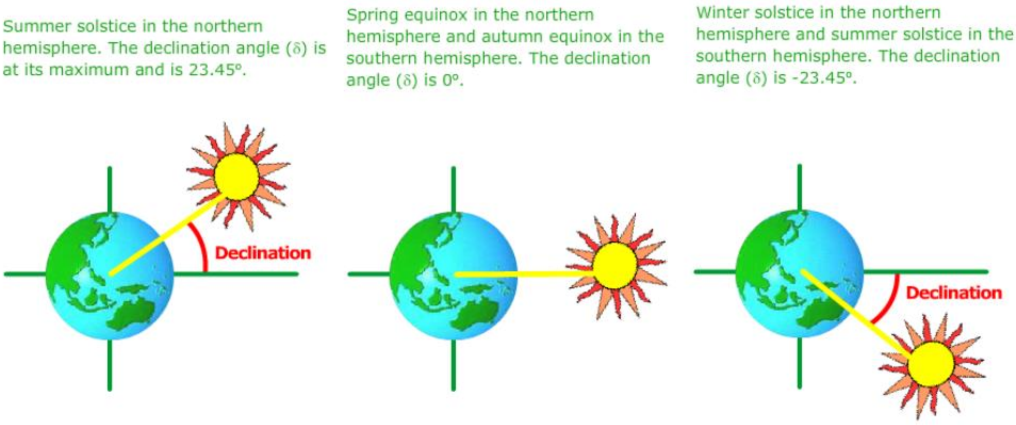

Figure 2. 4 Declination angle
(Honsberg & Bowden, n.d.)

The declination angle can be calculated by the equation:

$$\delta = -23.5° \times \cos\{(360/365) \times (d + 10)\}$$

where **d** is the day of the year with Jan 1 as d = 1

b. Hour angle (t)

The angle through which the earth would revolve to bring the point's meridian precisely under the sun is known as the hour angle, or t, of a point on the surface of the earth. With each 360/24 or 15 degrees of longitude equaling 1 hour and the afternoon hours is referred to as positive hours, the hour angle at local solar noon is 0. The hour angle is -15° at 11 am and 15° at 1 pm because the earth spins at a rate of 15 degrees each hour (Kalogirou, 2012). The AST, or the adjusted local solar time, may also be used to determine the hour angle:

$$t = (AST - 12)15$$

c. **Solar altitude angle (β)**

The solar altitude angle is the angle between the sun's rays and a horizontal plane as shown in Fig. It is related to the solar zenith angle Φ, being the angle between the sun's rays and the vertical (Kalogirou, 2012). Thus:

$$\Phi + \beta = \pi/2 = 90°$$

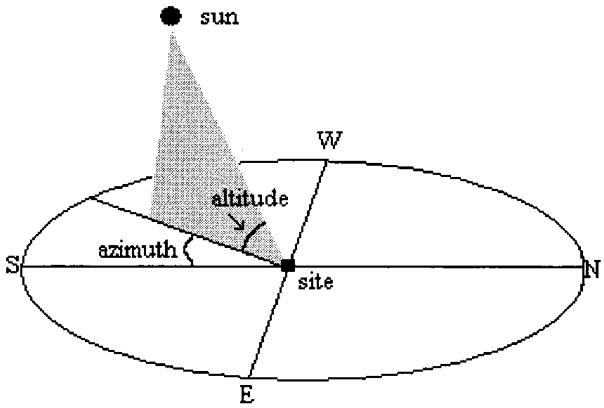

Figure 2. 5 solar azimuth angle and solar altitude angle (Kumar, et al., 1997)

The mathematical expression for the solar altitude angle is:

$$\sin\beta = (\cos(L) \times \cos(\delta) \times \cos(t) + \sin(L)\sin(\delta)$$

where,

L is local latitude, defined as the angle between a line from the center of the earth to the site of interest and the equatorial plane,

δ the solar declination (which is a function of the date and the time), and

t is the hour angle. Values north of the equator are positive and those of south are negative.

d. Solar azimuth angle (α)

The solar azimuth angle is the angle of the sun's rays measured in the horizontal plane from due south (true south) for the northern hemisphere or due north for the southern hemisphere; westward is designated as positive (Kalogirou, 2012).

The mathematical expression for the solar azimuth angle is:

$$\sin\alpha = (\cos(\delta) \times \sin(t))/\cos\beta$$

e. Ground shading factor

The shading factor is defined as the ratio between the global solar radiation received on a surface in presence of shading obstacles and in their absence (Cascone, et al., 2011).In an east-west oriented canyon of width W and wall height H, the width of the shade strip in the street x caused by the south wall is given by

$$x = (\cos\alpha/\tan\beta)\ H$$

where α is the solar azimuth and β is the solar altitude.

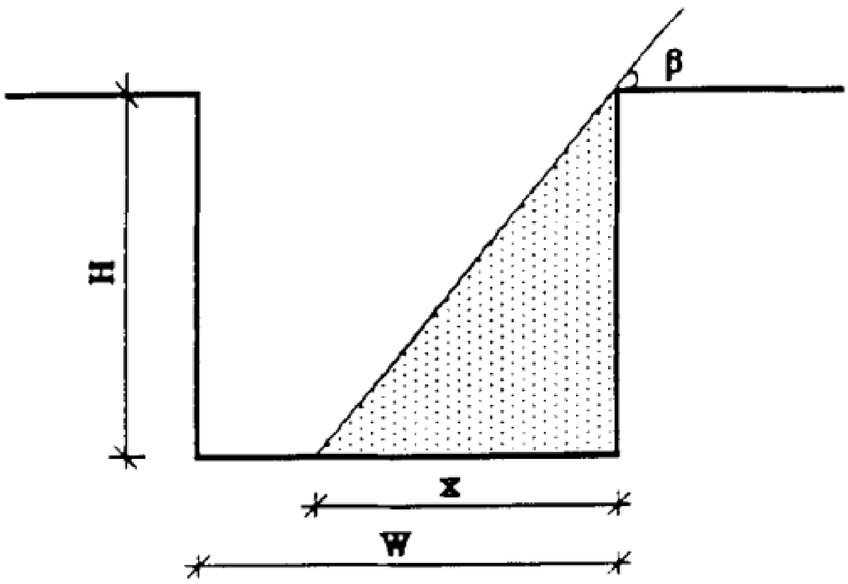

Figure 2. 6 Passive Solar Angle

The ratio of the shade strip width to the street width equals the ground shading factor (PSA), is given by,

$$PSA = x/W = (\cos\alpha/\tan\beta) \times H/W$$

$$\text{For } PSA = (H/W)\tan L$$

2.3. Street Canyon

Simply, street canyon is a rectangular trough (height H, width W) oriented at some angle (Arnfield, 1990). A street canyon is formed by two typically parallel rows of buildings separated by street (Syrios & Hunt, 2008). Bakarman and Chang (2015) claims that the exposure of the urban surfaces is a function of H/W ratio and orientation of the canyon. The amount of solar radiation received by canyon's surfaces depends on the aspect ratio and orientation of street. The air temperature in the street increases with decrease in height-width ratio and vice versa. The street exposure to sun decreases as the canyon becomes deep (Arnfield, 1990). The less solar radiation is received by the street, the less sensible heat is added into the ambient air resulting in decreasing the street temperature. The low temperature in street leads to comfortable street to the pedestrian in hot and humid climatic zone. Also, N-S oriented streets are more comfortable than E-W oriented streets.

2.3.1. Street Aspect Ratio

Street aspect ratio (AR) is defined as the ratio of height of the building surrounding the street to the width of the street. The more the height of the building the more will be the shadow length cast by those buildings, thereby, creating shaded streets. The canyon having aspect ratio around 1 is uniform street canyon, similarly, aspect ratio below 0.5 is shallow street canyon and aspect ratio of 2 represents deep street canyon (Shishegar, 2013). Aspect ratio along with orientation affect urban microclimate and solar access outdoor the building thereby affecting the pedestrian thermal comfort (Shishegar, 2013).

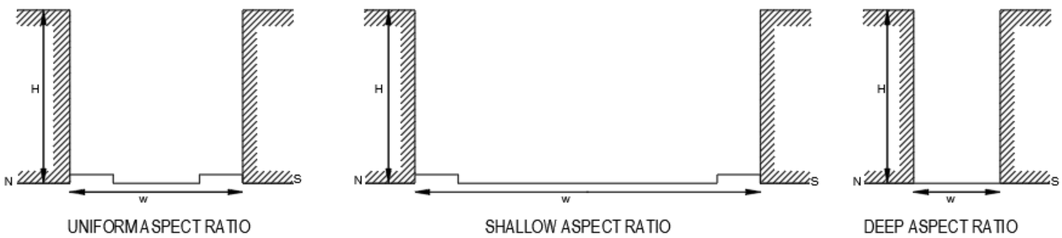

Figure 2. 7 street aspect ratio

De and Mukherjee (2018) looked at how different orientations and canyon aspect ratios affected the microclimate at street level in a warm, humid climate, and discovered that a canyon aspect ratio of 2.5 with taller buildings and more space between them provided the best thermal comfort for people walking around. In Columbo, Sri Lanka, where they studied various urban geometries on five different sites, Johansson and Emmanuel

(2006) discussed the impact of street canyon geometry on outdoor thermal comfort. They found that deeper street canyons provide shade at pedestrian level, creating comfortable pedestrian streets. Andreou and K. Axarli (2012) examined the microclimate of urban canyons in traditional (AR: 0.7-0.9) and modern (AR: 2-4) settings. He found that an increase in building height of one story, which corresponds to an increase in aspect ratio from 0.92 to 1.3, results in a 3°C fall in ground temperature.

Toudert (2005) looked into different street geometries, including aspect ratios, and came to the conclusion that wide streets with aspect ratios of less than or equal to 0.5 are thermally uncomfortable for the majority of the day. By increasing the aspect ratio, PET maxima for N-S streets noticeably decrease (by about 58 °C), but still increase by 66 °C for E-W canyons. Johansson (2006) compared an extremely deep and a shallow street canyon in Fez, Morocco, to examine the impact of urban geometry on outdoor thermal comfort. In the summer, the maximum difference was on average 6 K and as great as 10 K during the hottest days, indicating that in hot and dry climates, a compact urban design with very deep canyon is preferred.

(Jamei & Rajagopalan, 2019) investigated effect of orientation and aspect ratio in pedestrian thermal comfort under worse thermal conditions and concluded that with increase in aspect ratio from 0.1-0.85, diurnal temperature decreased by 1 °C and Mean radiant temperature by 14.2 °C. The deep canyon was found to be cooler than shallow one with an average variation of 4.3K by (Bakarman & Jae D. Chang, 2015,) in the city of Riyadh, Saudi Arabia. In subtropical latitudes, the shallow aspect ratio is highly stressful and almost independent of orientation (Ali-Toudert & Mayer, 2006).

A canyon aspect ratio of 2.5 with taller buildings and greater spacing in between them is optimal in terms of human thermal comfort at the pedestrian level (De & Mukherjee, 2018).The greater value of aspect ratio may be able to lower the amount of sun exposure to the structures, but effective ventilation at the building and neighborhood scales should be taken into account to ensure that it has no impact on the indoor thermal comfort.

2.3.2. Street Orientation

The orientation of the street directly influences the solar exposure of any street. Due to solar path, east-west oriented streets are exposed to solar radiation for most of the time all over the year while a part of a street is shaded for most of the time in case of north-south oriented streets. Parts of NE-SW and NW-SE streets with an intermediate orientation are always shaded during the day (Nasrollahi, et al., 2021,).

(Kushol, et al., 2013) studied the effects of orientation on microclimate comfort for the outdoors and observed that north-south canyons are cooler than east-west canyons by 0.9 K. (Toudert, 2005) also observed east-west street canyons less efficient than N-S in case of thermal comfort. (Rodríguez-Algeciras, et al., 2018) concluded that N-S orientation streets provide the comfort for pedestrians if the aspect ratio for east facing side is greater than 2 and for E-W orientation, deep canyon are recommended on the south facing side. The NS-EW streets are favorable during summer while NE-SW streets are favorable during winter for medium deep and medium wide canyons whereas for deeper canyons, E-W canyons are better for summer and N-S and NW-SE in winter (Chatzidimitriou & Yannas, 2017).

2.3.3. Relationship between street canyon and urban microclimate

A street is said to have a street canyon if buildings encircle it on all sides. Urban street canyons have unique microclimates that work together to influence the climate of the city. Solar access and shade conditions, among other factors, have a significant impact on the microclimate of urban street canyons, which modifies the air and surface temperatures. The length-to-height (L/H) ratio of a canyon also influences its ventilation conditions, which are determined by the geometry and features of the canyon, such as aspect ratio (or height to width ratio, H/W), and street orientation (LP, et al., 2019).

The climate of a small region that differs greatly from the general climate is called the microclimate. The temperature change in the region as a whole could not affect the specific area. As a result, both good and bad aspects of the transition are visible. A favorable microclimate refers to an atmosphere that is more appropriate to ecology and people. For instance, a cool climate in an excessively hot location, but a negative microclimate has a poorer environment than a larger region. The urban heat island may be the cause of the unfavorable microclimate. However, taking climate into account while constructing a city surely aids in creating a favorable microclimate.

Microclimatology focuses on the layer of air just above the earth's surface, where frictions, heating, and cooling are directly felt on temporal scales (Toudert, 2005). The air and mean temperature, wind, and humidity are the key microclimatic factors in an urban street canyon. Depending on the climate zone, the climatic characteristics affect how you feel thermally. One of the most significant natural variables influencing the microclimate is solar radiation, and latitude determines how intense it is. In cold climate zones, warm streets are favored; hence, the street canyon is built to maximize solar radiation. In a hot and humid climate, the situation is the exact reverse. As a result, climatic factors have a big impact on thermal comfort.

Mahmoud and Ghanem (2018) claims that air temperature has the largest share of effects on microclimate in hot arid area. Some studies pointed out solar radiation and mean radiant temperature as factors affecting microclimate of urban canyon (Bourbia & Awbi, 2004). Nakamura and oke (1998) investigated the canyon temperature and roof temperature in 63 measuring points of urban canyon and found the difference of 0.5-1K between roof and canyon temperature due to well mixed turbulent air within the canyon and above it.

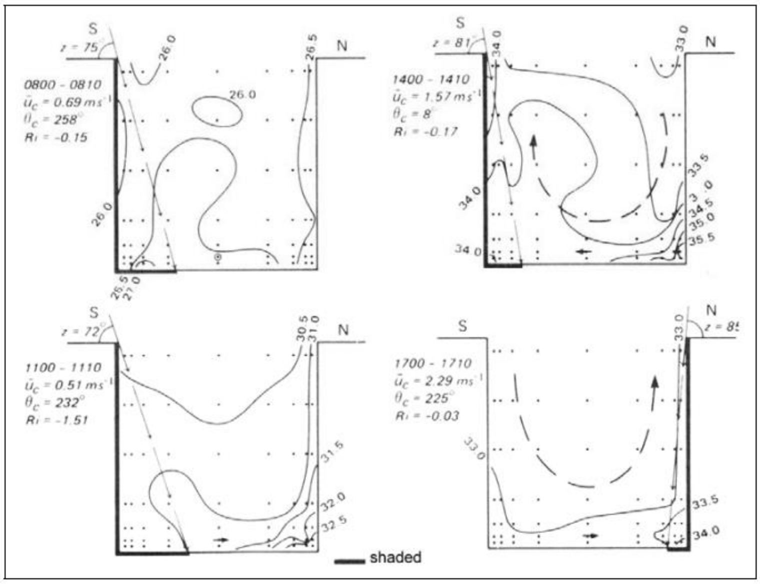

Figure 2. 8 Isotherm distribution across an E-W canyon at selected daytime hours *(Nakamura and Oke, 1998)*

The street canyon geometry, in terms of aspect ratio and orientation, is a key factor affecting exposure to sun and wind, and thus the formation of different street canyon microclimates (Chatzidimitriou & Yannas, 2017). The study also highlighted that solar radiation and air velocity are the parameters of the local microclimate which mostly influence thermal comfort for pedestrians. Hence, maintaining street air temperature at desired level by creating a mass around it and shading in hot and humid climatic zone results in comfortable street for pedestrians.

2.3.4. Street canyon and Pedestrian comfort

The concept of healthier and sustainable city includes people in movement performing physical activity that promotes sustainability and well-being. During this activity, people gather multisensory experiences that inform their state of comfort (Vasilikou & Nikolopoulou, 2019). Comfortable air temperature along with breeze creates thermally comfortable streets. Thermal comfort is one of the major factors affecting the quality of outdoors for pedestrians. Using the number of people performing activities on shaded or unshaded spaces shows that sunny and shaded spaces affect the people's willingness to leave or stay (Nasrollahi, et al., 2020).

In a study carried out in hot and arid city of Riyadh, Saudi Arabia, it was found that the street temperature was 5 °C-10 °C less in deep street canyon (2.2) than shallow street canyon (0.42) during the daytime at 14:00 hours (Bakarman & Chang, 2015). E. Johansson (2006) found out during the peak time of summer in city of Fez, Morocco, the physiologically equivalent temperature (PET) value in the deep canyon were stable at around 23 °C and 28 °C whereas in shallow canyon the PET value exceeded 40 °C between 11:00 and 17:00 hours. The peak street temperature was found to be 2.5-3.5 K lower than the reference temperature of meteorological station in case of deep canyon (2) in a study of El-Oued, Nigeria (Bourbia & Awbi, 2004). Also, the two thirds of street of shallow canyons (0.5) was receiving direct solar radiation at the rate of 846 W/m^2. A study in Rajarhat, Kolkata observed a canyon aspect ratio of 2.5 as optimal in terms of human thermal comfort at the pedestrian level for the region (De & Mukherjee, 2018).

Hence, several studies that measured PET values and street temperature have reported a clear correlation between pedestrian thermal comfort and aspect ratio. The deeper aspect ratio constricts direct solar radiation thus shading the streets. Shading has been reported as main parameter to reduce street temperature and PET resulting into a comfortable environment for pedestrians. Narrow streets with buildings provide better shading for sidewalk pedestrians than wide streets (Jamei & Rajagopalan, 2019).

2.3.5. Impact of street design on solar radiation

The exposure of direct solar radiation in the street is a critical parameter for pedestrian thermal comfort. Solar radiation incident on an urban area is received either by building facades and roof or the streets. The incident radiation during the day time makes the street thermally uncomfortable. Hence, urban streets should be designed in a way to utilize the solar access to improve urban microclimate and pedestrian thermal comfort.

Shishegar (2013) found out that increasing street width from 15 m to 20 m increases the radiation yield with 17–20%. She also found street orientation hardly influences the amount of solar radiation of canyon rather aspect ratio has great influence on the quantity of solar energy obtained by street. As discussed earlier, high aspect ratio yield lower amount of solar radiation. ARNFIELD (1990) emphasized that by increasing the aspect ratio, solar acess to walls and streets can always be decreased to larger values than those appropriate for the temperate latitudes.

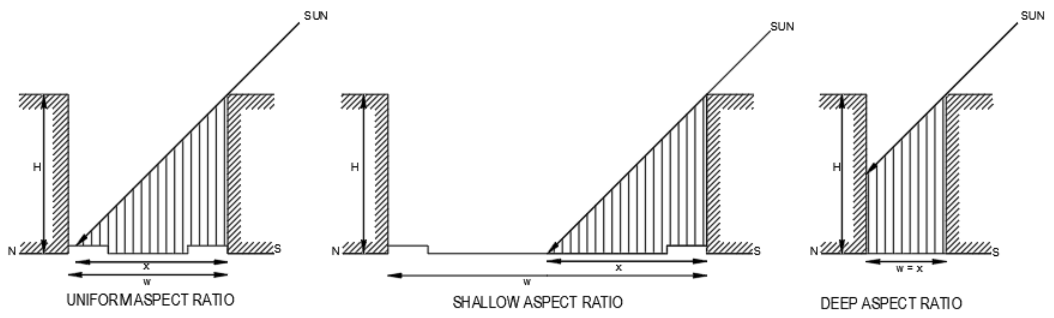

Figure 2. 9 Representation of solar incidence on street having different aspect ratio

The above figure shows that the street having deep aspect ratio can shade much of the street than streets with shallow and uniform aspect ratio. Low value of aspect ratio and high sky view factor allows street surfaces to receive highest solar radiation. Mohajeri, et al. (2019) conducted study in 1600 streets and found out the mean monthly radiation reaches highest i.e. 100KWh/m^2 for aspect ratio below about 0.5 in May and August and below about 1in June and July. Hence, street design influences the thermal comfort at pedestrian level considering the radiation received by street surfaces.

The street in N-S canyons limits solar exposure for the majority of the day and lowers direct solar radiation below 70% from early afternoon for 3 hours in wide canyons and hours in medium canyons both in summer and winter, whereas E-W canyons are exposed to solar for the majority of the time all through autumn and spring months and lowers direct solar radiation below 70% from early morning for more than 10 hours in wide and medium canyons and 4 hours in deep canyons during summer.

Between aspect ratios of greater than 2 and less than 1, it is possible to notice a difference in solar intensity of around 110–262 Wh/m2 from November to February and 482-2147 Wh/m2 from March to October.

2.3.6. Case of Rajasthan, India

Rajasthan is a state in northwest India that is bordered to the north and north-east by Punjab and Haryana, to the east by Uttar Pradesh and Madhya Pradesh, to the south-east and southwest by Gujarat, and to the west and northwest by Sindh and Punjab in Pakistan and India. With very little vegetation or water, and a hot, dry environment, it has incredibly difficult climatic conditions.

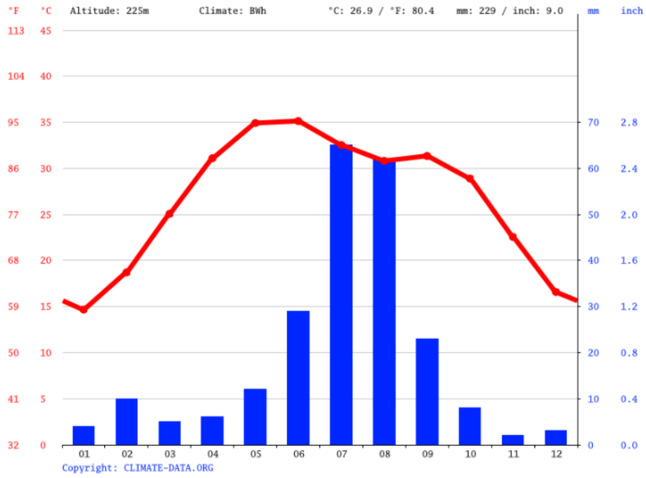

Chart 2. 1 Climate graph of Bikaner, Rajasthan (climatedata.org)

	January	February	March	April	May	June	July	August	September	October	November	December
Avg. Temperature °C (°F)	14.7 °C (58.4) °F	18.7 °C (65.7) °F	25.1 °C (77.1) °F	31.1 °C (88) °F	34.9 °C (94.9) °F	35.1 °C (95.2) °F	32.5 °C (90.6) °F	30.8 °C (87.5) °F	31.3 °C (88.4) °F	28.9 °C (84) °F	22.6 °C (72.6) °F	16.6 °C (61.8) °F
Min. Temperature °C (°F)	7.8 °C (46.1) °F	11.1 °C (52) °F	17 °C (62.5) °F	22.5 °C (72.6) °F	27.3 °C (81.2) °F	29.4 °C (84.9) °F	28.2 °C (82.8) °F	26.7 °C (80.1) °F	26.2 °C (79.2) °F	22 °C (71.5) °F	15.5 °C (59.9) °F	9.7 °C (49.5) °F
Max. Temperature °C (°F)	21.2 °C (70.2) °F	25.5 °C (77.9) °F	32 °C (89.6) °F	38 °C (100.4) °F	41.3 °C (106.4) °F	40.3 °C (104.5) °F	36.9 °C (98.5) °F	35.3 °C (95.5) °F	36.4 °C (97.5) °F	35.3 °C (95.6) °F	29.3 °C (84.7) °F	23.4 °C (74.1) °F

Chart 2. 2 Temperature of Bikaner, Rajasthan (climatedata.org)

The chart shows that the temperature of Rajasthan, Bikaner reaches 41.3°C during the month of May. The city experiences hot weather during the daytime for 8 months with maximum temperature above 30 °C. Despite the harsh temperature, it is observed that the streets are considerably a few degrees cooler than the overall temperature of the region due to the shadow cast by the building (Shabnaprarthana & Bhansali, 2021). The streetscape houses building up to two or three storeys high and often share a wall between the buildings.

Figure 2. 10 Streets of Jaisalmer,
(Timbukutu travel)

The streets are generally narrow not more than 8m wide. The buildings cast a shadow onto the street thus saving pedestrians from harsh overhead sun. Since every house on both sides of the street follows this in harmony, the street achieves a micro climate which is significantly cooler than the average microclimate of the region. The temperature of the street is pleasant as it's down by a few degrees, making the air sufficiently cool and moist.

Mawa patti street lies in old Bikaner. The street width is approximately 3m to 3.5m whereas building height varies from 9m to 15m (Suthar, 2020). The aspect ratio of the streets of Mawa patti varies from 3 to 5. The street canyon developed is deep canyon hence provides maximum shading to the street leading to comfortable streets for pedestrians.

Figure 2. 11 Street of Mawa Patti, Bikaner
(Suthar, 2020)

2.4. Building Byelaws

While carrying out building construction operations, a precise set of regulations must be observed, as is true of any type of development. This precise collection of restrictions that builders must follow in real estate is known as building bye-laws, and they are intended to provide orderly growth in cities. Cities will face excessive coverage, encroachment, and unplanned expansion in the absence of building bye-laws, resulting in chaotic situations, annoyance for users, and disregard for building aesthetics. Building bye-laws, which are largely formulated by a central body, guarantee that projects are not only safe but also meet aesthetic criteria. In that sense, these govern the construction and architectural components of building activity. Building bye-laws also control open space allowances in a project, with the goal of preventing developments from turning the city into a concrete jungle.

2.4.1. Ground Coverage

The ratio of the building area divided by the land area is ground coverage by building. Building area means the floor space of a building when looking down at it from the sky. It is calculated by

Ground coverage (%) = (Building area/Land area) x 100

2.4.2. Floor Area Ratio

The ratio of total floor area divided by land area is the floor area ratio. Here, total floor area refers to the total amount of floor space in a building. It is calculated by:

FAR = Total floor area/ Land area

2.4.3. Height of building

Building height is defined as the average maximum vertical height of a building or structure measured at a minimum of three equidistant places along each building elevation from completed grade to the highest point on the building or structure (division, n.d.).

2.4.4. Relationship between Ground coverage, FAR, and Height of building

Ground coverage (%) = (Building area/Land area) x 100

Maximum ground coverage area = (Ground coverage (%) x Land area)/100

FAR = Total floor area/ Land area

Total floor area = FAR x Land area

Area of one floor = Total floor area/ allowable ground coverage Area

No . of storey = Total Floor Area/ Area of one floor

2.4.5. Setback

The term "building setback" means the required separation between a street line (and/or right-of-way line) and a building or structure (Development, n.d.).

2.4.6. Bylaws of Lumbini Sanskritik Municipality

Building Type	Land Area	Maximum ground coverage	FAR
Residential	Upto 250 sq.m	70%	2.5
Residential	More than 250 sq.m	60%	2.5
Commercial cum Residential	Upto 250 sq.m	60%	3
Commercial cum Residential	More than 250 sq.m	50%	3
School, College		40%	1.25
Polyclinic, Nursing Home		35%	1.25
Hostel		50%	2

Table 2. 5 FAR and Ground Coverage

Setback

The minimum setback for highway roads is 6m while for inner roads the minimum setback is 1.5 m.

Building Type	Minimum Setback (m)	
	Front	Sides and back
Residential	1.5	1
Educational	5	3
Institutional	5	3
Theatre, community hall	15	6
Commercial	5	2
Hotel	5	2
Star Hotel	10	3

Table 2. 6 Setback for Lumbini Sanskritk Municipality

The minimum storey height for residential type is 2.9 m. The maximum permissible height of the building is 17m.

Shading devices used for rain and sun protection must be less than 1m in length and must be placed under setback.

The height of the boundary wall shall not exceed 4 feet when built with brick or stone masonry. If necessary, a 3ft height may be added with wire mesh.

2.5. Classification of Roads

Roads can be simply classified into four categories regarding the function and traffic and they are:

2.5.1. Arterial Roads:

For arterial highways, the right of way extends up to 50 meters and includes a bicycle lane in addition to four lanes for vehicles. Separate pedestrian pathwaysare available however crossing are allowed only at certain locations. Activities including parking, loading, and unloading are often regulated and limited.

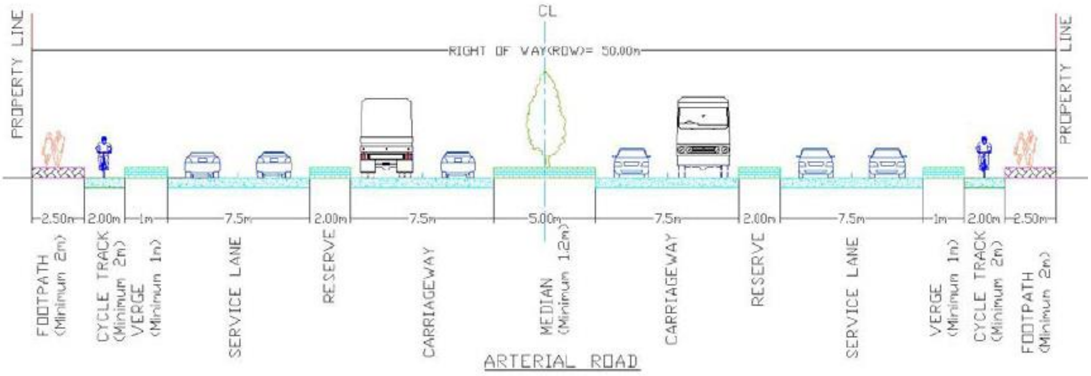

Figure 2. 12 Typical section of arterial roads
(Nepal Urban Road Standard, 2076)

For sub- arterial highways, the right of way extends up to 30 meters and includes a bicycle lane in addition to two lanes for vehicles. Separate pedestrian pathways are available however crossing are allowed only at certain locations. Activities including parking, loading, and unloading are often regulated and limited.

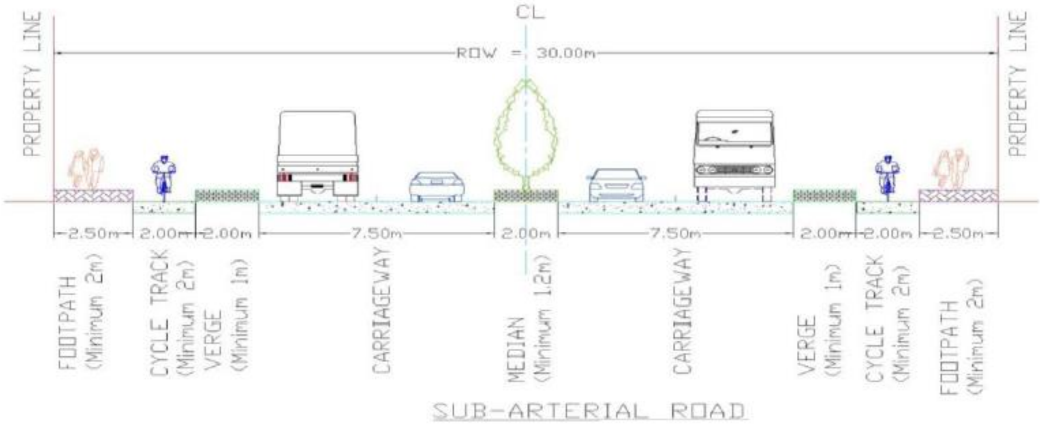

Figure 2. 13 Typical section of sub- arterial roads
(Nepal Urban Road Standard, 2076)

2.5.2. Collector Roads

A collector road is one that is designed to both provide access to arterial/sub-arterial roads and to collect and distribute traffic to and from local roads. Normally, collector roads are found in residential zones or business areas.

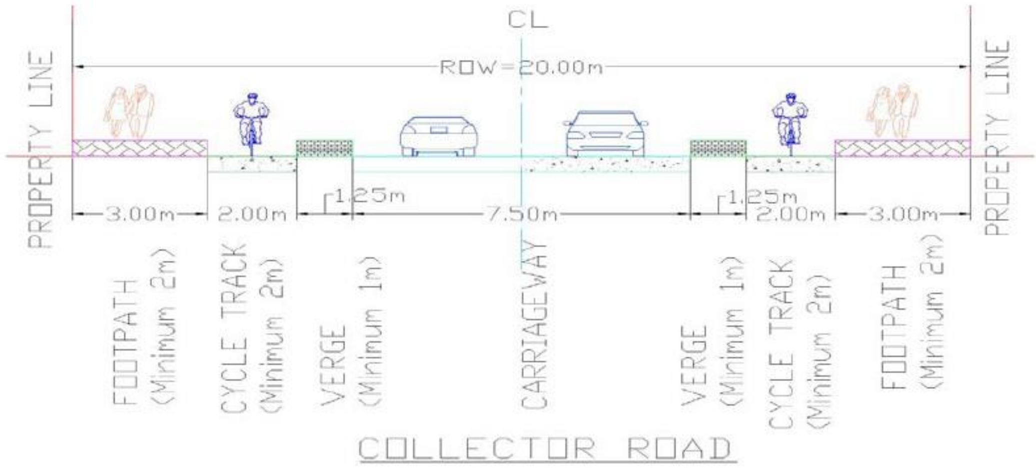

Figure 2. 14 Typical section of arterial roads (Nepal Urban Road Standard, 2076)

2.5.3. Local Road

A local road is one that is primarily designed to provide access to nearby homes, businesses, or other properties.

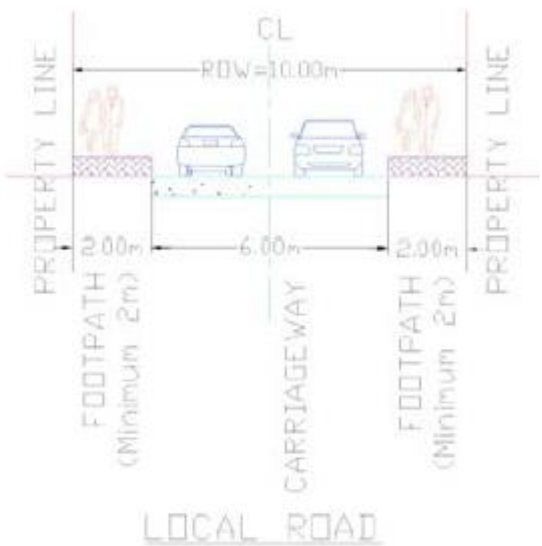

Figure 2. 15 Typical section of arterial roads (Nepal Urban Road Standard, 2076)

2.6. Previous research findings

Kushol, et al., (2013) studied the effects of street morphology (street orientation and aspect ratio) on the microclimate comfort criteria for outdoors in warm humid Dhaka and found out deep street canyons are suitable for N-S streets and shallow street canyons for E-W streets with the provision of tree shading. Also, front setbacks should be minimum to ensure deep canyon along the N-S direction while front setbacks should be maximum to create wide canyon along the EW direction. They suggested to place the open space adjacent to the street for plots along E-W street creating canyon of low H/W ratio while at the rear side of the building in plots adjacent to the N-S road.

Mohajeri, et al., (2019) concluded that the street surfaces receive the highest solar radiation when the aspect ratio is low. It was observed that the thermal comfort at the pedestrian level is highly influenced by street design due to amount radiation received by street surfaces.

The study carried out in hot and arid city of Riyad, Saudi Arabia evaluated the thermal performance of urban canyons with H/W ratios of 2.2 and 0.42. Bakarman and Chang (2015) concluded that the exposure of the urban surfaces to the solar radiation is a function of H/W ratio and orientation of canyon. The aspect ratio and orientation determines the quantity of solar radiation incident thus affecting the ambient surface temperature of street. The temperature increase with the decrease of aspect ratio.

(Nasrollahi, et al., 2020) on their study to develop strategies to mitigate heat to improve pedestrian comfort found mean radiant temperature has the greatest effect on outdoor thermal comfort among other factors such as wind speed and humidity. Hence, strategies that reduce mean radiant temperature such as shading are more effective way ti improve pedestrian comfort.

The effect of street design on pedestrian comfort was experimentally investigated by Jamei and Rajagopalan (2019). They reported that diurnal air temperature is decreased with the increase in aspect ratio. However, it is more perceptible in NW-SE oriented streets and least perceptible in E-W oriented streets. Similarly, they suggested shading through building is the key strategy for promoting pedestrian comfort because it leads to reduction in the ansorbed radiation by a standing person.

Johansson (2006) investigated the influence of urban geometry on outdoor thermal comfort by comparing an extremely deep and a shallow street canyon in Fez, Morocco. The continuous measurements showed that, by day, the deep canyon was considerably cooler than the shallow one. In summer, the maximum difference was on average 6 K and as great as 10 K during the hottest days. It indicates that in hot and dry climates, a compact urban design with very deep canyon is preferable.

De and Mukherjee (2018) investigated the impact of different orientations and canyon aspect ratios to improve street-level microclimate in a warm humid climate. A canyon aspect ratio of 2.5 with taller buildings and greater spacing in between them is optimal in terms of human thermal comfort at the pedestrian level.

Muniz-Gäal, et al. (2020) studied whether geometric parameters of urban street canyons affect their microclimates and pedestrian thermal comfort and revealed thatcanyons with higher aspect ratio increase the wind speed and shading by buildings, thereby improving the thermal comfort at the pedestrian level.

Ali-Toudert and Helmut Mayer (2006) discussed the contribution of street design towards the development of comfortable microclimate at street level for pedestrians. They concluded that in subtropical latitudes, shallow aspect ratio is highly stressful and almost independent of orientation. In contrast, high aspect ratio combined with N-S orientation provides much better thermal environment.

Shishegar (2013) analysed the effects of street geometry and orientation on airflow and solar access in urban canyons and concluded that aspect ratio affects the quantity of solar energy obtained by street facades. Decreasing the aspect ratio increases solar access in the street and street orientation hardly influences the amount of solar radiation of the canyon.

Chatzidimitriou and Yannas (2017) studied the influence of canyon aspect ratio and orientation on microclimate and outdoor comfort and observed differences upto 22K due to canyon orientations ans 4K due to aspect ratio in summer midday while 4K and 7K respectively during winter.

Johansson and Emmanuel (2006) discussed the influenced of street canyon geometry on outdoor thermal comfort in Columbo, Srilanka where they studied different urban geometry on five sites of Columbo. They observed deeper street canyons provide shade at pedestrian level creating comfortable pedestrian street however, deep canyons are seen not preferable in polluted areas since dispersion is less effective in shallow canyons.

Rodríguez-Algeciras, et al., (2018) studied the effect of asymmetrical street canyon profiles in warm-humid climate of Cuba simulating urban settings with five different aspect ratio and four street axis orientation. They found out N-S orientation provide the best comfort for pedestrians if the aspect ratio for east facing side is greater than 2. Similarly, for E-W orientation, deep canyon are recommended on the south facing side.

Andreou and K. Axarli (2012) investigated urban canyon micrclimate in traditional and contemporary environment experimentally and parametrically and discovered that the increase of building height by one storey which equals to increase of aspect ratio from 0.92 to 1.3 leads to decrease on ground temperature by 3°C.

Lee, et al., (2018) performed a detailed evaluation and comparison of three shading strategies: shade from building, from tree and from an umbrella and found out shading by building as the most effective strategy and recommend the cities to de designed in a way to have deeper canyons.

Toudert (2005) investigated street geometries including various aspect ratios, solar orientation and number of design details in Freiburg, Germany and Ghardaia, Algeria. He concluded that wide streets which has less or equal to 0.5 aspect ratio are thermally uncomfortable during the largest part of daytime. By increasing the aspect ratio, PET maxima decrease noticeably for N-S streets (about 58 °C) whereas still by 66 °C for E-W canyons.

(Muniz-Gäal, et al., 2020) studied whether geometric parameters of urban street canyons affect their microclimates and pedestrian thermal comfort and revealed that canyons with higher aspect ratios had increased shading from buildings, which decreased the variation in thermal comfort sensation during the day and lowered the peak PET values, thereby improving thermal comfort at pedestrian level, especially in summer. Furthermore, they claimed that the increase in the aspect ratio decreases the maximum air temperature.

2.7. Methodological review

The majority of research investigations have taken one of two methodologies, or a combination of these two approaches:

i. Experimental studies
ii. Numerical modeling studies

Field studies in the area of outdoor thermal comfort are limited in quantity due to the large number of urban elements and processes involved in street design. As a result, numerical methods outperform large field measurements, which are limited by a multiplicity of variables and processes. Arnfield (2003) agree that numerical simulation, which is defined as a methodology perfectly adapted to dealing with the complexities and non-linearities of urban climate systems, is gaining in favor.

In addition to the urban microclimate changes, only few microclimate models examine the resulting thermal comfort. This is primarily due to the difficulty in determining the radiation fluxes from a human body's surrounds in complicated urban locations. The problem of modeling outdoor thermal comfort is thus frequently addressed using simplified methods, in which many climatic processes are omitted and substituted by data entered by the user (for example, daily wind speed, air temperature, or humidity) (Ali-Toudert & Mayer, 2006). Several research (De & Mukherjee, 2018; Abdollahzadeh & Biloria, 2020; Ali-Toudert & Mayer, 2006; Chatzidimitriou & Yannas, 2017; Jamei & Rajagopalan, 2019; Makaremi, et al., 2012; Muniz-Gäal, et al., 2020; Qaid & Ossen, 2015) have used the CFD tool Envi-met since it is one of the first models to attempt to simulate the primary atmospheric processes that determine microclimate.

Only a small percentage of studies (Bakarman & Chang, 2015) succeed in achieving their goals through experimental research. A series of measurements were taken on specific days to investigate the influence of aspect ratio and shading effect. The ambient air temperature was the key climatic parameter measured. In order to determine the aspect ratio, the detail of the street section was also measured. (Lin, et al., 2010) took field measurements in a variety of sites with varying levels of shadowing and also conducted a questionnaire survey to assess thermal comfort.

Both experimental study and numerical simulation were used in some of the researches. Field surveys were conducted by (Johansson & Emmanuel, 2006) and (Johansson, 2006), who used RayMan software to calculate PET and MRT. Similarly, many studies (De & Mukherjee, 2018; Abdollahzadeh & Biloria, 2020; Ali-Toudert & Mayer, 2006; Chatzidimitriou & Yannas, 2017; Jamei & Rajagopalan, 2019; Makaremi, et al., 2012; Muniz-Gäal, et al., 2020; Qaid & Ossen, 2015) included field surveys as well as simulations utilizing the Envi-met software.

2.8. Software used

In order to carry out research projects in the field of architecture, there are basically two methods: Experimental Setup and Simulation Research. In the experimental setup, a real case model is developed and within constrained conditions experiments are performed, whereas, in simulation research virtual modelling of the real case scenario is done and simulation is carried out in digital framework. In simulation research, the real time data can be collected and used for accurate results. Experimental research and simulation research both have their pros and cons which decide their use in a certain field.

Advantages:

a. Experimental Research
    a. It gives more accurate results as compared to simulation research
    b. Multiple scenarios with different variables can be utilized at the same time
    c. It is versatile in nature and can be used in multiple sectors
    d. The results can be verified easily and also be duplicated multiple times
b. Simulation Research
    a. Requires less investments than experimental research
    b. This research can be carried out with just a computer in any location
    c. No foreign elements can affect the experiment
    d. The experiment and research can be obtained faster than experimental research
    e. Doesn’t require involvement of real objects or organisms.

Disadvantages:

a. Experimental Research
    a. Requires high investment throughout the research
    b. The external variables are very difficult to control
    c. Requires a standard laboratory condition to be carried out
    d. Same results may not be obtained in each iteration which increases the workload.
    e. The accuracy depends upon the human precision which is not always 100%.
    f. The results are affected by the subjectivity of the human participants.
b. Simulation Research
    a. The accuracy of the result is heavily dependent on the computation power.
    b. The results always need to be validated through either numerical or experimental modelling
    c. Heavily reliant on the information provided by the developers of the software.
    d. It cannot comprehend real life response of living subjects in research.

2.8.1. ENVI-met

ENVI- Met, a tridimensional model that models the interactions of the surface-vegetation-atmosphere and provides simulations for the microscale dimension, is one of the most well-known tools for urban climate modeling (Gusson & Duarte, 2016,). It is a Computational Fluid Dynamics (CFD) model that simulates the interaction between the built form, green cover and microclimate of urban setup in three dimensional grids (De & Mukherjee, 2018). ENVI-met models microclimatic dynamics in complex urban structures, such as buildings of varied shapes and heights, as well as vegetation, throughout the course of a day cycle (Ali-Toudert & Mayer, 2006).

Through simulation, this program enables for the examination and measurement of the impacts of urban planning and architecture on outdoor microclimate (Bruse & Fleer, 1998,). Envi-Met is remarkable for its capacity to mimic variations in solar radiation by constructing buildings and materials in a specific location's surroundings (Middel, et al., 2014). This program also calculates the impacts of vegetation, such as the potential temperature of leaves, by taking photosynthetic rates, soil moisture content, and local evaporation rates into account (Bruse & Fleer, 1998; Bruse, 2004).

One of its key advantages is that it reproduces the main atmospheric processes that determine microclimate, such as wind, turbulence, radiation fluxes, air temperature, and relative humidity, utilizing fundamental thermodynamic and fluid mechanics rules (Duarte, et al., 2015; McRae, et al., 2020,). From a microclimate standpoint, the models analyze daily cycles in complex urban structures, including buildings and plants of various forms and sizes (Cárdenas & Silva, 2018; Ali-Toudert, 2021). ENVI-Met has been used in a number of studies to simulate near-ground air temperatures and to better understand the influence of urban design on microclimate (Toudert et.al.,2006; Aslam & Rana, 2022; Tsoka et.al.,2018; Salata et.al.,2017). This program may be used to simulate scenarios, often evaluating the advantages of NBSs, and its results can be used as a reference for urban design, with the goal of reducing the impacts of heat islands in urban settings and enhancing user thermal comfort (Maleki et.al.,2016; Evola et.al.,2017; Tsilini et.al.,2015; Morakinyo and Lam, 2016; Lobaccaro and Acero; 2015).

ENVI-met is a microclimate modelling system with high resolution. It is a three-dimensional microclimate model developed to replicate surface-plant-air interactions in urban contexts, with a typical spatial resolution of 0.5 m and a temporal resolution of 1- 5 sec. Architecture, Landscape Architecture, Building Design, and Environmental Planning are just a few examples of typical applications. Envi-met can calculate air temperature, surface ground and wall energy budgets, wind velocity, and short-wave radiation flux (Qaid & Ossen, 2015). The input data for envi-met software are:

- position and height of buildings
- position of plants
- distribution of surface materials and soil types
- position of sources
- position of receptors
- geographic position of the location on earth (Envi-met 3.1 manual contents)

ENVI-met, a three-dimensional microclimate simulation model, enables users to create, simulate, and analyze the influence of various NBS on the urban microclimate for any urban environment in every temperature zone throughout the world, from the tropics to Central Europe and the northern regions. ENVI-met has been verified in over 3.000 scholarly articles during the last 20 years. ENVI-met is a prognostic model based on the fundamental laws of fluid dynamics and thermodynamics. The model includes the simulation of:

- Flow around and between buildings
- Exchange processes at the ground surface and at building walls

- Building physics
- Impact of vegetation of the local microclimate
- Bioclimatology
- Pollutant dispersion (MET, 2022)

It is the most frequently used urban environment model, with climate researchers using it in a variety of climate areas, including tropical climates and has been used in many aspect ratio researches (De & Mukherjee, 2018; Abdollahzadeh & Biloria, 2020; Ali-Toudert & Mayer, 2006; Chatzidimitriou & Yannas, 2017; Jamei & Rajagopalan, 2019; Makaremi, et al., 2012; Muniz-Gäal, et al., 2020; Qaid & Ossen, 2015).

Simply put, the software requires fewer parameters and estimates all critical meteorological characteristics such as air and surface temperatures, wind speed and direction, air humidity, short-wave and long-wave radiation fluxes, and the mean radiant temperature required for comfort studies (Ali-Toudert & Mayer, 2006).

2.8.2. Sketchup

SketchUp is a user-friendly 3D modelling tool that allows you to create and edit 2D and 3D models using a proprietary "Push and Pull" approach. Designers may use the Push and Pull tool to extrude any flat surface into 3D forms. All you have to do is click an object and pull it till you like what you see. SketchUp is a 3D modelling application that may be used for a variety of tasks such as architectural, interior design, landscape architecture, and video game design, to mention a few.

The software offers drawing layout capability, surface rendering, and compatibility for third-party Extension Warehouse plugins. The program has several uses, including architectural, interior design, gardening, and video game design. Sketchup is also popular among users who wish to create, distribute, or download 3D models for use with 3D printers.

@Last Software invented Sketchup in 1999. Google purchased SketchUp in 2006 after @Last Software built a Google Earth plugin that piqued Google's interest. Trimble Navigation (now Trimble Inc.) purchased Sketchup from Google in 2012 and enhanced the software by introducing a new website hosting plugins and extensions (Gavin, 2018,).

Solar Analysis in Sketchup

Any structure may be solar analyzed in Sketchup by first creating a 3D model of it via the user interface. Geolocation is used to input the location and solar angle into the program. The site's GIS coordinates, a satellite picture, and associated landscape are integrated into the model. Sketchup has a feature that allows users to project shadows at different times of day and on different days of the year, which may be used to do solar research.

3. Chapter 3. Methodology

3.1. Research Framework

The research is carried out in three phases basically, starting from literature review which includes a general description of street design and its relationship with microclimate, aspect ratio and solar access. The second phase deals with the field study and computational simulation using data from existing urban configuration. The findings will be evaluated and validated using field data.

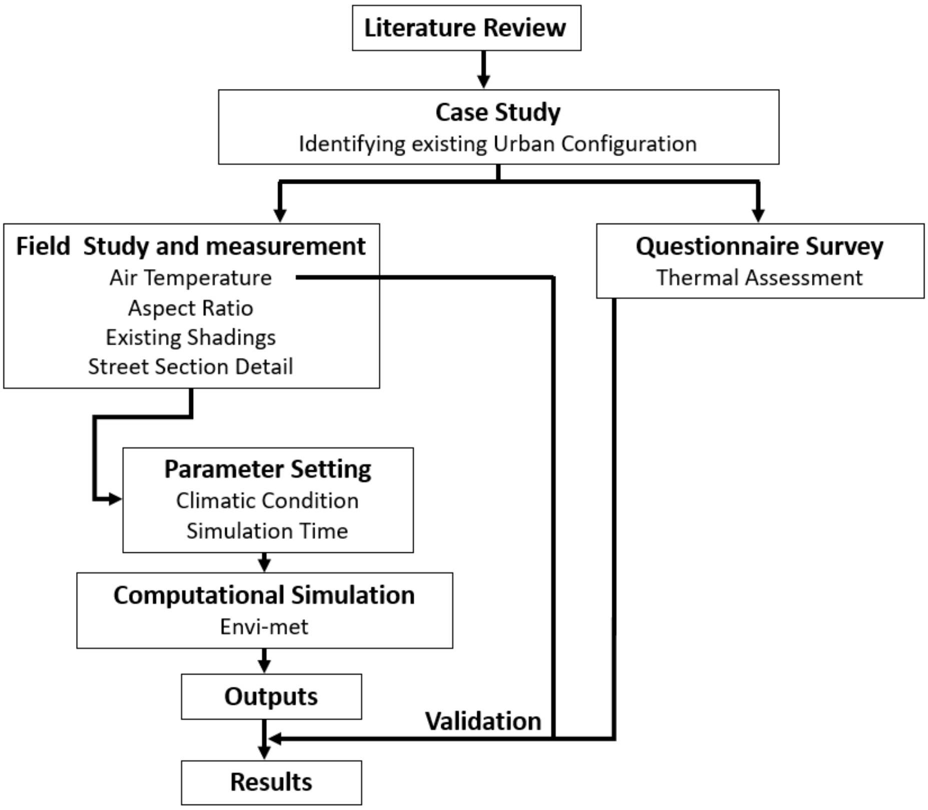

Chart 3. 1 Flowchart of Methodology

To carry out the research, both qualitative and quantitative data will be examined. A qualitative analysis will be performed to review and develop theoretical perceptions of street design and aspect ratio. Individual perceptions of outdoor thermal comfort and thermal sensation will be included in qualitative data. Meanwhile, the research will conduct both an experimental study and a numerical simulation to determine the results.

3.2. Research Methodology

This study employs a mixed methodology that includes a literature review, survey research, and simulation research. A thorough examination of the literature was conducted, referring to prior research articles and papers published on the issue. The survey research is the process of doing research by conducting surveys to targeted respondents and then evaluating statistically to get significant study results. Thus, a structured questionnaire survey was administered to pedestrians in the selected street of Lumbini Sanskritik Municipality. A total of thirty-two samples were gathered over the course of two days in June.

Another methodology used was simulation research. Simulation research stand for the research done by replicating exact same conditions in computer assisted virtual environment to determine the results. This research used ENVI-met 5.03 software student version for the process of simulation.

3.3. Research methods

3.3.1. Questionnaire survey

A structure questionnaire survey was conducted with the pedestrians in the selected street of Lumbini Sanskritik Municipality. Total of thirty-two samples were collected for two days June 16 and 17. The first of two days was partially overcast, while the second was sunny. The questionnaire consisted of three sections demographic details, thermal sensation survey and location related parameters.

Figure 3. 1 Conducting questionnaire survey

3.3.2. Field Survey

Figure 3. 2 Position of data logger

On the 17^{th} and 18^{th} of June, a complete field inspection was conducted along the selected road section. The field measurement primarily consisted of measurement of road section (length, width, and topography) with the help of laser measure (NOYAFA NF 271) and a standard 50 m measuring tape (Fibreglass Measuring Tape) along with the surrounding building height. The temperature and humidity of the site were measured from 17th June at 7:00 hrs to 1st July at 23:59 hrs. The data were recorded for each minute of the 24 hrs. time period. The data logger used was Onset Data logger (model no: MX2302A). The data logger was placed in the premise of a grocery shop due to safety and security region at a height of around 3m with the sensor hanging around 50cm below the device in the air for measurement of the required atmospheric data.

3.3.3. Simulation

To determine the results, the exact conditions of the site was simulated using ENVI-met 5.3 student version. The simulation time was determined by analyzing the climatic conditions and the recorded temperature humidity data from the site. The other input variables were exactly the same as the street section. For the improved results, different scenarios were created and simulated accordingly. The simulation was run for several times to ensure the accuracy.

4. Chapter 4: Study Area

The research site was chosen in Nepal's Lumbini Province, Rupandehi District, which is located in the Hot and Humid Climatic Zone. The study took place at a street right outside the Lumbini Masterplan Area, where a street section of 1000m was selected. The first 300m of street is oriented towards E-W direction whereas the remaining 700m is oriented NE-SW.

4.1. Introduction to site

Lumbini which is the birthplace of Siddhartha Gautama- Buddha in the 7th century BC, is located 22 kilometers west of Siddharthanagar (Bhairawa). In 1967, U Thant, Secretary-General of the United Nations, visited Lumbini and urged that it become a significant pilgrimage and peace destination. U Thant, a devout Buddhist from Myanmar, also felt that Lumbini should be built as a meeting place for religious and secular leaders to collaborate in order to build a world free of hunger and strife. As a result, the United Nations established a 15-member International Lumbini Development Committee. The Master Plan was designed by renowned architect Kenzo Tange and was approved in 1978 (LSSF, n.d.). The Lumbini Master Plan, spread in an area of 1×3 square mile, oriented along the north-south axis, encompasses three zones (1) the Sacred Garden, (2) the Monastic Zone, and (3) the New Lumbini Village, based on the notion of the path to enlightenment. Each of the zones covers an area of a square mile (LDT, n.d.).

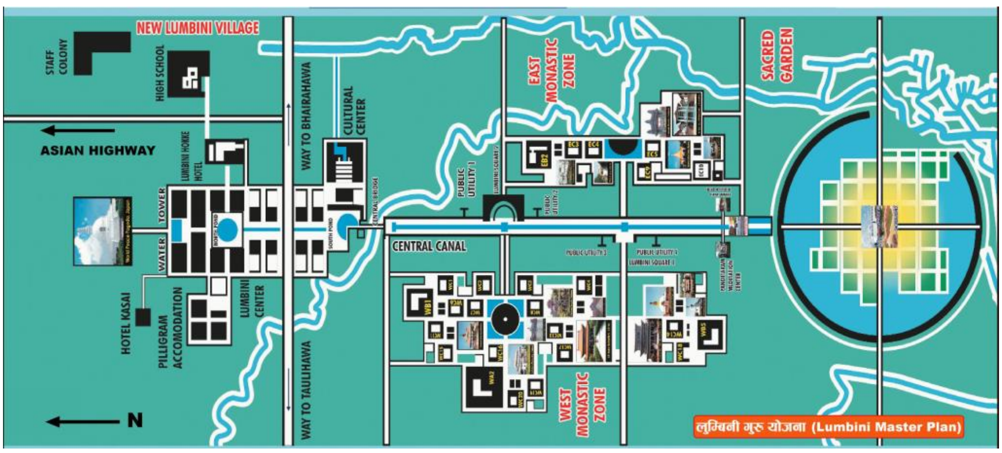

Figure 4. 1 Lumbini master plan
((LDT, n.d.)

Lumbini Sanskritik Municipality is one of the municipalities that is predicted to grow fast in the future due to the development potential of housing the world heritage site of Buddha's birthplace. Lumbini Sanskritik Municipality was founded by merging the existing Lumbini Adarsha Village Development Committee with six additional Village Development Committees, namely Bhagawanpur, Tenahawa, Ekala, Khudabazar, Madhuwani, and Masina.

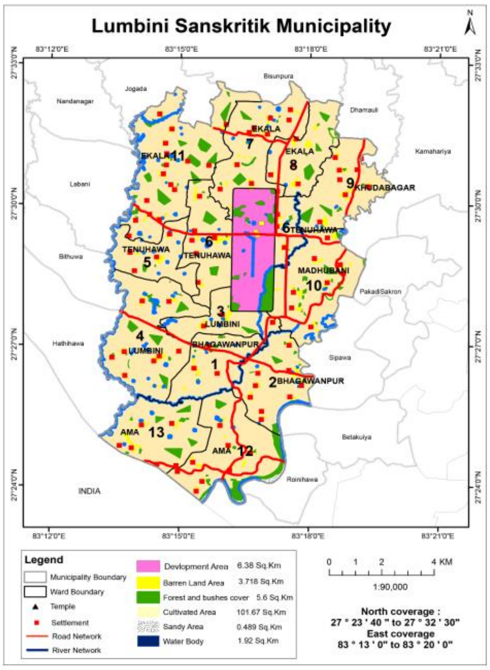

Figure 4. 2 Lumbini Sanskritik Municipality Map
(source: Lumbini Sanskritik Municipality)

The location is on the eastern edge of the sacred garden area. The roadway runs from Gate No. 5 to Mahilwar Chowk and goes to Lumbini's villages. The street near the Lumbini masterplan is made up of hotels and lodges with very few residences. The street width is 13.7m (45'), with a 2m (6.5') pedestrian sidewalk, while the surrounding buildings have 1 to 5 storeys. Because the average height of a one-story structure is 3.3m (10'-10”), the maximum height of a building on the street is 16.5m (54').

Figure 4. 3 Street view towards east

Figure 4. 5 street view towards south

Figure 4. 4 street view towards north

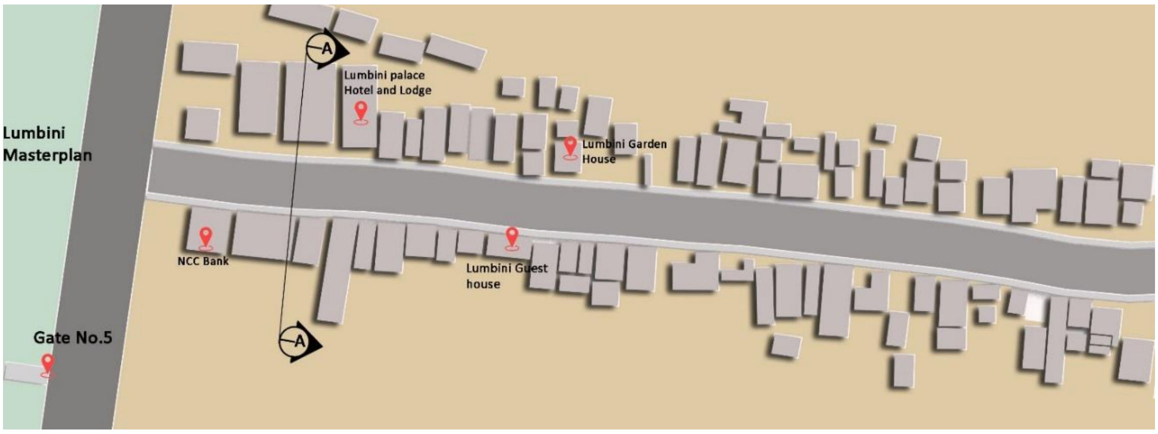

Figure 4. 6 Street map

The residential and commercial houses around that particular street was considered for aspect ratio calculation and further study. The section at A-A is taken from the building which is the tallest among the 100 m street section considered for this study.on the southern side of the road has two storey building of height around 6m which is the average height of building around that area.

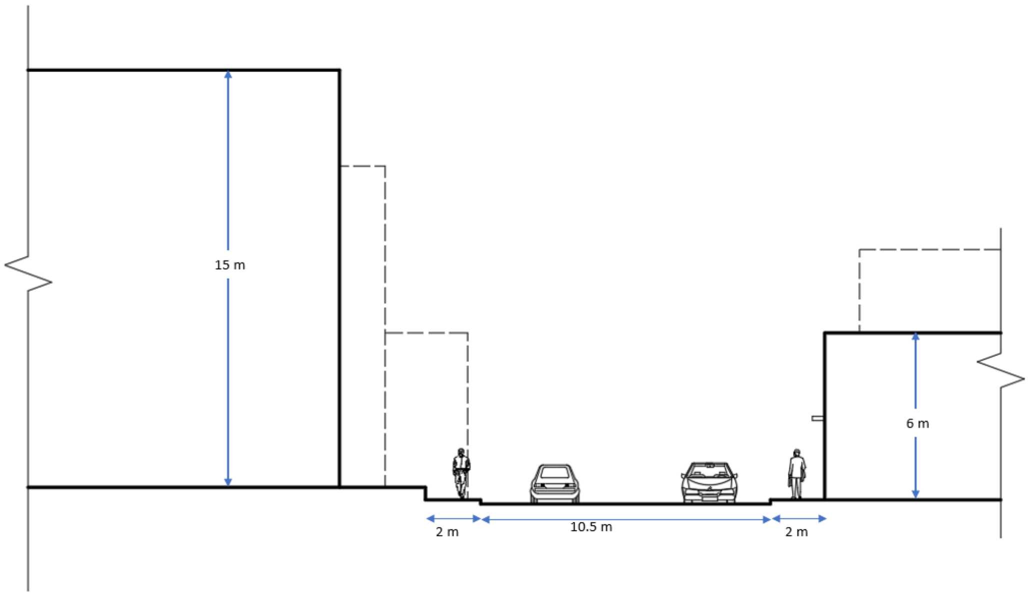

Figure 4. 7 Section at A-A

4.1.1. Aspect ratio Calculation

Storey	height of Building (in m)	Street width (m)	Pedestrian Walkway (m)	Aspect ratio
1	3.3	13.7	1.9	0.19
2	6.6	13.7	1.9	0.38
3	9.9	13.7	1.9	0.56
4	13.2	13.7	1.9	0.75
5	16.5	13.7	1.9	0.94

Table 4. 1 aspect ratio available in the street

The aspect ratio in the roadway is fairly low, and the canyon forms a shallow canyon. The shading on the street is determined by the aspect ratio. The greater the value of the aspect ratio, the more shade in the street. However, because the aspect ratio is low on this specific street, shading by the building is not conceivable if the aspect ratio is maintained as it is.

5. Chapter 5: Analysis and Findings

5.1 Climate Analysis of Lumbini

Climate data for the Lumbini region are acquired from a variety of sources. Secondary data sources included the Department of Hydrology and Meteorology (DOHM) in Nepal, as well as data from World Weather Online and Meteoblue, which are collected and analyzed. The Department of Hydrology and Meteorology does not have data for 2019 or 2020. Hence, data from 2010 to 2021, except 2019 and 2020, is utilized for climate analysis.

5.1.1. Data from Department of Hydrology and Meteorology

a) Temperature

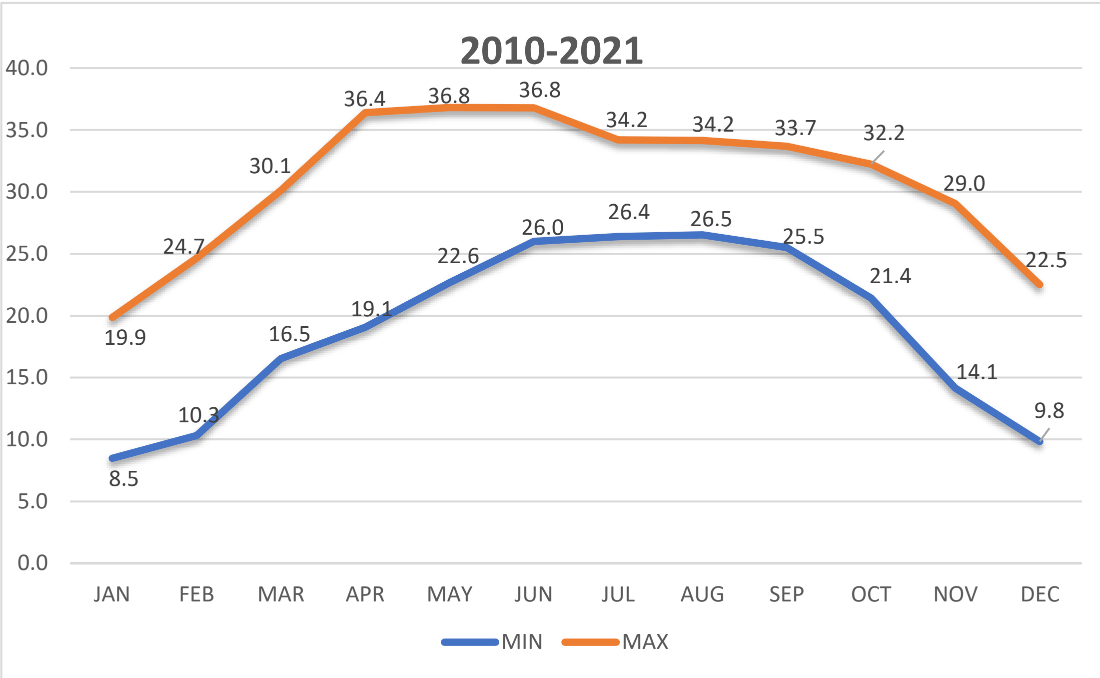

Chart 5. 1 Temperature from DOHM

The maximum average temperature of 10 years is 36.8°C in May and the minimum average temperature is 8.47°C in January. From March through October, the maximum temperature exceeds 30°C, and the lowest temperature exceeds 15°C. From November through February, the temperature falls below 15°C, while the maximum temperature rises beyond 20°C.

From March to October, the region has a hot climate since the temperature here exceeds 30°C. In June and May, the average maximum temperature is 36.8°C. In January, the average low temperature is 8.5°C. The appendix contains extensive temperature data for the last ten years.

b) Humidity

In January, the region's average maximum humidity is 91.47 percent, while in April, the average lowest humidity is 66.79 percent. The appendix contains humidity data for the last ten years.

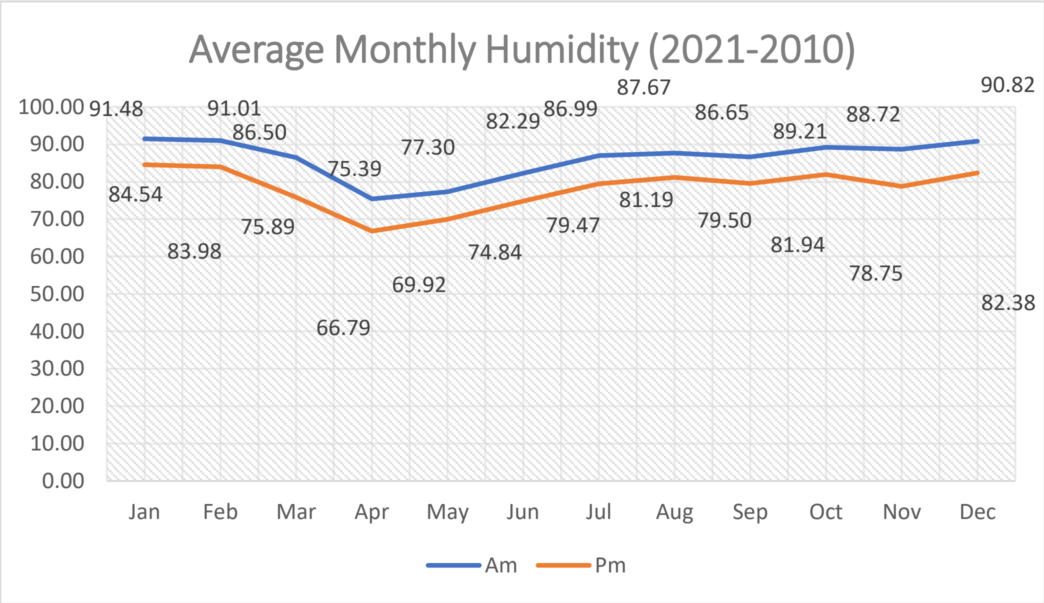

Chart 5. 2 Humidity data from DOHM

c) Rainfall

The region has rainfall above 80mm from May through September. During July, the average maximum rainfall is 379.3mm which is the highest. In November, there is no rain. The appendix contains rainfall data for the last ten years.

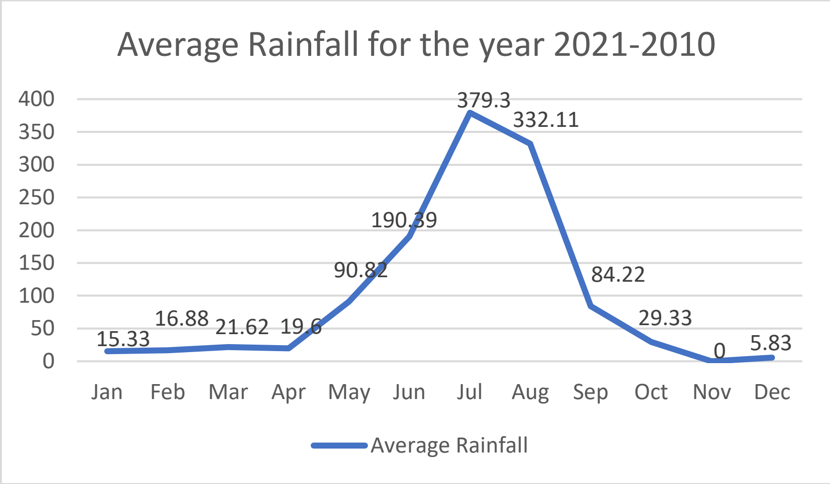

Chart 5. 3 Rainfall data from DOHM

5.1.2. Data from World Weather Online

a) Temperature

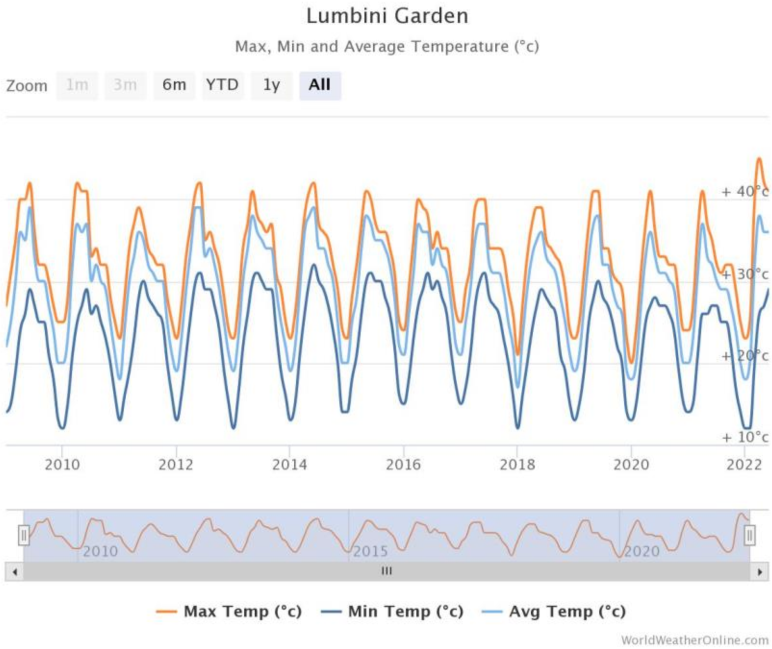

Chart 5. 4 Temperature data from World weather Online

According to the graph, the highest temperature exceeds 40°C. Throughout the year, the average temperature ranges from 39°C to 19°C. Throughout the 10 years, the average temperature did not go below 10°C.

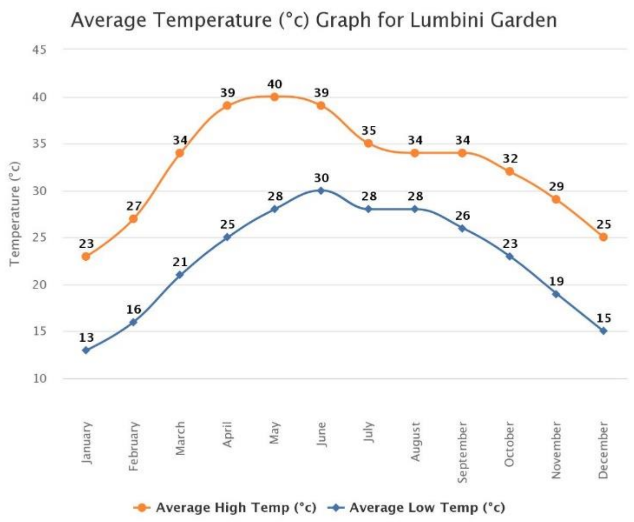

Chart 5. 5 Monthly Average Temperature data from World weather Online

The graph indicates that the hot climate in the Lumbini region begins in March and lasts until October. May had the highest average maximum temperature of 40°C. In January, the lowest average temperature is 13°C. It indicates that temperatures in the region exceed 20 degrees Celsius for nearly eight months, from March to October. Throughout the year, the temperature does not fall below 10°C.

b) Rainfall

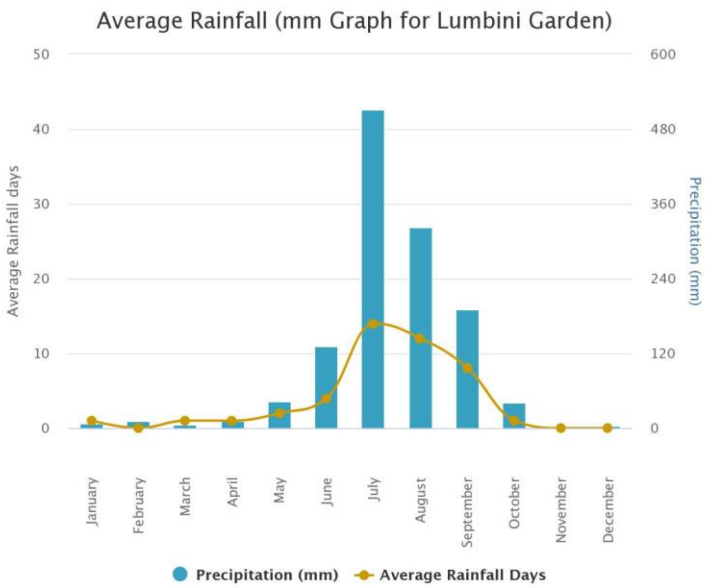

Chart 5. 6 Monthly Average Rainfall data from World weather Online

The chart indicates that the region receives more than 480mm of rain in July. From June through October, the area receives more than 10mm of rain. From November through March, there is no or very little rain.

c) Wind Speed

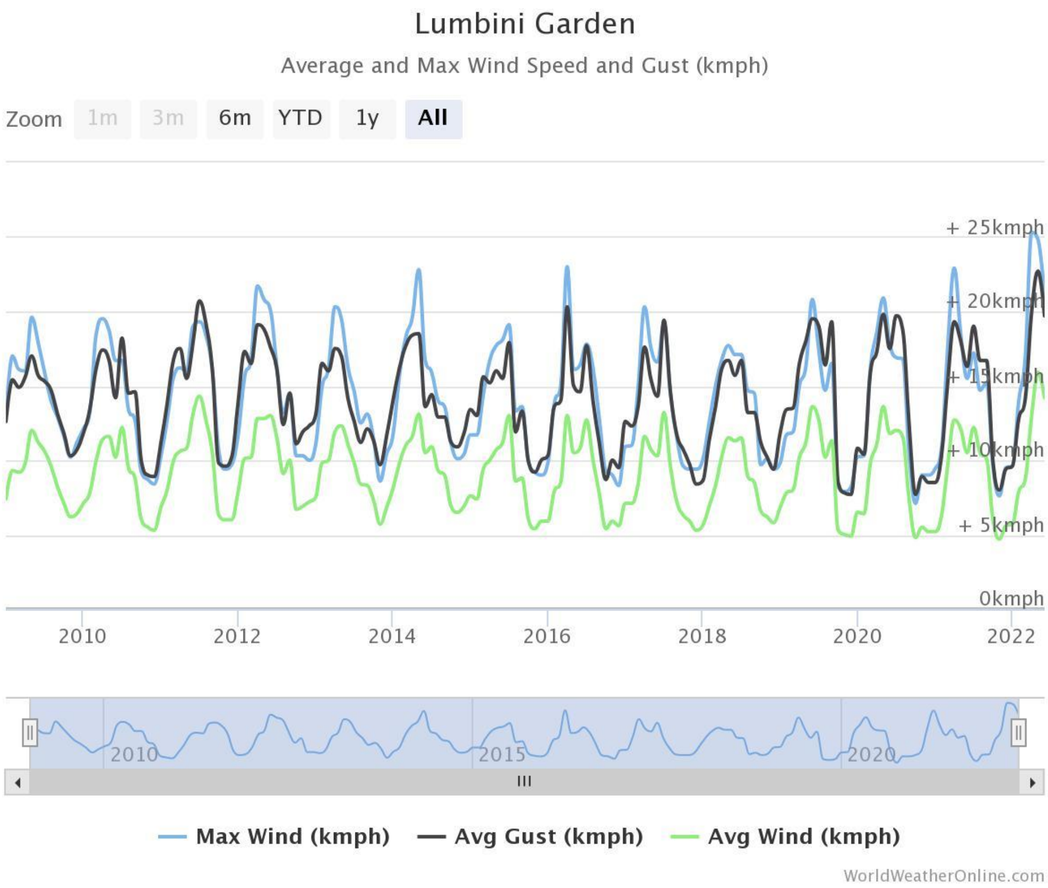

Chart 5. 7 Wind speed data from World weather Online

Maximum wind speeds in the area exceed 20 kilometers per hour. The average wind speed is between 15 and 5 kilometers per hour. The greatest average gust speed is greater than 15kmph.

d) Humidity and cloud

The region's average humidity level surpasses 70%. The humidity is high from July to September and low from March to May.

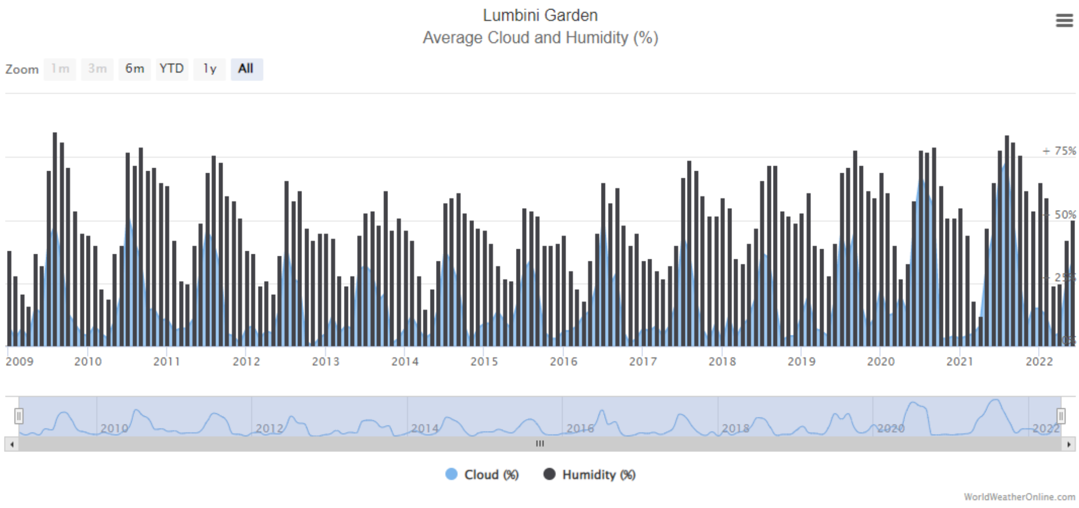

Chart 5. 8 Humidity data from World weather Online

e) Sun hours and sunny days

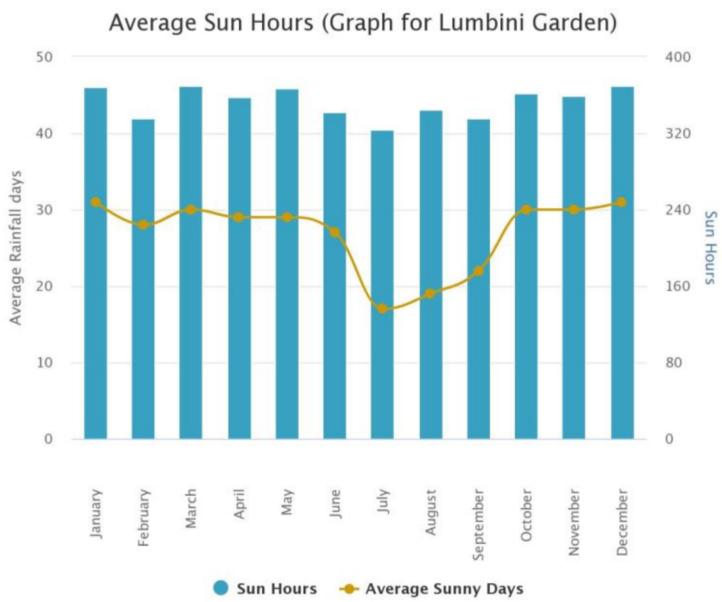

Chart 5. 9 Monthly Average sun hours and sunny days data from World weather Online

Every month of the year, the sun shines for more than 320 hours. The average number of bright days is more than 240 hours from November to March and less than 160 hours in July and August.

5.1.3. Data from Meteoblue Weather

a) Temperature

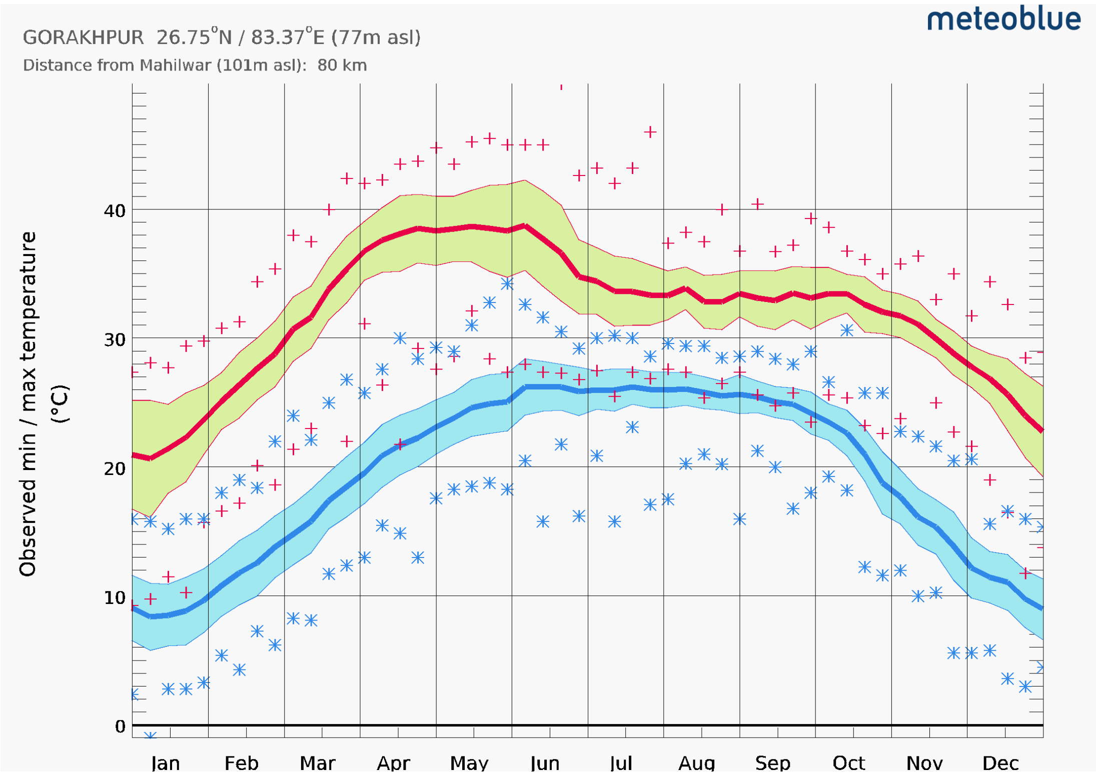

Chart 5. 10 Monthly Average Temperature data from Meteoblue weather

From late February to early November, the weather is scorching. From April through June, the temperature approaches 40°C. During these months, the temperature fluctuates from 20°C to 40°C. Temperatures vary from 35°C to 25°C from July to October. In January and December, the temperature drops below 10°C on some days. This region's climate is generally hot.

b) Windspeed

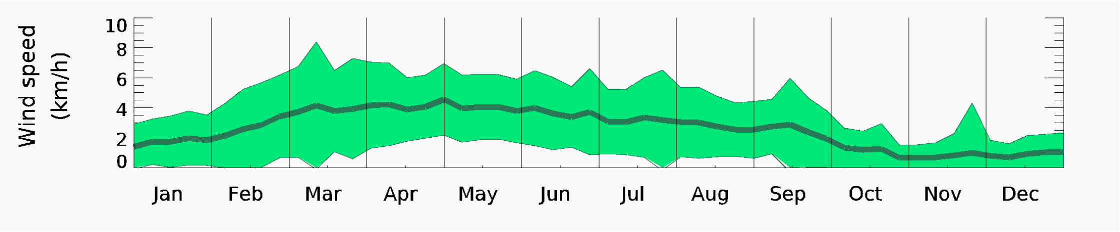

Chart 5. 11 Monthly Average Temperature data from Meteoblue weather

The average wind speed is between 2kmph to 4kmph throughout the year.

The climate in the Lumbini region is hot, with temperatures above 20°C for eight months of the year, according to all three meteorological data sets. May through July are the warmest months, and January and December are the coldest, with temperatures seldom falling below 10°C. Throughout the year, the sunlight hour exceeds 320 hours and the average humidity is greater than 70%. In July, the region receives more than 480mm of rain, however in June, there is nil or little rain between November through March.

5.2. Questionnaire survey

The questionnaire survey was conducted over the course of two days in June (June 16 and 17). A total of thirty-two samples were obtained where all of the respondents were pedestrians, with thirteen samples collected in the morning (6-7), five samples collected between 9 am and 10 am, eleven samples collected between 2 pm and 3 pm, and three samples collected after 6 pm. The first of two days was partially overcast, while the second was sunny.

When asked how they felt at that very moment, those who responded in the morning felt cool, slightly cool, neutral, and slightly warm, whereas those who responded after 9 a.m. felt neutral, slightly warm, and hot. In replies received in the afternoon, 6 were for hot, 4 were for warm, and 1 was for somewhat warm. After 6 p.m., respondents reported feeling slightly cool.

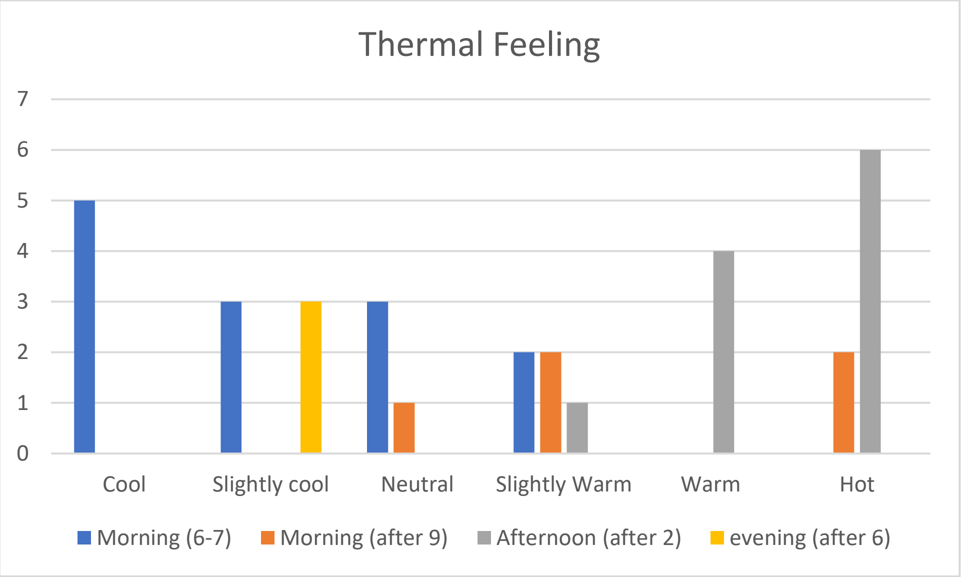

Chart 5. 12 Thermal feeling survey data

The respondents perceived an acceptable temperature environment in the morning and evening, while after 9 a.m., the acceptance range was greater than the non-acceptance range, and after 2 p.m., it was opposite. Six respondents found the temperature environment intolerable.

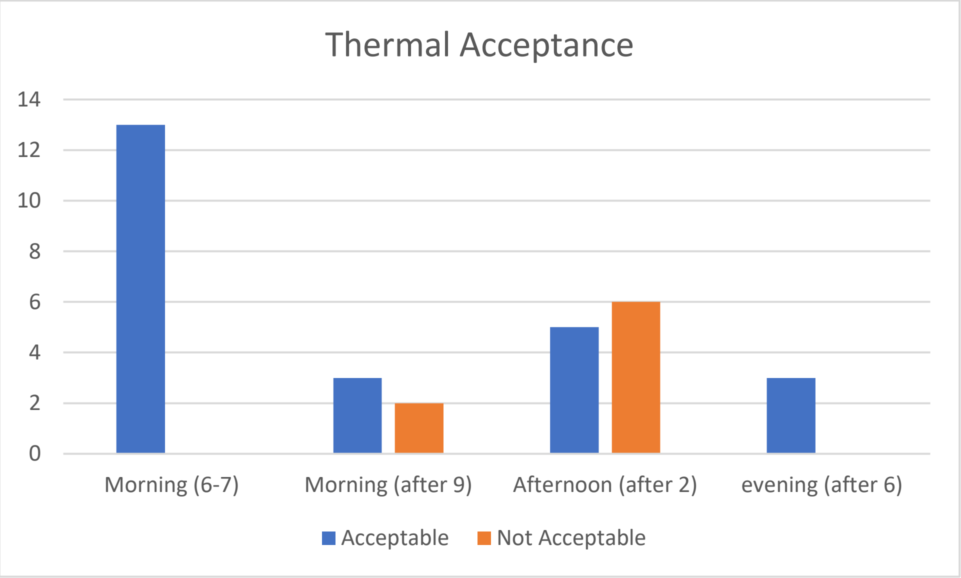

Chart 5. 13 Thermal Acceptance survey data

Few individuals find Lumbini's thermal condition to be comfortable. The majority of the respondents' responses were unpleasant. There were just a few persons who felt completely at ease.

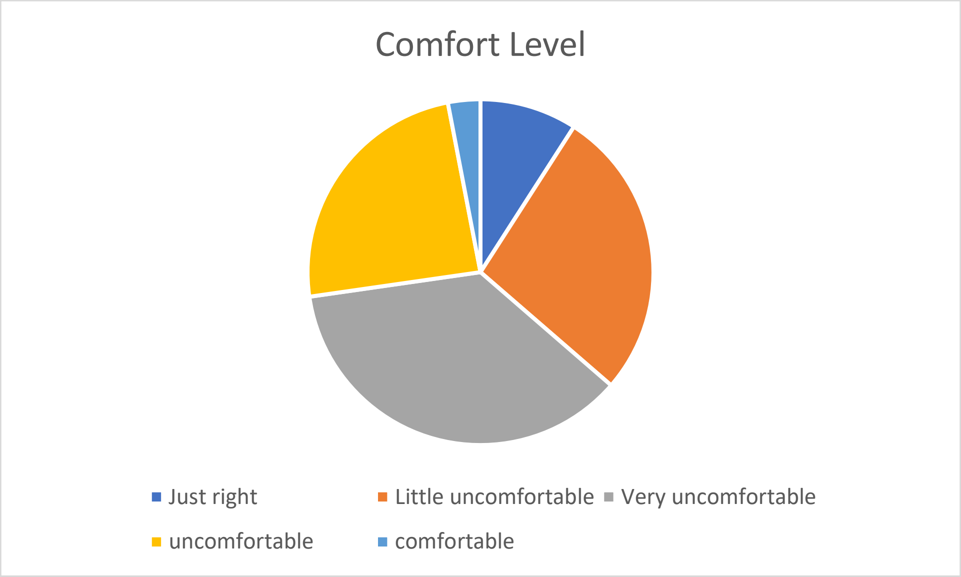

Chart 5. 14 Comfort level survey data

Only four respondents said their outside stay was unaffected by the temperature outside, while 27 said the temperature interfered with their outdoor visit. They like to spend their time outside in the evening or the morning.

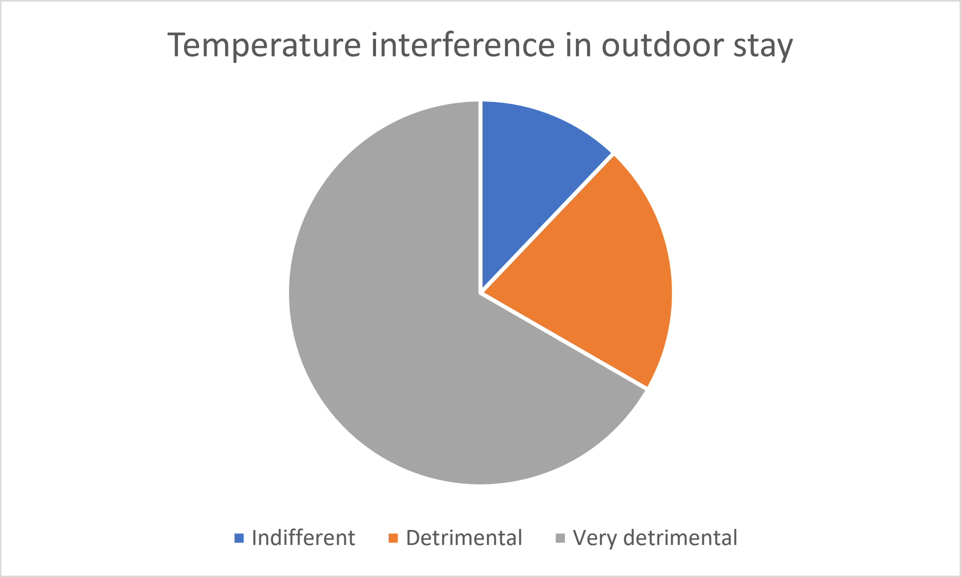

Chart 5. 15 Temperature Interference in Outdoor stay survey data

Respondents did not want to go outside in the afternoon. The majority of them prefer to walk outside in the morning, but there was also a positive reaction in the evening.

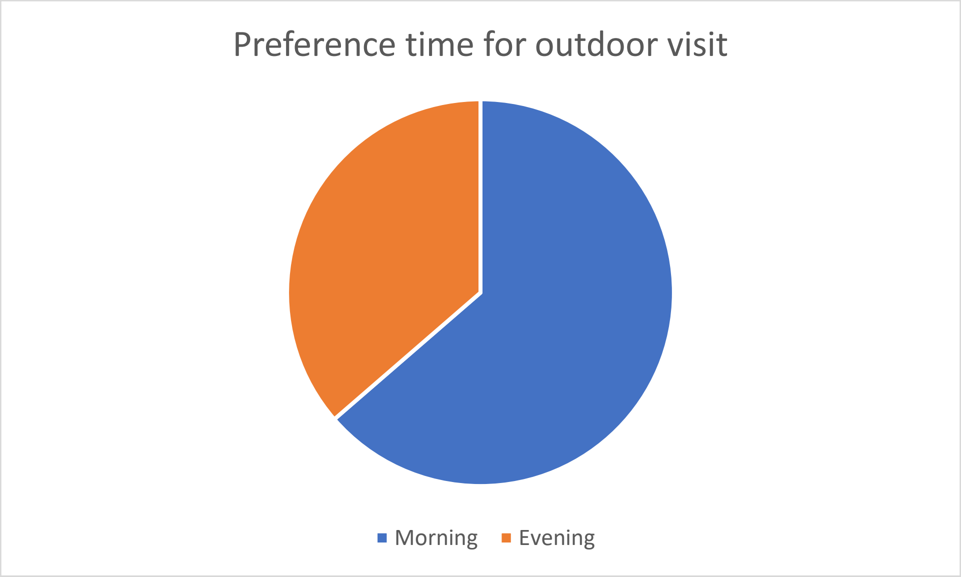

Chart 5. 16 Preference time for outdoor visit survey data

According to the respondents, the warmest months are Baisakh and Jestha. They have a scorching environment for over 5 months, beginning with Baisakh. Poush and Magh are the coldest months, with temperatures remaining mild for five months beginning with Kartik. The findings for Chaitra were divided; respondents reported a warm to somewhat cold thermal climate.

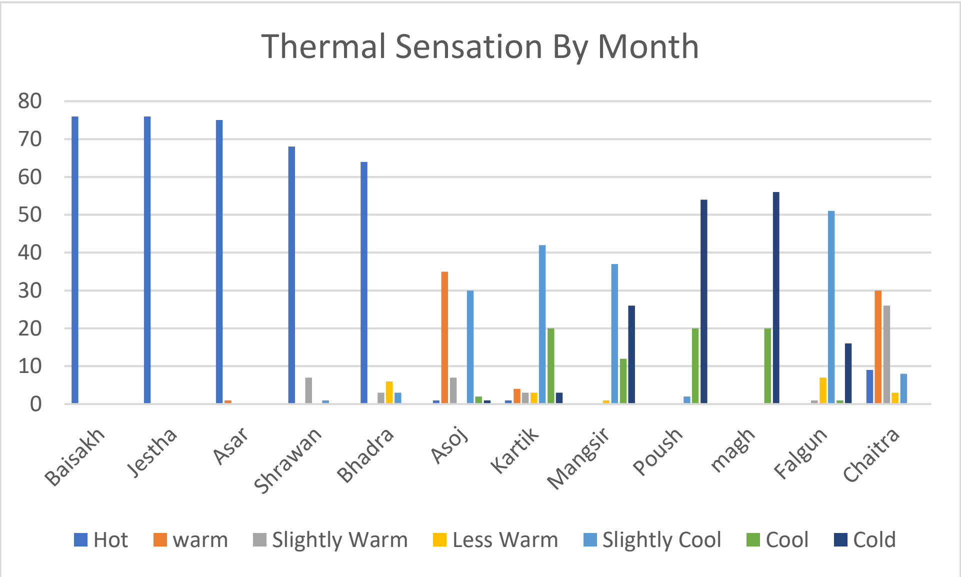

Chart 5. 17 Thermal sensation by month survey data

5.3. Simulation

5.3.1. Simulation scenarios on basis of Aspect Ratio

There are nine scenarios developed in all to establish the optimal aspect ratio for Nepal's hot and humid climate. The aspect ratio of the streets is increased from 1 to 3 in two directions regarding the streets. Although the base case or actual orientation of the selected street is east and west, the best aspect ratio is determined for the north south oriented street for general usage of aspect ratio in future design and planning.

Scenario Name	Aspect ratio	Orientation of street
Base case	0.19-0.96	East -West
AR1 (a)	1	East -West
AR1.5 (a)	1.5	East -West
AR2 (a)	2	East -West
AR3 (a)	3	East -West
AR1(b)	1	North- South
AR1.5 (b)	1.5	North- South
AR2 (b)	2	North- South
AR3 (b)	3	North- South

Table 5. 1 Simulation scenarios

5.3.2. Sensitivity Analysis on basis of Orientation

With an interval of 10° counterclockwise, the optimal aspect ratio is simulated in several orientations. By turning the model 180 degrees counterclockwise while maintaining the same aspect ratio of 1.5, a total of eighteen scenarios were created.

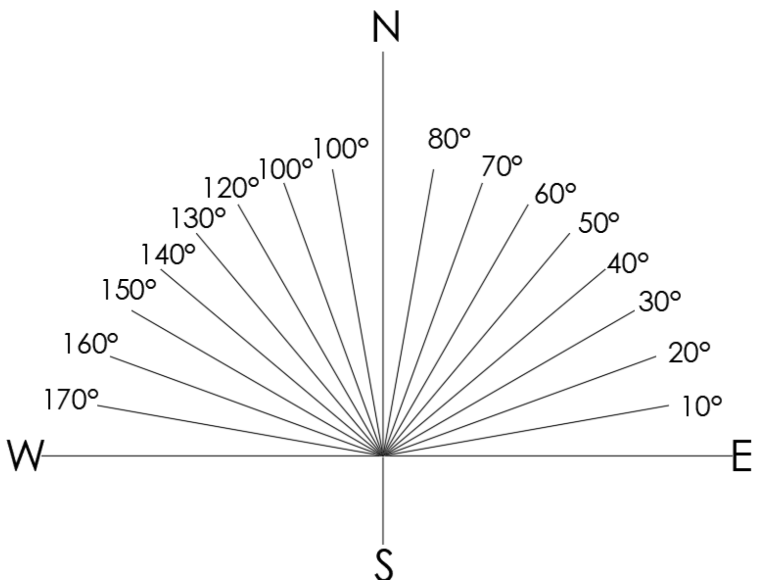

Figure 5. 1 scenario on the basis of orientation

The street layout was firstly simulated in 0/180 degrees and 90/270 degrees. The remaining angles were calculated to cover all four quadrants of angular distribution, meaning, each angle is supplemented with another of 180-degree angle. So, by covering 180 degrees of angles we can cover the remaining 180 degrees at the same time. So, keeping that in mind, 18 simulation scenarios were introduced to analyze the best street orientation for the site area.

5.3.3. Simulation Settings

The simulation process is carried out in Envi-met 5.3 Software Student version. The simulation setting is same for all the scenarios.

a) **Simulation Materials**

The model is a block model of the location. The road is asphalt, while the pedestrian walkway is concrete gray block pavement. The building' s walls are made of burned brick, while the roofs are made of concrete. In order to simulate the model as a real case scenario, the materials of the involved objects are taken as same as that in the field.

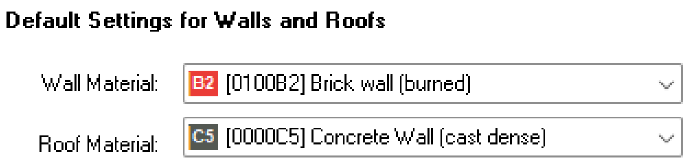

Figure 5. 2 Default settings for walls and roofs

a) Simulation Date

The 24th of June was chosen as the simulation date since it had the greatest temperature measured during the field visit. The simulation lasted 13 hours, beginning at 6:00 a.m. and ending at 18:00 p.m. The following are the day's statistics:

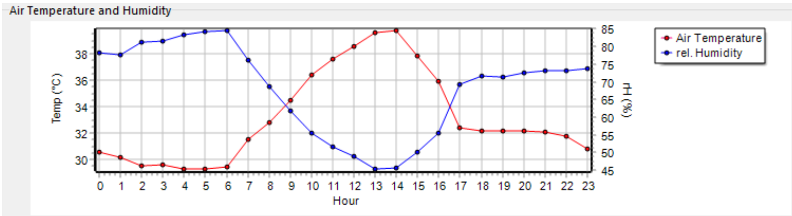

Manually adjust values

Time	T	rH
00:00	30.52	78.39
01:00	30.14	77.68
02:00	29.55	81.16
03:00	29.59	81.46
04:00	29.27	83.46
05:00	29.29	84.36
06:00	29.45	84.55
07:00	31.50	76.08
08:00	32.77	68.75
09:00	34.51	61.68
10:00	36.38	55.62
11:00	37.62	51.66
12:00	38.60	48.77
13:00	39.60	45.28
14:00	39.79	45.47
15:00	37.86	50.18
16:00	35.94	55.47
17:00	32.43	69.21
18:00	32.15	71.56
19:00	32.16	71.49
20:00	32.13	72.63
21:00	32.06	73.02
22:00	31.77	73.20
23:00	30.83	73.73

Figure 5. 3 Temperature and humidity data for simulation

Historically, June 24th is one of the hottest days in the case of Lumbini Sanskritik Municipality. The minimum temperature recorded was 27°C in 2021. The temperature was above 41°C for four years. This indicates that the temperature is mostly high during the 24th June according to the history of 14 years.

Lumbini Garden

Historical Weather on 24th June over the years

Year	Weather	Max	Min	Wind	Rain	Humidity	Cloud	Pressure
2009		41 °c	32 °c	16 km/h E	0.2 mm	39%	17%	1000 mb
2010		41 °c	29 °c	11 km/h ESE	2.4 mm	53%	29%	999 mb
2011		37 °c	31 °c	14 km/h ESE	7.8 mm	54%	31%	998 mb
2012		33 °c	28 °c	14 km/h ENE	45.4 mm	68%	41%	997 mb
2013		40 °c	32 °c	7 km/h SE	2.0 mm	42%	28%	999 mb
2014		41 °c	32 °c	11 km/h SSE	0.0 mm	33%	20%	997 mb
2015		40 °c	31 °c	8 km/h WSW	3.2 mm	41%	23%	998 mb
2016		36 °c	30 °c	8 km/h ESE	4.8 mm	56%	44%	1002 mb
2017		40 °c	32 °c	9 km/h ESE	0.4 mm	42%	17%	1000 mb
2018		41 °c	30 °c	9 km/h ESE	4.9 mm	49%	21%	999 mb
2019		39 °c	30 °c	11 km/h ESE	3.8 mm	47%	30%	1004 mb
2020		36 °c	28 °c	17 km/h E	11.1 mm	64%	61%	1004 mb
2021		33 °c	27 °c	11 km/h ESE	6.0 mm	75%	65%	1000 mb
2022		39 °c	30 °c	16 km/h E	0.6 mm	53%	54%	999 mb

Figure 5. 4 meteorological data history for 24th June

b) Wind setting for simulation

The wind considered was light breeze of 2 m/s from the North west direction.

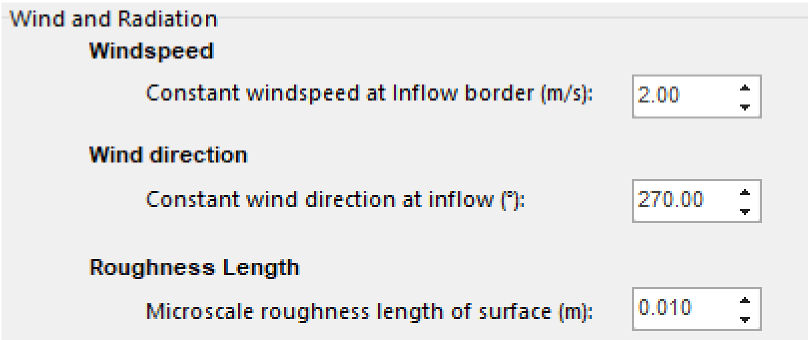

Figure 5. 5 Wind setting for simulation

c) PET calculation

A 35-year-old guy with a height of 1.75m and a weight of 75 kg was assumed for PET calculations. The clothing insulation is 0.4 (shorts and t-shirts), and the work metabolism is 80W since the guy is supposed to be walking.

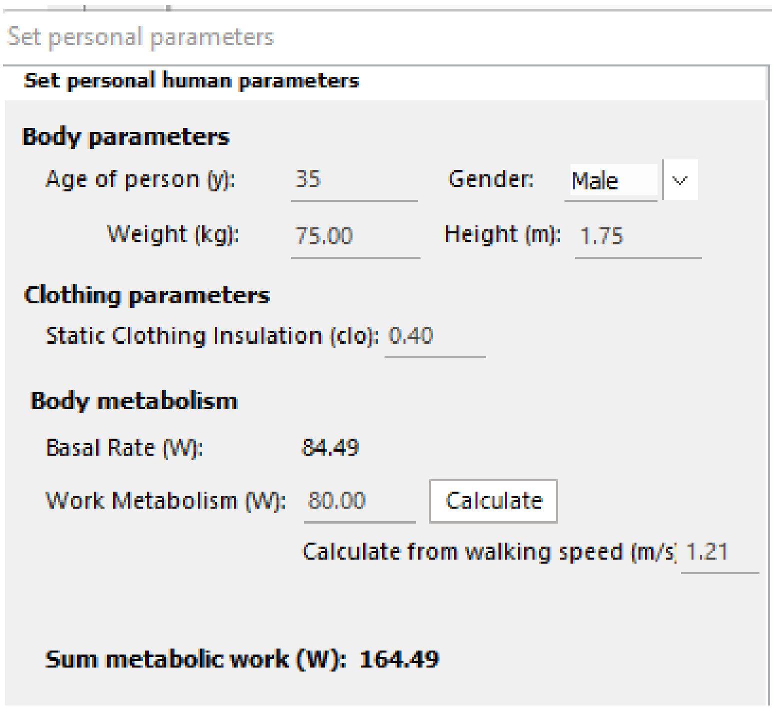

Figure 5. 6 Setting for PET calculation

5.3.4. Software User Interface

a. ENVI-met Headquarters

Figure 5. 7 envi-met headquarter interface

This is the first user interface that the users get once you start the software. This part of GUI, allows the user to reach multiple cores of the software for different parts of the simulation such as ENVI-core, BIO-met, Leonardo, etc.

b. Data and Settings

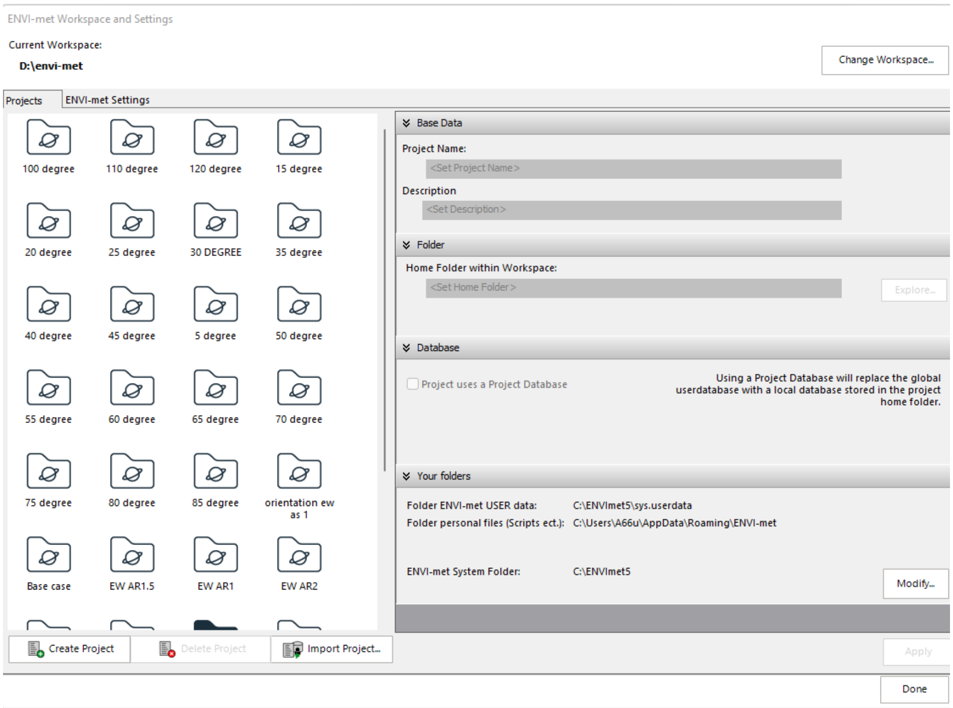

Figure 5. 8 data and setting interface

After, clicking the Data and settings in the ENVI-met headquarters interface, we reaching this screen where we create a project for the start of our simulation. We enter the project details and start.

c. Spaces

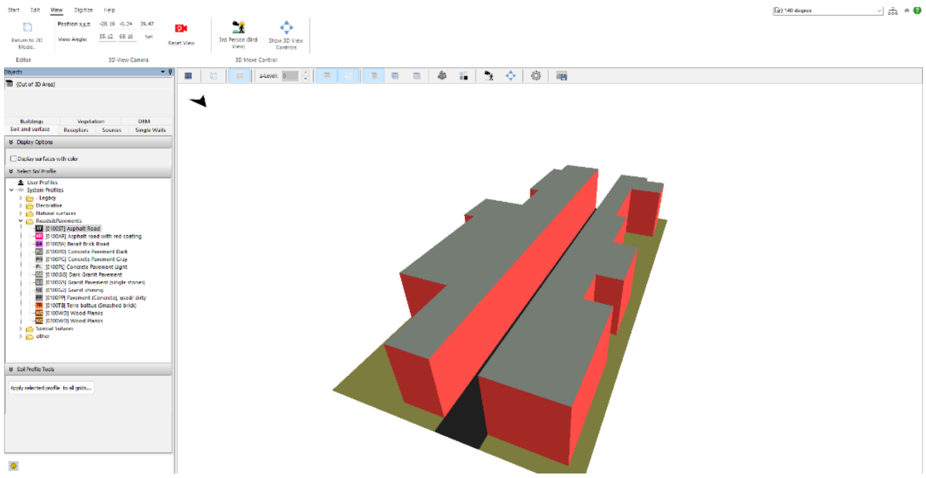

Figure 5. 9 envi-met spaces interface

Here, we start our 3D modelling process of the real case scenario. We acquire the simulation weather data through geolocation and if necessary, assign vegetations and building materials according to need.

d. ENVI-guide

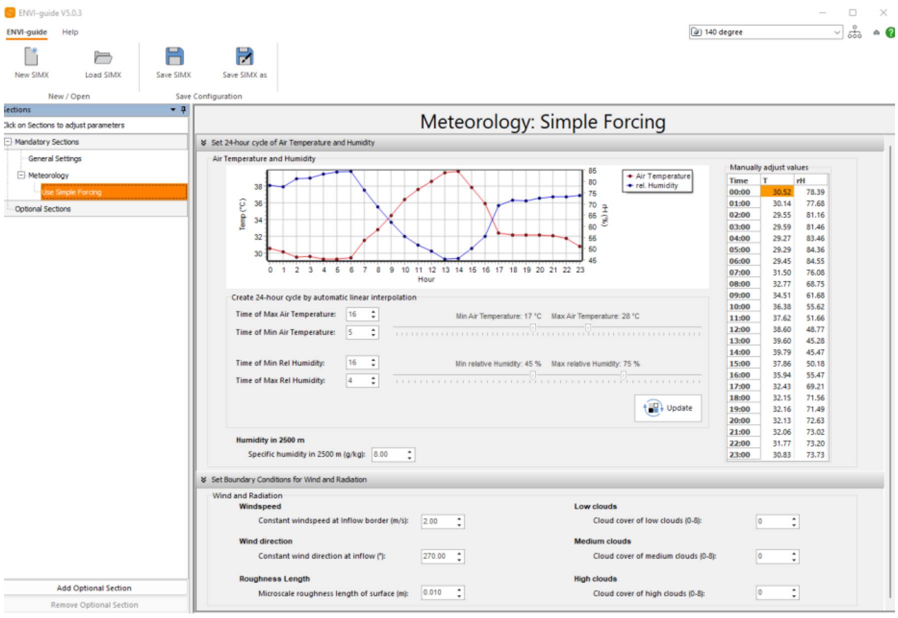

Figure 5. 10 envi-guide interface

Here, we enter the weather data as measured in the field in the form of temperature, wind, humidity and also set the time of simulation as required by the user.

e. ENVI-core

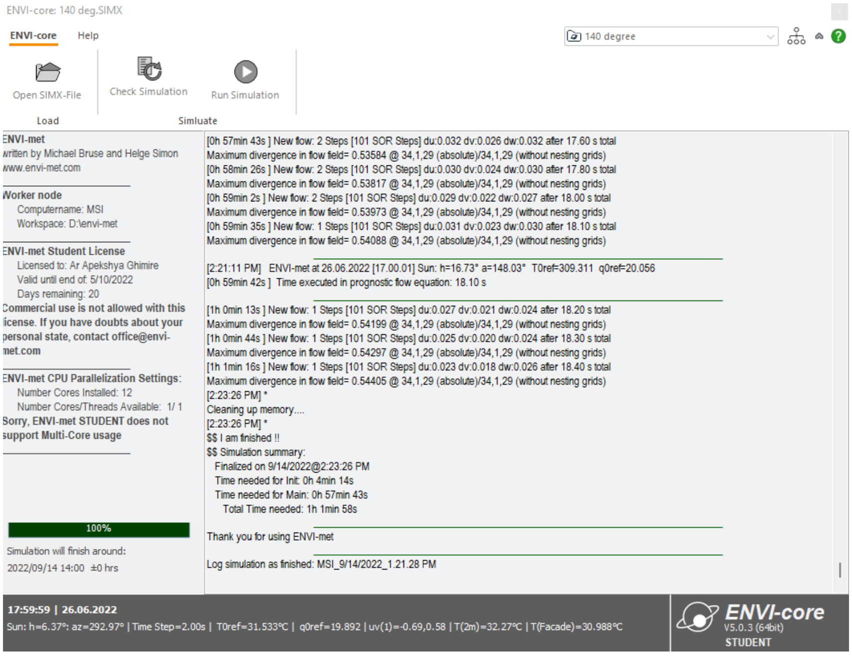

Figure 5. 11 envi-core interface

In this interface, we start the simulation process the file exported from the ENVI-guide. We can also check the simulation progress reports along with any errors faced during the simulation.

f. Leonardo

Figure 5. 12 Leonardo interface

This is the final interface where we obtain the results of the simulation in the form of 2D graphs. The results are presented in a multicolor chart with appropriate legends beside it. Also, we can simulate the 3D results in the form of animation if required. The main function of Leonardo is to interpret the obtain results from simulation.

5.4. Base Model

The base model is the exact replication of the selected site. However, due to the constraints of software only 100 m street section has been selected for the simulation process. The aspect ratio of the building is maintained as it is. The aspect ratio is different for different sections throughout the road and varies from 0.1 to 0.9.

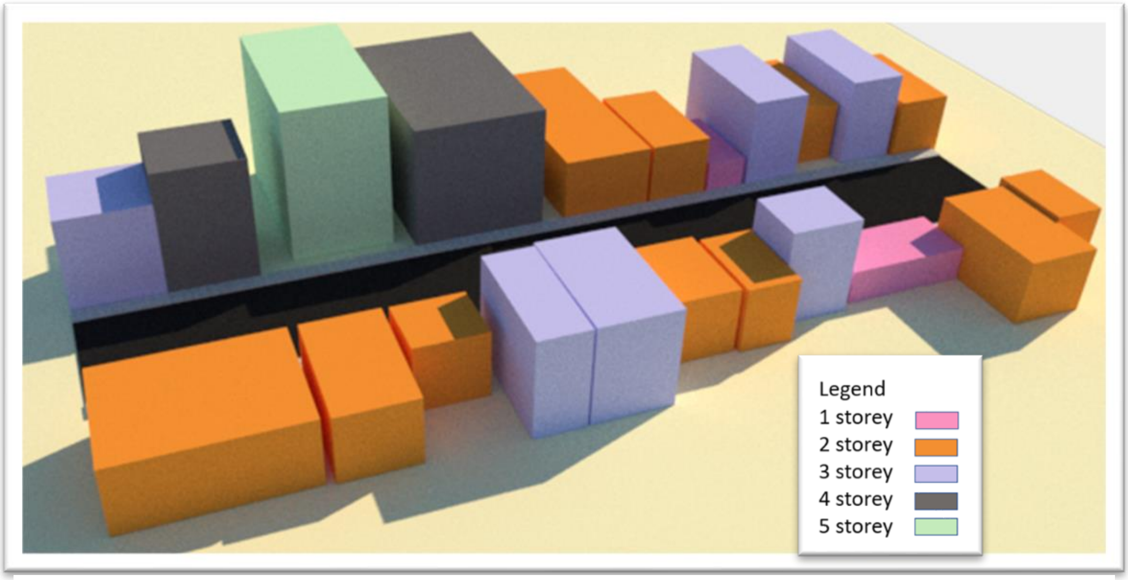

Figure 5. 13 base model representation for storey

The figure 22 shows the base case scenario with difference in height of the building indicated by different colors. The building height varies from 3.3 m to 16.5 m. The section below shows the width of the street and height of the building in the base case scenario. The aspect ratio is different for each building in the case of base case.

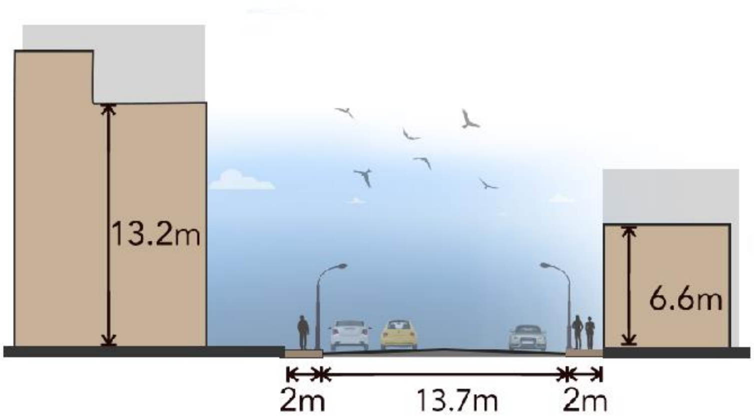

Figure 5. 14 section of the base case

The figure 24 is the 3d model designed in Envi-met software. The red color of the wall represents the burnt brick wall that was chosen for simulation and the grey color of the ceiling is representation of material concrete.

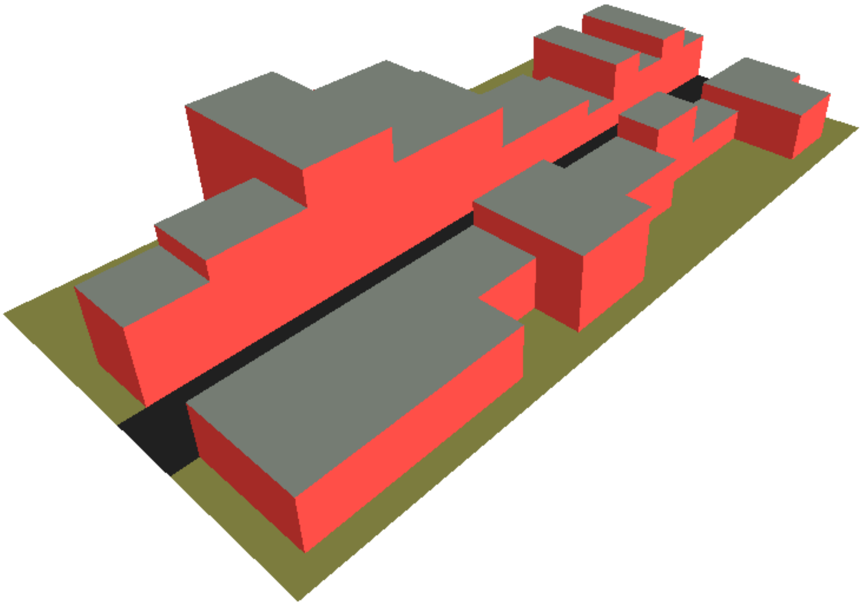

Figure 5. 15 base model designed in Envi-met

5.4.1. Solar analysis of the base model

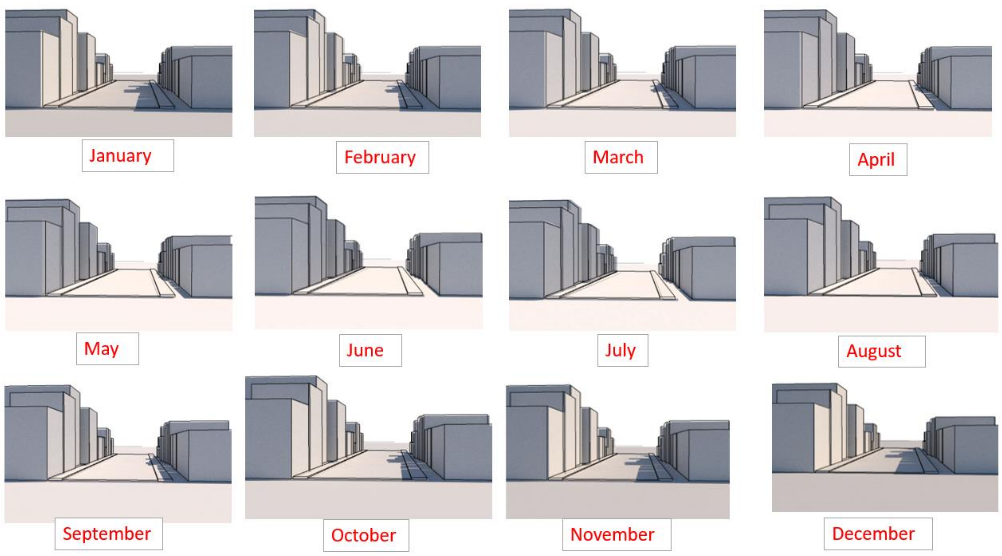

Figure 5. 16 Shadow condition on 24th of each month

The figure 21 depicts the site's shadow status on the 24th of each month. Because the sun angle is normally low throughout the winter, the southern side of the road is entirely shaded from October to February. During the summer, from March to August, the sun angle is high and the streets aren't shadowed at all by buildings. Due to the high temperatures, a shaded street is an essential component of that location in order to provide a comfortable pedestrian route and to encourage walkability.

Figure 22 displays the shadow situation of the location from 6 a.m. to 6 p.m. on June 24th. The northern side of the road appears to be shaded for 3-4 hours in the morning, yet the streets are open to direct sun radiation during the daylight when necessary. Thus, it shows that some intervention is required at the location to prevent direct sun radiation and create pedestrian thermal comfort.

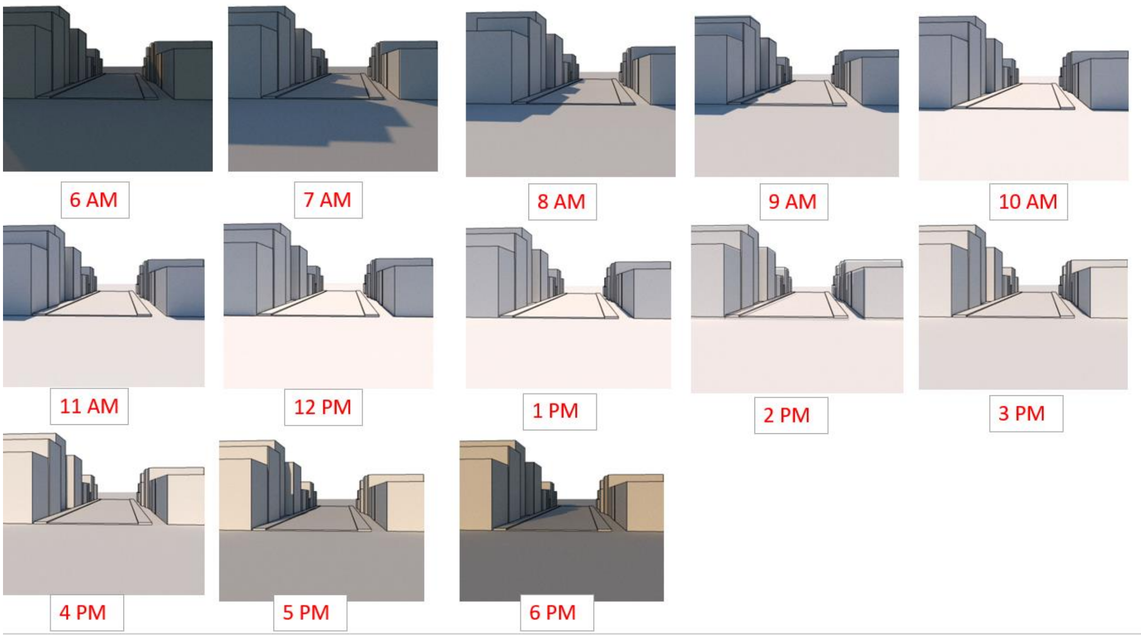

Figure 5. 17 Shadow condition of 24th June for 12 hours

According to solar analysis, the streets of the Lumbini Sanskritik Municipality are exposed to direct solar radiation throughout the day during the summer months. During the winter, the southern section of the streets is shaded by the buildings. The direct sun radiation that strikes the street has made it hard for people to travel during the day.

5.4.2. Simulation Results

The simulation was run with the above-mentioned variables, and the software detected the probable air temperature surrounding the building and in the streets at 1.5 m above ground.

a) Ambient Air Temperature

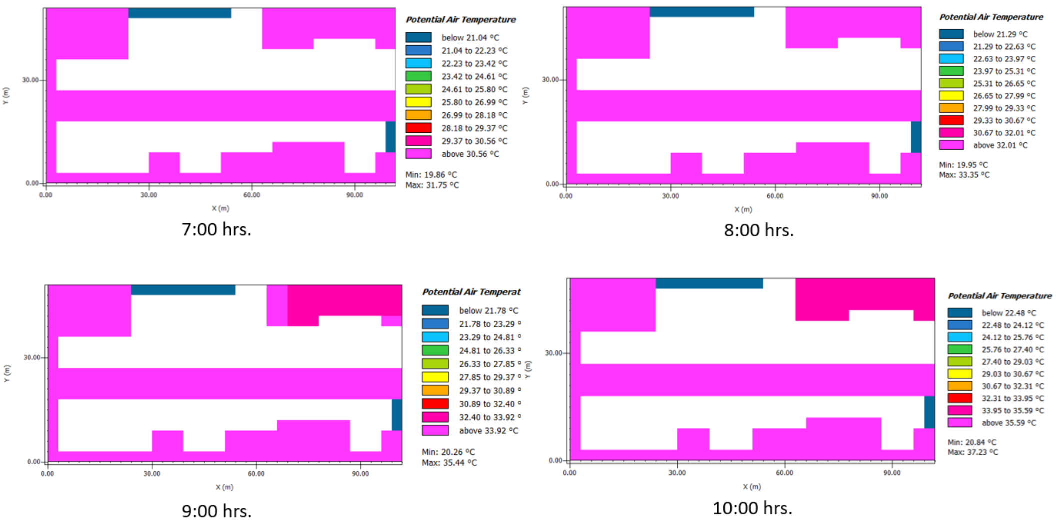

Figure 5. 18 Potential Air Temperature from 7:00 hrs. to 10:00 hrs. at 1.5m above ground level

The figure shows that the temperature is lower than 31.75 °C at 7:00 hrs but increases slowly by at least 2°C in every two hours. At 10:00 hrs, the temperature is around 37.23°C from 35.44°C at 9:00 hrs. The temperature is quite high for the morning time.

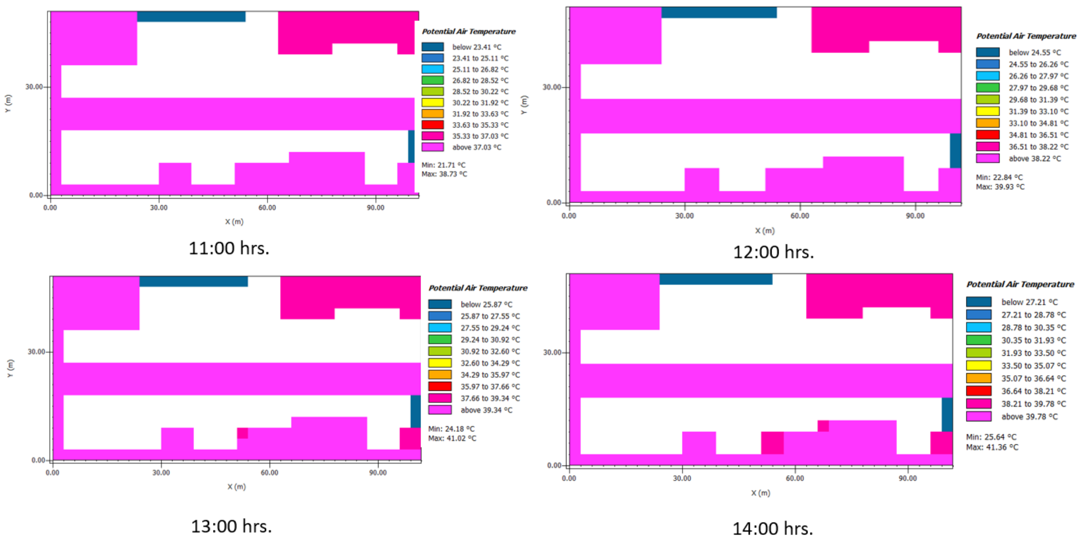

Figure 5. 19 Potential Air Temperature from 11:00 hrs. to 14:00 hrs. at 1.5m above ground level

The temperature is rising at least a degree Celsius from 11:00 hrs. The temperature reached 38.73°C at 11:00 hours and reaches 39.93°C at 12:00 hours. The temperature rises up to 41.02°C at 13:00 hrs and 41.36°C at 14:00 hrs. The temperature is maximum during this time period.

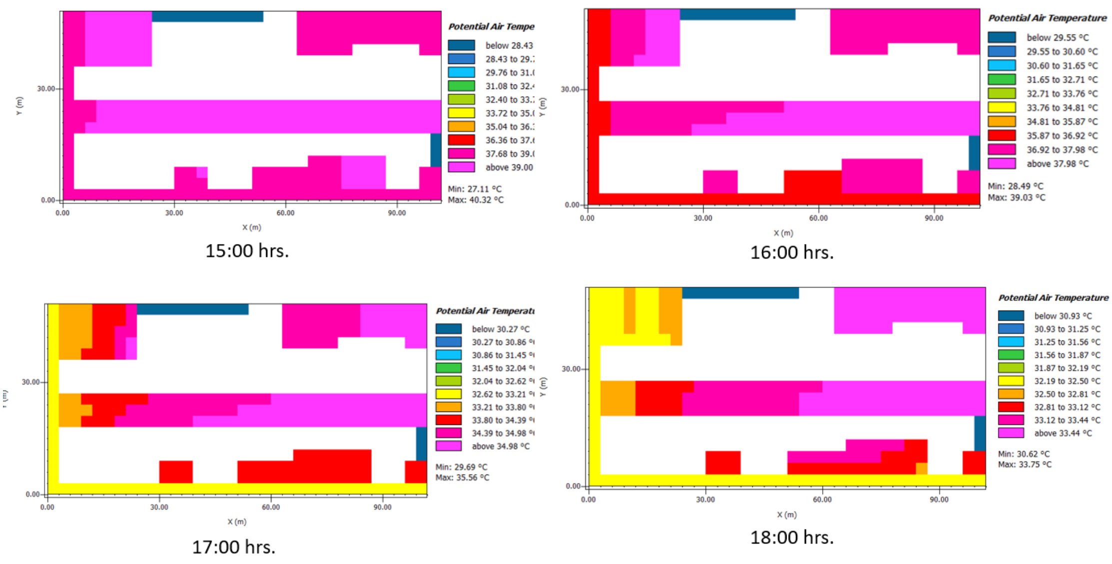

Figure 5. 20 Potential Air Temperature from 15:00 hrs. to 18:00 hrs. at 1.5m above ground level

The temperature begins to fall from the western end of the street at 15:00 hrs. the maximum temperature is 40.32 °C at 15:00 hrs and gradually decrease to 39.03 °C on next hour. The graph shows the change in temperature from the western side of the street. The temperature drops down to 33.75 °C at 18:00 hrs.

The graph illustrates that the temperature peaks around 14:00 hours and then drops to roughly 40 °C the following hour. From 9:00 a.m. until 17:00 p.m., the temperature rises over 35 °C. According to this graph, the streets are a little more pleasant in the morning between 7:00 to 9:00 a.m. and after 17:00 p.m. The street is too hot for pedestrians to walk all day.

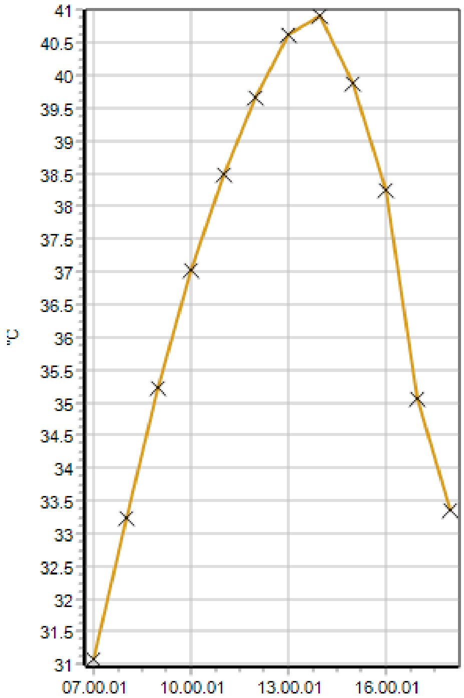

Graph 5. 1 Potential air temperature predicted by Envi-met

b) Mean Radiant temperature

The mean radiant temperature rises sharply after 8:00 hours and reaches 70.9 °C by 14:00 hours. At 17:00 hours, the temperature drops to 34.3 °C. This table also illustrates that the streets are thermally uncomfortable for pedestrians.

Time	Mean Radiant Temperature (°C)
07.00.01	29.215
08.00.01	55.344
09.00.01	58.992
10.00.01	60.26
11.00.01	61.021
12.00.01	64.469
13.00.01	68.842
14.00.01	70.912

15.00.01	68.776
16.00.01	62.841
17.00.01	34.309
17.59.59	26.587

Table 5. 2 Mean Radiant temperature predicted by Envi-met

c) PET calculation

The temperature is very high after 8:00 hours since the PET temperature is above 43 °C. The PET temperature drops only after 17:00 hours. This means the streets are extremely hot throughout the day.

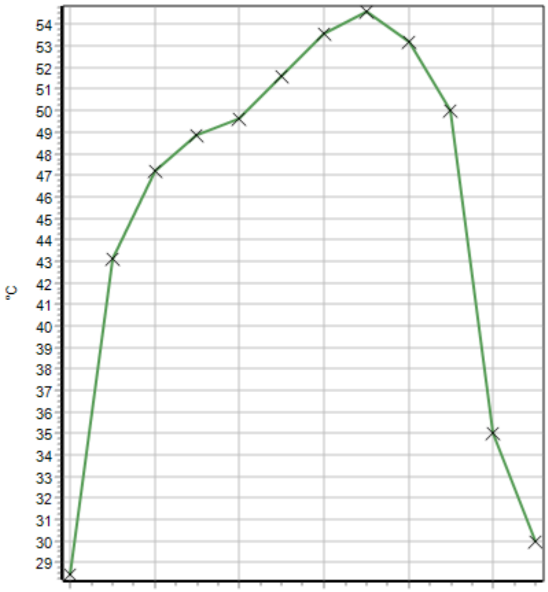

Graph 5. 2 PET temperature predicted by Envi-met

d) UTCI calculation

The temperature starts to rise right after 7:00 hours and reach to the peak 49.5 °C at 14:00 hours. After 15:00 hours the temperature drops gradually and reach to 32.9°C at 18:00 hours. This means the streets are extremely hot throughout the day. The UTCI temperature is also similar to base case scenario.

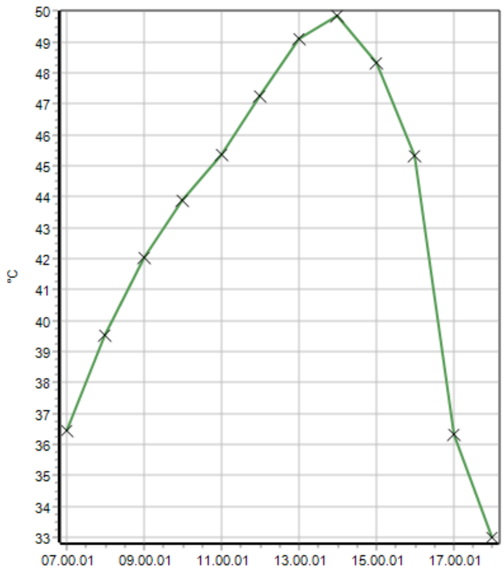

Graph 5. 3 UTCI temperature predicted by Envi-met

5.5. Scenario 2: AR1 (a)

The streets width is kept as it is but the height is improvised maintaining the aspect ratio 1. The height of the building is same as the width of the street and the canyon formed is called uniform canyon. In this case H=W and aspect ratio is 1.

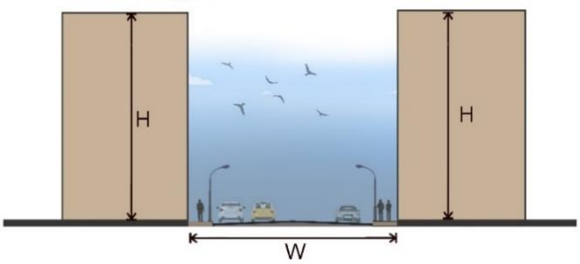

Figure 5. 21 Scenario AR1 (a), H=W

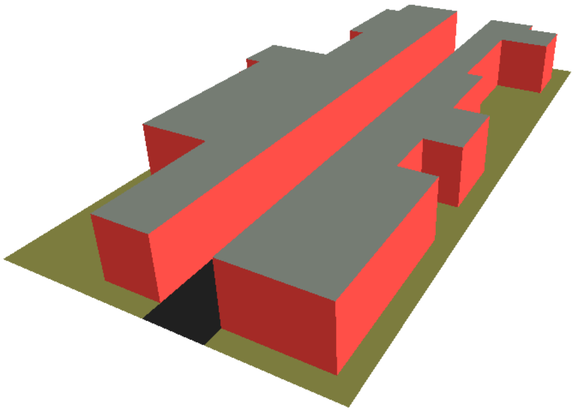

Figure 5. 22 3d model designed for scenario AR1 (a) by Envi-met

5.5.1. Solar analysis

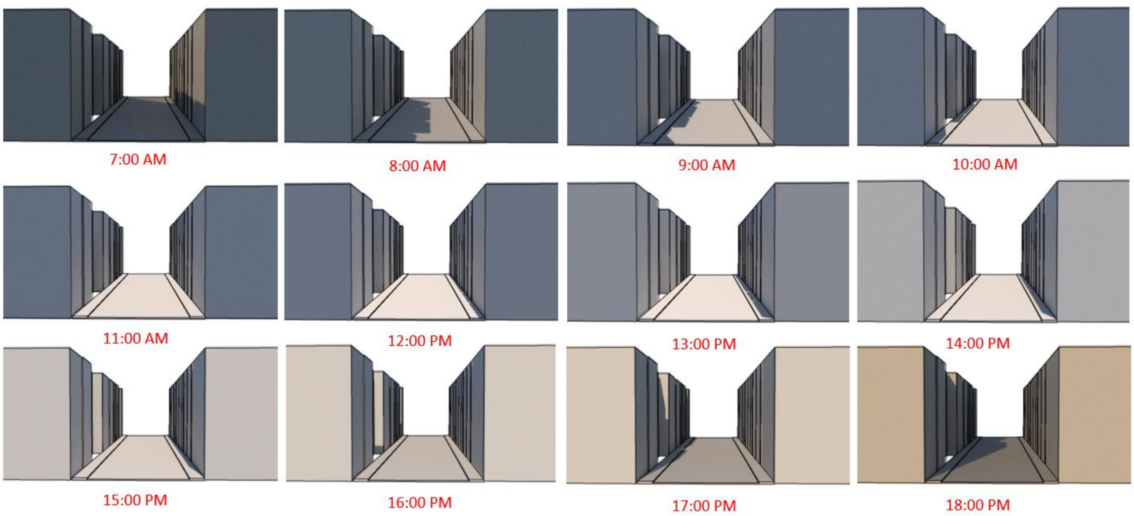

Figure 5. 23 solar analysis of scenario AR1 (a)

When the building height is equivalent to the street width, the northern half of the street is shaded in the morning, while the southern section of the street is somewhat shaded between 12:00 and 2:00 p.m. After 15:00 p.m., the streets are not even partially shaded. From 17:00 hours, the northern section of the streets begins to become shaded. The street is not shaded at 11:00 hours, and 16:00 hours at all. The shading during 15:00 hours is not enough for comfortable streets.

5.5.2. Simulation Results

a) Ambient air temperature

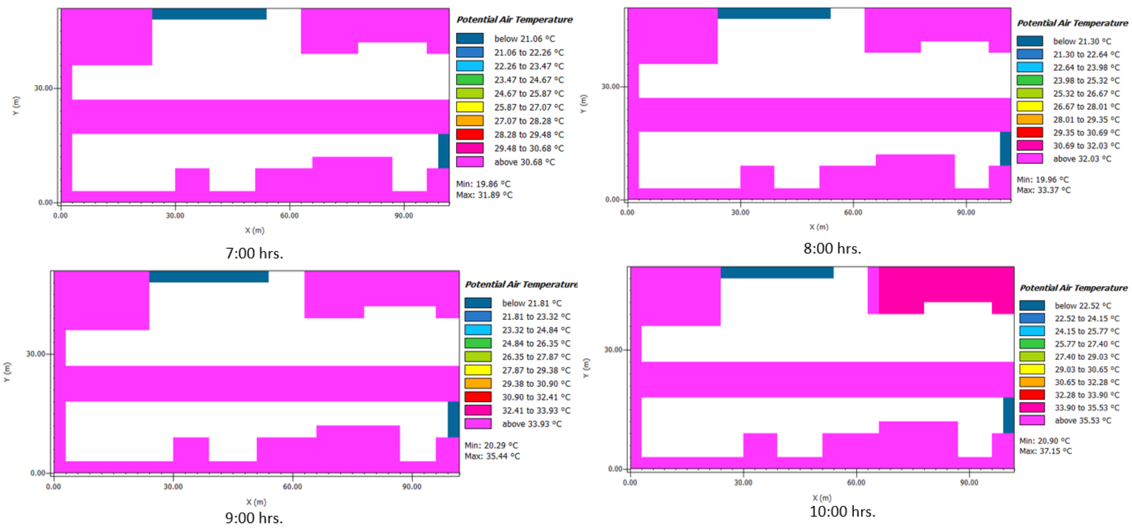

Figure 5. 24 Potential Air Temperature from 07:00 hrs. to 10:00 hrs. of scenario AR1 (a)

The figure shows that the temperature is lower than 31.89 °C at 7:00 hours but increases slowly by at least 2°C in every two hours. At 10:00 hours, the temperature is around 37.15 °C from 35.44 °C at 9:00 hrs. The temperature is still quite high for the morning time.

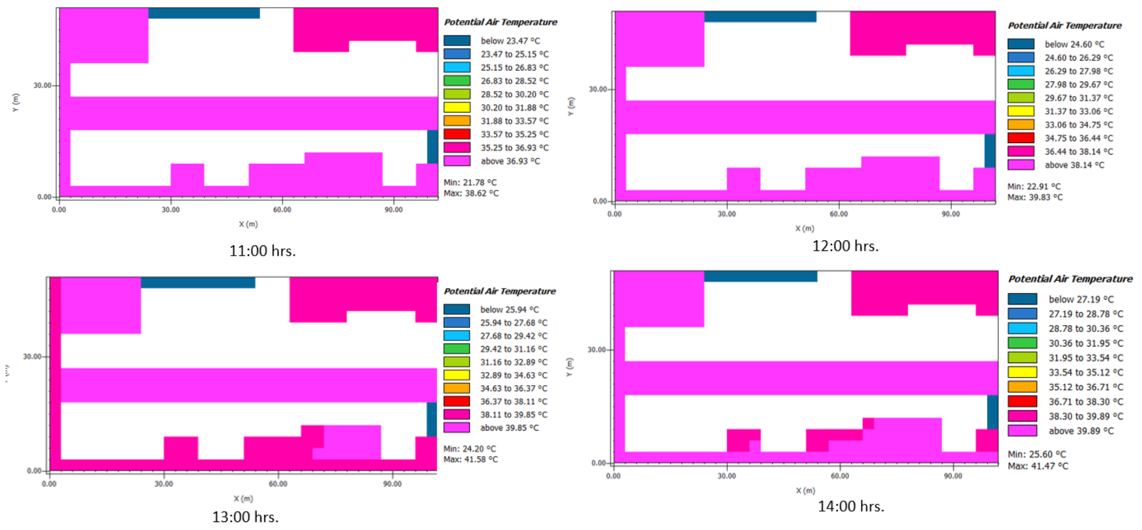

Figure 5. 25 Potential Air Temperature from 11:00 hrs. to 14:00 hrs. of scenario AR1 (a)

The temperature is rising at least a degree Celsius from 11:00 hrs. The temperature reached 38.62 °C at 11:00 hours and reaches 39.83 °C at 12:00 hours. The temperature rises up to 41.58 °C at 13:00 hours and 41.47 °C at 14:00 hours. The temperature is maximum during this time period.

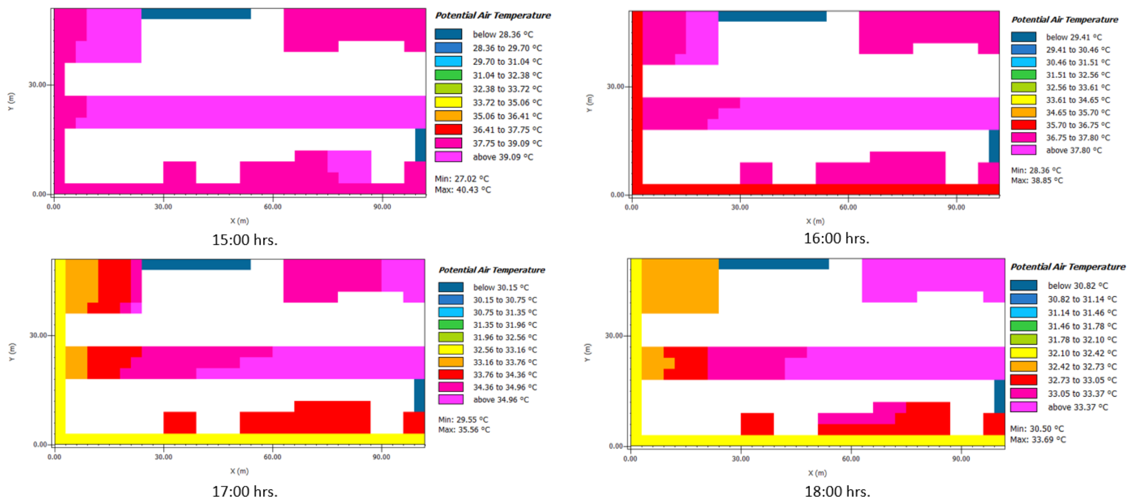

Figure 5. 26 Potential Air Temperature from 15:00 hrs. to 18:00 hrs. of scenario AR1 (a)

The temperature begins to fall from the western end of the street at 15:00 hours same as in base model. the maximum temperature is 40.43 °C at 15:00 hours and gradually decrease to 38.85 °C on next hour. The graph shows the changes in temperature from the western side of the street. The temperature drops down to 33.69 °C at 18:00 hours.

The graph illustrates that the temperature peaks around 14:00 hours and then drops to roughly 40 °C the following hour. From 9:00 a.m., until 17:00 p.m., the temperature rises over 35 °C. According to this graph, the streets are a little more pleasant in the morning between 7:00 to 9:00 a.m. and after 17:00 p.m. The street is too hot for pedestrians to walk all day. The results are same as in base model.

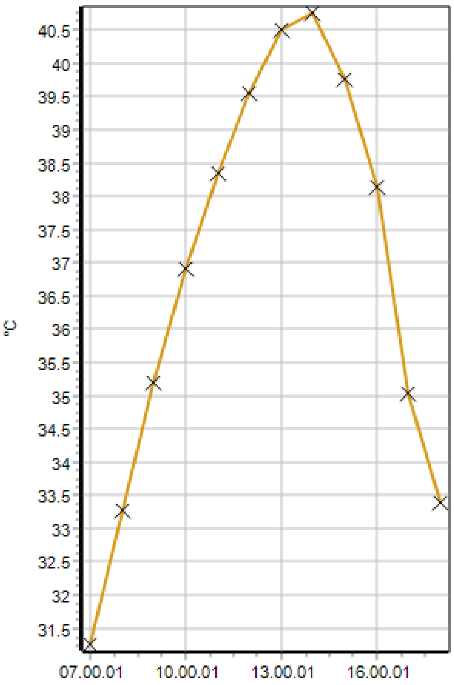

Graph 5. 4 Predicted Potential air temperature (Envi-met) for scenario AR1 (a)

b) Mean Radiant temperature

The mean radiant temperature rises sharply after 8:00 hours and reaches 70.28 °C by 14:00 hours. At 17:00 hours, the temperature drops to 47.01 °C. This table also illustrates that the streets are thermally uncomfortable for pedestrians and the temperature is similar as in base model.

Table 5. 3 MRT temperature predicted by Envi-met for scenario AR1 (a)

Time	Mean Radiant Temperature (°C)
07.00.01	49.844
08.00.01	55.478
09.00.01	59.249
10.00.01	60.028
11.00.01	60.378
12.00.01	64.309
13.00.01	68.731
14.00.01	70.286
15.00.01	68.206
16.00.01	62.63
17.00.01	47.014
17.59.59	26.375

c) PET calculation

The temperature is very high after 8:00 hours since the PET temperature is above 43 °C. The PET temperature drops only after 17:00 hours. This means the streets are extremely hot throughout the day. The PET temperature is also similar to base case scenario.

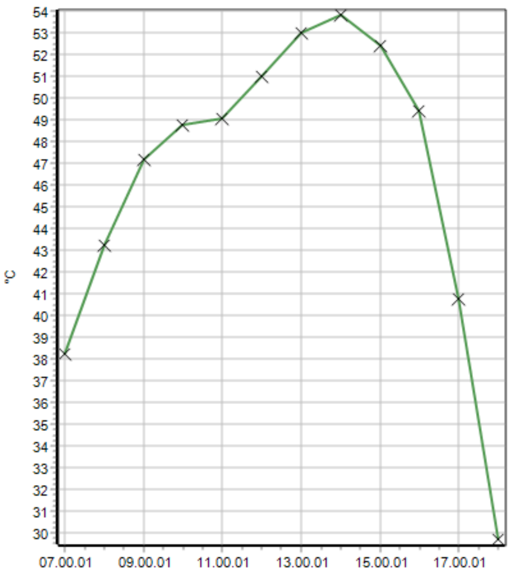

Graph 5. 5 PET temperature predicted by Envi-met for scenario AR1 (a)

d) UTCI calculation

The temperature starts to rose right after 7:00 hours and reach to the peak 49.5 °C at 14:00 hours. After 15:00 hours the temperature drops gradually and reach to 32.9°C at 18:00 hours. This means the streets are extremely hot throughout the day. The UTCI temperature is also similar to base case scenario.

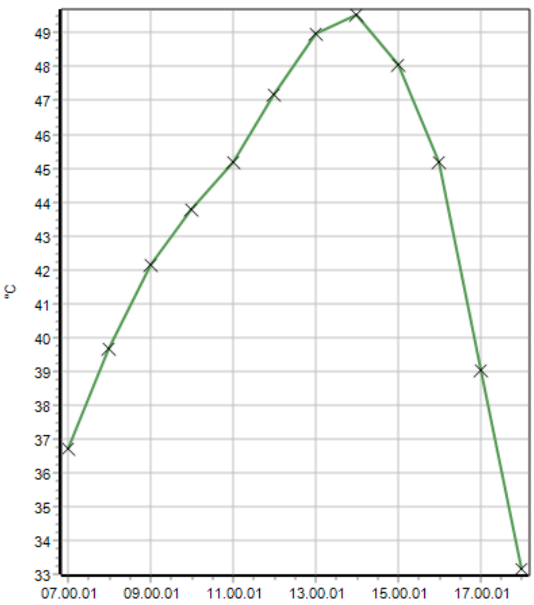

Graph 5. 6 UTCI temperature predicted by Envi-met for scenario AR1 (a)

5.6. Scenario 3: AR1.5 (a)

The height of building is 1.5 times the width of the street in this scenario. The aspect ratio formed is 1.5.

Aspect ratio = H/W

1.5 = H/W

H= Wx1.5

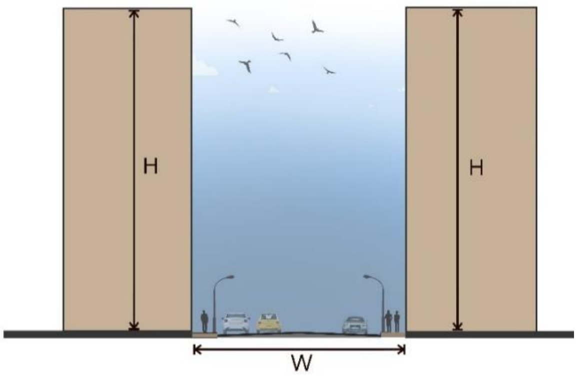

Figure 5. 27 section of street of scenario AR 1.5 (a)

For the street of 17 m, the building height should be 25.5 m in order to create canyon of aspect ratio 1.5.

5.6.1. Solar analysis

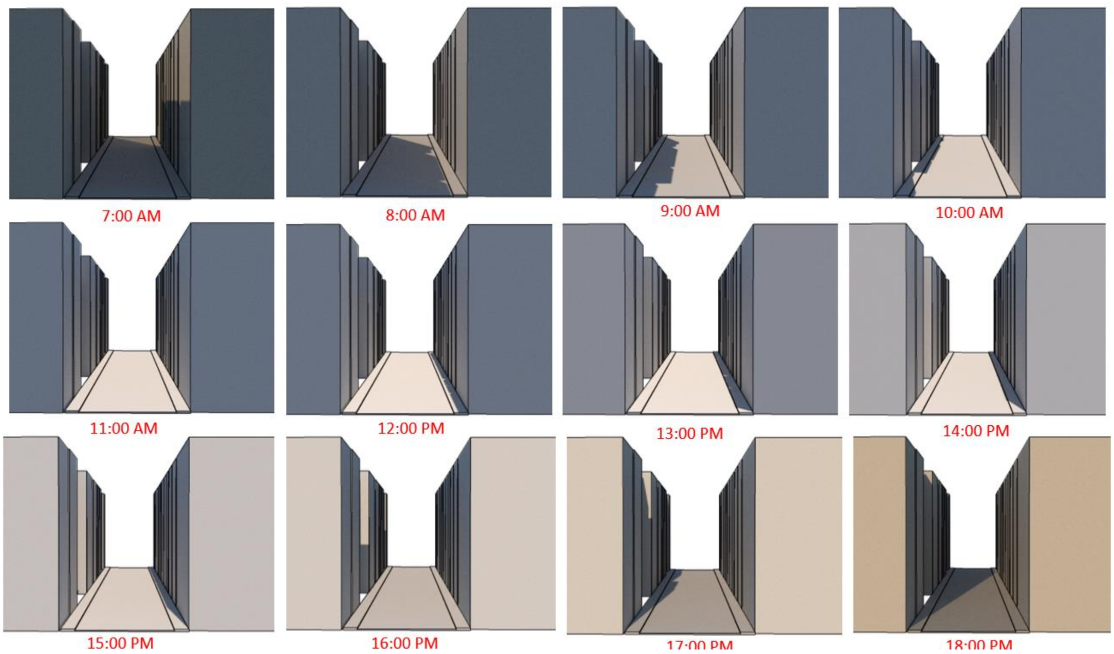

Figure 5. 28 solar analysis of scenario AR1.5 (a)

When the building height is 1.5 times the width of the street, the shadowed portion of the street is somewhat more than the base case and street with aspect ratio 1. The northern section of the street is shaded until 10:00 a.m., while the southern portion begins to gain shade around 12:00 p.m. At 11:00 a.m. and 16:00 p.m., the street is not shaded at all. During the remaining hours, at least one section of the roadway is shaded making the streets thermally comfortable during those hours.

5.6.2. Simulation Results

a) Ambient air temperature

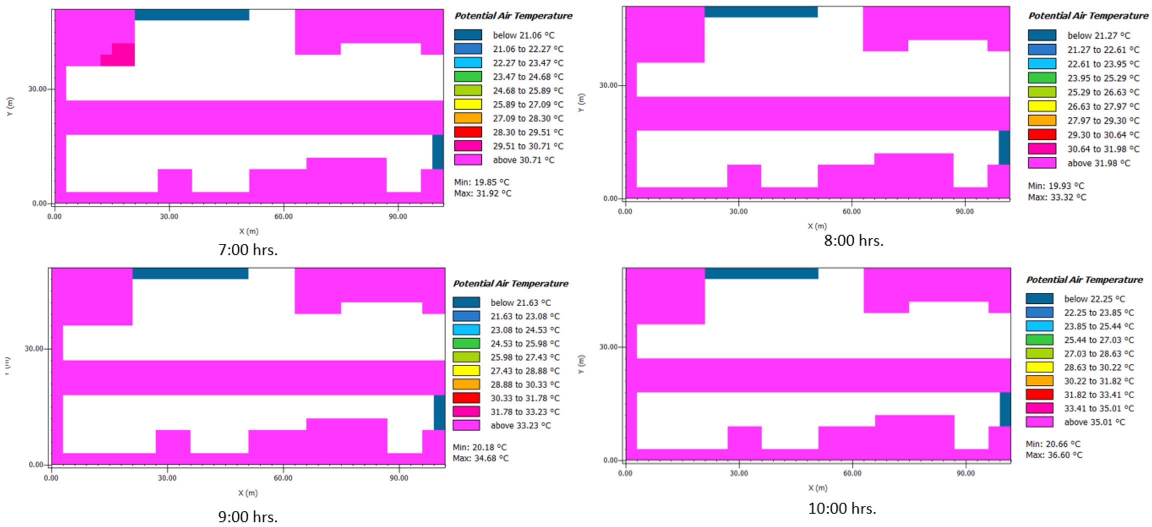

Figure 5. 29 Potential Air Temperature from 07:00 hrs. to 10:00 hrs. of scenario AR1.5 (a)

The figure shows that the temperature is lower than 31.92 °C at 7:00 hours but increases slowly by at least 2 °C in every two hours. At 10:00 hours, the temperature is around 36.60 °C from 34.68 °C at 9:00 hours which is 1 °C less than the base model. The temperature is still quite high for the morning time.

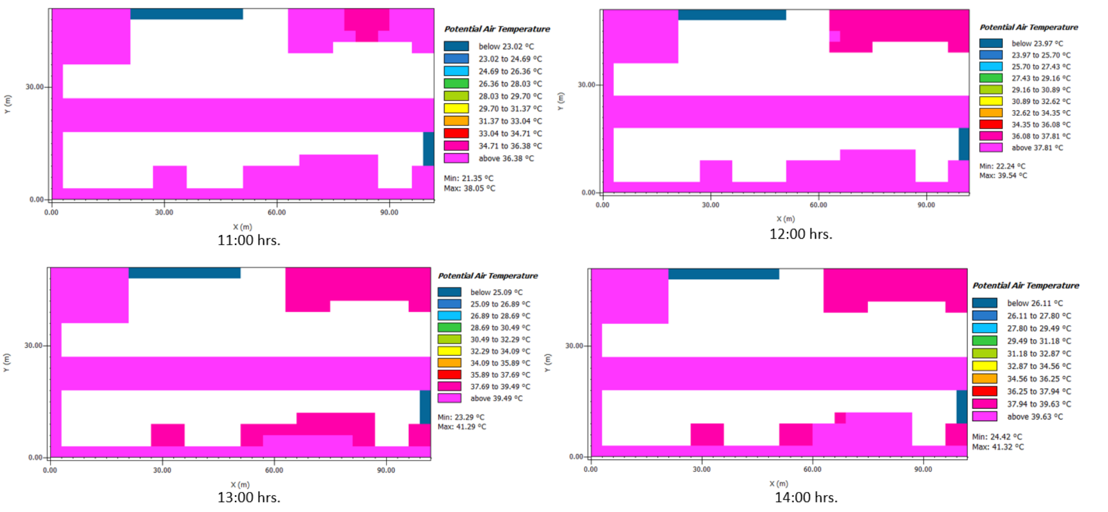

Figure 5. 30 Potential Air Temperature from 11:00 hrs. to 14:00 hrs. of scenario AR1.5 (a)

The temperature is rising at least a degree Celsius from 11:00 hrs. The temperature reached 38.05 °C at 11:00 hours and reaches 39.54 °C at 12:00 hours. The temperature rises up to 41.29 °C at 13:00 hours and 41.32 °C at 14:00 hours which is similar to base model. The temperature is maximum during this time period.

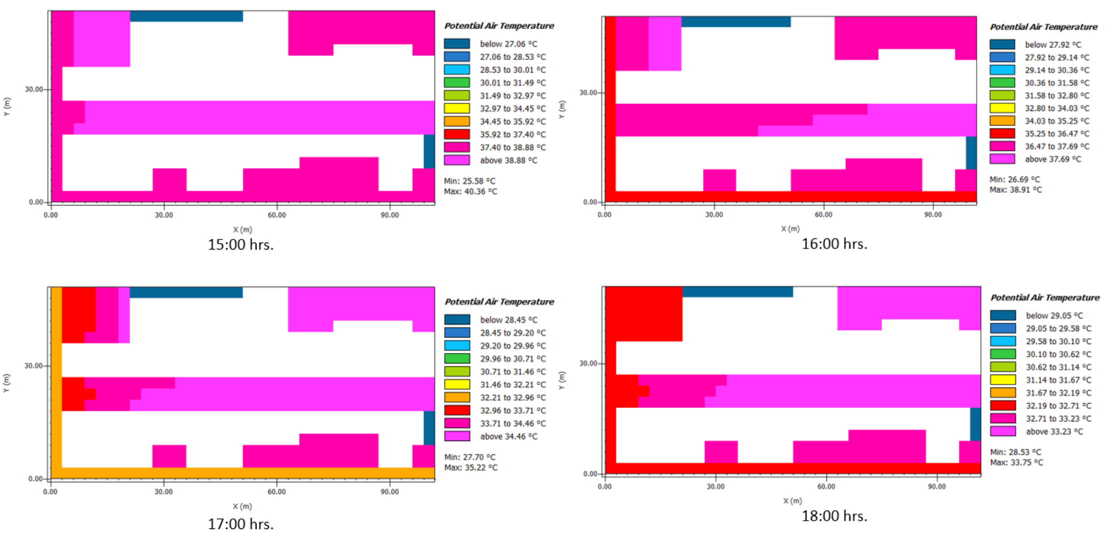

Figure 5. 31 Potential Air Temperature from 15:00 hrs. to 18:00 hrs. of scenario AR1.5 (a)

The temperature begins to fall from the western end of the street at 15:00 hours same as in base model. The maximum temperature is 40.36 °C at 15:00 hours and gradually decrease to 38.91 °C on next hour. The graph shows the change in temperature from the western side of the street. The temperature drops down to 33.75 °C at 18:00 hours.

The graph illustrates that the temperature peaks around 14:00 hours and then drops to roughly 39 °C the following hour which is almost 1 °C less than the base model. The temperature is less than 34.5 °C before 10: 00 am in the morning. The temperature drops below 35 after 17:00 hours. The temperature is 0.5 °C -1 °C less than base model throughout the day.

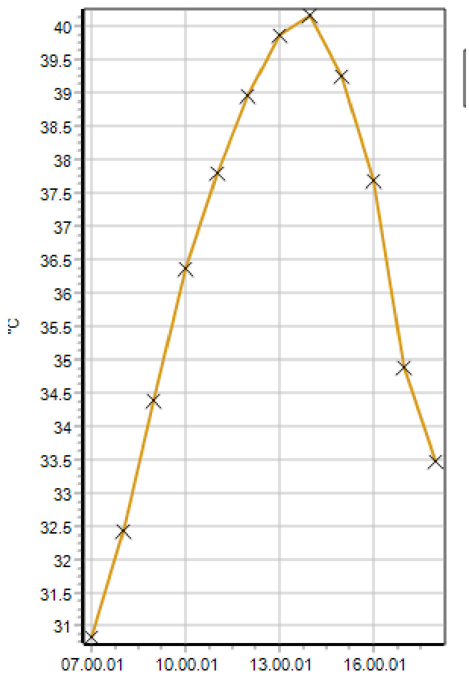

Graph 5. 7 Potential air temperature predicted by Envi-met for scenario AR1.5 (a)

b) Mean Radiant temperature

The mean radiant temperature rises sharply after 8:00 hours and reaches 69.45 °C by 14:00 hours. At 17:00 hours, the temperature drops to 33.79 °C. The mean radiant temperature is 0.1 °C -2.5 °C less than base model after 10:00 hours to 15:00 hours. There is slight change in mean radiant temperature when aspect ratio is increased to 1.5.

Table 5. 4 MRT temperature predicted by Envi-met for scenario AR1.5 (a)

Time	Mean Radiant Temperature (°C)
07.00.01	28.451
08.00.01	34.079
09.00.01	56.502
10.00.01	59.224
11.00.01	59.847
12.00.01	63.798
13.00.01	67.726
14.00.01	69.458
15.00.01	67.322
16.00.01	42.806
17.00.01	33.779
17.59.59	26.174

PET calculation

The PET temperature reaches 44.5 °C at 9:00 hours which is very high temperature. The PET temperature drops to 34.34 °C only after 17:00 hours. This means the streets are extremely hot throughout the day. The PET temperature is 0.3 °C -2.6 °C less than the base model during the noon.

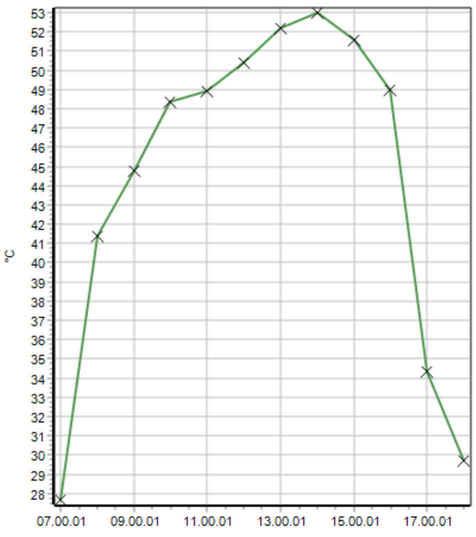

Graph 5. 8 PET temperature predicted by Envi-met for scenario AR1.5 (a)

5.7. Scenario 4: AR2 (a)

The aspect ratio is 2 in this scenario that means the height of building is twice the width of street. For the street of 17 m, the building height should be 34 m in order to create canyon of aspect ratio 2.

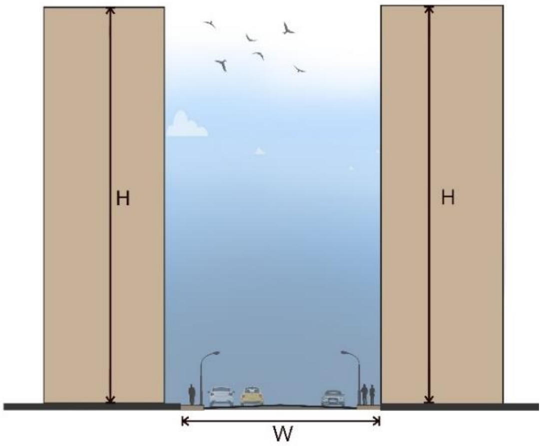

Figure 5. 32 Street section for scenario AR2 (a)

5.7.1. Solar analysis

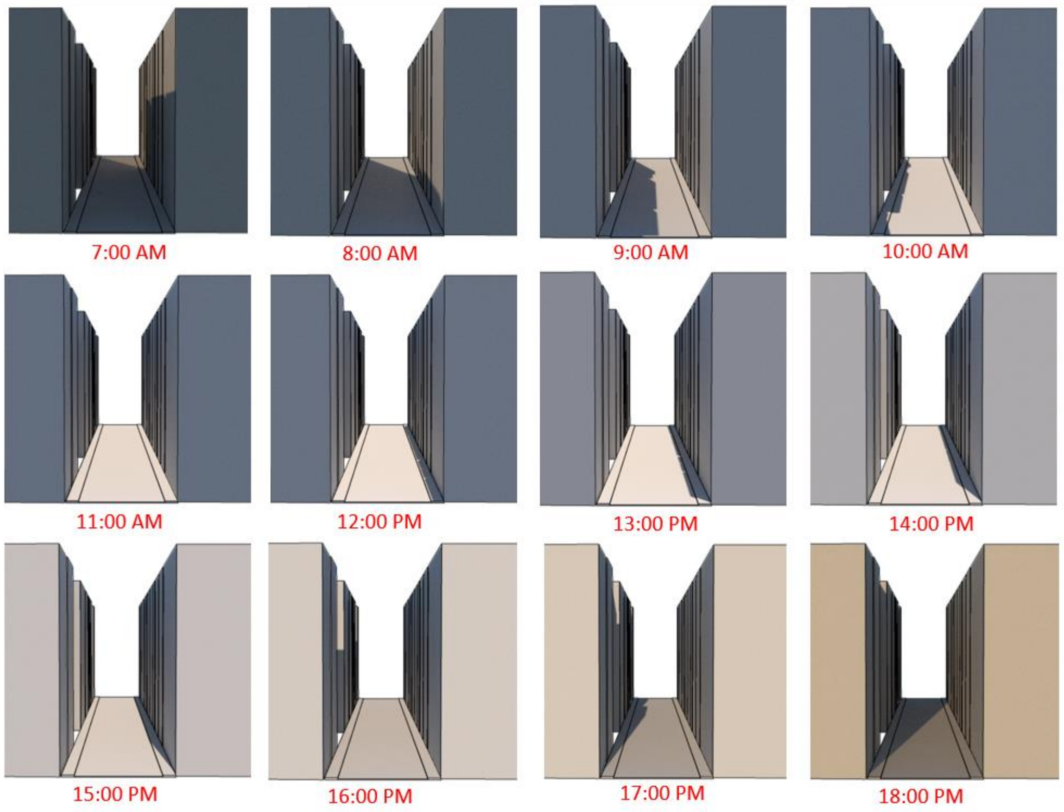

Figure 5. 33 solar analysis of scenario AR 2(a)

The time of shaded street is increased with increase in aspect ratio. The streets are completely shaded during two hours starting from 7:00 hours. The northern portion of streets are shaded till 10:00 hours and from 12:00 hours to 15:00 hours, the northern part of the street is completely shaded. The streets are not shaded for only two hours throughout the day. During the remaining hours, at least one section of the roadway is shaded making the streets thermally comfortable during those hours.

5.7.2. Simulation Results

a) Ambient air temperature

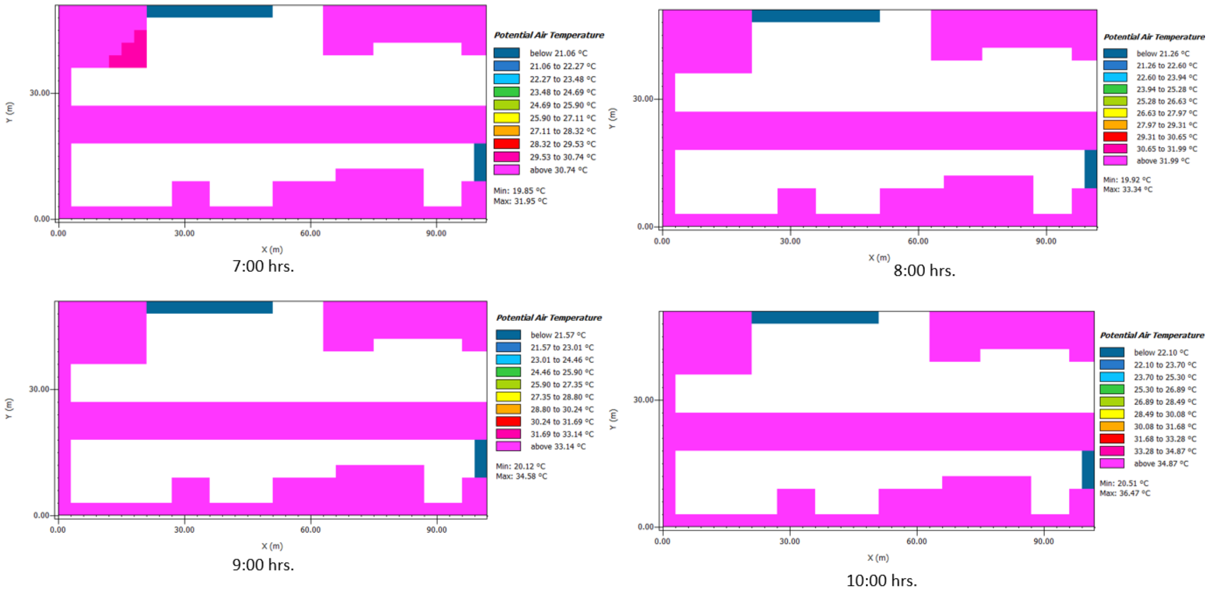

Figure 5. 34 Potential Air Temperature from 07:00 hrs. to 10:00 hrs. of scenario AR2 (a)

The graph shows that the temperature is lower than 31.95 °C at 7:00 hours but increases slowly by at least 2 °C in every two hours. At 10:00 hours, the temperature is around 36.47 °C from 34.58 °C at 9:00 hours which is 1 °C less than the base model. The temperature is still quite high for the morning time.

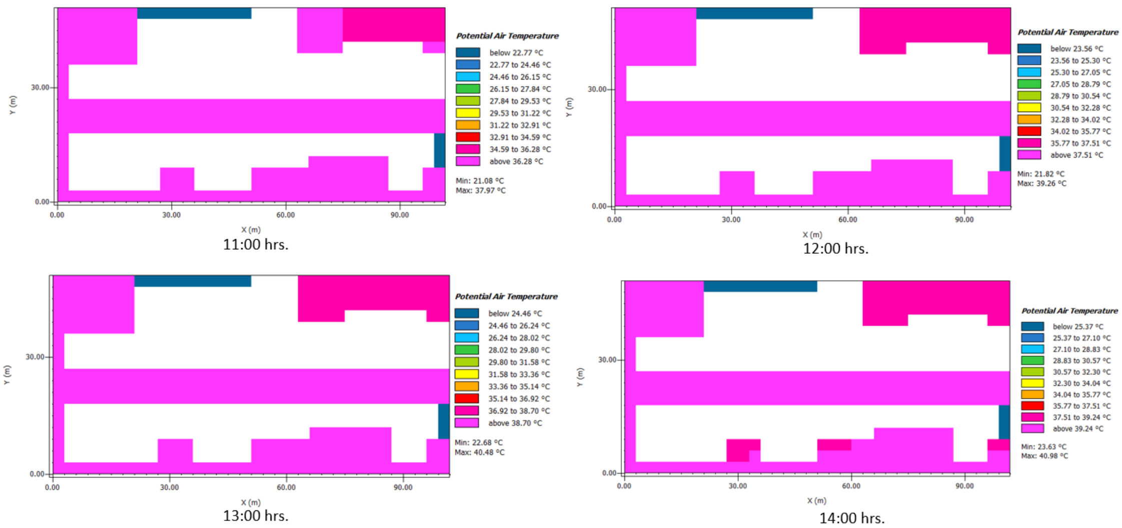

Figure 5. 35 Potential Air Temperature from 11:00 hrs. to 14:00 hrs. of scenario AR2 (a)

The temperature is rising at least a degree Celsius from 11:00 hrs. The temperature reached 37.97 °C at 11:00 hours and reaches 39.26 °C at 12:00 hours. The temperature rises up to 40.48 °C at 13:00 hours and 40.98 °C at 14:00 hours which is 1 °C less than base model. The temperature is maximum during this time period.

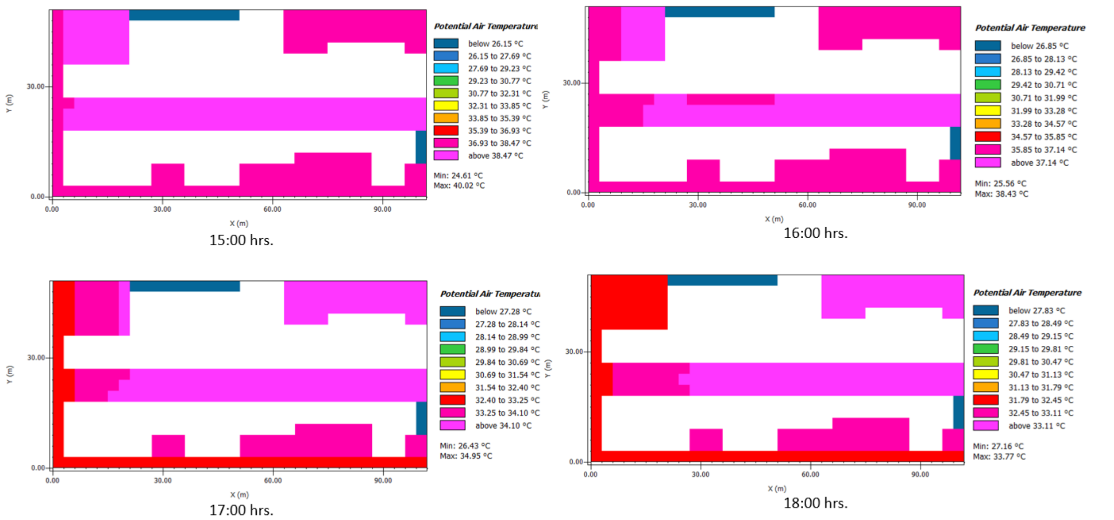

Figure 5. 36 Potential Air Temperature from 15:00 hrs. to 18:00 hrs. of scenario AR2 (a)

The temperature begins to fall from the western end of the street at 15:00 hours same as in base model. The maximum temperature is 40.02 °C at 15:00 hours and gradually decrease to 38.43 °C on next hour. The graph shows the change in temperature from the western side of the street. The temperature drops down to 33.77 °C at 18:00 hours.

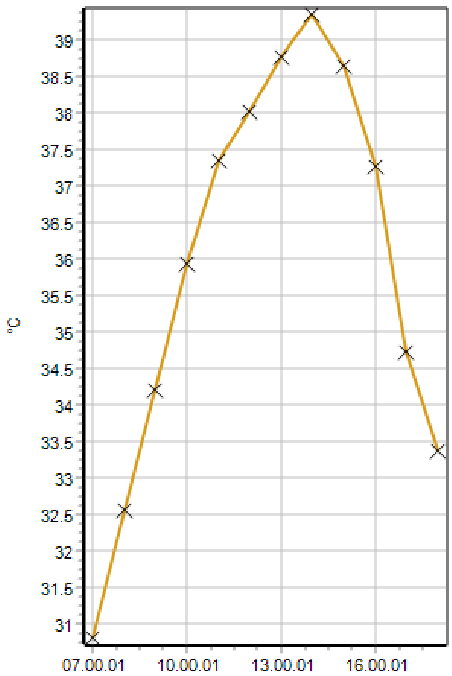

Graph 5. 9 Potential air temperature predicted by Envi-met for scenario AR2 (a)

The graph illustrates that the temperature peaks around 14:00 hours same as in other scenarios and then drops to roughly 38.5 °C the following hour which is almost 1.5 °C less than the base model. The temperature is less than 34.5 °C before 10: 00 am in the morning. The temperature drops below 35 after 17:00 hours. The temperature is 0.5 °C -2 °C less than base model throughout the day.

b) Mean Radiant temperature

The mean radiant temperature rises sharply after 8:00 hours and reaches 68.11 °C by 14:00 hours. At 17:00 hours, the temperature drops to 33.35 °C. The mean radiant temperature is 0.7 °C -4 °C less than base model after 10:00 hours to 15:00 hours. There is change in mean radiant temperature when aspect ratio is increased to 2.

Table 5. 5 MRT temperature predicted by Envi-met for scenario AR2 (a)

Time	Mean Radiant Temperature (°C)
07.00.01	28.105
08.00.01	33.772
09.00.01	56.196
10.00.01	58.803
11.00.01	59.898
12.00.01	60.678
13.00.01	64.51
14.00.01	68.11
15.00.01	66.522
16.00.01	60.067
17.00.01	33.355
17.59.59	26.073

c) PET calculation

The PET temperature reaches 44.5 °C at 9:00 hours which is very high temperature. The PET temperature drops to 34.34 °C only after 17:00 hours. This means the streets are extremely hot throughout the day. The PET temperature is 0.5 °C -3 °C less than the base model during the noon.

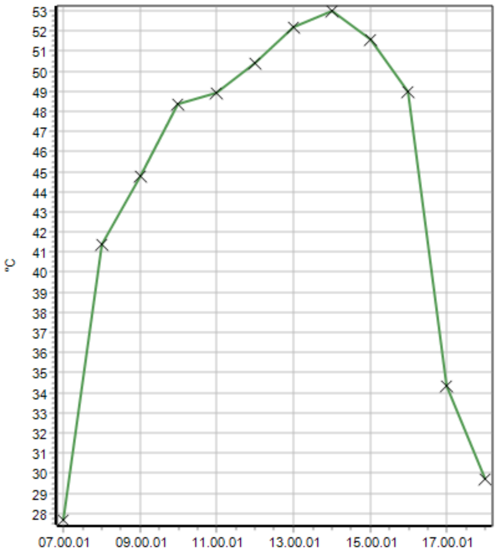

Graph 5. 10 PET temperature predicted by Envi-met for scenario AR 2(a)

d) UTCI calculation

The UTCI temperature reaches 39.8 °C at 9:00 hours which is high temperature. The UTCI temperature drops to 35.17 °C only after 17:00 hours. This means the streets are extremely hot throughout the day. The UTCI temperature is 0.4 °C -6.2 °C less than the base model during the noon.

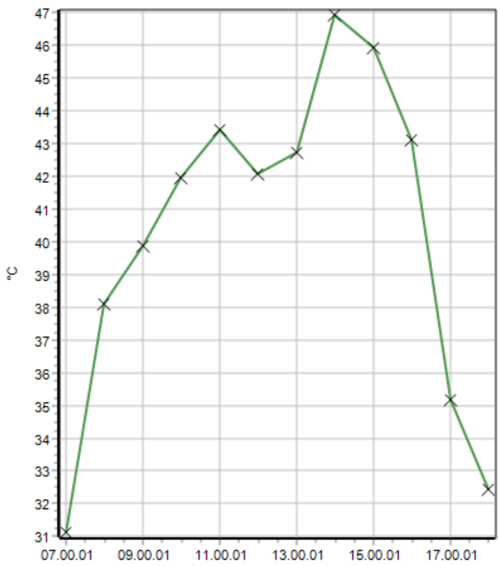

Graph 5. 11 UTCI temperature predicted by Envi-met for scenario AR 2(a)

5.8. Scenario 5: AR 3 (a)

The aspect ratio is 3 in this scenario that means the height of building is thrice the width of street. For the street of 17 m, the building height should be 54 m in order to create canyon of aspect ratio 3. Aspect ratio 3 is quite high for the context of Nepal.

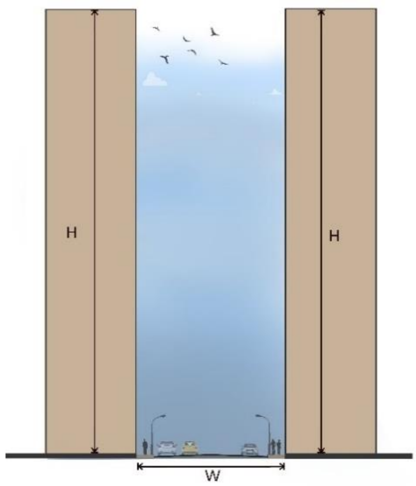

Figure 5. 37 Street section for scenario AR 3 (a)

5.8.1. Solar analysis

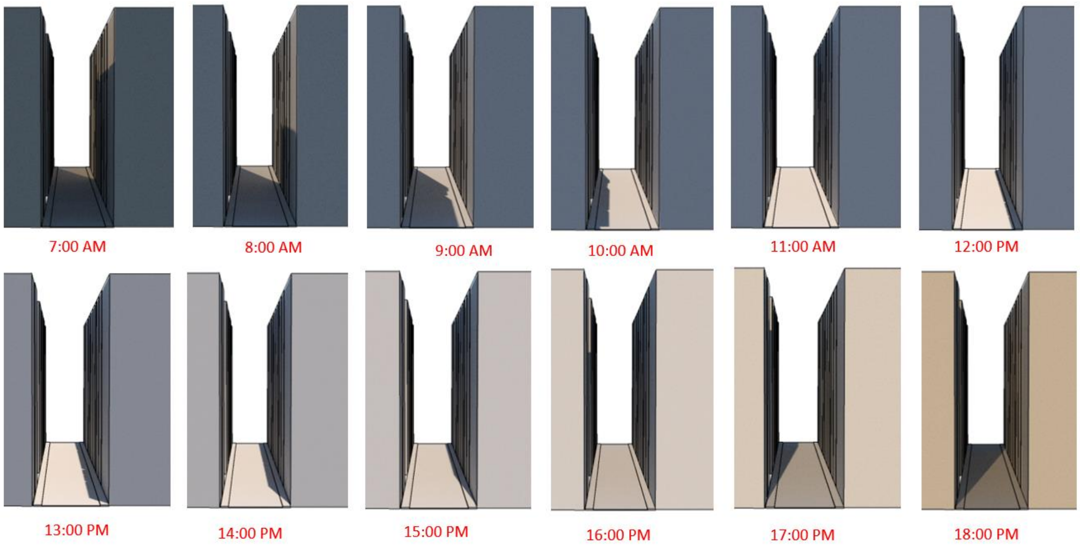

Figure 5. 38 solar analysis of scenario AR 3(a)

The time of a shaded street increases as the aspect ratio increases. Beginning at 7:00 a.m., the streets are entirely shaded for two hours. The northern portion of the roadway is shaded until 10:00 a.m., and from 12:00 a.m. to 15:00 a.m., southern part is totally shaded. The streets are not shaded for only for two hours. During the remaining hours, at least one part of the streets is shaded, allowing the streets to be thermally pleasant.

5.8.2. Simulation Results

a) Ambient air temperature

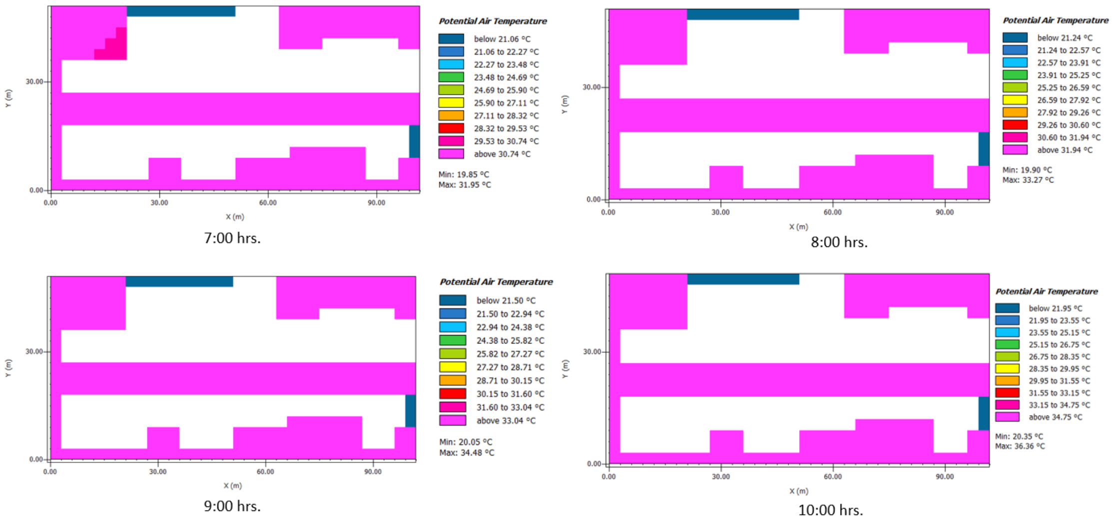

Figure 5. 39 Potential Air Temperature from 07:00 hrs. to 10:00 hrs. of scenario AR3 (a)

The graph shows that the temperature is lower than 31.95 °C at 7:00 hours but increases slowly by at least 2 °C in every two hours. At 10:00 hours, the temperature is around 36.36 °C from 34.48 °C at 9:00 hours which is 1 °C less than the base model. The temperature is still quite high for the morning time.

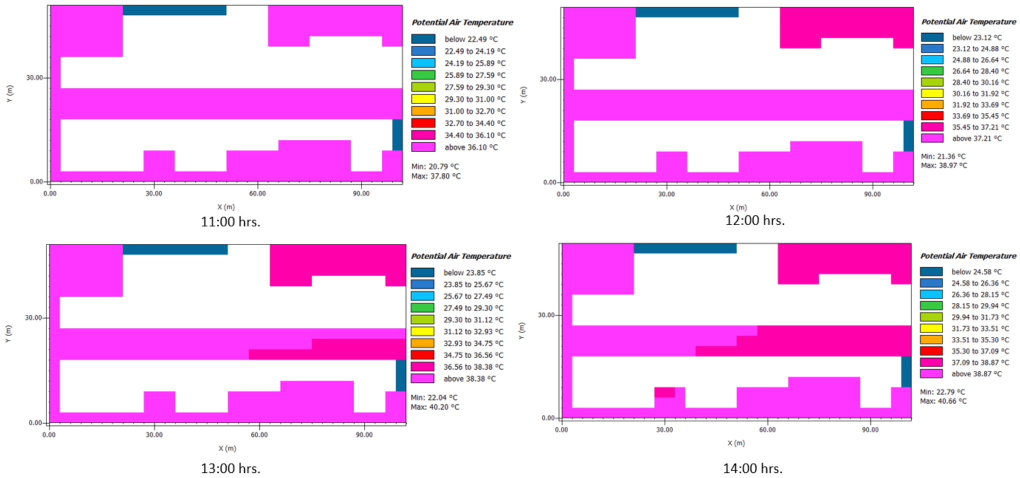

Figure 5. 40 Potential Air Temperature from 11:00 hrs. to 14:00 hrs. of scenario AR3 (a)

The temperature is rising at least a degree Celsius from 11:00 hrs. The temperature reached 37.8 °C at 11:00 hours and reaches 38.97 °C at 12:00 hours. The temperature rises up to 40.20 °C at 13:00 hours and 40.66 °C at 14:00 hours which is 1 °C less than base model. The temperature is maximum during this time period. After 13:00 hours, the temperature begins to drop slowly from the south eastern part of the street. The south eastern portion of the street have 38 °C which is 2 °C less than the western part of the street.

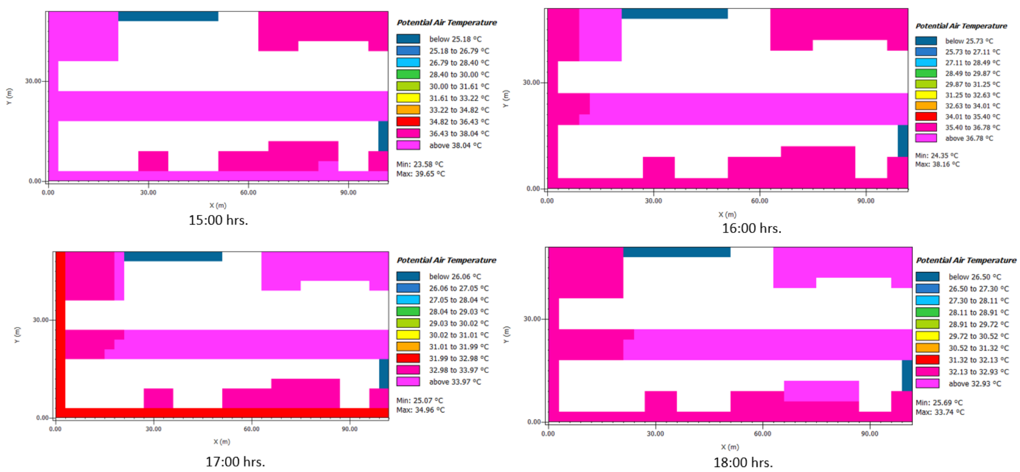

Figure 5. 41 Potential Air Temperature from 15:00 hrs. to 18:00 hrs. of scenario AR3 (a)

The temperature begins to fall from the western end of the street after 16:00 hours in this scenario. The maximum temperature is 39.65 °C at 15:00 hours and gradually decrease to 38.16 °C on next hour. The graph shows the change in temperature from the western side of the street. The temperature drops down to 33.74 °C at 18:00 hours.

The graph illustrates that the temperature is different for two ends of the street. The south eastern portion of the street has maximum temperature at 38.7 °C at 14:00 hours while the south western part has temperature 39.2 °C at 14:00 hours. The difference of about 0.5 °C can be seen on two parts of the street throughout the day. The temperature in both case drops down in average to around 38 °Cat 15:00 hrs which is around 2°C less than the base model. The temperature is less than 34.5 °C before 10: 00 am in the morning. The temperature drops below 35 after 17:00 hours. The temperature is 0.5 °C -2 °C less than base model throughout the day.

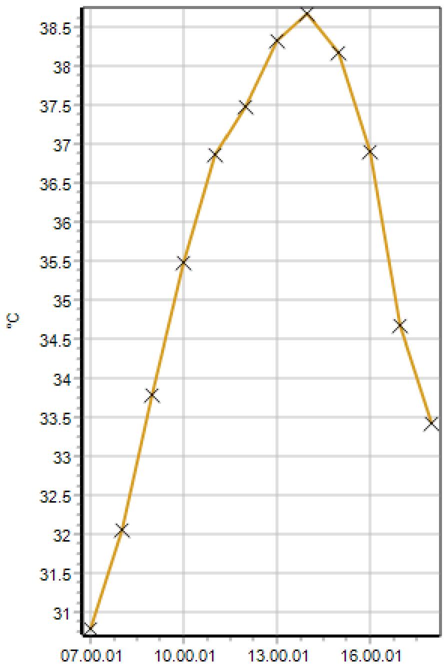

Graph 5. 12 Potential air temperature predicted by Envi-met for scenario AR3 on the south eastern side of street(a)

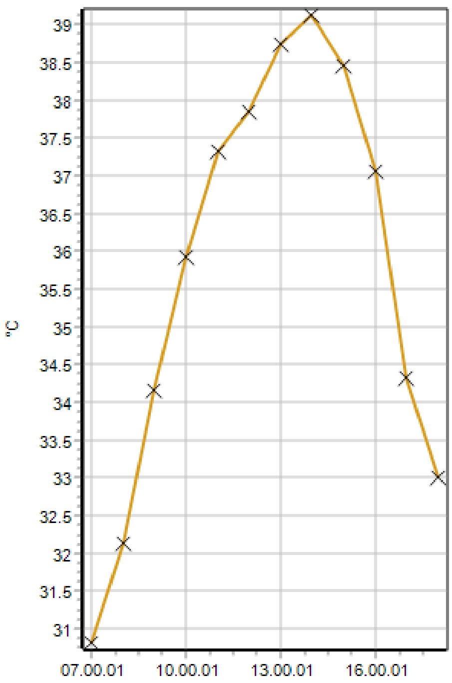

Graph 5. 13 Potential air temperature predicted by Envi-met for scenario AR3 on the south western side of street(a)

b) Mean Radiant temperature

The mean radiant temperature rises sharply after 8:00 hours and reaches 49.56 °C by 14:00 hours. At 17:00 hours, the temperature drops to 32.90 °C. The mean radiant temperature is 2.7 °C -21.1 °C less than base model after 10:00 hours to 16:00 hours. There is a huge change in mean radiant temperature when aspect ratio is increased to 3.

Table 5. 6 MRT temperature predicted by Envi-met for scenario AR3 (a)

Time	Mean Radiant Temperature (°C)
07.00.01	28.017
08.00.01	52.592
09.00.01	55.108
10.00.01	57.23
11.00.01	49.065
12.00.01	49.411
13.00.01	50.571
14.00.01	49.564
15.00.01	64.895
16.00.01	59.014
17.00.01	32.901
17.59.59	25.652

c) PET calculation

The PET temperature reaches 43.4 °C at 9:00 hours which is very high temperature. The PET temperature drops to 33.617 °C only after 17:00 hours. This means the streets are extremely hot throughout the day. The PET temperature is 0.5 °C -12.6 °C less than the base model throughout the day.

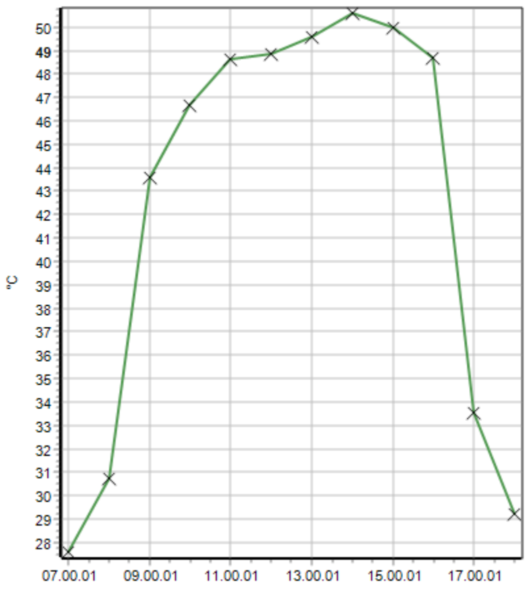

Graph 5. 14 PET temperature predicted by Envi-met for scenario AR3 (a)

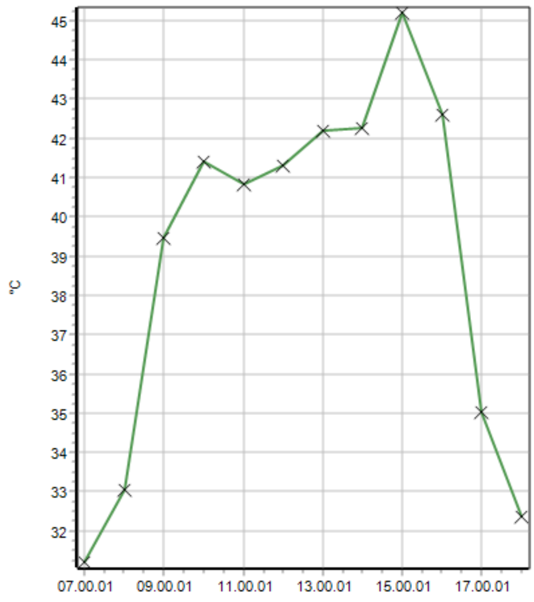

Graph 5. 15 Graph 16 UTCI temperature predicted by Envi-met for scenario AR3 (a)

d) UTCI calculation

The UTCi temperature reaches 45.2 °C at 15:00 hours which is very high temperature. The UTCI temperature drops to 32.4 °C only after 17:00 hours. This means the streets are extremely hot throughout the day. The UTCI temperature is 0.5 °C -7.5 °C less than the base model throughout the day.

5.9. Scenario 6: AR1 (b)

The aspect ratio is 1 in this scenario that means the height of building is equal to the width of street. For the street of 17 m, the building height should be 17 m in order to create canyon of aspect ratio 1. The difference between this scenario and AR1 (a) is that the street of scenario AR1(a) is oriented toward North-South direction while the street of this scenario AR1 (b) is oriented towards the East-West direction.

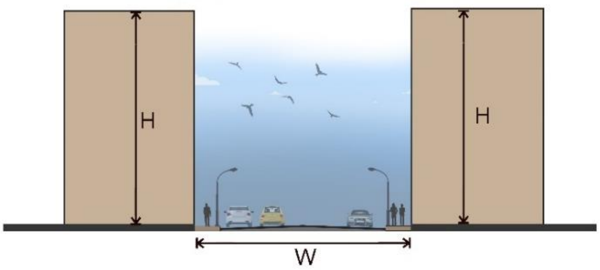

Figure 5. 42 Scenario AR1 (b), H=W

The orientation of the scenarios is changed so that there will be optimum aspect ratio for both orientation streets for future planning and design.

5.9.1. Solar analysis

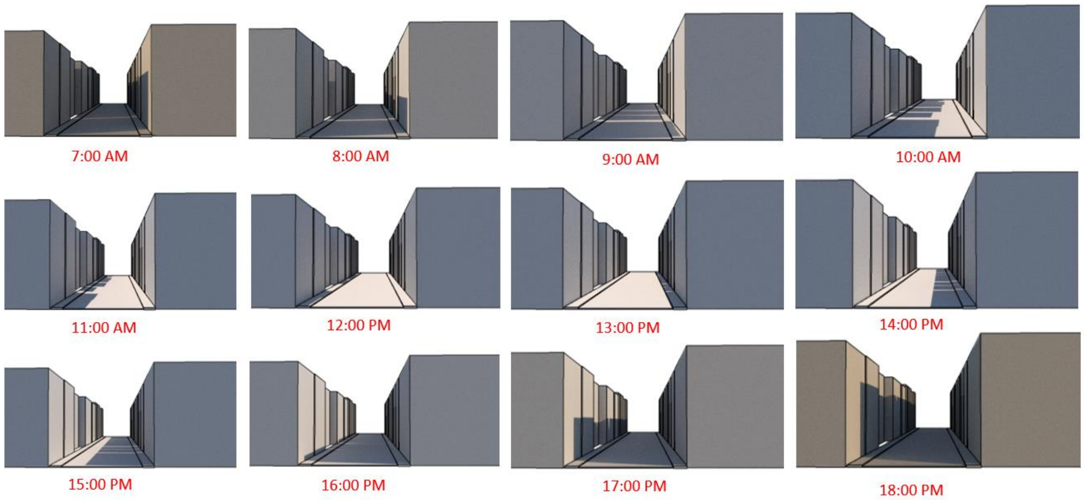

Figure 5. 43 solar analysis of scenario AR 1(b)

The shading pattern of the street changes with the change in orientation. The north south oriented streets are more shaded throughout the day than east west oriented streets. The figure above shows that at least one portion of the street is shaded always even with uniform aspect ratio. The streets are little shaded at 12:00 hours otherwise the streets look thermally comfortable throughout day when analyzing the shading.

5.9.2. Simulation Results

a) Ambient air temperature

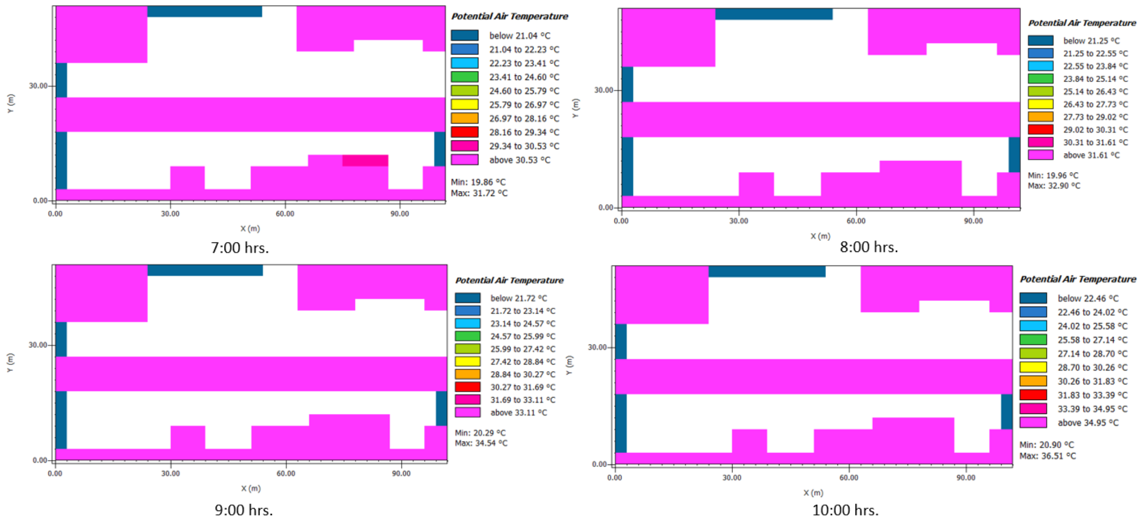

Figure 5. 44 Potential Air Temperature from 07:00 hrs. to 10:00 hrs. of scenario AR1 (b)

The graph shows that the temperature is lower than 31.72 °C at 7:00 hours but increases slowly by at least 2 °C in every two hours. At 10:00 hours, the temperature is around 36.51 °C from 34.54 °C at 9:00 hours which is 1 °C less than the base model. The temperature is still quite high for the morning time.

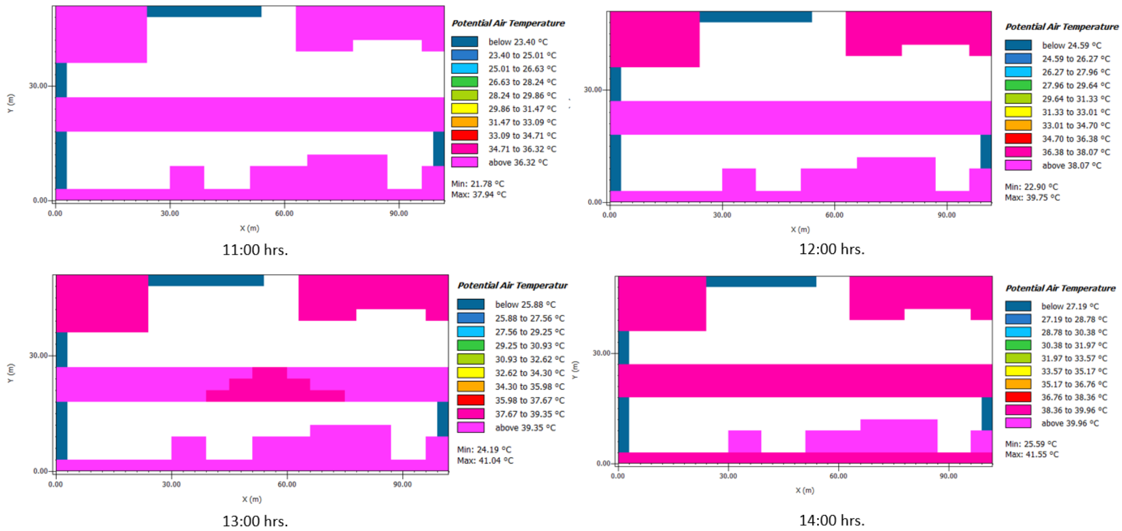

Figure 5. 45 Potential Air Temperature from 11:00 hrs. to 14:00 hrs. of scenario AR1 (b)

The temperature is rising at least a degree Celsius from 11:00 hrs. The temperature reached 37.94 °C at 11:00 hours and reaches 39.75 °C at 12:00 hours. The temperature slowly decreases in the middle part of the street and reach to 37.6 °C. The temperature remains same throughout the street on the next hour. The temperature in the street at 14:00 hours is between 38.36 °C to 39.96 °C which is almost 2 °C than the base model.

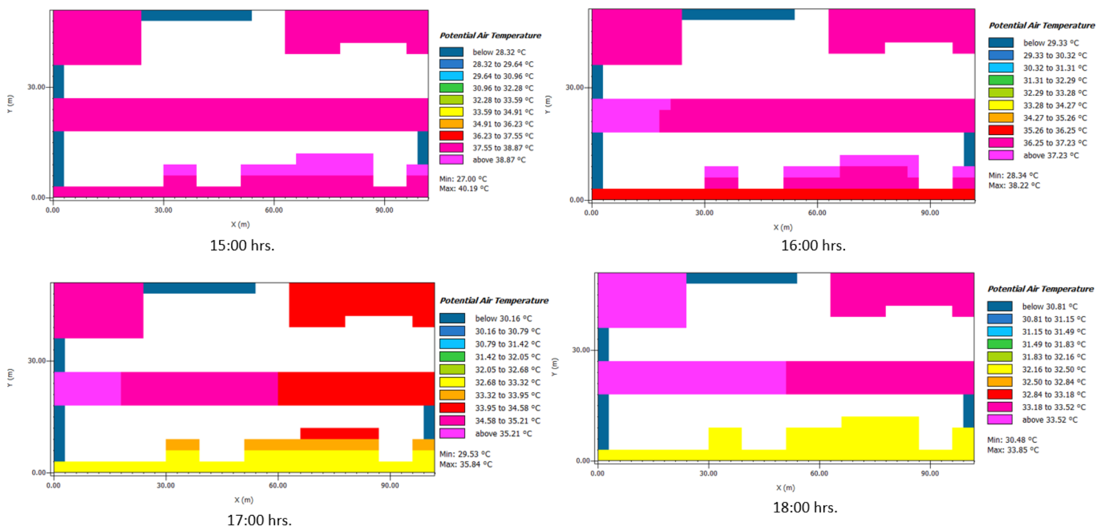

Figure 5. 46 Potential Air Temperature from 15:00 hrs. to 18:00 hrs. of scenario AR1 (b)

The temperature is less than 38.87 °C at 15:00 hours which then decreases below 37.23 °C at 16:00 hrs. the temperature is constantly decreasing with the time. The maximum temperature is 33.52 °C at 18:00 hours. The temperature is different for two ends of the street. The northern part of the streets has little high temperature than the southern.

The graph illustrates that the temperature peaks around 14:00 hours and then drops to roughly 38.2 °C the following hour which is almost 2 °C less than the base model. From 9:00 a.m. until 17:00 p.m., the temperature rises over 34.5 °C. According to this graph, the temperature is below 36 °C before 10:00 hours and after 17:00 hours. The temperature doesn't reach above 40 °C in this scenario even the aspect ratio is uniform i.e., 1. The streets are a little more pleasant than the base model.

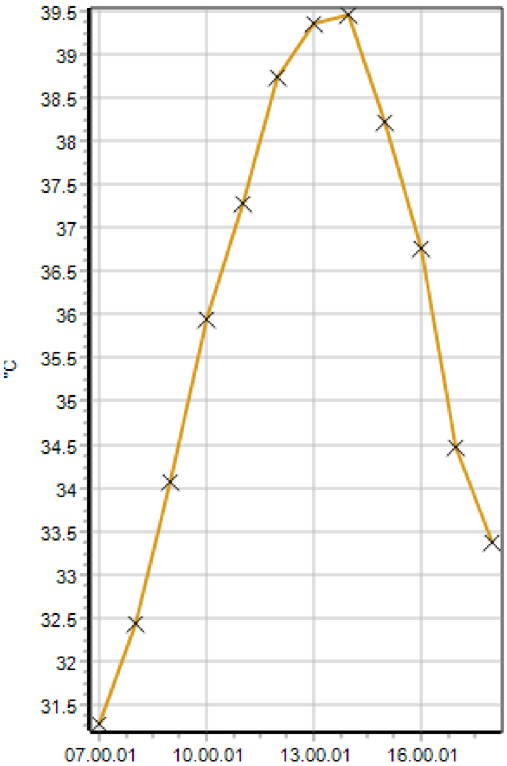

Graph 5. 16 Graph 18 Air temperature predicted by Envi-met for scenario AR1 (b)

b) Mean Radiant temperature

The mean radiant temperature rises sharply after 8:00 hours and reaches 58.70 °C by 9:00 hours and starts to decrease right after 10:00 hours. The MRT is maximum at 14:00 hours however it decreases afterwards and reach 35.294 at 17:00 hours. During the peak time i.e., after 13:00 hours there is a difference of 13.5 °C to 19.7 °C in MRT between this scenario and base model. Due to the shading cast by buildings, there is drop in Mean Radiant temperature in this scenario.

Table 5. 7 MRT temperature predicted by Envi-met for scenario AR1 (b)

Time	Mean Radiant Temperature (°C)
07.00.01	30.211
08.00.01	35.885

09.00.01	58.707
10.00.01	60.149
11.00.01	58.247
12.00.01	63.479
13.00.01	55.055
14.00.01	53.754
15.00.01	48.985
16.00.01	43.328
17.00.01	35.294
17.59.59	26.211

c) PET calculation

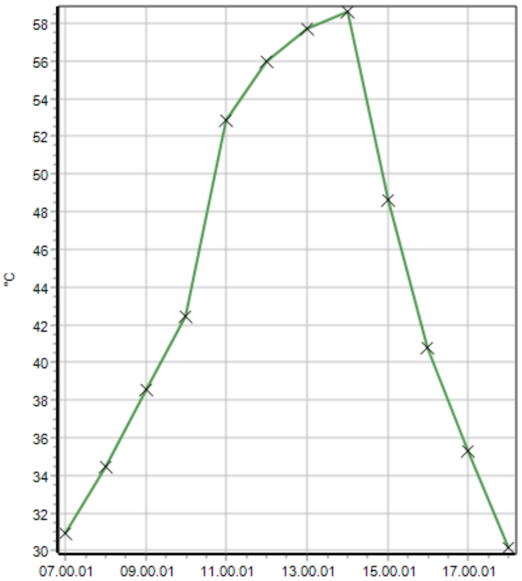

Graph 5. 18 PET calculated by Envi-met for scenario AR1 (b) in eastern side of the road

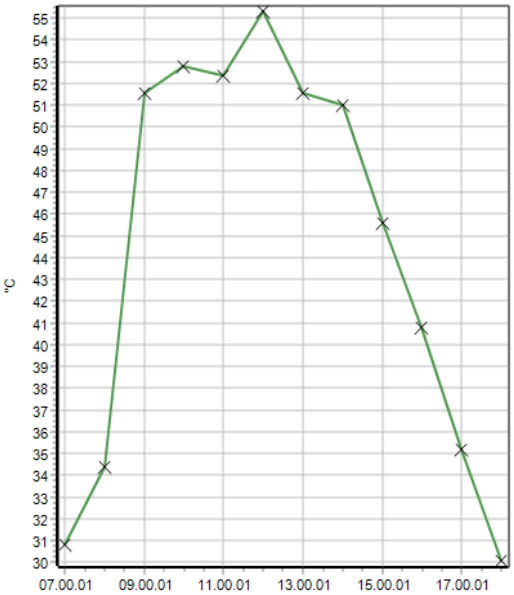

Graph 5. 17 PET calculated by Envi-met for scenario AR1 (b) in western side of the road

The graph 12 demonstrates that the temperature peaks around 12:00 p.m. on the western side of the street, where total shade was seen on solar analysis, and then begins to fall during peak hours. However, on the eastern side, where no shade was accessible after 12:00 hours, the temperature peaks at 14:00 hours and falls after 16:00 hours when the shading is visible. Hence, this proves that the shading of the street decreases the PET temperature.

d) UTCI calculation

The UTCI temperature reaches 47 °C at 12:00 hours which is very high temperature. The UTCI temperature drops to 33.8 °C only after 17:00 hours. This means the streets are extremely hot throughout the day.

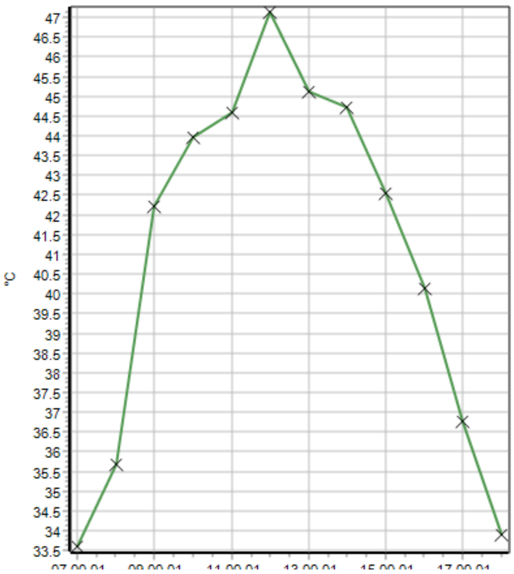

Graph 5. 19 UTCI temperature predicted by Envi-met for scenario AR1 (b)

5.10. Scenario 7: AR 1.5 (b)

In this scenario, the height of building is 1.5 times the width of the street in this scenario. The aspect ratio formed is 1.5.

For the street of 17 m, the building height should be 25.5 m in order to create canyon of aspect ratio 1.5.

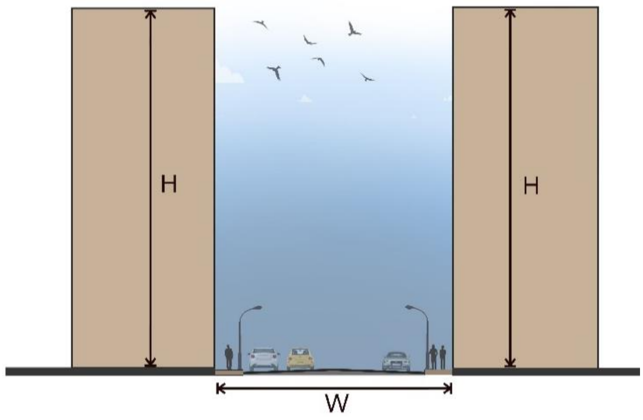

Figure 5. 47 section of street of scenario AR 1.5 (b)

5.10.1.Solar analysis

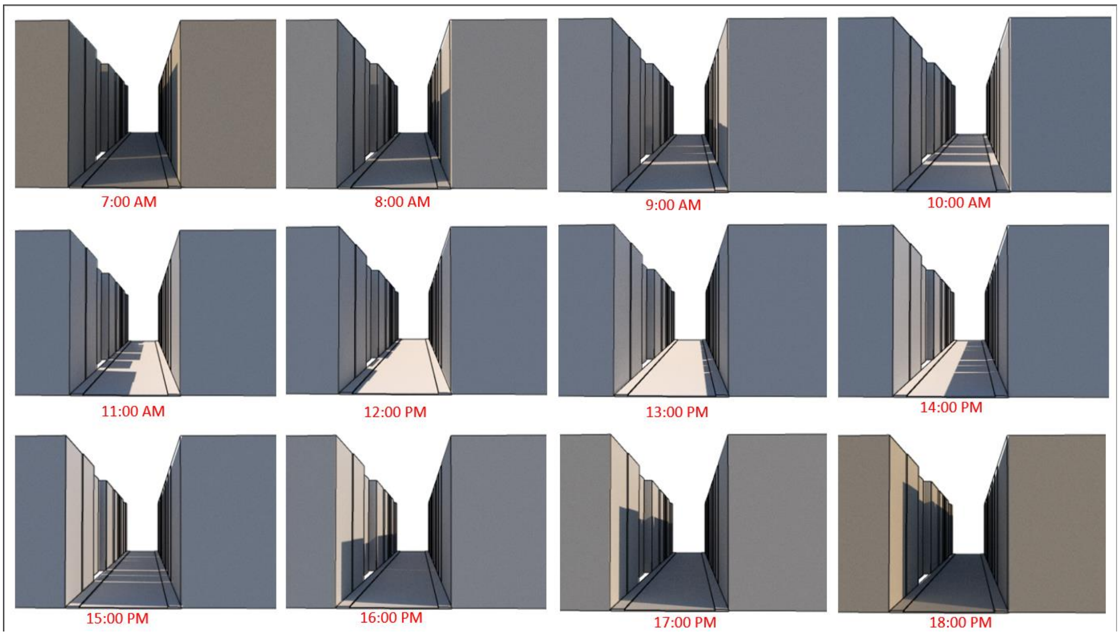

Figure 5. 48 solar analysis of scenario AR1.5 (b)

The shading pattern of the street changes with the change in orientation. The north south oriented streets are more shaded throughout the day than east west oriented streets. The figure above shows that at least one portion of the street is shaded always. The streets are little shaded at 12:00 hours otherwise the streets look thermally comfortable throughout day when analyzing the shading.

5.10.2.Simulation Results

a) Ambient air temperature

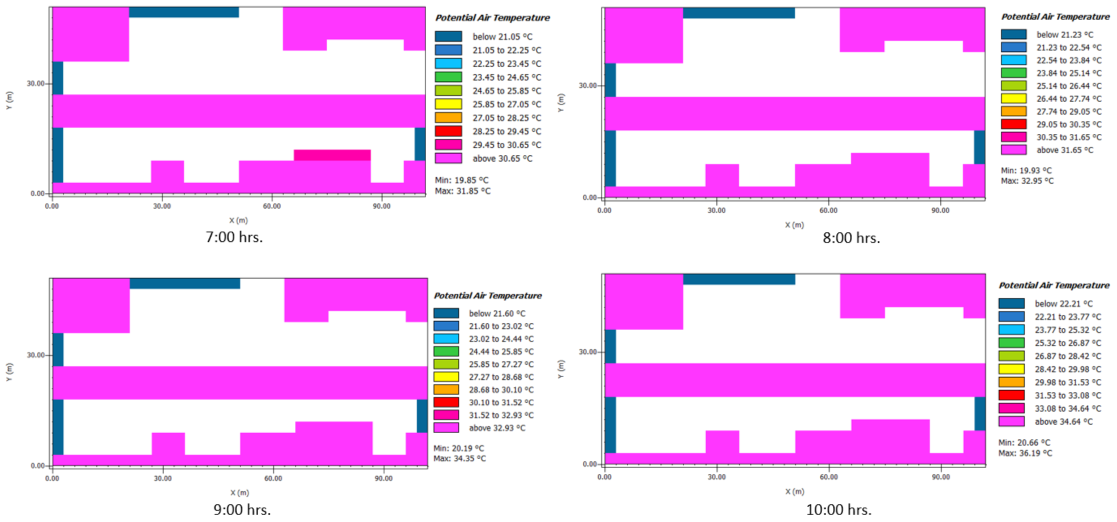

Figure 5. 49 Potential Air Temperature from 07:00 hrs. to 10:00 hrs. of scenario AR1.5 (b)

The graph shows that the temperature is lower than 31.85 °C at 7:00 hours but increases slowly by 1 °C -2 °C in every two hours. At 10:00 hours, the temperature is around 36.19 °C from 34.35 °C at 9:00 hours which is 1 °C less than the base model. The temperature is still quite high for the morning time.

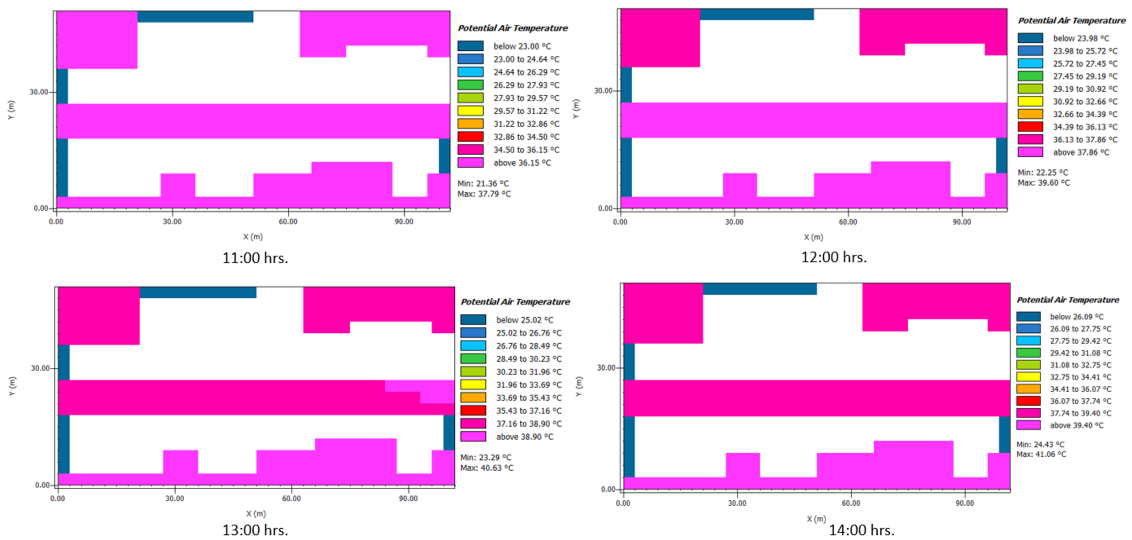

Figure 5. 50 Potential Air Temperature from 11:00 hrs. to 14:00 hrs. of scenario AR1.5 (b)

The temperature is rising at least a degree Celsius from 11:00 hours to 12:00 hours. However, the temperature drops below 38.90 °C from the north western side of the road at 13:00 hours. At 14:00 hours, the temperature of the street is 38.71 °C which is 2.5

°C less than the base model. During the peak hours the temperature of the streets is 1.5 °C to 2.5 °C less than the base model.

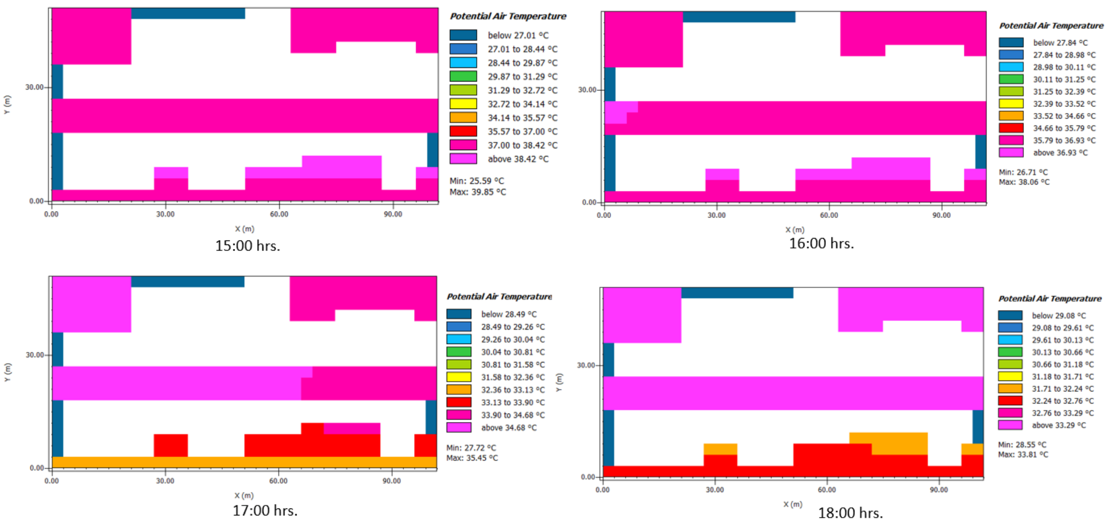

Figure 5. 51 Potential Air Temperature from 15:00 hrs. to 18:00 hrs. of scenario AR1.5 (b)

After 15:00 hours, the temperature continues to decline and reaches 37.79 °C. The temperature subsequently begins to fall from the southern side of the street, reaching 36.61 °C around 16:00 p.m. After 17:00 hours, like in previous scenarios, the streets are comfortable since the temperature falls below 35 °C.

The graph shows that the temperature peaks between 13:00 and 14:00 hours and then falls to about 37.7 °C the following hour, which is nearly 2.4 °C lower than the base model. Before 10:00 a.m., the temperature is less than 34 degrees Celsius. After 17:00 p.m., the temperature falls below 35 °C. Throughout the day, the temperature is 0.6 °C -2.4 °C lower than the base model.

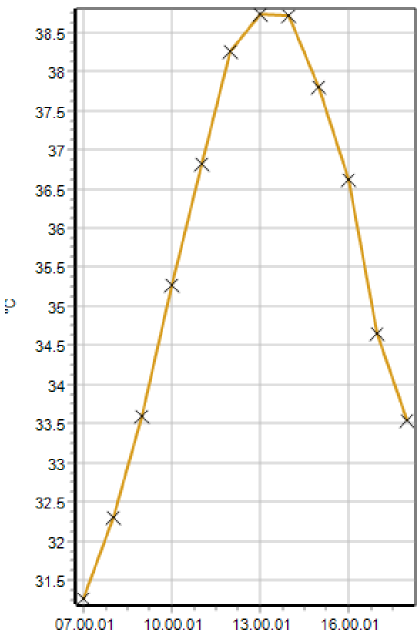

Graph 5. 20 air temperature predicted by Envi-met for scenario AR 1.5 (b)

b) Mean Radiant temperature

The mean radiant temperature rises sharply after 9:00 hours and reaches 57.63 °C by 11:00 hours the it starts to drop gradually. The MRT is 10 °C to 22.3 °C less than the base model during the peak hours. Since, the western part of the streets are partially or completely shaded after 12:00 hours, there is huge difference seen in mean radiant temperature for aspect ratio 1.5 in streets oriented to north south direction.

Table 5. 8 MRT temperature predicted by Envi-met for scenario AR1.5 (b)

Time	Mean Radiant Temperature (°C)
07.00.01	29.88
08.00.01	34.671
09.00.01	38.495
10.00.01	57.437
11.00.01	57.631
12.00.01	54.163
13.00.01	52.371
14.00.01	49.751
15.00.01	46.323
16.00.01	42.562
17.00.01	34.997
17.59.59	25.915

c) PET calculation

The graph 15 demonstrates that the temperature peaks around 11:00 hours on the western side of the street, where total shade was seen on solar analysis, and then begins to fall during peak hours. However, on the eastern side, where no shade was accessible after 12:00 hours, the temperature peaks at 13:00 hours and falls after 14:00 hours when the shading is visible. Hence, this proves that the shading of the street decreases the PET temperature.

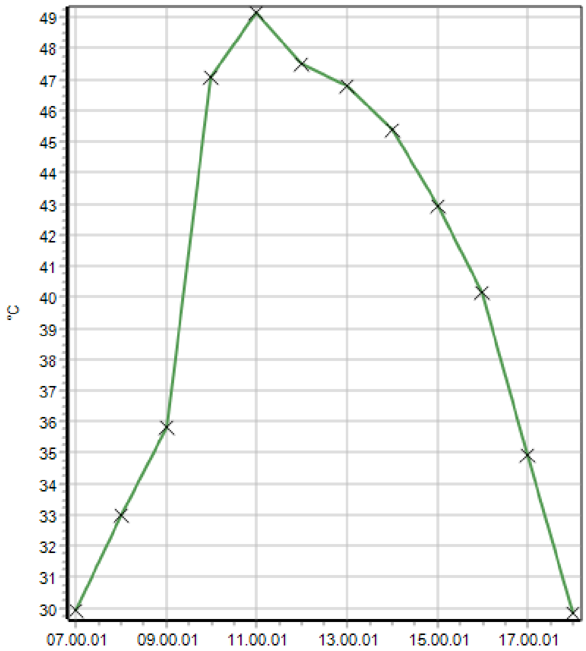

Graph 5. 22 calculated by Envi-met for scenario AR1.5 (b) in western side of the road

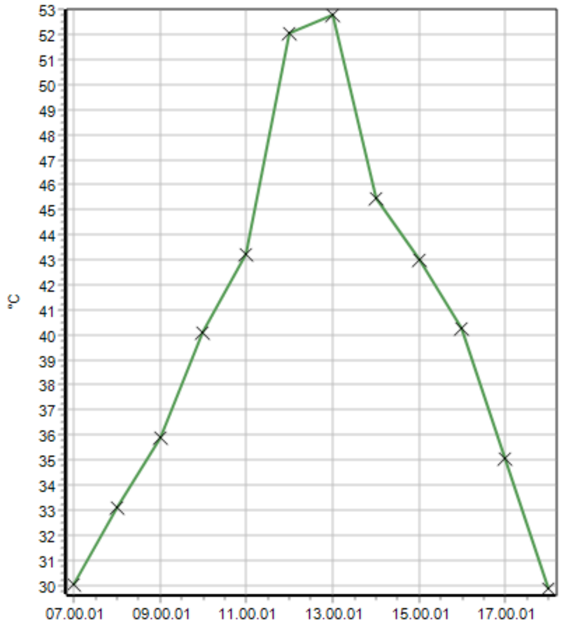

Graph 5. 21 PET calculated by Envi-met for scenario AR1.5 (b) in eastern side of the road

d) UTCI calculation

The UTCI temperature reaches 44 °C at 12:00 hours which is very high temperature. The UTCI temperature drops to 33.4 °C only after 17:00 hours. This means the streets are extremely hot throughout the day. The UTCI temperature is 1.7 °C - 6.8 °C less than the base model throughout the day.

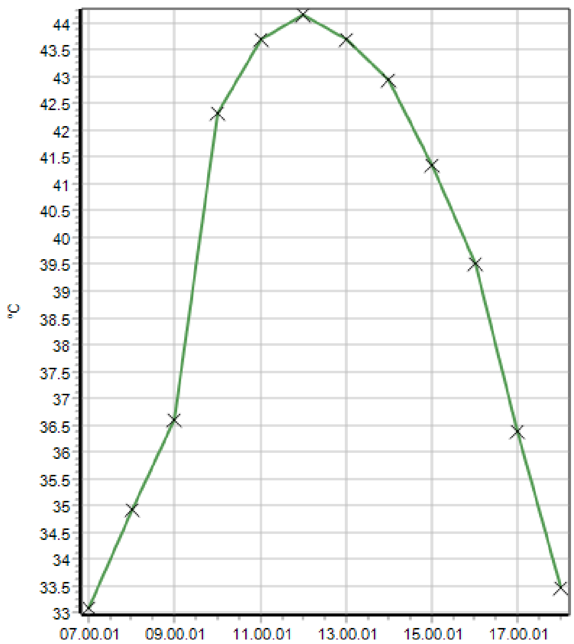

Graph 5. 23 UTCI calculated by Envi-met for scenario AR1.5 (b)

5.11. Scenario 8: AR 2 (b)

In this scenario, the height of building is twice the width of the street in this scenario. The aspect ratio formed is 2.

Aspect ratio = H/W

2 = H/W

H= Wx2

For the street of 17 m, the building height should be 34 m in order to create canyon of aspect ratio 2.

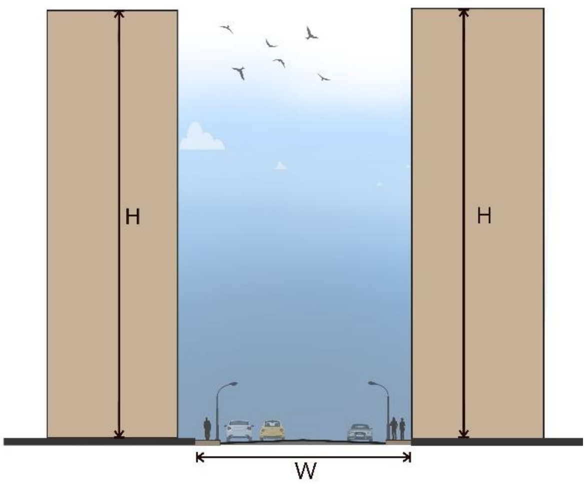

Figure 5. 52 section of street of scenario AR 2 (b)

5.11.1.Solar analysis

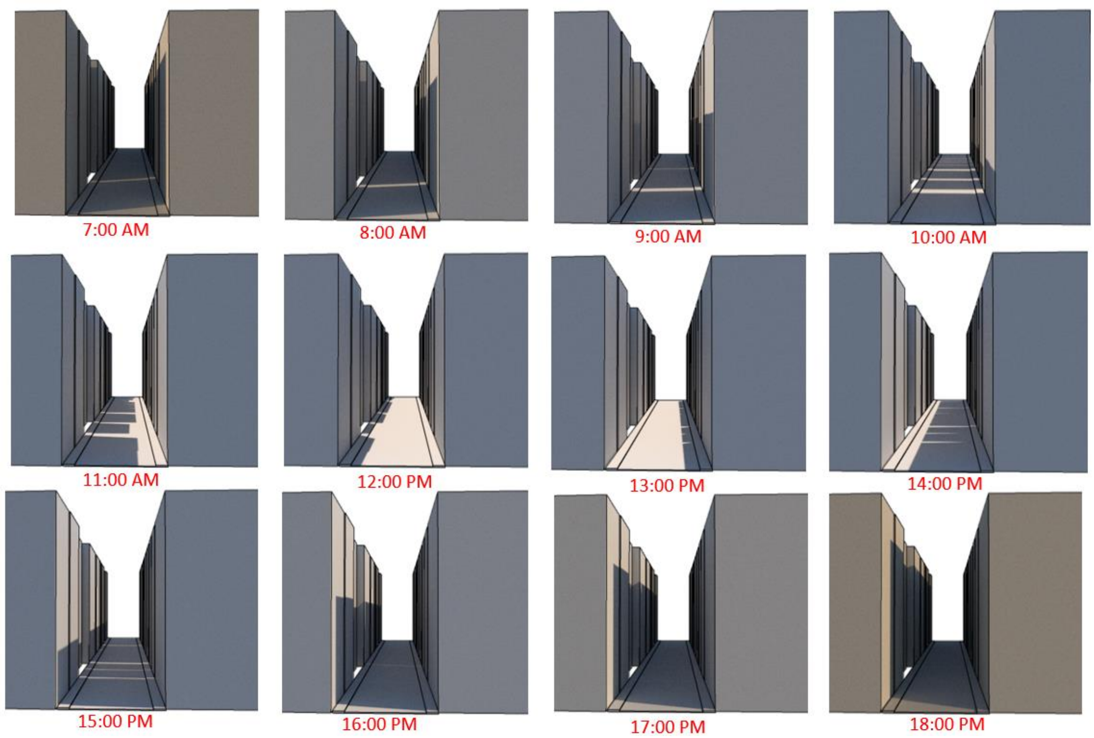

Figure 5. 53 solar analysis of scenario AR 2(b)

Throughout the day, the street is entirely or partially shaded. In the morning hours from 7 :00 to 9 :00 hours, the sunrays start invading the western side of the street section through narrow openings between the buildings, slightly lighting the eastern face of the western side buildings in streaks. 9 AM onwards the western buildings start getting illuminated by the solar radiation almost completely. From 11 AM onwards the street also starts getting illuminated quarterly till 12:00 when it is completely illuminated. The solar position changes after 12 PM as the east side of the street starts getting illuminated. After 14:00 hours, almost whole street is shaded, and after 15:00 hours, the building façade of one side of the road is also shaded, potentially reducing the building's cooling demand. According to solar study, streets aligned towards north-south with aspect ratio 2 appear thermally pleasant.

5.11.2.Simulation Results

a) Ambient air temperature

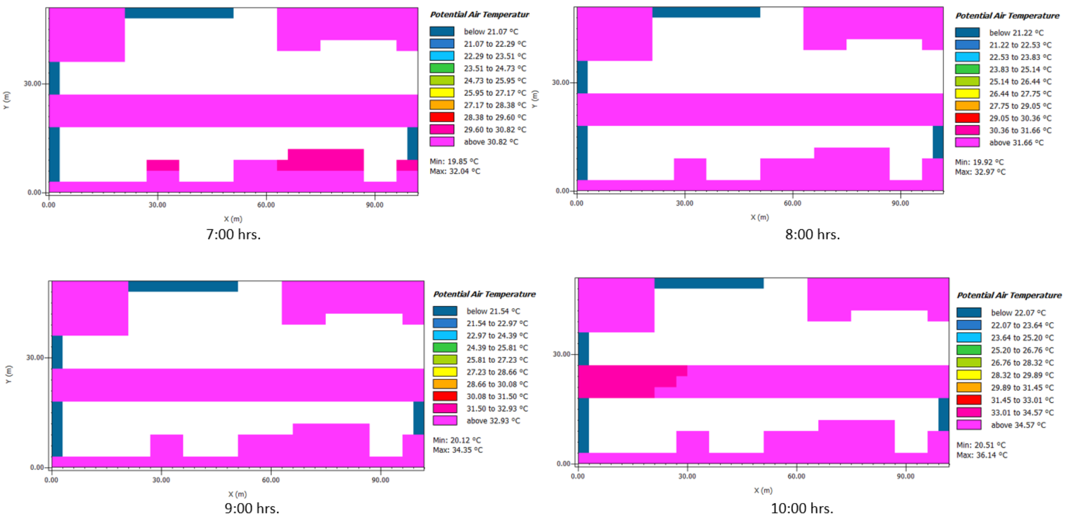

Figure 5. 54 Potential Air Temperature from 07:00 hrs. to 10:00 hrs. of scenario AR 2 (b)

The graph shows that the temperature is lower than 32.04 °C at 7:00 hours but increases slowly by 1 °C -2 °C in every two hours. At 10:00 hours, the temperature is around 36.14 °C from 34.35 °C at 9:00 hours which is 1 °C less than the base model. The temperature is still quite high for the morning time.

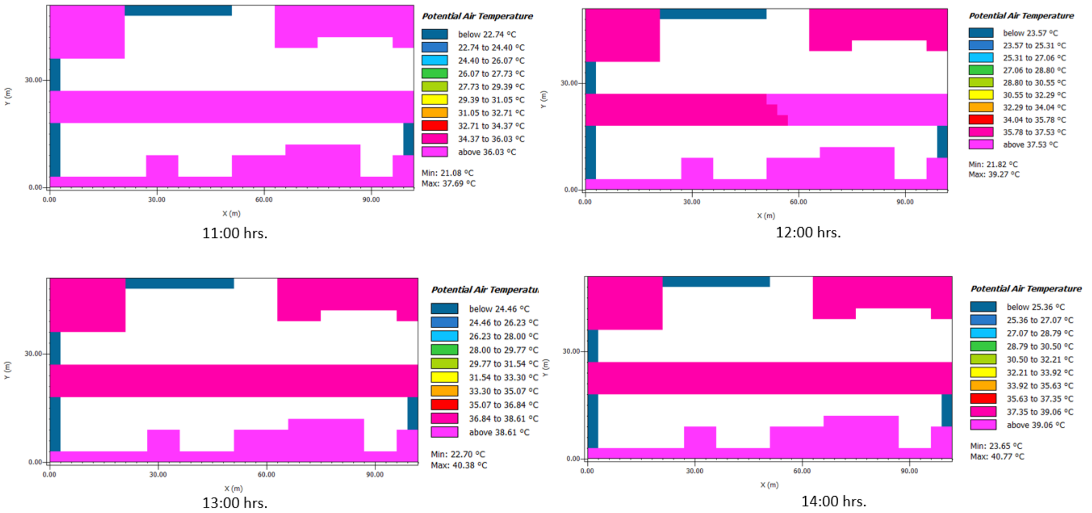

Figure 5. 55 Potential Air Temperature from 11:00 hrs. to 14:00 hrs. of scenario AR2 (b)

The temperature is rising at least a degree Celsius from 11:00 hours to 12:00 hours. However, the temperature drops below 38.61 °C from the north western side of the road at 13:00 hours. At 14:00 hours, the temperature of the street is 39.06 °C which is 2.3 °C less than the base model. During the peak hours the temperature of the streets is 2.4 °C less than the base model.

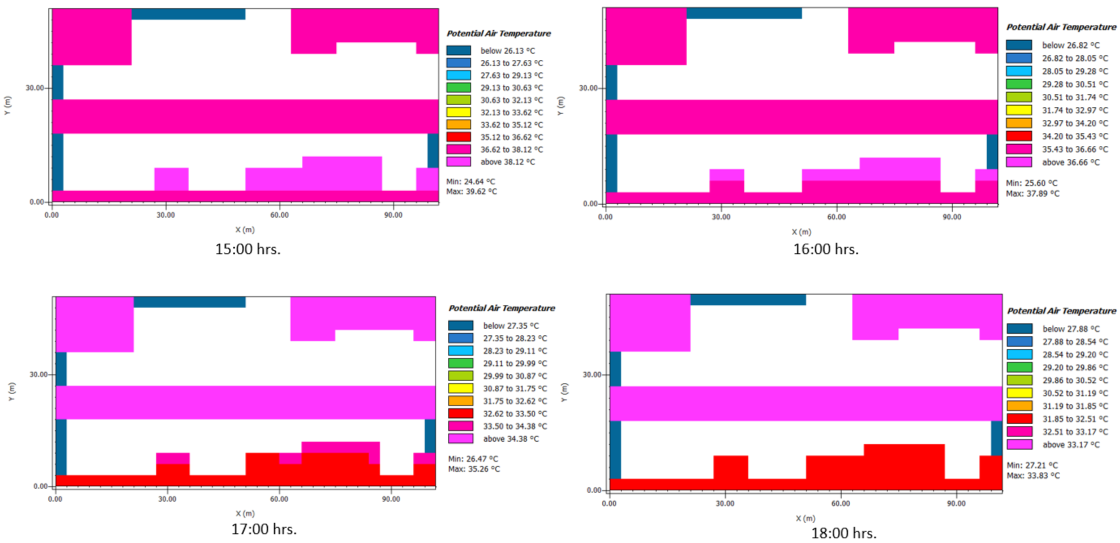

Figure 5. 56 Potential Air Temperature from 15:00 hrs. to 18:00 hrs. of scenario AR2 (b)

After 15:00 hours, the temperature continues to decline and reaches 39.62 °C. The temperature subsequently begins to fall from the northern side of the street, reaching 36.66 °C around 16:00 p.m. After 17:00 hours, like in previous scenarios, the streets are comparatively comfortable since the temperature falls below 35 °C.

The graph shows that the temperature peaks between 13:00 and 14:00 hours and then falls to about 37.6 °C the following hour, which is nearly 4 °C lower than the base model. Before 10:00 a.m., the temperature is less than 35 degrees Celsius. After 17:00 p.m., the temperature falls below 35 °C. Throughout the day, the temperature is 0.75°C - 2.4°C lower than the base model.

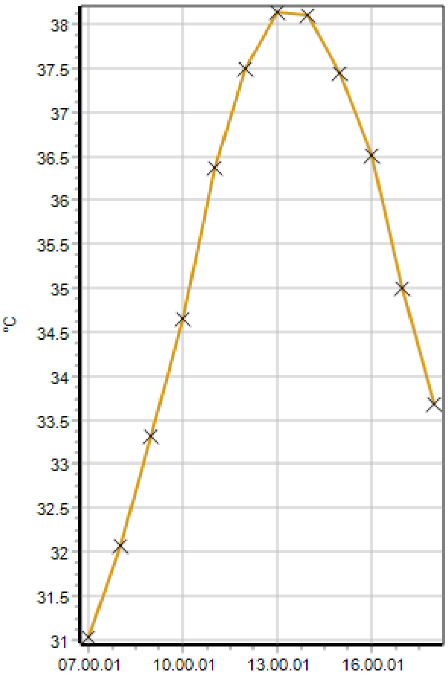

Graph 5. 24 Air temperature calculated by Envi-met for scenario AR2 (b)

b) Mean Radiant temperature

The mean radiant temperature rises sharply after 9:00 hours and reaches 57.03 °C by 11:00 hours the it starts to drop gradually. The MRT is 18 °C to 23.65 °C less than the base model during the peak hours. Since, the eastern part of the streets are partially or completely shaded after 14:00 hours, a huge difference is seen in mean radiant temperature for aspect ratio 2 in streets oriented to north south direction.

Table 5. 9 MRT temperature predicted by Envi-met for scenario AR 2(b)

Time	Mean Radiant Temperature (°C)
07.00.01	30.019
08.00.01	34.493
09.00.01	37.887
10.00.01	54.641
11.00.01	57.033
12.00.01	50.689
13.00.01	50.923
14.00.01	47.267
15.00.01	45.294
16.00.01	41.903
17.00.01	34.832

17.59.59	25.696

c) PET calculation

The graph 15 demonstrates that the temperature peaks around 11:00 hours on the western side of the street, where somewhat total shade was seen on solar analysis, and then begins to fall during peak hours. However, on the eastern side, where no shade was accessible after 12:00 hours, the temperature peaks at 13:00 hours and falls after 13:00 hours when the shading is visible. Hence, this proves that the shading of the street decreases the PET temperature.

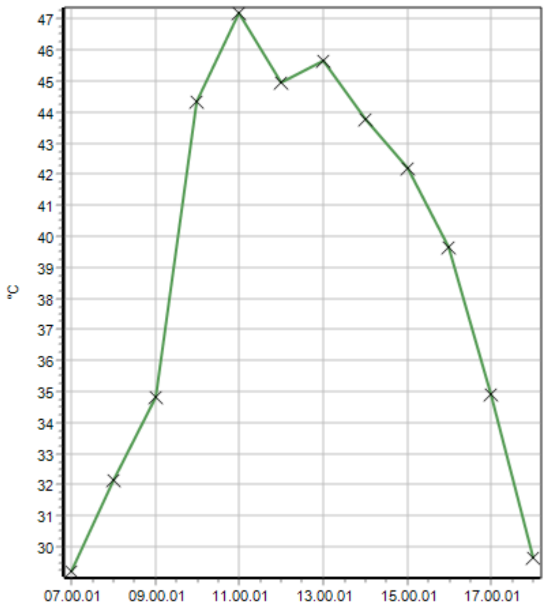

Graph 5. 26 PET calculated by Envi-met for scenario AR 2 (b) in western side of the road

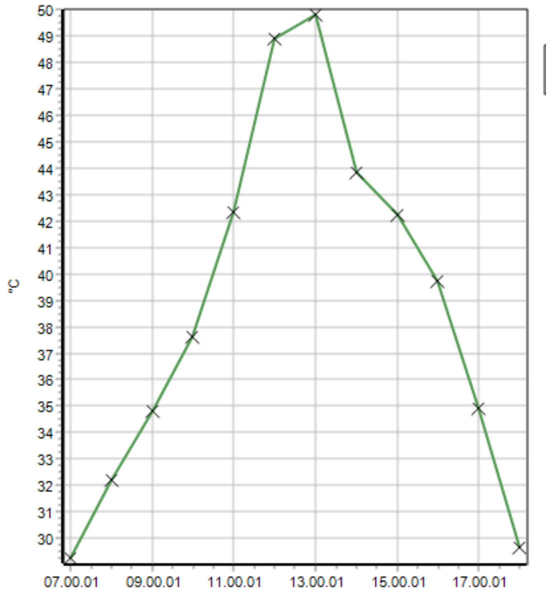

Graph 5. 25 PET calculated by Envi-met for scenario AR 2 (b) in eastern side of the road

d) UTCI calculation

The UTCI temperature reaches 42.6 °C at 11:00 hours which is very high temperature and then drops to 41.8°C at 12:00 hours only to rise back to 42.4°C at 13:00 hours. The UTCI temperature drops to 32.5 °C only after 17:00 hours. This means the streets are extremely hot throughout the day. The UTCI temperature is 0.4 °C – 8.5 °C less than the base model throughout the day.

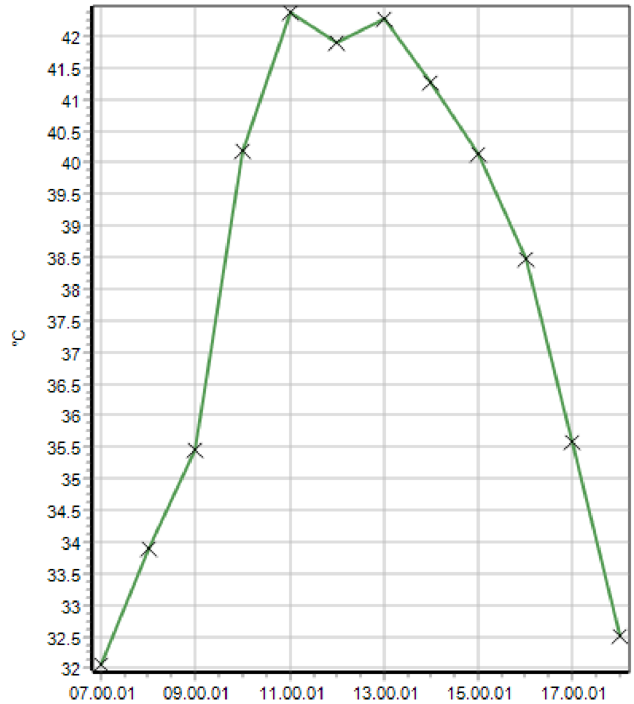

Graph 5. 27 UTCI calculated by Envi-met for scenario AR2 (b)

5.12. Scenario 9: AR 3 (b)

In this scenario, the height of building is three times the width of the street in this scenario. The aspect ratio formed is 3.

For the street of 17 m, the building height should be 51 m in order to create canyon of aspect ratio 3.

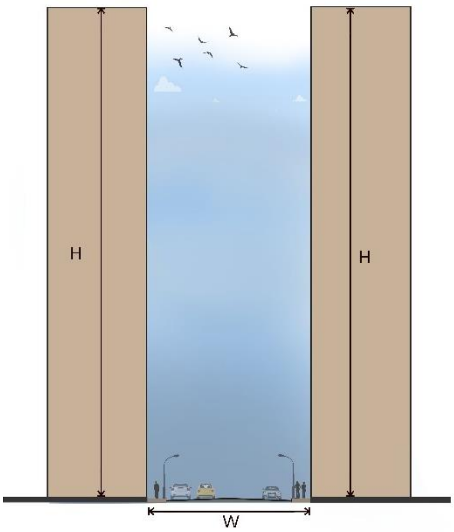

Figure 5. 57 section of street of scenario AR 3(b)

5.12.1.Solar analysis

Figure 5. 58 solar analysis of scenario AR 3(b)

Throughout the day, the street is entirely or partially shaded. The street is illuminated only between 12:00 hours and 14:00 hours. After 14:00 hours, practically the whole street is shaded, and after 15:00 hours, the façade of the building is also shaded, potentially reducing the building's cooling demand. According to solar study, streets aligned towards north-south with aspect ratio 3 appear thermally pleasant.

5.12.2.Simulation Results

a) Ambient air temperature

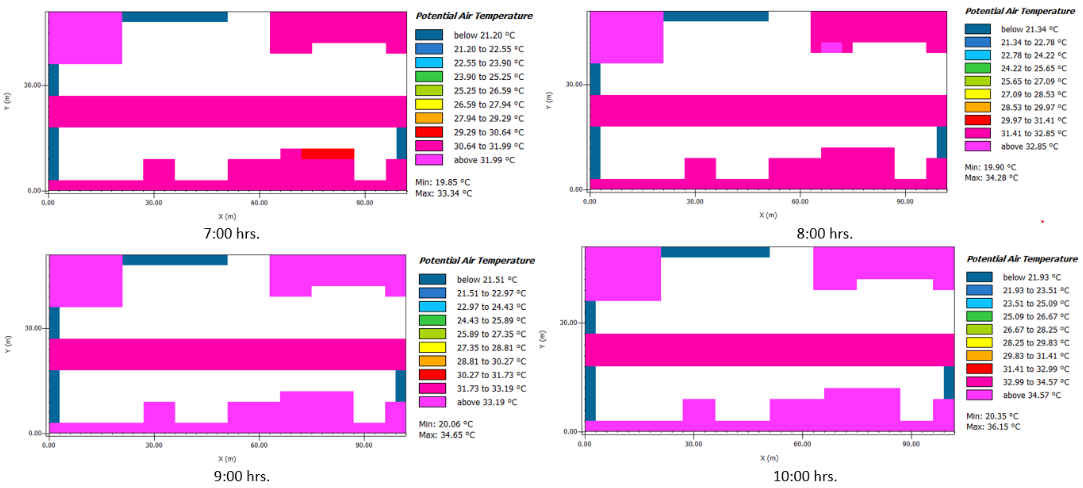

Figure 5. 59 Potential Air Temperature from 07:00 hrs. to 10:00 hrs. of scenario AR 3 (b)

The graph shows that the temperature is lower than 33.34 °C at 7:00 hours but increases slowly by 1 °C -2 °C in every two hours. At 10:00 hours, the temperature is around 36.15 °C from 34.65 °C at 9:00 hours which is around 1 °C less than the base model. The temperature is still quite high for the morning time.

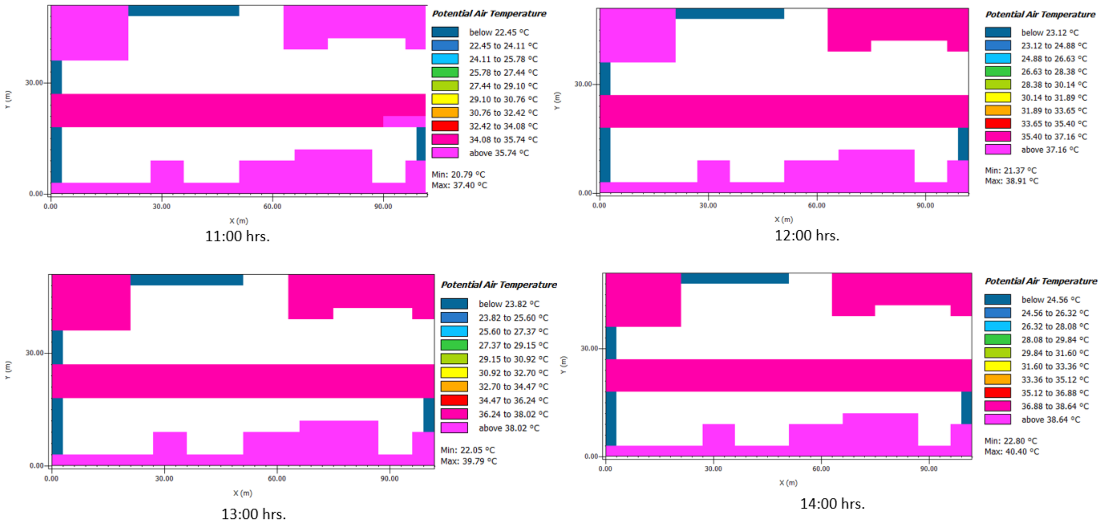

Figure 5. 60 Potential Air Temperature from 11:00 hrs. to 14:00 hrs. of scenario AR 3 (b)

The temperature is rising at least a degree Celsius from 11:00 hours to 12:00 hours. However, the temperature drops below 38.02 °C from the north western side of the road at 13:00 hours. At 14:00 hours, the temperature of the street is 38.64 °C which is 2.72°C less than the base model. During the peak hours the temperature of the streets is 2.72 °C to 3 °C less than the base model.

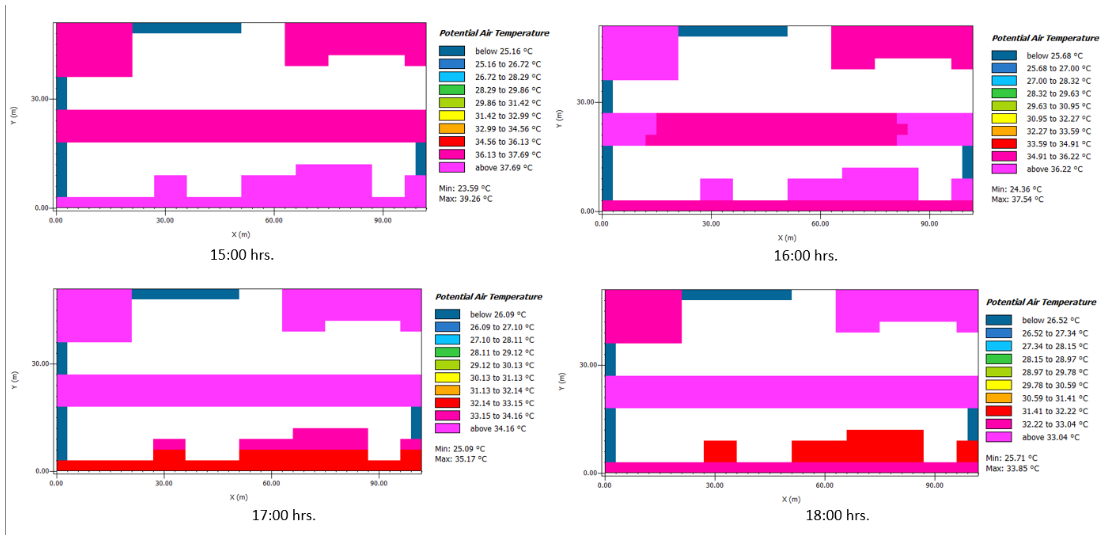

Figure 5. 61 Potential Air Temperature from 15:00 hrs. to 18:00 hrs. of scenario AR 3 (b)

After 15:00 hours, the temperature continues to decline and reaches 39.26 °C. The temperature subsequently begins to fall from the middle of the street, reaching 36.22 °C around 16:00 p.m. After 17:00 hours, like in previous scenarios, the streets are comfortable since the temperature falls below 35 °C.

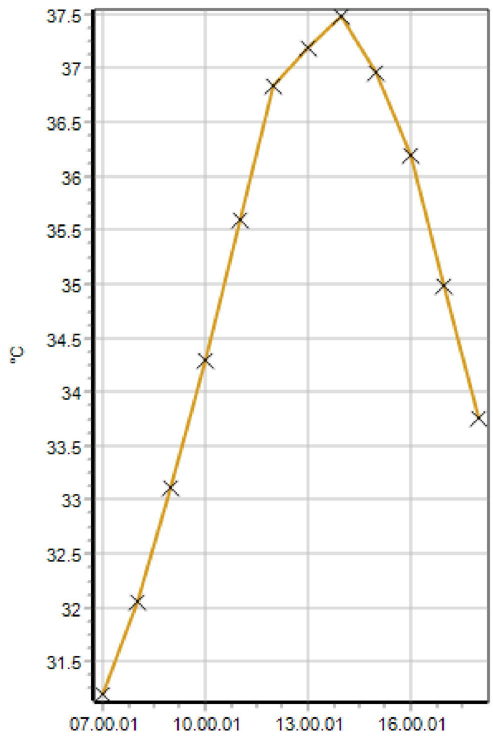

Graph 5. 28 Air temperature calculated by Envi-met for scenario AR3 (b)

The graph shows that the temperature peaks between 14:00 hours and 15:00 hours and then falls to about 36.3 °C the following hour, which is nearly 2.72 °C lower than the base model. Before 10:00 a.m., the temperature is less than 34.5 degrees Celsius. After 17:00 p.m., the temperature falls below 35 °C. Throughout the day, the temperature is 1.5 °C - 3.86 °C lower than the base model.

b) Mean Radiant temperature

The mean radiant temperature rises sharply after 9:00 hours and reaches 53.34 °C by 11:00 hours the it starts to drop gradually. The MRT is 1 °C to 17.6 °C less than the base model during the peak hours. Since, the western part of the streets are partially or completely shaded after 12:00 hours, there is huge difference seen in mean radiant temperature for aspect ratio 3 in streets oriented to north south direction.

Table 5. 10 MRT temperature predicted by Envi-met for scenario AR 3 (b)

Time	Mean Radiant Temperature (°C)
07.00.01	30.552
08.00.01	34.848
09.00.01	37.758
10.00.01	40.171
11.00.01	53.336
12.00.01	48.443
13.00.01	45.652
14.00.01	45.188
15.00.01	44.115
16.00.01	41.288

17.00.01	34.587
17.59.59	25.466

c) PET calculation

The graph 15 demonstrates that the temperature peaks around 11:00 hours on the western side of the street, where total shade was seen on solar analysis, and then begins to fall during peak hours. However, on the eastern side, where shade was accessible after 13:00 hours, the temperature peaks at 13:00 hours and falls after 14:00 hours when the shading is visible. Hence, this proves that the shading of the street decreases the PET temperature.

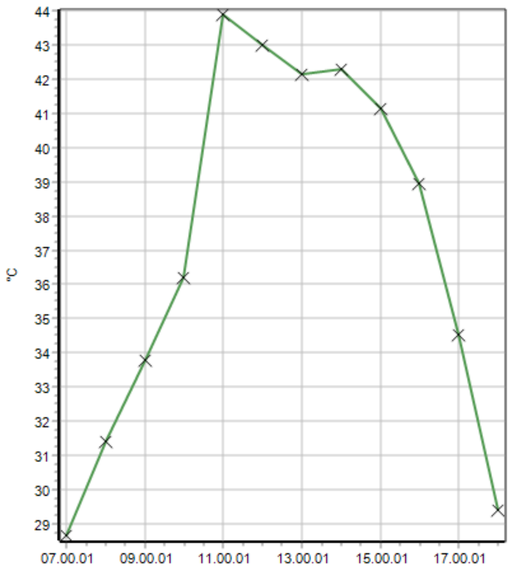

Graph 5. 30 PET calculated by Envi-met for scenario AR 3 (b) in western side of the road

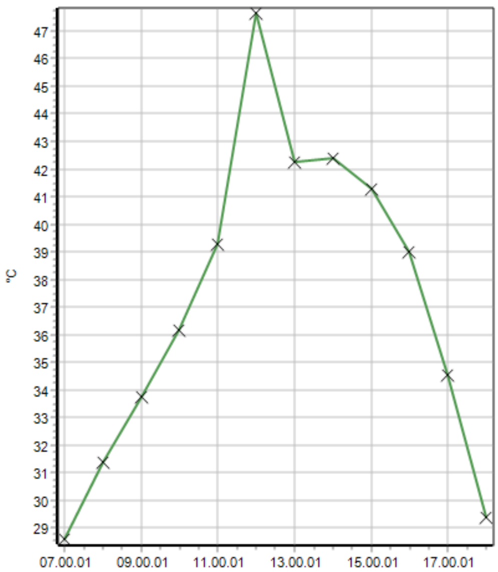

Graph 5. 29 PET calculated by Envi-met for scenario AR 3 (b) in eastern side of the road

d) UTCI calculation

The UTCi temperature reaches 39.5 °C at 12:00 hours which is very high temperature and then drops to 39.2℃ at 13:00 hours only to rise back to 39.4℃ at 14:00 hours. The UTCI temperature drops to 31.3 °C only after 17:00 hours. This means the streets are extremely hot throughout the day. The UTCI temperature is 1.6 °C – 10.6 °C less than the base model throughout the day.

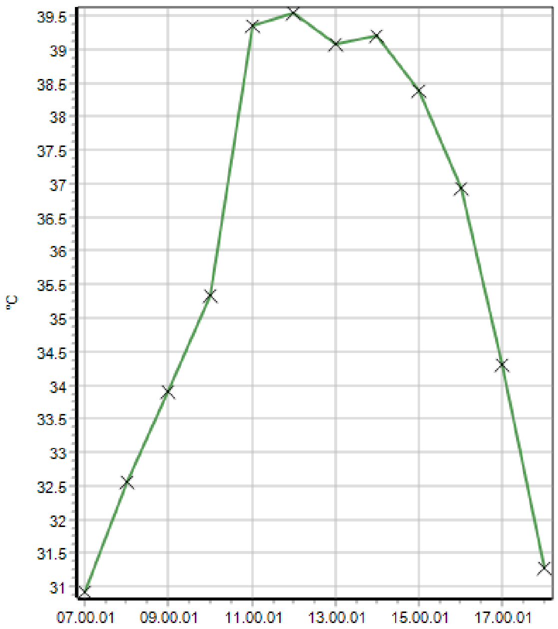

Graph 5. 31 UTCI calculated by Envi-met for scenario AR 3 (b)

After validation of the best-case scenario of 1.5 aspect ratio, further simulations were carried out covering all possible street orientation from 0 to 360 degrees. The results obtained were in the form of Air temperature, MRT, PET and UTCI.

5.13. Sensitivity Analysis

1. 10 degrees

Here, the street north was rotated by an angle of 10 degrees towards west in an anticlockwise direction which also covers an inclination of 190 degrees.

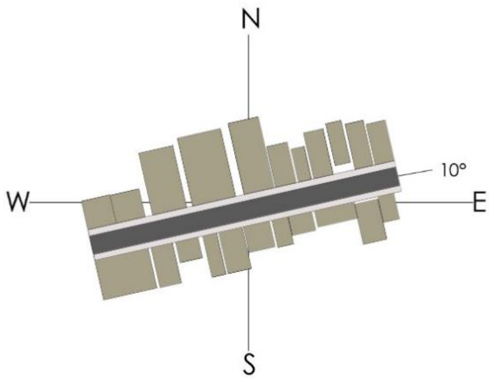

Figure 5. 62 sensitivity analysis 10 degrees

a. Air Temperature

Beginning from 7 AM, we can see gradual increase of air temperature in this street section which peaks at about 2PM with the value of 39.5°C. As the day passes on, the temperature changes to 39.3°C and then finally reaching 33.5°C at 6PM. As expected, due to the change in sun position, we can observe this changing behavior of the air temperature graph as shown in graph 5.33.

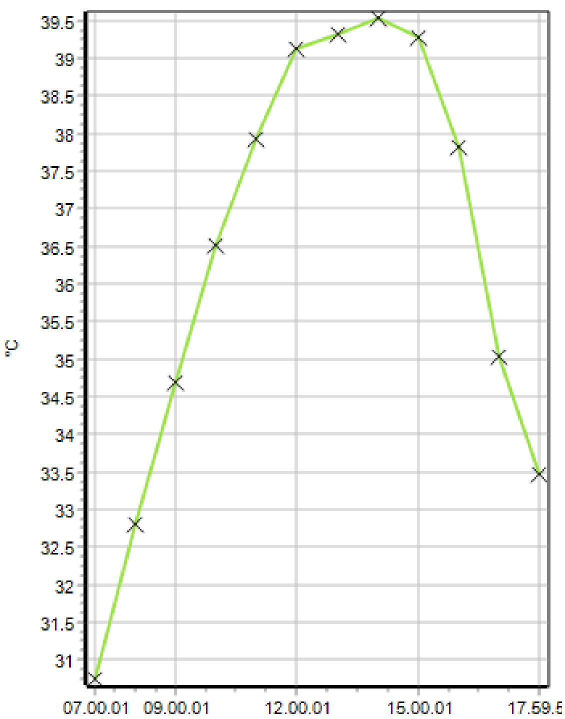

Graph 5. 33 Air Temperature of 1.5/10 degrees

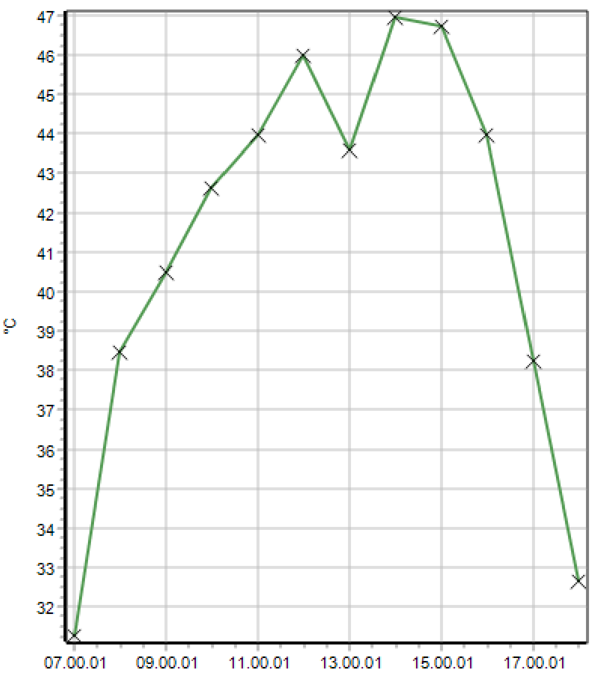

Graph 5. 32 UTCI graph for 1.5/10 degrees

b. UTCI

The graph of UTCI is a bit different than that of the air temperature as the first peak of 46°Cis reached at 12PM and then massively drops at 1PM to 43.5°C. Then again, the value rises to 47°C and finally reaching 32.5°C at 6PM. This creates an M shaped curve.

2. **20 Degrees**

Here, the street north was rotated by an angle of 20 degrees towards west in an anticlockwise direction which also covers an inclination of 200 degrees.

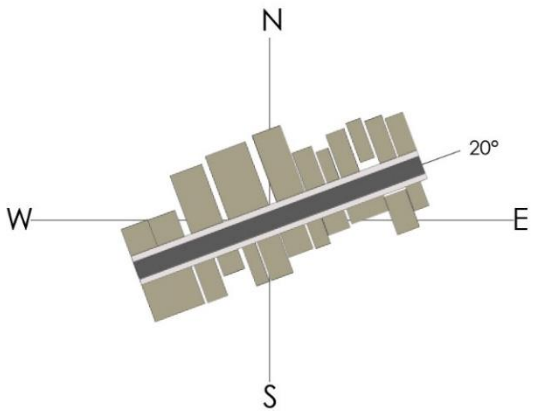

Figure 5. 63 sensitivity analysis for 20 degrees

a. Air Temperature

Beginning from 7 AM, we can see gradual increase of air temperature in this street section which peaks at about 12PM with the value of 39°C. As the day passes on, the temperature changes to 39.3°C and then finally reaching 33.5°C at 6PM. As expected, due to the change in sun position, we can observe this changing behavior of the air temperature graph as shown in graph 5.35.

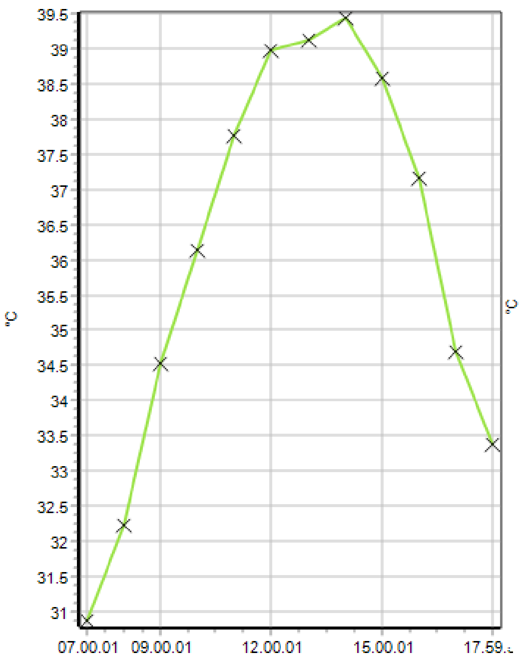

Graph 5. 35 Air temperature graph for 1.5/20 degrees

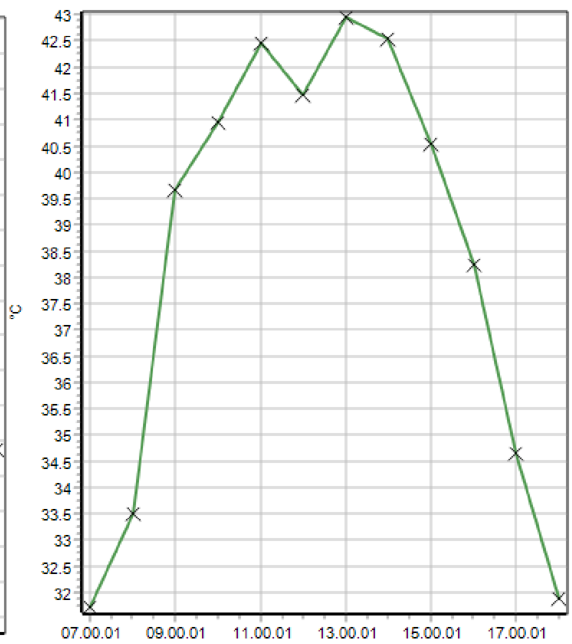

Graph 5. 34 UTCI graph for 1.5/20 degrees

b. UTCI

The graph of UTCI is a bit different than that of the air temperature as the first peak of 42.5°C is reached at 11PM and then drops at 12 PM to 41.5°C. Then again, the value rises to 43°C and finally reaching 32°C at 6PM. This creates an M shaped curve.

3. 30 Degrees

Here, the street north was rotated by an angle of 30 degrees towards west in an anticlockwise direction which also covers an inclination of 210 degrees.

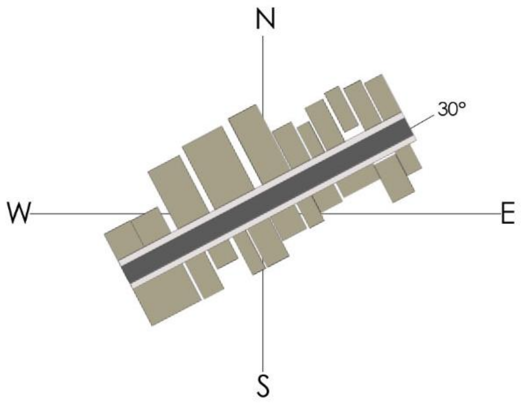

Figure 5. 64 sensitivity analysis for 30 degrees

a. Air Temperature

Beginning from 7 AM, we can see gradual increase of air temperature in this street section which peaks at about 2PM with the value of 39.5℃. As the day passes on, the temperature changes to 39.3℃ and then finally reaching 33.5℃ at 6PM. As expected, due to the change in sun position, we can observe this changing behavior of the air temperature graph as shown in graph 5.36.

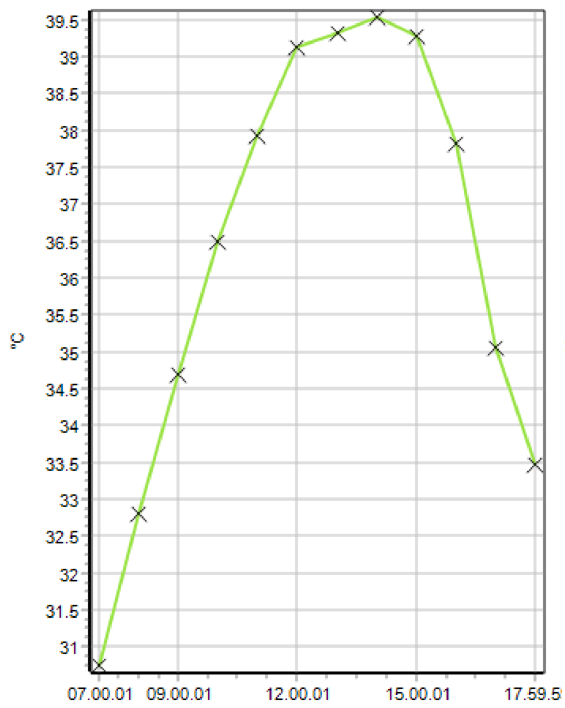

Graph 5. 36 Air temperature graph for 1.5/30 degrees

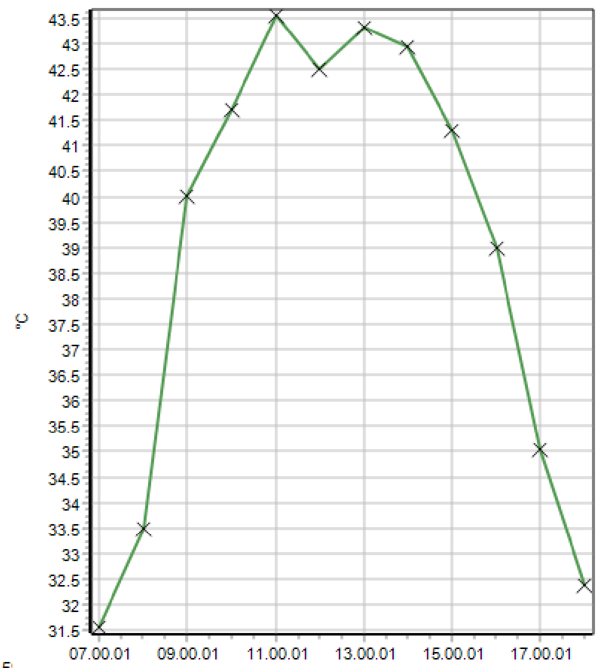

Graph 5. 37 UTCI graph for 1.5/30 degrees

b. UTCI

The graph of UTCI is a bit different than that of the air temperature as the first peak of 43.5℃ is reached at 11PM and then drops at 1PM to 42.5℃. Then again, the value rises to 43.3℃ and finally reaching 32.5℃ at 6 PM. This creates an M shaped curve.

4. **40 Degrees**

Here, the street north was rotated by an angle of 40 degrees towards west in an anticlockwise direction which also covers an inclination of 220 degrees.

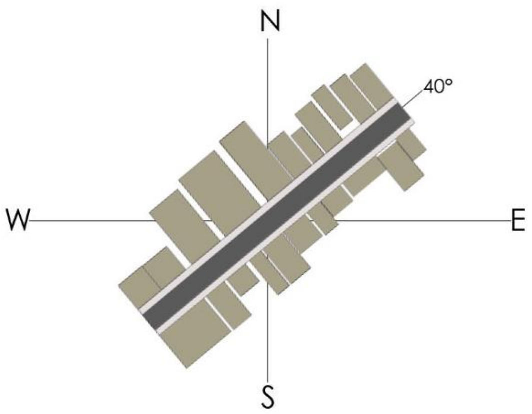

Figure 5. 65 sensitivity analysis for 40 degrees

a. Air Temperature

Beginning from 7 AM, we can see gradual increase of air temperature in this street section which peaks at about 2PM with the value of 38.5℃. As the day passes on, the temperature changes to 37.7℃ and then finally reaching 33℃ at 6PM. As expected, due to the change in sun position, we can observe this changing behavior of the air temperature graph as shown in graph 5.39.

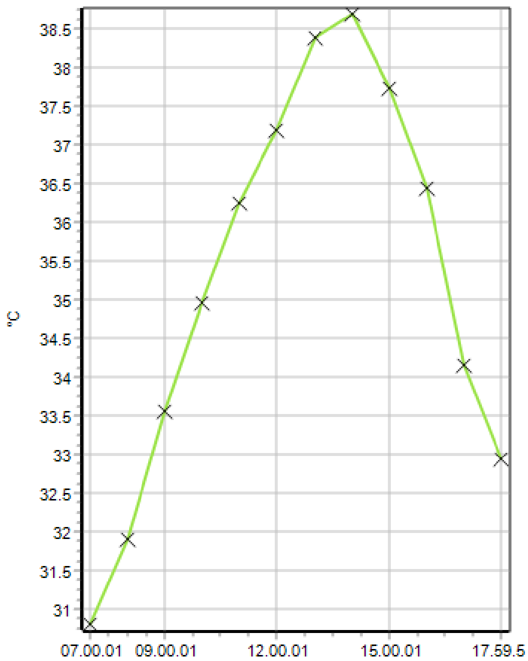

Graph 5. 39 Air Temperature graph for 1.5/40 degrees

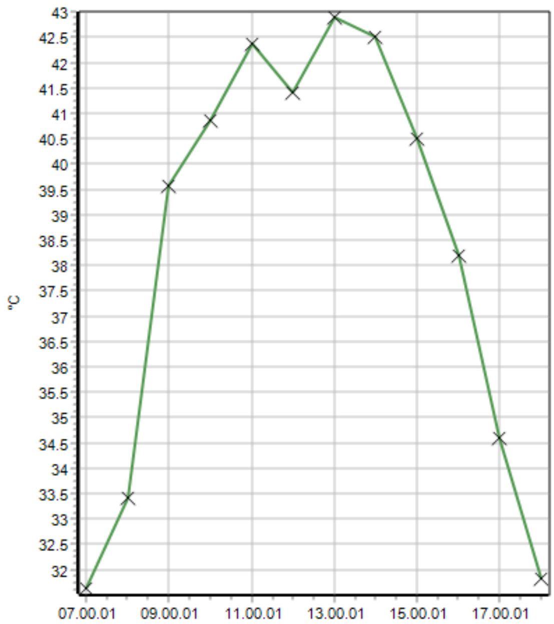

Graph 5. 38 UTCI graph for 1.5/40 degrees

b. UTCI

The graph of UTCI is a bit different than that of the air temperature as the first peak of 42.3℃ is reached at 11PM and then drops at 12PM to 41.5℃. Then again, the value rises to 42.8℃ and finally reaching 31.8℃ at 6 PM. This creates an M shaped curve.

5. 50 Degrees

Here, the street north was rotated by an angle of 50 degrees towards west in an anticlockwise direction which also covers an inclination of 230 degrees.

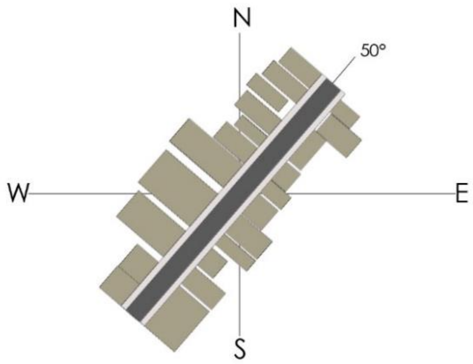

Figure 5. 66 sensitivity analysis for 50 degrees

a. Air Temperature

Beginning from 7 AM, we can see gradual increase of air temperature in this street section which peaks at about 2PM with the value of 38.8°C. As the day passes on, the temperature changes to 38°C and then finally reaching 33.4°C at 6PM. As expected, due to the change in sun position, we can observe this changing behavior of the air temperature graph as shown in graph 5.40.

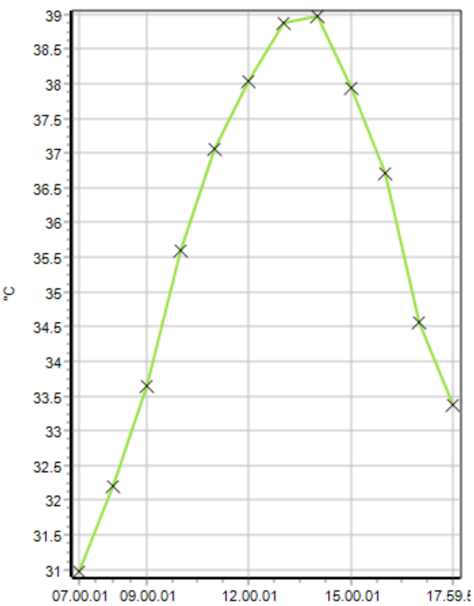

Graph 5. 40 Air temperature graph for 1.5/50 degrees

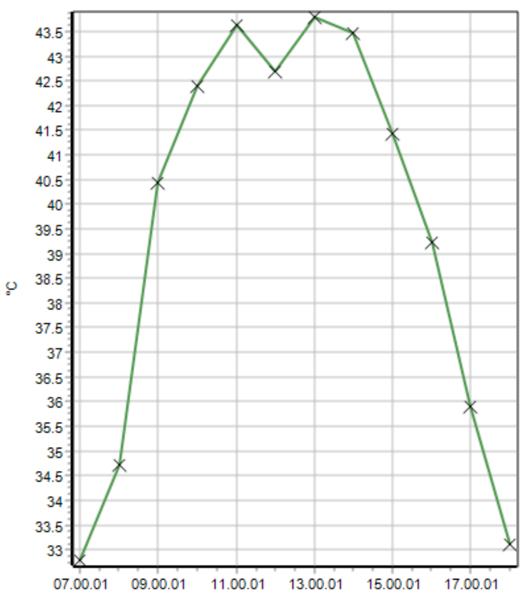

Graph 5. 41 UTCI graph for 1.5/50 degrees

b. UTCI

The graph of UTCI is a bit different than that of the air temperature as the first peak of 43.5°C is reached at 11PM and then drops at 12PM to 42.7°C. Then again, the value rises to 43.8°C and finally reaching 33°C at 6 PM. This creates an M shaped curve.

6. 60 Degrees

Here, the street north was rotated by an angle of 30 degrees towards west in an anticlockwise direction which also covers an inclination of 240 degrees.

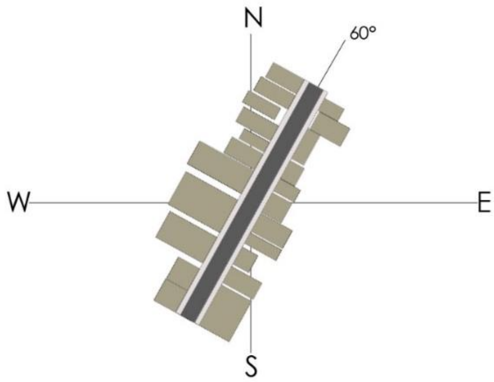

Figure 5. 67 sensitivity analysis for 60

a. Air Temperature

Beginning from 7 AM, we can see gradual increase of air temperature in this street section which peaks at about 2PM with the value of 38.8°C. As the day passes on, the temperature changes to 37.6°C and then finally reaching 33.4°C at 6PM. As expected, due to the change in sun position, we can observe this changing behavior of the air temperature graph as shown in graph 5.43.

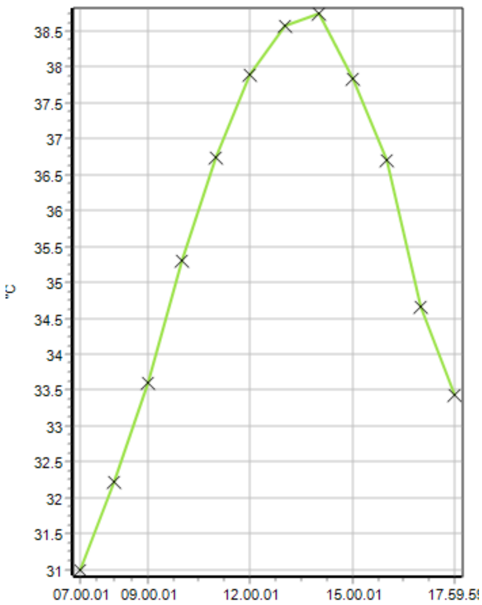

Graph 5. 43 Air temperature graph for 1.5/60 degrees

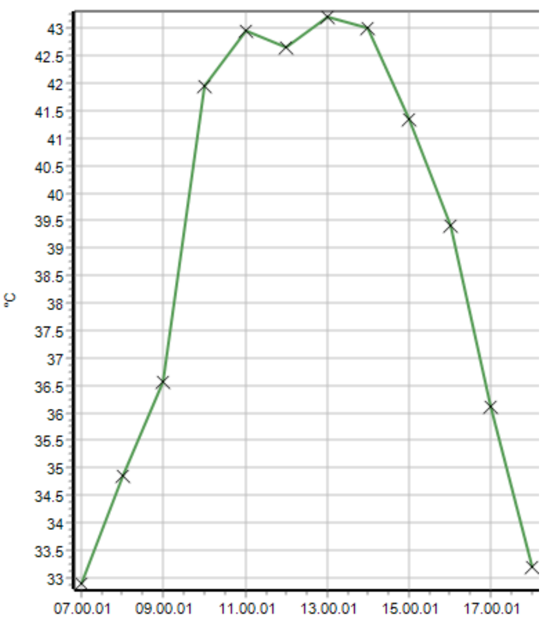

Graph 5. 42 UTCI graph for 1.5/60 degrees

b. UTCI

The graph of UTCI is a bit different than that of the air temperature as the first peak of 43°C is reached at 11PM and then drops at 12PM to 42.5°C. Then again, the value rises to 43.5°C and finally reaching 33.4°C at 6 PM. This creates an M shaped curve.

7. **70 Degrees**

Here, the street north was rotated by an angle of 70 degrees towards west in an anticlockwise direction which also covers an inclination of 250 degrees.

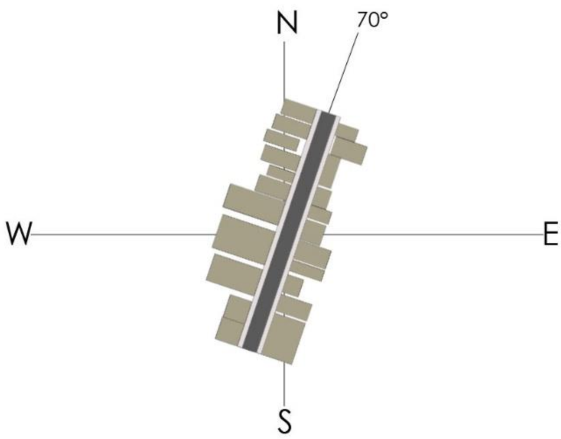

Figure 5. 68 sensitivity analysis for 70 degrees

a. Air Temperature

Beginning from 7 AM, we can see gradual increase of air temperature in this street section which peaks at about 2PM with the value of 38.8°C. As the day passes on, the temperature changes to 37.6°C and then finally reaching 33.6°C at 6PM. As expected, due to the change in sun position, we can observe this changing behavior of the air temperature graph as shown in graph 5.45.

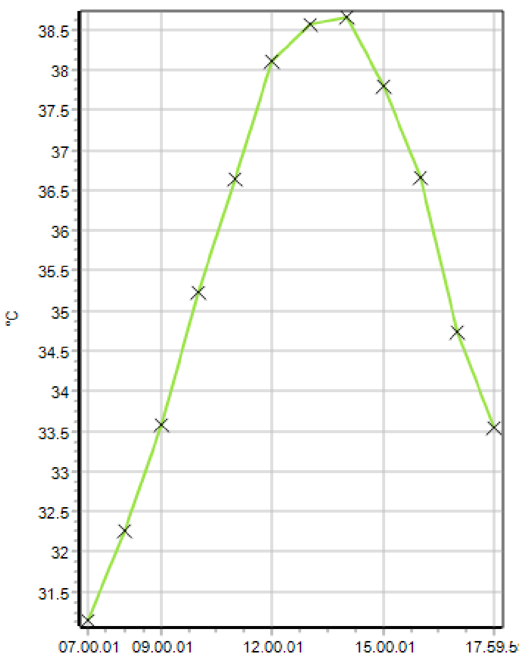

Graph 5. 45 Air temperature graph for 1.5/70 degrees

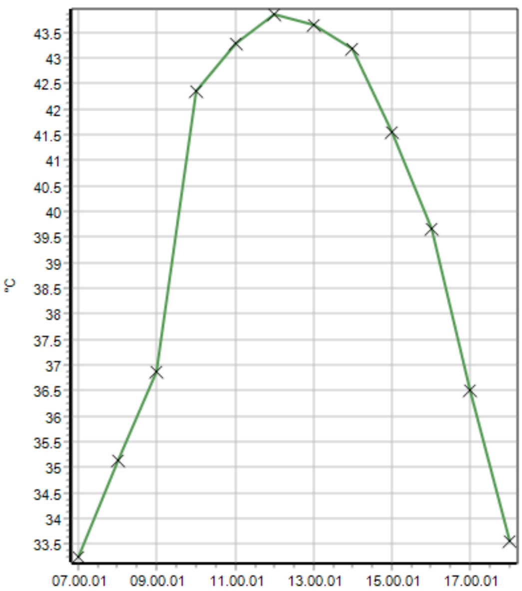

Graph 5. 44 UTCI graph for 1.5/70 degrees

b. UTCI

The graph of UTCI is a bit different than that of the air temperature as the first peak of 43.7°C is reached at 12PM and then drops at 2PM to 43.3°C and finally reaching 33.5°C at 6 PM.

8. 80 Degrees

Here, the street north was rotated by an angle of 80 degrees towards west in an anticlockwise direction which also covers an inclination of 260 degrees.

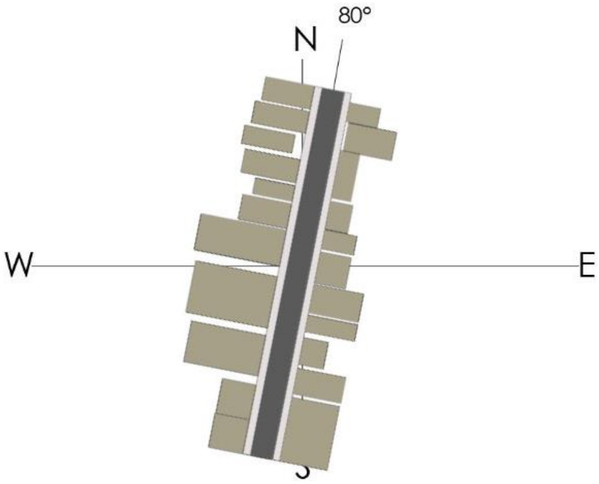

Figure 5. 69 sensitivity analysis for 80 degree

a. Air Temperature

Beginning from 7 AM, we can see gradual increase of air temperature in this street section which peaks at about 1PM with the value of 38.8°C. As the day passes on, the temperature changes to 37.7°C and then finally reaching 33.6°C at 6PM. As expected, due to the change in sun position, we can observe this changing behavior of the air temperature graph as shown in graph 5.46.

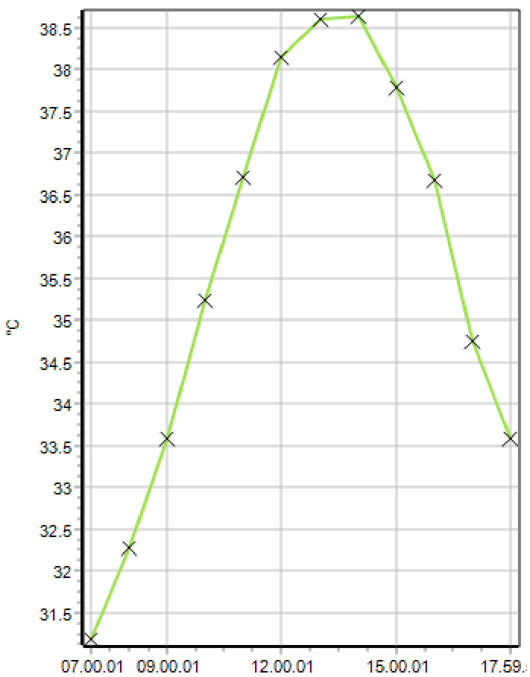

Graph 5. 47 Air temperature graph for 1.5/80 degrees

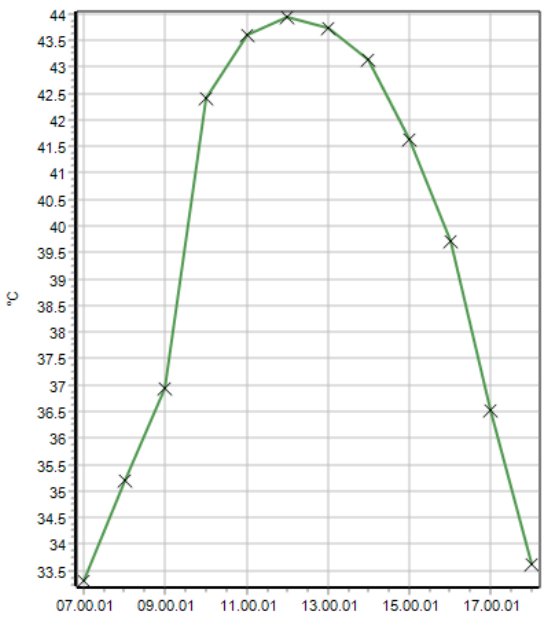

Graph 5. 46 UTCI graph for 1.5/80 degrees

b. UTCI

The graph of UTCI is a bit different than that of the air temperature as the first peak of 43.8°C is reached at 12PM and then drops at 2PM to 43.3°C and finally reaching 33.6°C at 6 PM.

9. 100 Degrees

Here, the street north was rotated by an angle of 100 degrees towards west in an anticlockwise direction which also covers an inclination of 280 degrees.

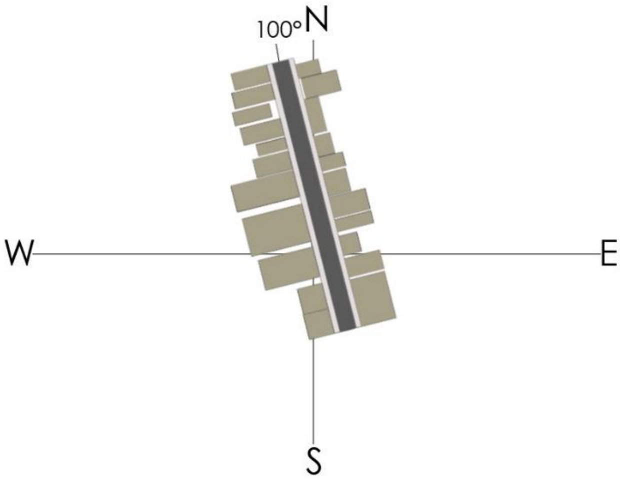

Figure 5. 70 sensitivity analysis for 100 degrees

a. Air Temperature

Beginning from 7 AM, we can see gradual increase of air temperature in this street section which peaks at about 1PM with the value of 38.8°C. As the day passes on, the temperature changes to 37.7°C and then finally reaching 33.6°C at 6PM. As expected, due to the change in sun position, we can observe this changing behavior of the air temperature graph as shown in graph 5.48.

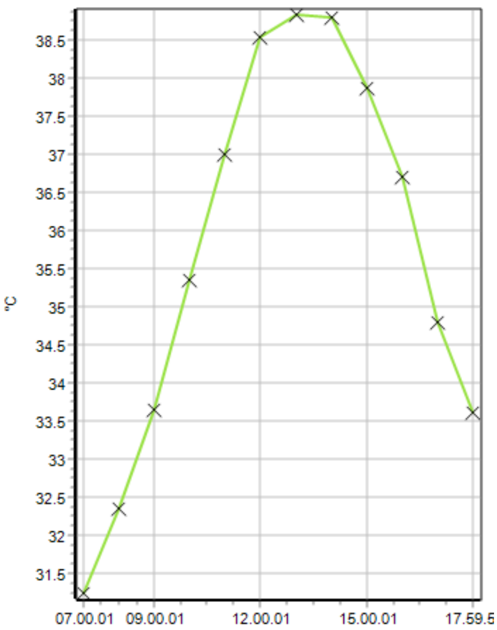

Graph 5. 48 Air temperature graph for 1.5/100 degrees

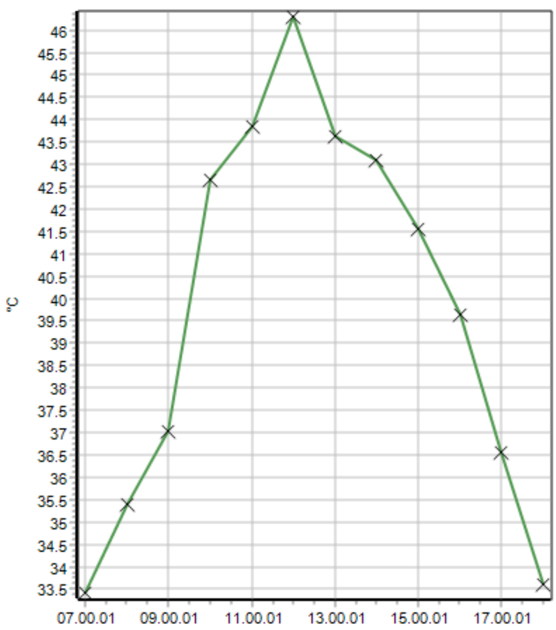

Graph 5. 49 UTCI graph for 1.5/70 degrees

b. UTCI

The graph of UTCI is a bit different than that of the air temperature as the first peak of 46.3°C is reached at 12PM and then drops at 1PM to 43.5°C and finally reaching 33.6°C at 6 PM.

10. 110 Degrees

Here, the street north was rotated by an angle of 110 degrees towards west in an anticlockwise direction which also covers an inclination of 290 degrees.

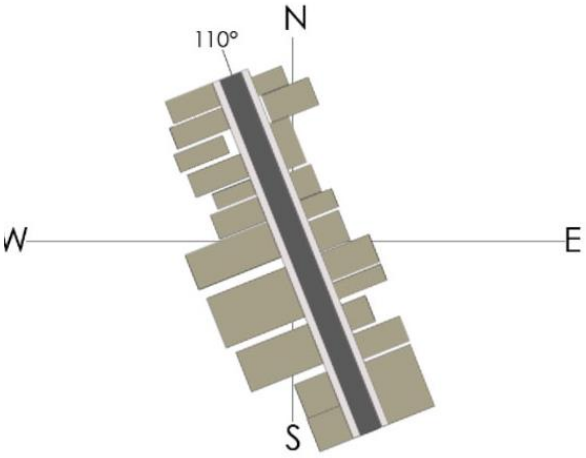

Figure 5. 71 sensitivity analysis for 110 degrees

a. Air Temperature

Beginning from 7 AM, we can see gradual increase of air temperature in this street section which peaks at about 1PM with the value of 39.4℃. As the day passes on, the temperature changes to 39℃ and then finally reaching 33.5℃ at 6PM. As expected, due to the change in sun position, we can observe this changing behavior of the air temperature graph as shown in graph 5.50.

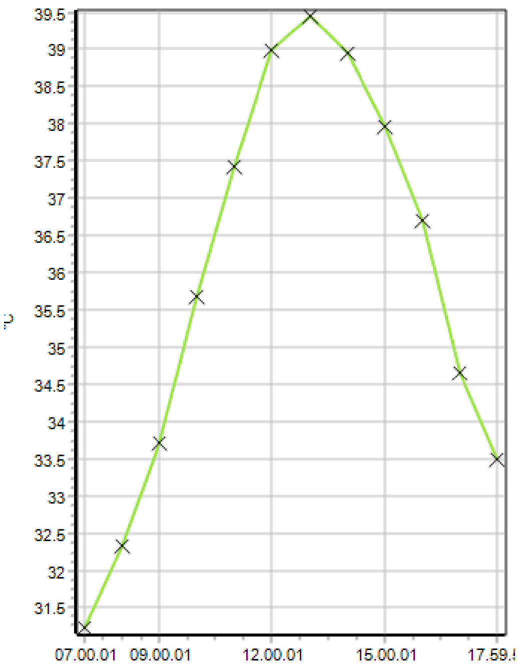

Graph 5. 50 Air temperature graph for 1.5/110 degrees

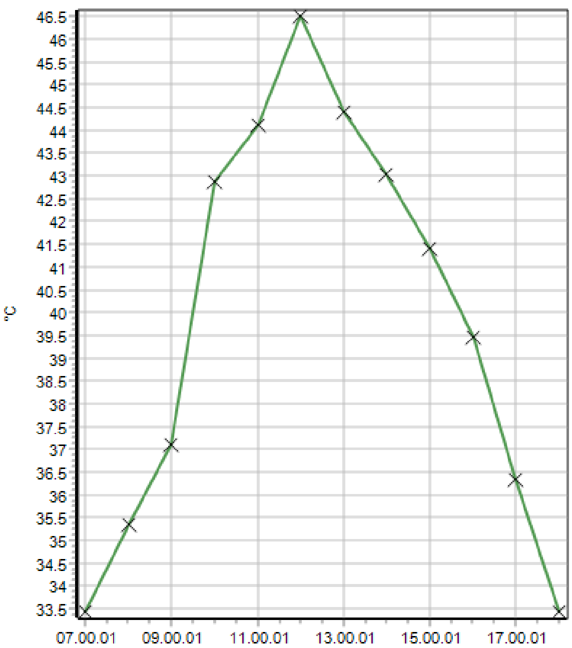

Graph 5. 51 UTCI graph for 1.5/110 degrees

b. UTCI

The graph of UTCI is a bit different than that of the air temperature as the first peak of 46.5℃ is reached at 12PM and then drops at 2PM to 44.4℃ and finally reaching 33.4℃ at 6 PM.

11. 120 Degrees

Here, the street north was rotated by an angle of 120 degrees towards west in an anticlockwise direction which also covers an inclination of 300 degrees.

a. Air Temperature

Beginning from 7 AM, we can see gradual increase of air temperature in this street section which peaks at about 1PM with the value of 39.4°C. As the day passes on, the temperature changes to 38.2°C and then finally reaching 33.3 at 6PM. As expected, due to the change in sun position, we can observe this changing behavior of the air temperature graph as shown in graph 5.53.

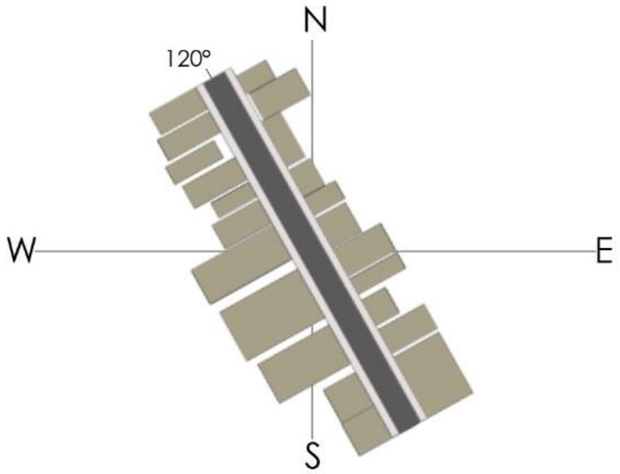

Figure 5. 72 sensitivity analysis for 120 degrees

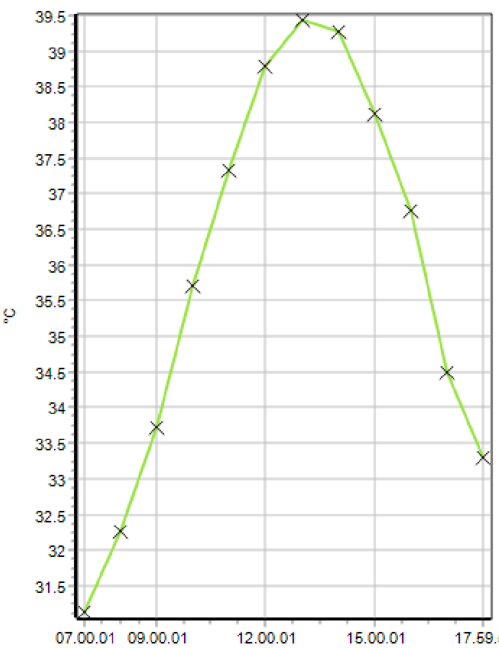

Graph 5. 53 Air temperature graph for 1.5/120 degrees

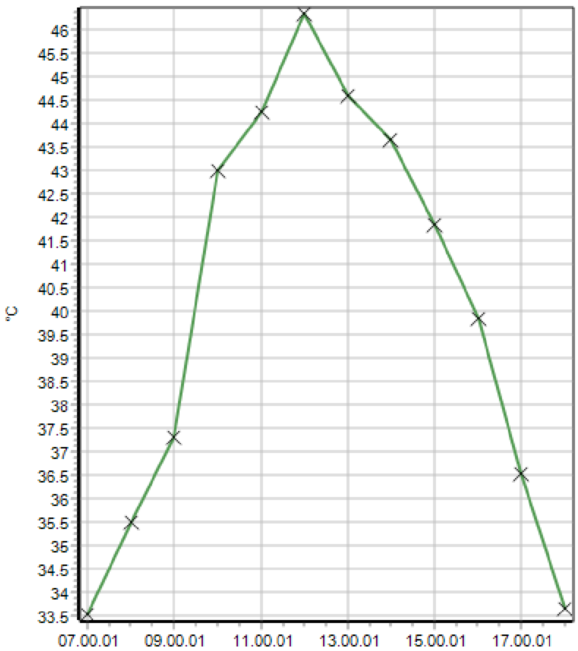

Graph 5. 52 UTCI graph for 1.5/120 degrees

b. UTCI

The graph of UTCI is a bit different than that of the air temperature as the first peak of 46.5°C is reached at 12PM and then drops at 2PM to 44.5°C and finally reaching 33.6°C at 6 PM.

12. 130 Degrees

Here, the street north was rotated by an angle of 130 degrees towards west in an anticlockwise direction which also covers an inclination of 310 degrees.

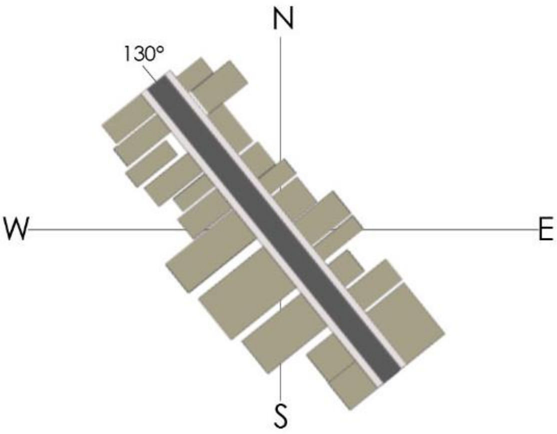

Figure 5. 73 sensitivity analysis for 130 degrees

a. Air Temperature

Beginning from 7 AM, we can see gradual increase of air temperature in this street section which peaks at about 2PM with the value of 39.6℃. As the day passes on, the temperature changes to 38.6℃ and then finally reaching 33.3℃ at 6PM. As expected, due to the change in sun position, we can observe this changing behavior of the air temperature graph as shown in graph 5.55.

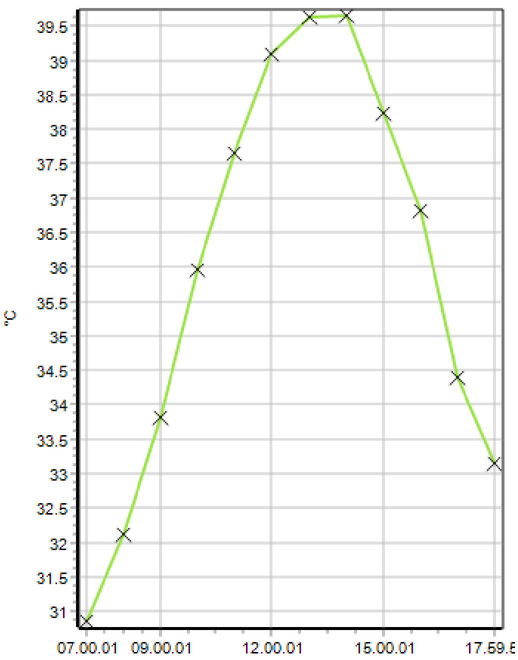

Graph 5. 55 Air temperature graph for 1.5/130 degrees

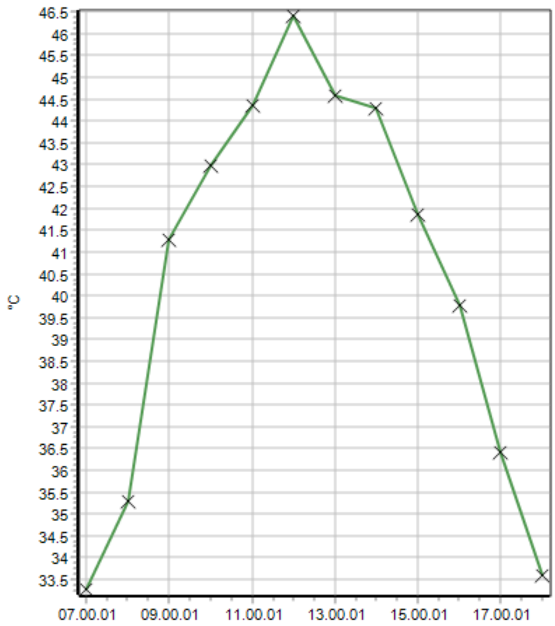

Graph 5. 54 UTCI graph for 1.5/130 degrees

b. UTCI

The graph of UTCI is a bit different than that of the air temperature as the first peak of 46.4℃ is reached at 12PM and then drops at 1PM to 44.5℃ and finally reaching 33.6℃ at 6 PM.

13. 140 Degrees

Here, the street north was rotated by an angle of 140 degrees towards west in an anticlockwise direction which also covers an inclination of 320 degrees.

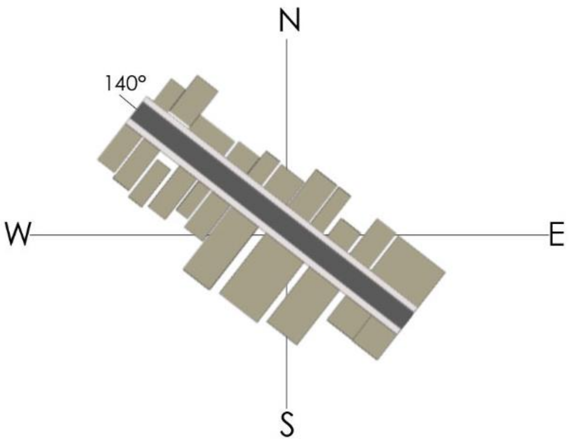

Figure 5. 74 sensitivity analysis for 140 degrees

a. Air Temperature

Beginning from 7 AM, we can see gradual increase of air temperature in this street section which peaks at about 1PM with the value of 39.8℃. As the day passes on, the temperature changes to 38.4℃ and then finally reaching 33.2℃ at 6PM. As expected, due to the change in sun position, we can observe this changing behavior of the air temperature graph as shown in graph 5.56.

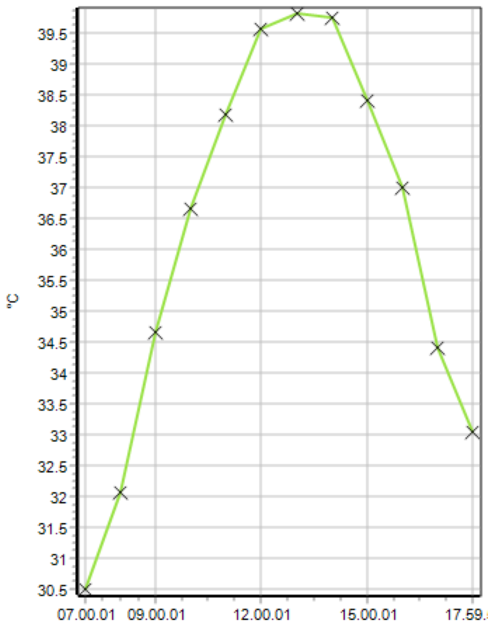

Graph 5. 56 Air temperature graph for 1.5/140 degrees

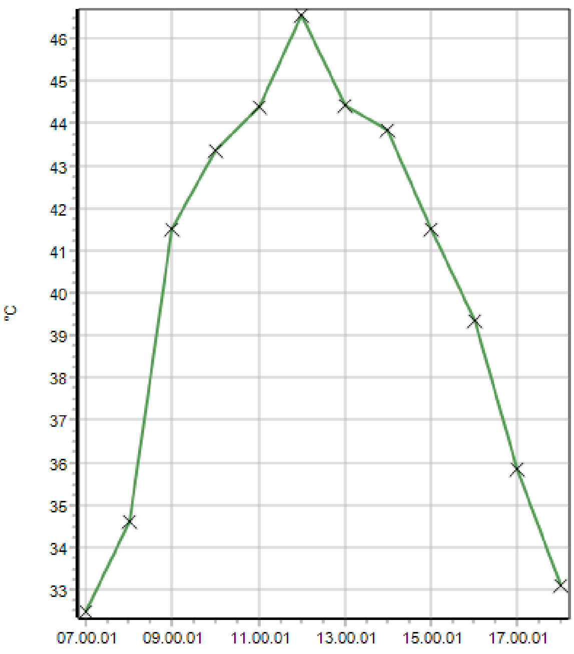

Graph 5. 57 UTCI graph for 1.5/140 degrees

b. UTCI

The graph of UTCI is a bit different than that of the air temperature as the first peak of 46.5℃ is reached at 12PM and then drops at 2PM to 43.8℃ and finally reaching 33.4℃ at 6 PM.

14. 150 Degrees

Here, the street north was rotated by an angle of 150 degrees towards west in an anticlockwise direction which also covers an inclination of 330 degrees.

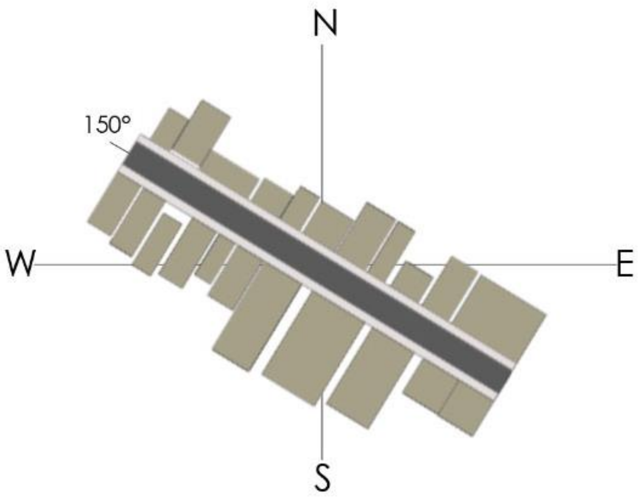

Figure 5. 75 sensitivity analysis for 150 degrees

a. Air Temperature

Beginning from 7 AM, we can see gradual increase of air temperature in this street section which peaks at about 1 PM with the value of 40°C. As the day passes on, the temperature changes to 38.5°C and then finally reaching 33.1°C at 6 PM. As expected, due to the change in sun position, we can observe this changing behavior of the air temperature graph as shown in graph 5.59.

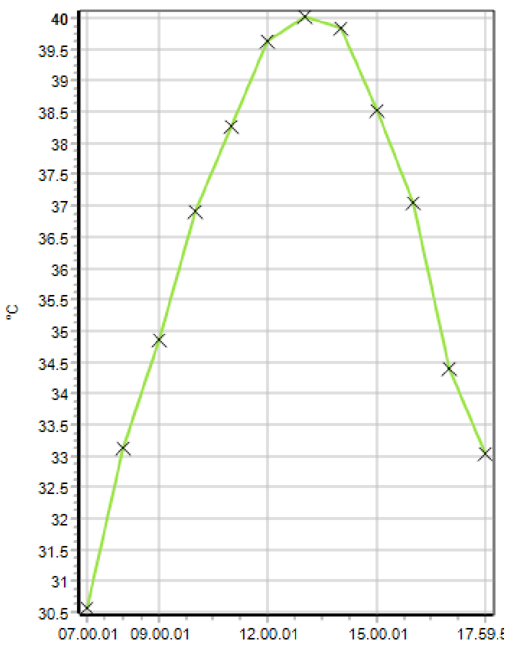

Graph 5. 59 Air temperature graph for 1.5/150 degrees

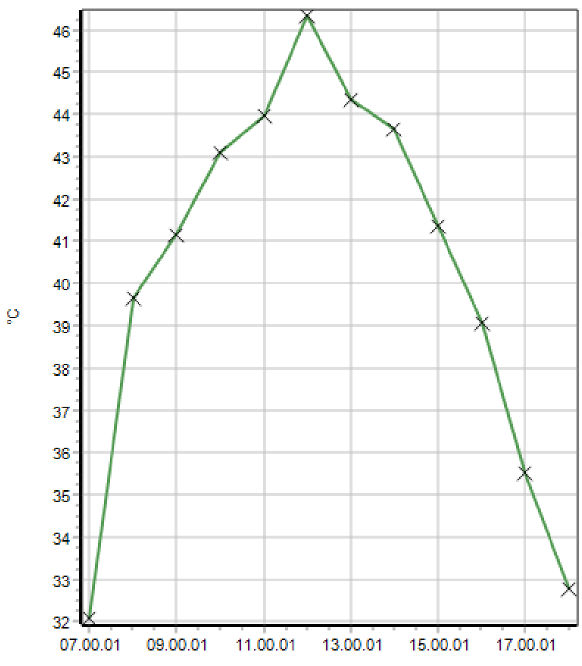

Graph 5. 58 UTCI graph for 1.5/150 degrees

b. UTCI

The graph of UTCI is a bit different than that of the air temperature as the first peak of 46.4°C is reached at 12PM and then drops at 2PM to 43.8°C and finally reaching 32.8°C at 6 PM.

15. 160 Degrees

Here, the street north was rotated by an angle of 160 degrees towards west in an anticlockwise direction which also covers an inclination of 340 degrees.

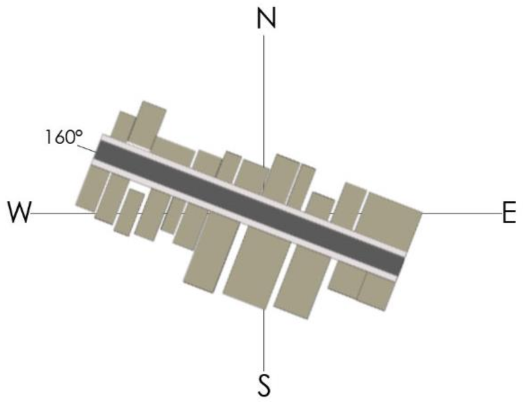

Figure 5. 76 sensitivity analysis for 160 degrees

a. Air Temperature

Beginning from 7 AM, we can see gradual increase of air temperature in this street section which peaks at about 1 PM with the value of 40.5°C. As the day passes on, the temperature changes to 37.2°C at 4 PM and then finally reaching 33.2°C at 6 PM. As expected, due to the change in sun position, we can observe this changing behavior of the air temperature graph as shown in graph 5.61.

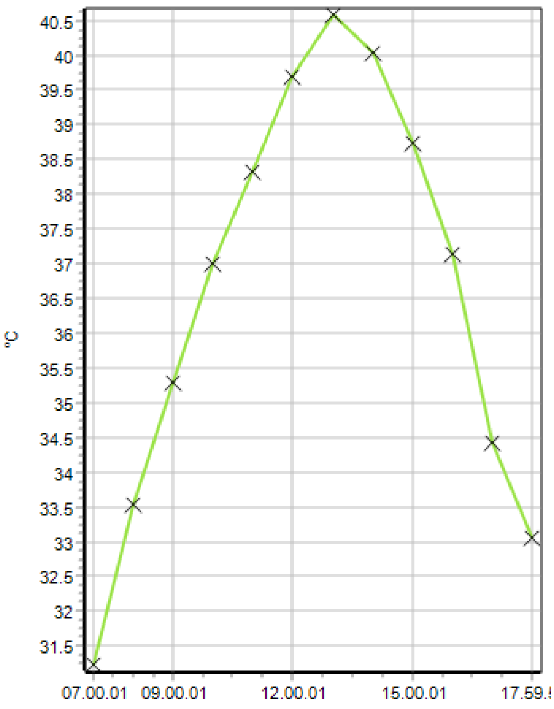

Graph 5. 61 Air temperature graph for 1.5/160 degrees

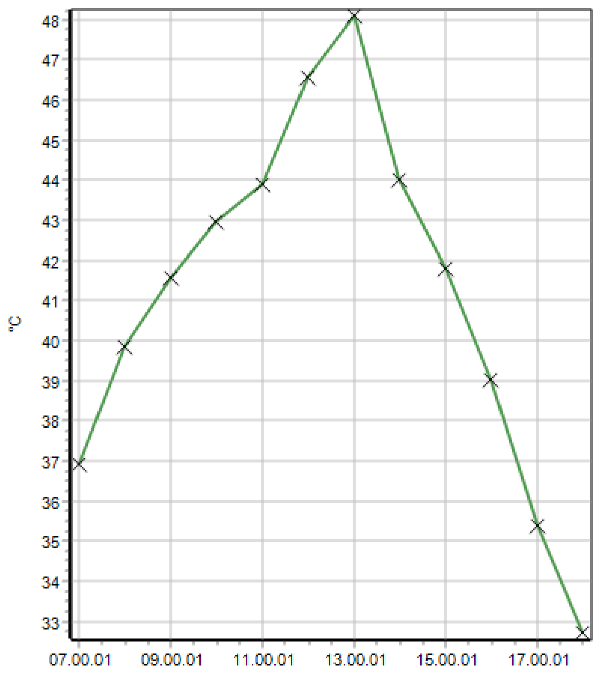

Graph 5. 60 UTCI graph for 1.5/160 degrees

b. UTCI

The graph of UTCI is a bit different than that of the air temperature. The first peak of 48°C is reached at 1PM and then drops at 2PM to 44°C and finally reaching 32.5°C at 6 PM.

16. 170 Degrees

Here, the street north was rotated by an angle of 170 degrees towards west in an anticlockwise direction which also covers an inclination of 350 degrees.

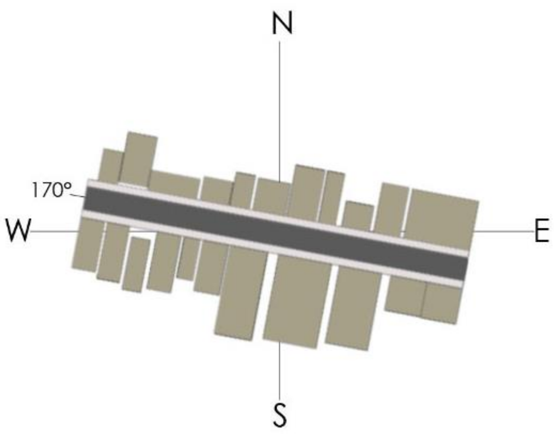

Figure 5. 77 sensitivity analysis for 170 degrees

a. Air Temperature

Beginning from 7 AM, we can see gradual increase of air temperature in this street section which peaks at about 1PM with the value of 38.8°C. As the day passes on, the temperature changes to 37.7°C and then finally reaching 33.6°C at 6PM. As expected, due to the change in sun position, we can observe this changing behavior of the air temperature graph as shown in graph 5.63.

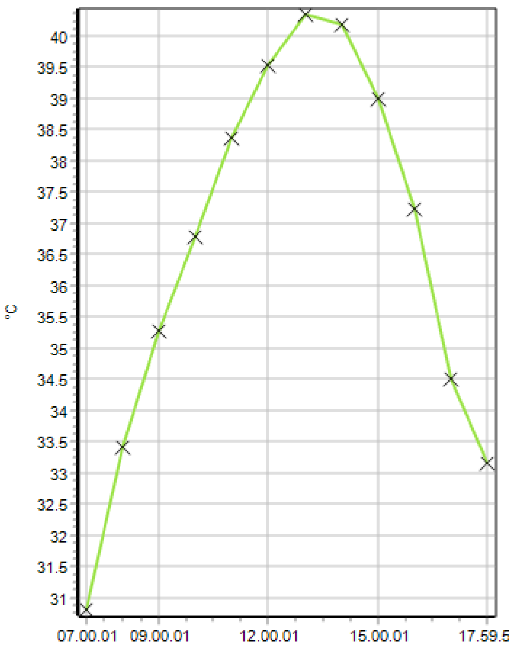

Graph 5. 62 Air temperature graph for 1.5/170 degrees

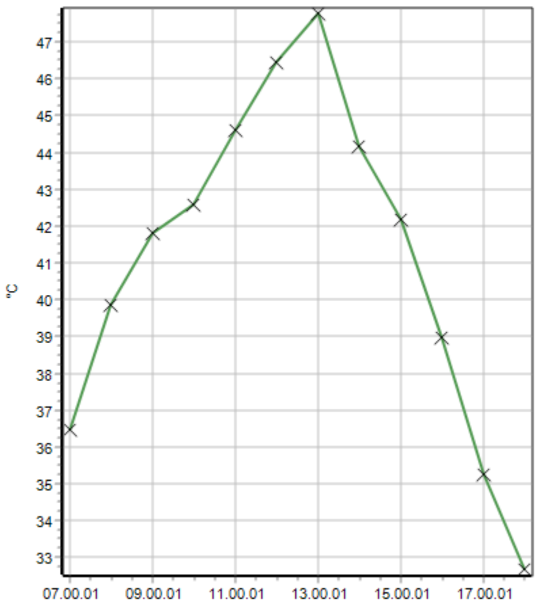

Graph 5. 63 UTCI graph for 1.5/170 degrees

b. UTCI

The graph of UTCI is a bit different than that of the air temperature. The first peak of 47.8°C is reached at 1 PM and then drops at 2 PM to 44.1°C and finally reaching 32.5°C at 6 PM.

6. Chapter 6: Discussion

The review investigated at the best aspect ratio for Nepal's hot and humid environment. Along with the base case, nine alternative scenarios with varying aspect ratios and orientations were developed. The orientation of the same base case was adjusted in order to identify the ideal aspect ratio for different orientations, which may be used in future urban planning and design in Nepal's hot and humid climate. Envi-met 5.3 student version was used for the simulation. The optimal aspect ratio is determined by analyzing the air temperature, mean radiant temperature, and physiologically equivalent temperature.

6.1. Comparison between scenarios based on Aspect Ratio

6.1.1. Air temperature

The air temperature is found to decrease moderately with increase in aspect ratio. This is more perceptible after 10:00 hours to 16:00 hours with aspect ratio more than 1.5. The scenario with aspect ratio 1 showed similar air temperature to the base case scenario. The difference of 1 °C can be seen between the base case and canyon with aspect ratio 1.5 during 14:00 hours and similarly difference of 1.5 °C can be seen between the base case and canyon with aspect 2 and difference of 2 °C with aspect ratio 3. This shows that with increase in aspect ratio, there is reduction of air temperature by certain degree Celsius which conforms the findings of other researchers (Toudert, 2005; De & Mukherjee, 2018; Jamei & Rajagopalan, 2018; Qaid & Ossen, 2015).

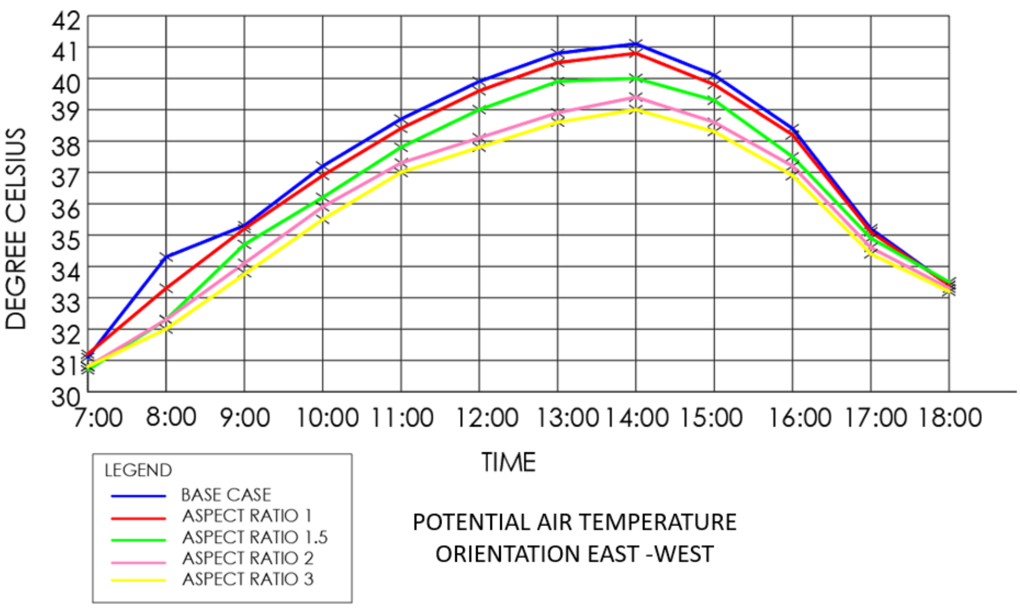

Graph 6. 1 Comparison of potential air temperature of different aspect ratio for E-W street

When the orientation of the street is changed to north-south from east- west, the temperature was reduced by 1.7 °C on aspect ratio 1 at 14:00 hours. With further increment of aspect ratio to 1.5, 2, and 3, the temperature was reduced by 2.4 °C, 3 °C, 3.6 °C respectively on the same time. The north south oriented street performed better than east-west oriented street with a difference of roughly 0.8 °C - 1.3 °C between 8:00 hours and 16:00 hours. North-south oriented streets are cooler in hot and humid climates than east-west oriented ones, which agrees to (KUSHOL, et al., 2013).

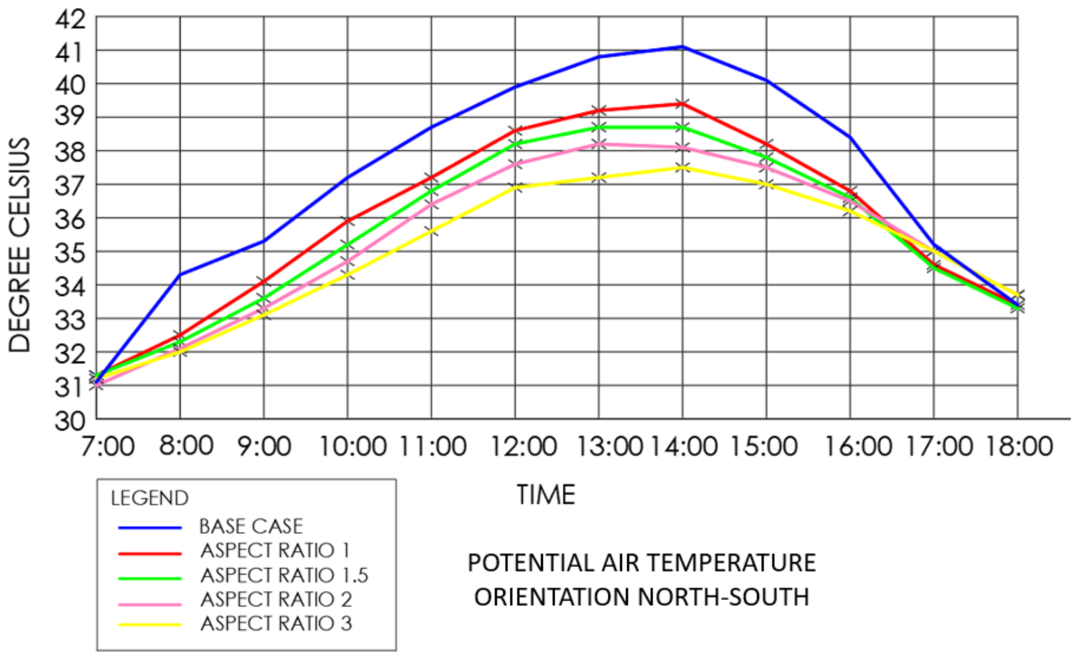

Graph 6. 2 comparison of potential air temperature of different aspect ratio for N-S street

6.1.2. Mean Radiant Temperature

The change in Mean radiant temperature was seen when the aspect ratio is above 2. The mean radiant temperature drops to 51 °C at 12:00 hours to 14:00 hours and increases readily on scenario with aspect ratio above 2. The results show that with increase in aspect ratio, the mean radiant temperature decreases during the peak hour due to the shading by building.

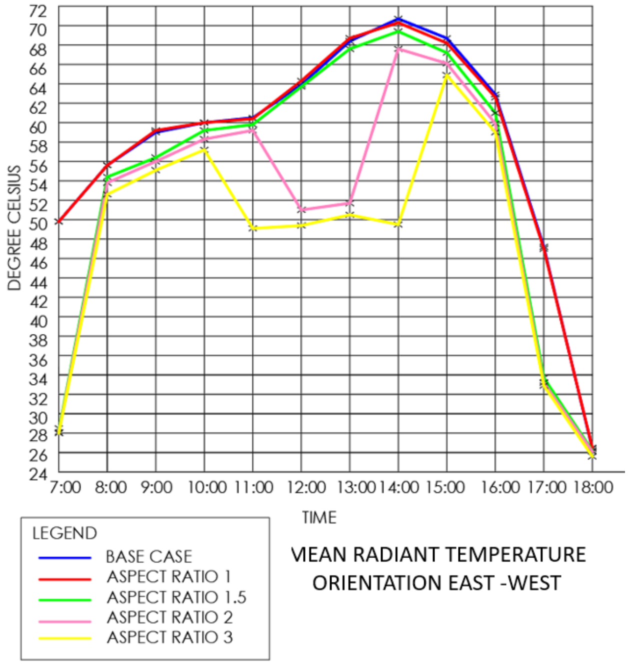

Graph 6. 3 comparison of mean radiant temperature of different aspect ratio for E-W street

For north south oriented streets, the reduction in mean radiant temperature can be seen after 11:00 hours till 15:00 hours. The street with aspect ratio 1 show difference of 13.6 °C at 13:00 hours with base case. The street with aspect ratio 1.5 in north south direction shows similar thermal performance with street of aspect ratio 3 in east west direction.

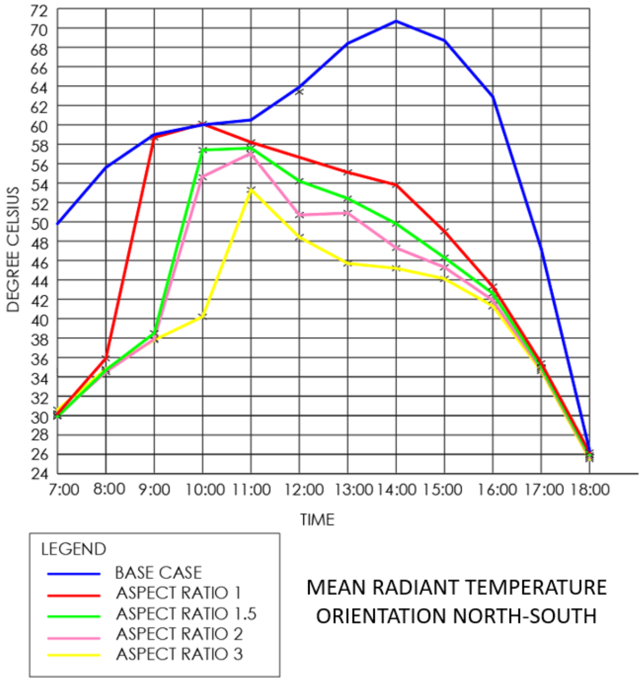

Graph 6. 4 comparison of mean radiant temperature of different aspect ratio for N-S street

6.1.3. Physiologically Equivalent Temperature

As similar to mean radiant temperature, the street with aspect ratio above 2 shows better result in case of PET temperature. There is reduction of 5 °C at 12:00 hours in street with aspect ratio 2. The PET reduces after 12:00 hours to 14:00 hours on the street with aspect ratio above 2. There is no or very less difference between base model and street with aspect ratio 1 and 1.5.

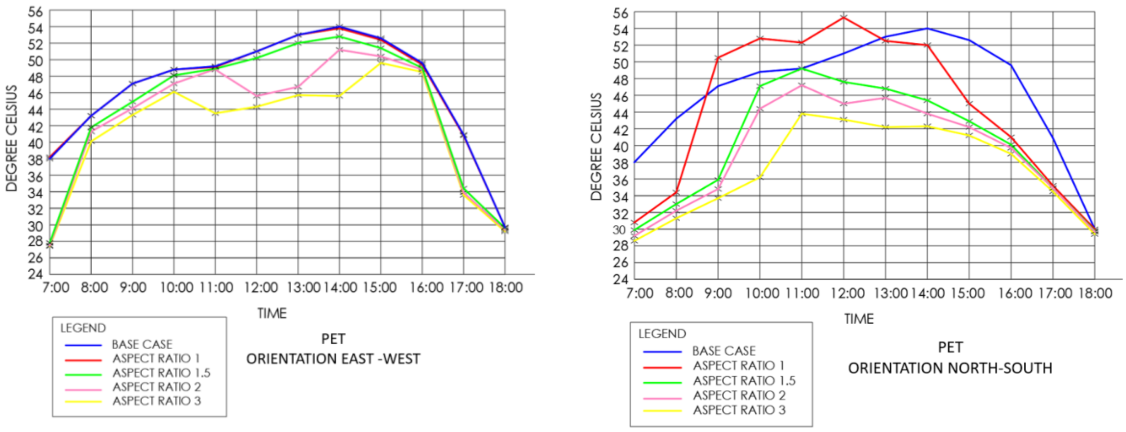

Graph 6. 5 comparison of mean radiant temperature of different aspect ratio

The street with aspect ratio 1 did not show better result than base model in north-south oriented streets. However, the street with aspect ratio above 1.5 shows the reduction of PET by 6.2 °C – 11.7 °C during 10:00 hours to 14:00 hours. The street with aspect ratio 1.5 in north south direction is better than street with aspect ratio 3 in East-west direction when comparing the PET temperature. However, the temperature is still high and the streets are thermally uncomfortable considering the temperature only.

The difference in height of building could change the temperature at 14:00 hours from 41 °C to 38.7 °C in East West oriented streets and to 37.5 °C in North South direction which is still high temperature. The reduction of 3.5 °C due to aspect ratio alone is still appreciable however, further studies to reduce more temperature should be carried out considering other variables that affects thermal comfort.

6.2. Comparison between scenarios based on Orientation

After the completion of simulation, all the scenarios were compared in different metrics of MRT, Air Temperature, PET and UTCI.

6.2.1. Air Temperature

a. 0-90 Degrees

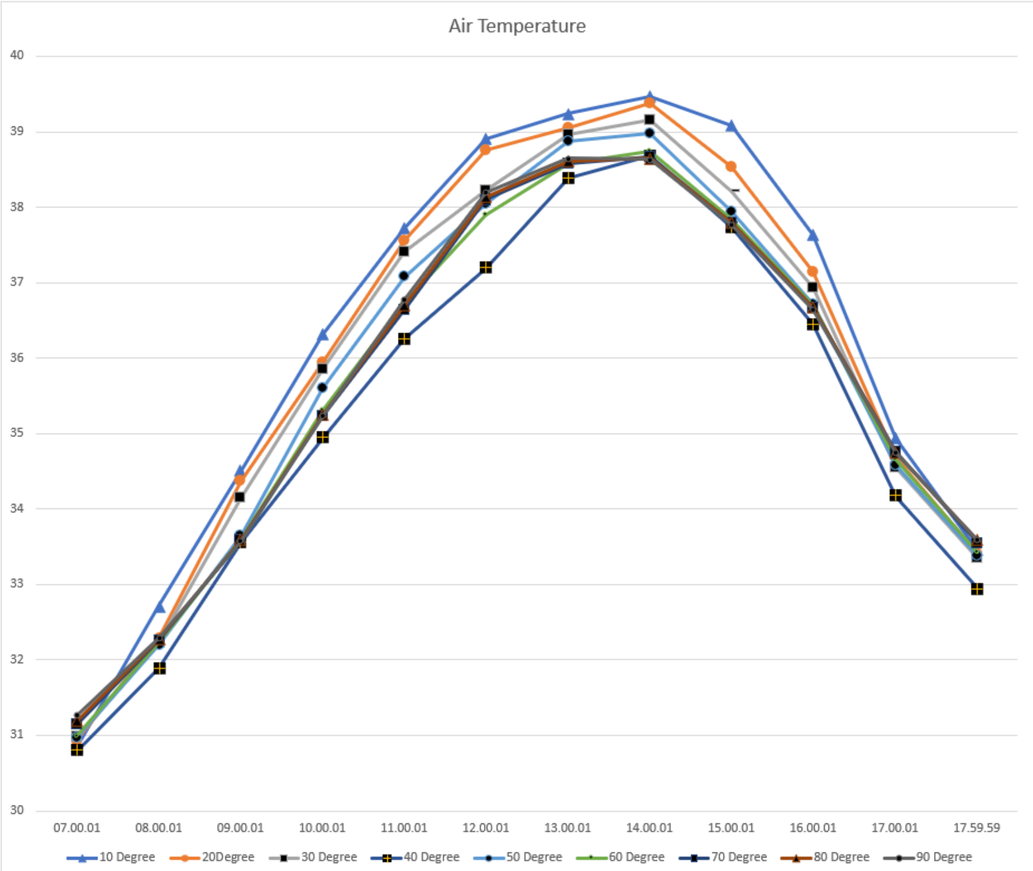

Graph 6. 6 comparison of air temperature of different orientation (10 degree -90 degree)

Looking at graph, the curves of all scenarios follow similar path with linear increase in every time period with the graph of 40 degrees performing the best. Starting from 7 AM we see a slight increase in Air temperature which follows the trend till the peak time of around 2PM validated by the solar positions at those times. The air temperatures then gradually decrease as the sun position also lowers from the zenith reaching the lowest at 6PM corelated by the temperature graph. There seems a gradual decrease in air temperature with rotation of 10°. The orientation 40° shows the lowest temperature.

b. 100-180 Degrees

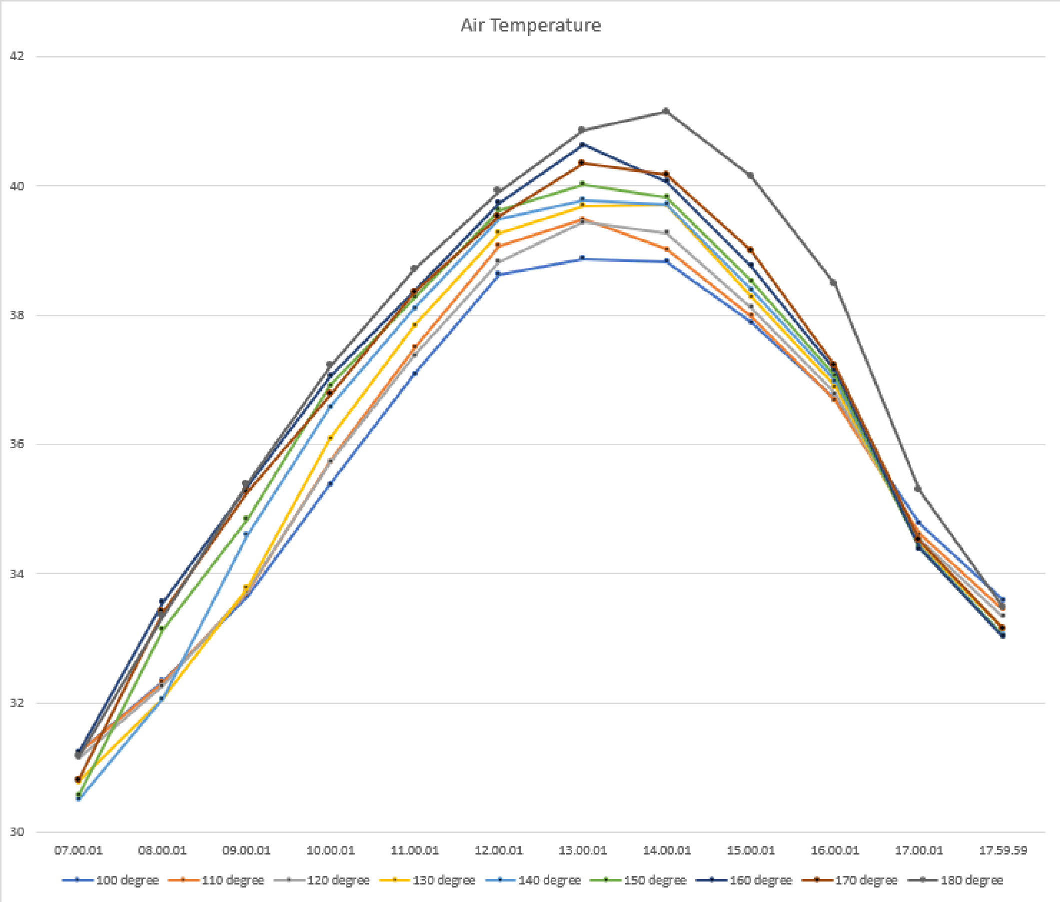

Graph 6. 7 comparison of air temperature of different orientation (100 degree -180 degree)

The air temperature begins to increase when the street is rotated 10°. The orientation after 160- degree NW shows worst result in air temperature as it reaches above 40 °C at 1 PM. The orientation up to 150 ° has temperature below 40°C which is around 2.3 °C less than the exact E-W oriented streets.

6.2.2. MRT

a) **0-90 Degrees**

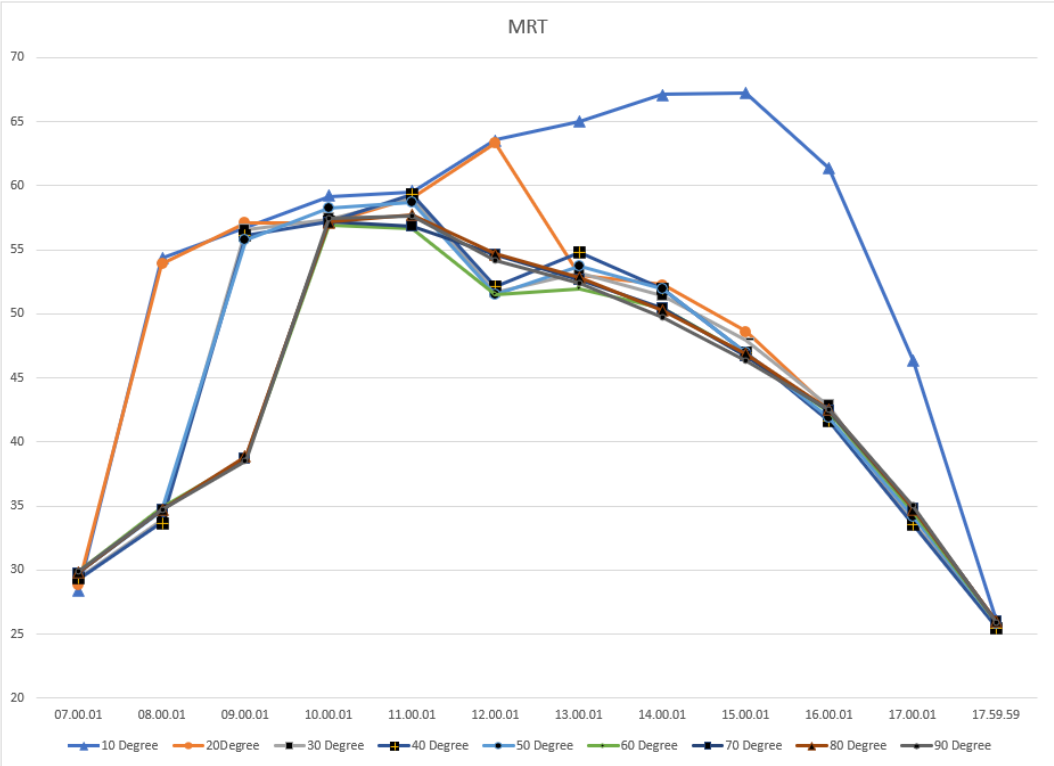

Graph 6. 8 comparison of MRT of different orientation (10 degrees -90 degree)

Looking at the graphs, we observe a steep increase in MRT in 20-degree curve while the remaining follow similar path. The anomaly can be observed in the 50-degree graph which reaches a record peak of 67℃ while the second highest peak is only 63℃. At the end of the day at 6PM, all the graphs converge at a single temp of 25℃.

b) 100-180 Degrees

The MRT begins to increase when the street is rotated 10°. The 170-degree NW shows worst result in air temperature as it reaches above 50 ℃ at 1 PM. The orientation up to 150 ° has temperature below 40℃ which is around 2.3 ℃ less than the exact E-W oriented streets.

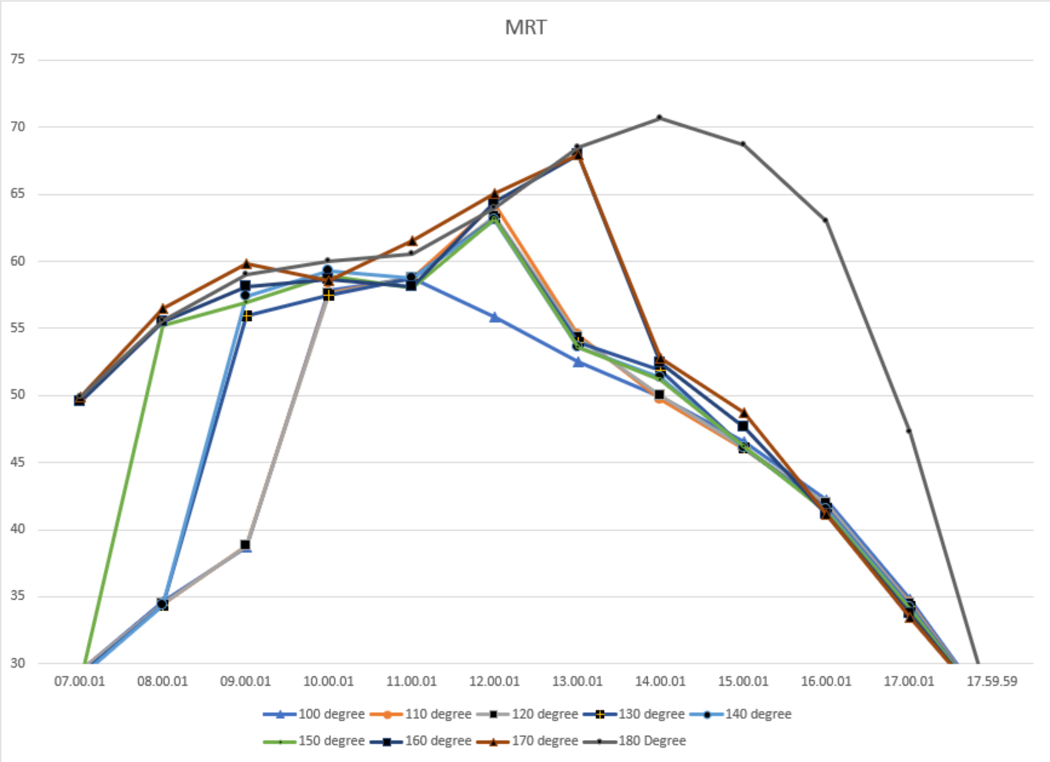

Graph 6. 9 comparison of air temperature of different orientation (100-degree -180 degree)

6.2.3. PET

e. 0-90 degrees

From scenario 0-90 degrees, the nature of graph is similar except in the case of 50 degrees. In 10 degrees, the temperature is high throughout the day from morning till evening while in the case of 20-degree, temperature is as high as 10 degrees in the morning till 12 and then the PET decreases by about 5 degrees in the remaining time of the day. From 30-50 degrees, the PET starts decreasing from 8 AM and then the rest of the day, the graph follows the similar pattern of 20 degrees. From 60-90 degrees, the performance of the street section is similar as the PET drops from 8AM to 9 AM by about 8°C compared to 30–50-degree scenarios. From 10 AM to 1 PM we can observe gradual increase and then the graph follows a decreasing patter compared to the 20-degree scenario graph for the rest of the day.

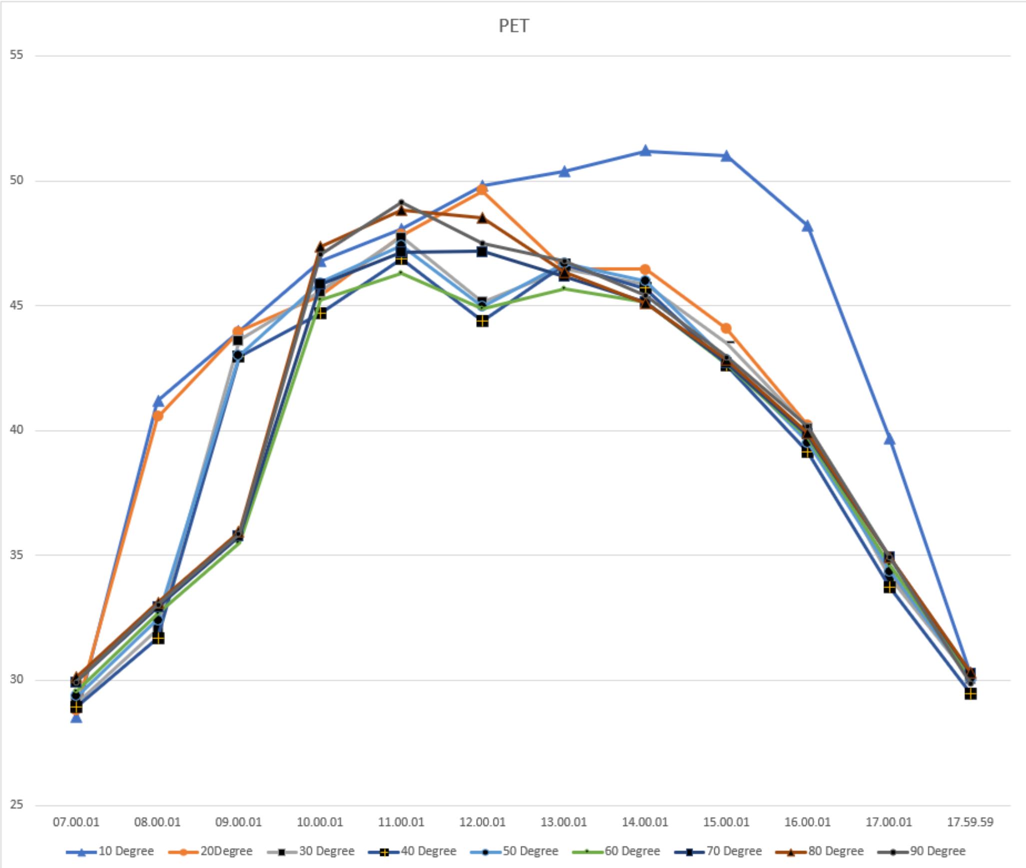

Graph 6. 10 comparison of PET of different orientation (10 degrees -90 degree)

f. 100-180 Degrees

From scenario 100-180 degrees, the nature of graph is highly variable in the beginning of the simulation time to the end for different orientations. For the start of simulation at 6:00 hours, there is a considerable difference in the observed PET ranging from (28-38) °C. The average peak PET observed is around 53°C with an exception of 110 degrees where the peak PET was observed at 62°C. At the end of the simulation time at 18:00 hours, all the graphs converged at a common temperature of 30°C.

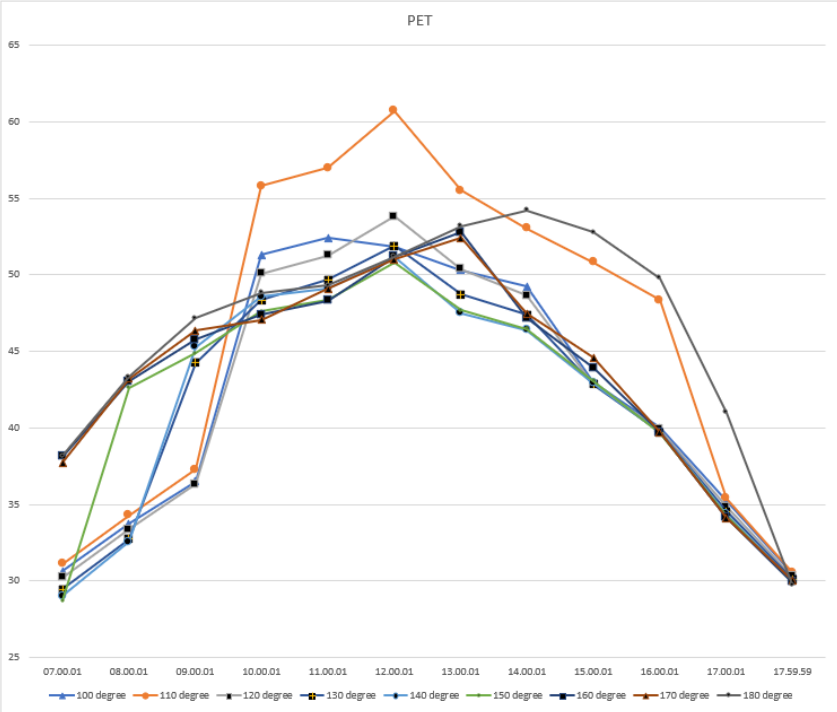

Graph 6. 11 comparison of PET of different orientation (100 degrees -180 degree)

6.2.4. UTCI

1. 0-90 Degrees

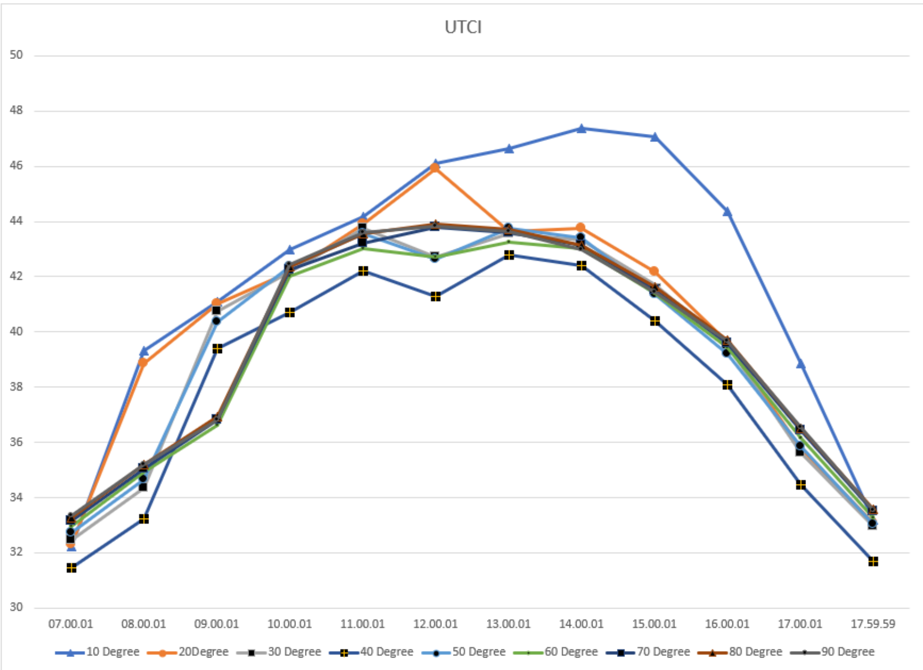

Graph 6. 12 comparison of UTCI of different orientation (10 degrees -90 degree)

Looking at the graphs, we observe a steep increase in UTCI in 10 and 20-degree curve while the remaining follow similar path. The anomaly can be observed in the 50-degree graph which reaches a record peak of 47℃ while the second highest peak is only 46℃. At the end of the day at 6PM, all the graphs converge at a single temp of 32-33℃.

2. 100- 180 Degrees

The graph shows that the orientation below 150 ° NW starts with low temperature but reaches maximum 46 ℃ at 12 PM and gradually decrease. However, the orientation above 150 ° NW reaches maximum 48 ℃ at 1 PM and starts to decrease gradually. During the peak hour i.e., 12PM – 2 PM, the streets oriented from 100 ° to 150 ° shows better performance as the temperature drops abruptly. The 180 degrees shows the worst performance as shown by the graph.

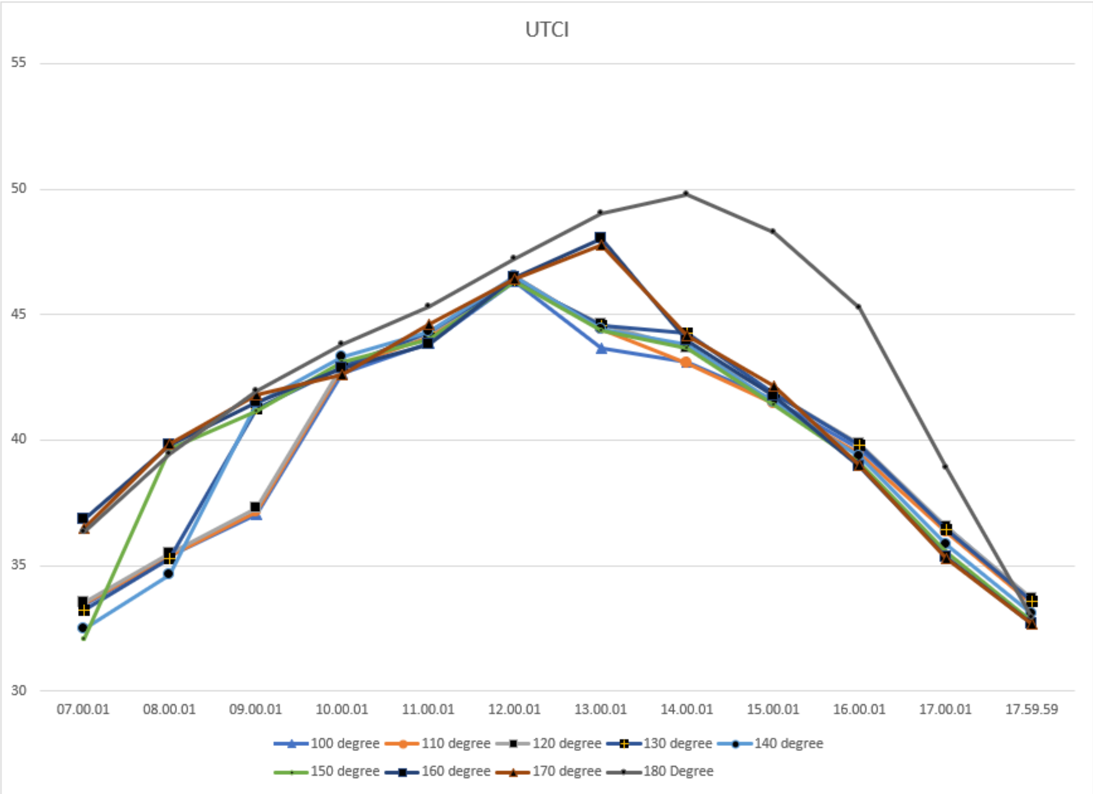

Graph 6. 13 comparison of UTCI of different orientation (100 degrees -180 degree)

7. Chapter 7: Conclusion and Recommendation

7.1. Conclusion

For a town like Lumbini in hot and humid climatic zone, the street oriented towards north-south is more favorable since, at least one side of the street is always shaded even with low building height. For east-west street, the aspect ratio above 2 is suitable regarding the shading and low temperature, however, in case of Lumbini aspect ratio 3 or more seems unsuitable as the height of the building will be above the prevailing byelaws. Hence, aspect ratio 2 is optimum for east west oriented streets in case of hot and humid climate of Nepal.

The north-south street with aspect ratio 1.5 performs better thermally than street in east west with aspect ratio. The street is completely or partially shaded throughout the day with aspect ratio above 1.5 in Nort-south direction. Hence, aspect ratio 1.5 is optimum for north-south oriented streets in case of hot and humid climate of Nepal.

The north-south oriented streets performs better than east-west oriented streets, since, the results shows that there is a difference of 2.5 °C between E-W oriented streets and N-S oriented streets. The air temperature starts to decrease during the peak hour when the street is rotated 40 ° NE. The orientation between 40 ° NE to 90 ° NS performs similar in case of air temperature when the aspect ratio is 1.5. When the orientation is changed from 100° NW to exact E-W, the air temperature gradually increases and reaches 41.1 °C with difference of 2.3 °C. Hence, the orientation from 40 ° NE to 150 ° NW performs better thermally.

The difference in temperature between E-S and N-S oriented streets in the MRT is 20.9 °C. When the direction is between 20 ° NE and 150 ° NW, the MRT starts to decline, and it then begins to ascend after 150 ° NW. When the orientation is changed by 10 degrees in the case of PET, the temperature drops by 3 degrees, and by another 10 degrees, the temperature drops by 4.8 degrees. The difference of around 10 °C between the orientations of 30 °NE and 150 ° NW may be noted. Similarly in case of UTCI, the temperature drops by 2.4 °C after rotating the street by 10 °NE and by 3.6 °C after another 10 ° rotation. The actual E-W orientation reveals a variation of around 7.3 °C in the direction from 30 ° NE to 150 ° NW.

This research revealed that proper street orientation and the use of the most suitable canyon aspect ratio can decrease pedestrian thermal stress. This study presents a paradigm for optimizing canyon aspect ratio and orientation in a hot and humid climatic region. Though just temperature and aspect ratio are studied in this study, the developed methodology may be modified and carried forward to include other parameters such as wind velocity, humidity and vegetations, surface material, and so on.

7.2. Research Validation

- This research concludes that with increase in aspect ratio, there is reduction of air temperature by certain degrees Celsius which conforms the findings of other researchers (Toudert, 2005; De & Mukherjee, 2018; Jamei & Rajagopalan, 2018; Qaid & Ossen, 2015).

- North-south oriented streets are cooler in hot and humid climates than east-west oriented ones, which agrees to Kushol, et al., 2013; Toudert, 2005; Chatzidimitriou and Yannas, 2017.

7.3. Recommendation

- In climates like that of Lumbini Sanskritik municipality, it is recommended that road orientation and aspect ratio also be given priority during future road planning to enhance walkability.
- Orientation of 30 ° to 150° anticlockwise along with aspect ratio 1.5 is strongly recommended for future road plans.
- It is imperative that we consider pedestrian comfort in equal importance with road safety plans for any road design.

7.4. Further research

- Since the research ignore all other prevailing variables that can affect pedestrian thermal comfort of the region such as wind corridors, vegetations, water bodies and cool pavements, further research can be done to understand the effect of these variables for the same region.

- Further research can be carried out in the orientation other than the ones studied in this research.

- Research was carried out in a short amount of time focusing only on the summer conditions, so, further research needs to be done on the effect on pedestrian comfort for the same region for other seasons.

- Further research can be carried out on the economic and social viability of the solutions provided in this research for the same region.

References

Abdollahzadeh, N., & Biloria, N. (2020). Outdoor thermal comfort: Analyzing the impact of urban configurations on the thermal performance of street canyons in the humid subtropical climate of Sydney. *Frontiers of Architectural Research*. doi:https://doi.org/10.1016/j.foar.2020.11.006

Ahmed, K. S. (2003). Comfort in urban spaces: defining the boundaries of outdoor thermal comfort for the tropical urban environments. *Energy and Buildings, 35*(1), 103-110. doi:https://doi.org/10.1016/S0378-7788(02)00085-3.

Ali-Toudert, F., & Mayer, H. (2006). Numerical study on the effects of aspect ratio and orientation of an urban street canyon on outdoor thermal comfort in hot and dry climate. *Building and Environment, 41*(2), 94-108. doi:https://doi.org/10.1016/j.buildenv.2005.01.013

Asarpota, K., & Nadin, V. (2020). Energy Strategies, the Urban Dimension,and Spatial Planning. *Energies*.

Azmi, D. I., & Karim, H. A. (2012). Implications of Walkability Towards Promoting Sustainable Urban Neighbourhood,. *Social and Behavioral Sciences,, 50*(1877-0428,), 204-213. doi:https://doi.org/10.1016/j.sbspro.2012.08.028.

Bodach, S. (2014, December.). Developing Bio-climatic Zones and Passive Solar Design Strategies for Nepal. *30th International PLEA Conference*, (pp. 16-18). Ahmedabad, India .

Chatzidimitriou, A., & Yannas, S. (2017). Street canyon design and improvement potential for urban open spaces; the influence of canyon aspect ratio and orientation on microclimate and outdoor comfort. *Sustainable Cities and Society*, *33*, 85-101. doi:https://doi.org/10.1016/j.scs.2017.05.019.

Chatzipoulka, C., Nikolopoulou, M., & Watkins, R. (2015). The impact of urban geometry on the radiant environment in outdoor spaces. *ICUC9 - 9th*

International Conference on Urban Climate jointly with 12th Symposium on the Urban Environment. Retrieved June 15, 2015

Cocci grifoni, R., Passerini, G., & Pierantozzi, M. (2013). Assessment of outdoor thermal comfort and its relation to urban geometry. *173*. SUSTAINABLE DEVELOPMENT AND PLANNING 2013. doi:http://dx.doi.org/10.2495/SDP130011

De, B., & Mukherjee, M. (2018). Optimisation of canyon orientation and aspect ratio in warm-humid climate: Case of Rajarhat Newtown, India. *Urban Climate, 24*, 887-920. doi:https://doi.org/10.1016/j.uclim.2017.11.003.

Grifoni, R. C., Passerini, G., & Pierantozzi, M. (2013). Assessment of outdoor thermal comfort and its relation to urban geometry. *Sustainable Development and Planning VI, 173*. doi:doi:10.2495/SDP130011

Johansson, E. (2006). Influence of urban geometry on outdoor thermal comfort in a hot dry climate: A study in Fez, Morocco. *Building and Environment, 41*(10), 1326-1338. doi:https://doi.org/10.1016/j.buildenv.2005.05.022.

Johansson, E., & Emmanuel, R. (2006). The influence of urban design on outdoor thermal comfort in the hot, humid city of Colombo, Sri Lanka. *Int J Biometeorol, 51*, 119–133. doi:https://doi.org/10.1007/s00484-006-0047-6

Kakon, A., Mishima, N., & Kojima, S. (2009). Simulation of the urban thermal comfort in a high density tropical city: Analysis of the proposed urban construction rules for Dhaka, Bangladesh. *Building Simulation, 2*. doi:https://doi.org/10.1007/s12273-009-9321-y

Lee, I., Voogt, J., & Gillespie, T. (2018). Analysis and Comparison of Shading Strategies to Increase Human Thermal Comfort in Urban Areas. *Atmosphere*. doi: https://doi.org/10.3390/atmos9030091

Lenzholzer, S. (2012). Research and design for thermal comfort in Dutch urban squares. *Resources Conservation and Recycling, 64*. doi:10.1016/j.resconrec.2011.06.015.

Lin, T.-P. (2009). Thermal perception, adaptation and attendance in a public square in hot and humid regions. *Elsevier Building and environment*, *44*(10), 2017-2026. doi:https://doi.org/10.1016/j.buildenv.2009.02.004

NIKOLOPOULOU, M., BAKER, N., & STEEMERS, K. (2001). THERMAL COMFORT IN OUTDOOR URBAN SPACES: UNDERSTANDING THE HUMAN PARAMETER. *Solar Energy*, *Vol. 70*, 227–235,. doi:10.1016/S0038-092X(00)00093-1.

Rodríguez-Algeciras, J., Tablada, A., & Matzarakis, A. (2018, August). Effect of asymmetrical street canyons on pedestrian thermal comfort in warm-humid climate of Cuba. *Theor Appl Climatol*, *133*, 663-679. doi:https://doi.org/10.1007/s00704-017-2204-8

Shafaghat, A., Manteghi, G., Keyvanfar, A., Lamit, H., Saito, K., & Ossen, D. (2016). Street Geometry Factors Influence Urban Microclimate in Tropical Coastal Cities: A Review. *Environmental and Climate Technologies*, *17*, 61-75. doi:10.1515/rtuect-2016-0006.

https://www.questionpro.com/article/survey-research.html

Blog, F. (2022, September 14). Experimental Vs Non-Experimental Research: 15 Key Differences. Formpl. https://www.formpl.us/blog/experimental-non-experimental-research

Annex 1 Filled Questionnaire Survey

Thermal Sensation Survey

Demographic Details

Name

Narottam Kasaudhan

Age

- ( ) 0-10
- ( ) 11-20
- ( ) 21-30
- (•) 31-40
- ( ) 41-50
- ( ) 51-60
- ( ) 61-70
- ( ) 71 above

Gender

- (•) Male
- ( ) Female
- ( ) Others

Nationality

- (•) Nepali
- ( ) Indian
- ( ) Foreigner

City

Lumbini

For how long have you been staying in the place?

2

Clothing

- ( ) Naked
- ( ) Underpants only
- (•) Shorts and Tshirt
- ( ) Trousers and shirt
- ( ) Light Business suit
- ( ) Business suit + Thermals
- ( ) Jacket and Overcoat
- ( ) Heavy winter Gear
- ( ) Arctic type clothing

State of Interviewee

- ( ) Sedentary
- ( ) Walking
- ( ) Exercising
- ( ) Lying
- (•) Resting
- ( ) Dancing

Thermal Sensation

How do you feel?

- ( ) Cold
- ( ) Cool
- ( ) Slightly Cool
- ( ) Neutral
- ( ) Slightly warm
- ( ) Warm
- (•) Hot

how do you rate the overall acceptability to the thermal environment at this moment

- ( ) Acceptable
- (•) Not Acceptable

what is the temperature state that you expect?

- (•) Cooler
- ( ) No change
- ( ) Warmer

Do you feel comfortable now?

- ○ Very uncomfortable
- ◉ uncomfortable
- ○ Little uncomfortable
- ○ Just right
- ○ Little comfortable
- ○ comfortable
- ○ very comfortable

The environment in your opinion is

- ○ Perfectly Tolerable
- ○ Easily Tolerable
- ◉ Difficult to tolerate
- ○ Intolerable

In general, how does the temperature interfere with or enhance your outdoor stay?

- ◉ Very detrimental
- ○ Detrimental
- ○ Indifferent
- ○ Slightly Helps
- ○ Helps a lot

At what time, do you prefer to visit the street?

- ○ Morning (6-11)
- ○ Midday (11-2)
- ○ Afternoon (2-5)
- ◉ Evening (5-8)
- ○ Night (after 8)
- ○ None

Location related parameters

Time of Response

2022-06-18 | 02:30 PM

Place of interviewe

- (•) Shaded
- ( ) Unshaded
- ( ) partially Shaded

Sky conditions

- (•) Clear Sky
- ( ) partly cloudy
- ( ) Overcast
- ( ) Rain
- ( ) Fog

Air speed

- ( ) Still
- ( ) Not Noticeable
- ( ) Barely Noticeable
- (•) Pleasant Breeze
- ( ) Light Breeze
- ( ) Hair and Papers move
- ( ) Noticeable Draughty
- ( ) Unpleasant Breeze
- ( ) Gusting

What brings you to the street?

- (•) Shopping
- ( ) Traveling
- ( ) Walking
- ( ) Hanging out

What feature do you find attractive of this street?

Nothing

How often do you come to/pass this street?

- (•) Regular
- ( ) Often
- ( ) Occasionally
- ( ) Never

Where were you 15 minutes prior to this survey?

Shop

If you were outdoor, how long have you spent in this particular street?

0

What measures would you like to take to feel more comfortable?

- [ ] Umbrella/hat
- [x] Move to shaded area
- [ ] Reduce clothing
- [ ] No change
- [ ] Others

ANNEX 2- Simulation Results Data

Scenarios

Base Case					
Date	**Time**	**Air Temperature**	**MRT**	**PET**	**UTCI**
22.06.2022	07.00.01	31.1	50.0	38.0	36.355
22.06.2022	08.00.01	33.3	55.8	43.2	39.449
22.06.2022	09.00.01	35.3	59.2	47.1	41.961
22.06.2022	10.00.01	37.1	60.1	48.8	43.787
22.06.2022	11.00.01	38.6	60.7	49.2	45.3
22.06.2022	12.00.01	39.8	64.1	51.0	47.197
22.06.2022	13.00.01	40.8	68.7	53.0	49.031
22.06.2022	14.00.01	41.1	70.9	54.0	49.783
22.06.2022	15.00.01	40.0	68.9	52.6	48.269
22.06.2022	16.00.01	38.4	63.2	49.6	45.263
22.06.2022	17.00.01	35.2	47.4	40.9	38.905
22.06.2022	17.59.59	33.4	26.4	29.7	32.927

AR1 (a)					
Date	**Time**	**Air Temp.**	**MRT**	**PET**	**UTCI**
22.06.2022	07.00.01	31.2	49.8	38.2	36.718
22.06.2022	08.00.01	33.3	55.5	43.2	39.66
22.06.2022	09.00.01	35.3	59.2	47.1	42.134
22.06.2022	10.00.01	37.0	60.0	48.8	43.8
22.06.2022	11.00.01	38.4	60.4	49.1	45.167
22.06.2022	12.00.01	39.6	64.3	51.0	47.19
22.06.2022	13.00.01	40.6	68.7	53.0	48.974
22.06.2022	14.00.01	40.8	70.3	53.8	49.538
22.06.2022	15.00.01	39.9	68.2	52.4	48.078
22.06.2022	16.00.01	38.3	62.6	49.4	45.195
22.06.2022	17.00.01	35.2	47.0	40.8	39.006
22.06.2022	17.59.59	33.5	26.4	29.7	33.15

AR1.5 (a)					
Date	**Time**	**Air Temp.**	**MRT**	**PET**	**UTCI**
22.06.2022	07.00.01	30.8	28.4	27.8	31.443
22.06.2022	08.00.01	32.7	54.0	41.8	38.589
22.06.2022	09.00.01	34.5	56.4	44.9	40.611
22.06.2022	10.00.01	36.4	59.2	48.1	42.852
22.06.2022	11.00.01	37.8	59.8	48.9	44.255
22.06.2022	12.00.01	39.0	63.7	50.2	46.228
22.06.2022	13.00.01	39.9	67.6	52.0	47.843
22.06.2022	14.00.01	40.2	69.4	52.8	48.484
22.06.2022	15.00.01	39.3	67.2	51.4	47.071
22.06.2022	16.00.01	37.8	61.0	49.0	44.119
22.06.2022	17.00.01	35.0	33.7	34.4	35.748
22.06.2022	17.59.59	33.5	26.2	29.6	32.869

AR2 (a)					
Date	**Time**	**Air Temp.**	**MRT**	**PET**	**UTCI**
22.06.2022	07.00.01	30.8	28.1	27.5	31.13
22.06.2022	08.00.01	32.5	53.8	41.3	38.107
22.06.2022	09.00.01	34.2	56.0	44.1	39.886
22.06.2022	10.00.01	35.9	58.3	47.1	41.945
22.06.2022	11.00.01	37.3	59.2	48.8	43.421
22.06.2022	12.00.01	38.0	51.0	45.6	42.075
22.06.2022	13.00.01	38.7	51.7	46.7	42.744
22.06.2022	14.00.01	39.3	67.6	51.2	46.934
22.06.2022	15.00.01	38.7	66.1	50.4	45.915
22.06.2022	16.00.01	37.3	59.9	48.8	43.101
22.06.2022	17.00.01	34.8	33.2	33.9	35.167
22.06.2022	17.59.59	33.4	25.9	29.4	32.459

AR3 (a)					
Date	**Time**	**Air Temp.**	**MRT**	**PET**	**UTCI**
22.06.2022	07.00.01	30.8	28.0	27.4	31.207
22.06.2022	08.00.01	32.0	52.6	40.1	33.041
22.06.2022	09.00.01	33.8	55.1	43.3	39.456
22.06.2022	10.00.01	35.5	57.2	46.1	41.392
22.06.2022	11.00.01	36.9	49.1	43.5	40.832
22.06.2022	12.00.01	37.5	49.4	44.3	41.296
22.06.2022	13.00.01	38.3	50.6	45.7	42.192
22.06.2022	14.00.01	38.7	49.6	45.6	42.257
22.06.2022	15.00.01	38.2	64.9	49.6	45.195
22.06.2022	16.00.01	36.9	59.0	48.5	42.596
22.06.2022	17.00.01	34.6	32.9	33.6	35.019
22.06.2022	17.59.59	33.4	25.7	29.2	32.374

AR1 (b)					
Date	**Time**	**Air Temp.**	**MRT**	**PET**	**UTCI**
22.06.2022	07.00.01	31.3	30.2	30.8	33.607
22.06.2022	08.00.01	32.5	35.9	34.4	35.689
22.06.2022	09.00.01	34.1	58.7	51.5	42.23
22.06.2022	10.00.01	35.9	60.1	52.8	43.984
22.06.2022	11.00.01	37.2	58.2	52.3	44.582
22.06.2022	12.00.01	38.6	63.5	55.3	47.136
22.06.2022	13.00.01	39.2	55.1	51.5	45.134
22.06.2022	14.00.01	39.4	53.8	51.0	44.734
22.06.2022	15.00.01	38.2	49.0	45.6	42.555
22.06.2022	16.00.01	36.8	43.3	40.8	40.129
22.06.2022	17.00.01	34.6	35.3	35.2	36.777
22.06.2022	17.59.59	33.4	26.2	30.1	33.912

AR1.5 (b)					
Date	**Time**	**Air Temp.**	**MRT**	**PET**	**UTCI**
22.06.2022	07.00.01	31.3	29.9	29.9	33.363
22.06.2022	08.00.01	32.3	34.7	33.0	35.197
22.06.2022	09.00.01	33.6	38.5	35.9	36.83
22.06.2022	10.00.01	35.2	57.4	47.1	42.458
22.06.2022	11.00.01	36.8	57.6	49.2	43.604
22.06.2022	12.00.01	38.2	54.2	47.6	43.833
22.06.2022	13.00.01	38.7	52.4	46.8	43.64
22.06.2022	14.00.01	38.7	49.8	45.4	42.989
22.06.2022	15.00.01	37.8	46.3	42.9	41.449
22.06.2022	16.00.01	36.6	42.6	40.1	39.67
22.06.2022	17.00.01	34.7	35.0	34.9	36.54
22.06.2022	17.59.59	33.6	25.9	29.8	33.552

AR2 (b)					
Date	**Time**	**Air Temp.**	**MRT**	**PET**	**UTCI**
22.06.2022	07.00.01	31.0	30.0	29.2	32.061
22.06.2022	08.00.01	32.1	34.5	32.2	33.909
22.06.2022	09.00.01	33.3	37.9	34.8	35.451
22.06.2022	10.00.01	34.7	54.6	44.4	40.196
22.06.2022	11.00.01	36.4	57.0	47.2	42.378
22.06.2022	12.00.01	37.6	50.7	45.0	41.906
22.06.2022	13.00.01	38.2	50.9	45.7	42.273
22.06.2022	14.00.01	38.1	47.3	43.8	41.273
22.06.2022	15.00.01	37.5	45.3	42.2	40.13
22.06.2022	16.00.01	36.5	41.9	39.7	38.47
22.06.2022	17.00.01	35.0	34.8	34.9	35.589
22.06.2022	17.59.59	33.7	25.7	29.6	32.521

AR3 (b)					
Date	**Time**	**Air Temp.**	**MRT**	**PET**	**UTCI**
22.06.2022	07.00.01	31.2	30.6	28.6	30.916
22.06.2022	08.00.01	32.0	34.8	31.3	32.567
22.06.2022	09.00.01	33.1	37.8	33.7	33.896
22.06.2022	10.00.01	34.3	40.2	36.2	35.33
22.06.2022	11.00.01	35.6	53.3	43.9	39.36
22.06.2022	12.00.01	36.9	48.4	43.1	39.547
22.06.2022	13.00.01	37.2	45.7	42.2	39.092
22.06.2022	14.00.01	37.5	45.2	42.3	39.202
22.06.2022	15.00.01	37.0	44.1	41.2	38.392
22.06.2022	16.00.01	36.2	41.3	39.0	36.94
22.06.2022	17.00.01	35.0	34.6	34.5	34.298
22.06.2022	17.59.59	33.7	25.5	29.4	31.283

10 Degree				
Time	**Air Temp.**	**MRT**	**PET**	**UTCI**
07.00.01	30.9	28.4	28.6	32.242
08.00.01	32.7	54.4	41.2	39.317
09.00.01	34.5	56.8	44.0	41.093
10.00.01	36.3	59.2	46.8	42.999
11.00.01	37.7	59.5	48.1	44.184
12.00.01	38.9	63.6	49.8	46.107
13.00.01	39.2	65.0	50.4	46.641
14.00.01	39.5	67.1	51.2	47.36
15.00.01	39.1	67.2	51.0	47.05
16.00.01	37.6	61.4	48.2	44.387
17.00.01	34.9	46.4	39.7	38.841
17.59.59	33.5	26.1	30.2	33.209

20 Degree				
Time	**Air Temp.**	**MRT**	**PET**	**UTCI**
07.00.01	30.9	28.9	28.8	32.32
08.00.01	32.3	53.9	40.5	38.842
09.00.01	34.4	57.1	44.0	41.024
10.00.01	35.9	57.1	45.4	42.163
11.00.01	37.6	59.0	47.8	43.891
12.00.01	38.8	63.4	49.6	45.907
13.00.01	39.1	53.0	46.5	43.632
14.00.01	39.4	52.3	46.5	43.742
15.00.01	38.5	48.6	44.1	42.173
16.00.01	37.1	42.6	40.2	39.638
17.00.01	34.7	33.6	34.3	35.757
17.59.59	33.4	26.0	30.1	33.067

30 Degree				
Time	**Air Temp.**	**MRT**	**PET**	**UTCI**
07.00.01	31.0	29.3	29.1	32.441
08.00.01	32.2	33.9	32.1	34.332
09.00.01	34.2	56.6	43.6	40.748
10.00.01	35.9	57.4	45.6	42.172
11.00.01	37.4	59.0	47.7	43.768
12.00.01	38.2	51.7	45.2	42.703
13.00.01	39.0	53.2	46.5	43.575
14.00.01	39.2	51.4	45.9	43.32
15.00.01	38.2	48.0	43.5	41.728
16.00.01	36.9	42.8	40.1	39.496
17.00.01	34.6	33.6	34.1	35.623
17.59.59	33.4	25.9	30.0	32.948

40 Degree				
Time	**Air Temp.**	**MRT**	**PET**	**UTCI**
07.00.01	30.8	29.3	28.9	31.45
08.00.01	31.9	33.7	31.7	33.248
09.00.01	33.6	56.2	43.0	39.394
10.00.01	34.9	57.2	44.7	40.693
11.00.01	36.2	59.4	46.9	42.231
12.00.01	37.2	52.1	44.4	41.293
13.00.01	38.4	54.8	46.7	42.795
14.00.01	38.7	52.0	45.7	42.404
15.00.01	37.7	47.0	42.6	40.398
16.00.01	36.4	41.7	39.2	38.093
17.00.01	34.2	33.5	33.7	34.476
17.59.59	33.0	25.5	29.5	31.693

50 Degree				
Time	**Air Temp.**	**MRT**	**PET**	**UTCI**
07.00.01	31.0	29.8	29.3	32.718
08.00.01	32.2	34.6	32.4	34.656
09.00.01	33.6	55.8	43.0	40.37
10.00.01	35.6	58.3	45.9	42.348
11.00.01	37.1	58.7	47.4	43.575
12.00.01	38.0	51.5	45.0	42.649
13.00.01	38.9	53.8	46.7	43.754
14.00.01	39.0	52.0	46.0	43.42
15.00.01	37.9	47.0	42.8	41.38
16.00.01	36.7	41.9	39.5	39.198
17.00.01	34.6	34.2	34.4	35.853
17.59.59	33.4	25.9	30.1	33.049

60 Degree				
Time	**Air Temp.**	**MRT**	**PET**	**UTCI**
07.00.01	31.0	29.9	29.6	32.965
08.00.01	32.2	34.8	32.7	34.928
09.00.01	33.6	38.7	35.5	36.629
10.00.01	35.3	56.9	45.2	42.012
11.00.01	36.7	56.7	46.3	43.006
12.00.01	37.9	51.5	44.9	42.694
13.00.01	38.6	52.0	45.7	43.246
14.00.01	38.7	50.5	45.1	43.033
15.00.01	37.8	46.7	42.7	41.394
16.00.01	36.7	42.3	39.7	39.439
17.00.01	34.7	34.5	34.6	36.15
17.59.59	33.4	25.9	30.1	33.259

70 Degree				
Time	**Air Temp.**	**MRT**	**PET**	**UTCI**
07.00.01	31.1	29.8	29.9	33.156
08.00.01	32.3	34.7	32.9	35.059
09.00.01	33.6	38.7	35.8	36.803
10.00.01	35.2	57.2	45.8	42.261
11.00.01	36.6	56.9	47.1	43.211
12.00.01	38.1	54.6	47.2	43.796
13.00.01	38.6	52.7	46.2	43.614
14.00.01	38.7	50.4	45.2	43.137
15.00.01	37.8	46.7	42.7	41.518
16.00.01	36.7	42.4	39.8	39.609
17.00.01	34.8	34.8	34.9	36.447
17.59.59	33.6	26.0	30.3	33.504

80 Degree				
Time	**Air Temp.**	**MRT**	**PET**	**UTCI**
07.00.01	31.2	29.8	30.1	33.28
08.00.01	32.3	34.7	33.1	35.178
09.00.01	33.6	38.9	36.0	36.918
10.00.01	35.2	57.2	47.4	42.384
11.00.01	36.7	57.7	48.8	43.576
12.00.01	38.1	54.7	48.5	43.919
13.00.01	38.6	52.8	46.3	43.732
14.00.01	38.6	50.2	45.1	43.126
15.00.01	37.8	46.9	42.8	41.622
16.00.01	36.7	42.5	39.9	39.69
17.00.01	34.7	34.7	34.9	36.5
17.59.59	33.6	26.0	30.3	33.59

90 Degree				
Time	**Air Temp.**	**MRT**	**PET**	**UTCI**
07.00.01	31.3	29.9	29.9	33.363
08.00.01	32.3	34.7	33.0	35.197
09.00.01	33.6	38.5	35.8	36.83
10.00.01	35.2	57.4	47.1	42.458
11.00.01	36.8	57.6	49.2	43.604
12.00.01	38.2	54.2	47.5	43.833
13.00.01	38.6	52.4	46.8	43.64
14.00.01	38.6	49.8	45.4	42.989
15.00.01	37.8	46.3	42.9	41.449
16.00.01	36.6	42.6	40.2	39.67
17.00.01	34.7	35.0	34.9	36.54
17.59.59	33.6	25.9	29.8	33.552

100 Degree				
Time	**Air Temp.**	**MRT**	**PET**	**UTCI**
07.00.01	31.2	29.5	30.6	33.435
08.00.01	32.3	34.6	33.8	35.401
09.00.01	33.6	38.7	36.5	37.061
10.00.01	35.4	57.8	51.3	42.677
11.00.01	37.1	58.8	52.4	43.879
12.00.01	38.6	55.9	51.8	46.322
13.00.01	38.9	52.5	50.3	43.66
14.00.01	38.8	49.9	49.3	43.126
15.00.01	37.9	46.5	43.0	41.58
16.00.01	36.7	42.2	40.0	39.642
17.00.01	34.8	34.8	35.2	36.546
17.59.59	33.6	26.4	30.5	33.602

110 Degree				
Time	**Air Temp.**	**MRT**	**PET**	**UTCI**
07.00.01	31.2	29.5	31.1	33.455
08.00.01	32.3	34.5	34.3	35.362
09.00.01	33.7	38.8	37.3	37.13
10.00.01	35.7	57.6	55.8	42.876
11.00.01	37.5	58.7	57.0	44.127
12.00.01	39.1	64.3	60.7	46.51
13.00.01	39.5	54.5	55.5	44.404
14.00.01	39.0	49.7	53.0	43.071
15.00.01	38.0	46.0	50.8	41.432
16.00.01	36.7	41.8	48.4	39.47
17.00.01	34.6	34.5	35.4	36.351
17.59.59	33.5	26.3	30.6	33.459

120 Degree				
Time	**Air Temp.**	**MRT**	**PET**	**UTCI**
07.00.01	31.1	29.5	30.2	33.54
08.00.01	32.3	34.5	33.3	35.491
09.00.01	33.7	38.7	36.4	37.313
10.00.01	35.7	57.5	50.1	42.982
11.00.01	37.4	58.8	51.3	44.244
12.00.01	38.8	63.4	53.8	46.335
13.00.01	39.4	54.3	50.4	44.591
14.00.01	39.3	50.0	48.7	43.653
15.00.01	38.1	46.1	42.9	41.841
16.00.01	36.8	41.9	39.9	39.844
17.00.01	34.5	34.5	34.8	36.537
17.59.59	33.3	26.2	30.3	33.676

130 Degree				
Time	Air Temp.	MRT	PET	UTCI
07.00.01	30.8	29.2	29.4	33.243
08.00.01	32.1	34.3	32.7	35.272
09.00.01	33.8	56.0	44.3	41.274
10.00.01	36.1	57.5	48.4	42.93
11.00.01	37.8	58.8	49.7	44.311
12.00.01	39.3	63.2	51.9	46.353
13.00.01	39.7	54.0	48.7	44.569
14.00.01	39.7	51.9	47.4	44.284
15.00.01	38.3	46.1	42.8	41.872
16.00.01	36.9	41.6	39.7	39.776
17.00.01	34.4	34.3	34.5	36.435
17.59.59	33.2	26.2	30.1	33.596

140 Degree				
Time	Air Temp.	MRT	PET	UTCI
07.00.01	30.5	29.0	29.0	32.466
08.00.01	32.1	34.3	32.5	34.617
09.00.01	34.6	57.4	45.3	41.456
10.00.01	36.6	59.3	48.6	43.296
11.00.01	38.1	58.7	49.1	44.329
12.00.01	39.5	63.1	51.2	46.498
13.00.01	39.8	53.6	47.5	44.405
14.00.01	39.7	51.3	46.4	43.827
15.00.01	38.4	46.1	42.9	41.501
16.00.01	37.0	41.5	39.7	39.328
17.00.01	34.4	34.2	34.4	35.843
17.59.59	33.1	26.2	30.0	33.083

150 Degree				
Time	Air Temp.	MRT	PET	UTCI
07.00.01	30.6	28.6	28.7	32.08
08.00.01	33.1	55.2	42.6	39.672
09.00.01	34.8	57.0	44.9	41.144
10.00.01	36.9	58.9	47.6	43.103
11.00.01	38.3	58.1	48.3	43.988
12.00.01	39.6	63.2	50.8	46.337
13.00.01	40.0	53.6	47.7	44.364
14.00.01	39.8	51.2	46.4	43.659
15.00.01	38.5	46.2	43.1	41.378
16.00.01	37.1	41.3	39.7	39.082
17.00.01	34.4	34.1	34.3	35.521
17.59.59	33.0	26.2	29.9	32.786

160 Degree				
Time	Air Temp.	MRT	PET	UTCI
07.00.01	31.2	49.6	38.1	36.861
08.00.01	33.6	55.5	43.0	39.797
09.00.01	35.3	58.2	45.8	41.508
10.00.01	37.1	58.6	47.4	42.854
11.00.01	38.4	58.1	48.3	43.796
12.00.01	39.7	64.4	51.2	46.463
13.00.01	40.6	68.0	52.8	48.024
14.00.01	40.1	52.4	47.2	43.972
15.00.01	38.8	47.6	43.9	41.75
16.00.01	37.2	41.2	39.7	38.969
17.00.01	34.4	33.8	34.1	35.326
17.59.59	33.0	26.2	29.9	32.672

170 Degree				
Time	Air Temp.	MRT	PET	UTCI
07.00.01	37.709	30.805	49.871	36.492
08.00.01	43.223	33.411	56.516	39.845
09.00.01	46.367	35.268	59.834	41.795
10.00.01	47.042	36.776	58.572	42.603
11.00.01	49.087	38.357	61.526	44.607
12.00.01	51	39.528	65.028	46.439
13.00.01	52.4	40.344	67.924	47.775
14.00.01	47.476	40.171	52.817	44.157
15.00.01	44.586	38.995	48.711	42.178
16.00.01	39.734	37.217	41.158	38.991
17.00.01	34.105	34.51	33.499	35.259
17.59.59	30.059	33.154	26.286	32.683

180 Degree (Base Case)				
Time	Air Temp.	MRT	PET	UTCI
31.168	49.864	38.158	36.355	31.168
33.338	55.617	43.329	39.449	33.338
35.387	59.029	47.175	41.961	35.387
37.21	59.997	48.815	43.787	37.21
38.713	60.59	49.304	45.3	38.713
39.911	63.965	51.201	47.197	39.911
40.856	68.492	53.201	49.031	40.856
41.142	70.699	54.2	49.783	41.142
40.144	68.707	52.801	48.269	40.144
38.477	62.994	49.8	45.263	38.477
35.283	47.252	41.007	38.905	35.283
33.481	26.413	29.761	32.927	33.481

ANNEX 3- IOE GC article

Proceedings of 12th IOE Graduate Conference
[Peer Reviewed]
ISSN: 2350-8914 (Online), 2350-8906 (Print)
Year: 2022, Month: September, Volume: 12

Analysis of Solar Radiation for Pedestrian comfort in the streets of hot and humid climate, A case of Lumbini, Nepal

Apekshya Ghimire [a], Sanjaya Uprety [b], Ashim Ratna Bajracharya [c]

[a] *Department of Architecture, Institute of Engineering*
[b] *Associate Professor, Department of Architecture, Institute of Engineering*
[c] *Associate Professor, Department of Architecture, Institute of Engineering*
[a] 076mseeb002.apekshya@pcampus.edu.np, [b] suprety@ioe.edu.np, [c] ashim@ioe.edu.np

Abstract

The development of road sections is a very important and critical responsibility in changing the local pedestrian behavior. The construction of roadside building structures should be carried out keeping in mind the solar shading it provides to that road section, especially in hot and humid regions. Walking outside in Lumbini's hot and humid climate is challenging, even for short distances, due to the bright sunshine during the day. Shading of the walkways influences the commuting behavior of pedestrians significantly. So, the study seeks to examine the effect of buildings and vegetation on pedestrian thermal comfort due to shading by existing buildings and vegetation. A structured questionnaire and solar analysis using Sketchup were used to examine the present conditions of the street connecting Mahilwar to Majhediya and the comfort it provides to pedestrian. In a typical east-west oriented street section, it was found that buildings over three stories performed better as shading agents compare to the buildings less than 2 stories on the southern side while plantation of local trees provides shading all over the year regardless of the direction. The buildings present in the street of Lumbini Sanskritik Municipality performed poorly in providing shade to the pedestrian walkway during the summer when it is mostly desired. Thus, this study concludes that constructing buildings over three stories provides shading to the southern walkway, and planting local trees helps in shading of the pedestrian walkways even in the north direction.

Keywords

Shading, Pedestrian Thermal comfort, Solar Analysis, Walkability, Walkway

1. Introduction

Walking outside Lumbini Sankskritik Municipality is challenging, even for short distances, due to the bright sunshine during the day. Since direct sun radiation and high temperatures cause thermal stress on the human body, pedestrians tend to change their outgoing time during the morning or evening. Direct sun radiation exposure can lead to health issues such as heat exhaustion and dehydration. Furthermore, people's preference for going outdoors has a detrimental impact on the region's economic and tourism activity [1]. As a result, the streets must be shaded to increase the number of people and their thermal comfort.

Basically, thermal comfort refers to a condition where people feel neutral and do not desire to change the thermal condition. According to [2], thermal comfort is the state of mind that is assessed by subjective evaluation that expresses satisfaction with the thermal environment. Outdoor thermal comfort is an important issue that seems to be neglected most of the time, especially in the context of Nepal. The energy consumption pattern of the households along with internal thermal comfort has been studied in past but there is less importance given to outdoor and pedestrian thermal comfort. Department of road and Department of Urban Planning have looked into pedestrian comfort from the field of safety but pedestrian thermal comfort is yet to be studied.

A route that can be walked from start to finish without raising the core temperature of the human body or causing perceived discomfort is a thermally comfortable pedestrian route (TCPR) [3]. Shading the streets by any means such as vegetation, artificial shading devices or building itself makes the route thermally comfortable. Many types of research claim shading as an effective way to reduce thermal discomfort in outdoor thermal conditions [4][5] [6]. For a route to be comfortable for all the summer days, the shading coverage should be more than 62 percent [3].

Thermally as well as aesthetically comfortable streets promote walkability and sustainability as it encourages people to not rely on a vehicle for short distances. In order to establish and sustain walkability, it is important to make urban streets comfortable as far as the ambient climate permits [7]. The configuration of buildings and vegetation creates an obstruction to the direct solar radiation that strikes the street thus helping in the reduction of temperature thereby improving thermal comfort. Hence, it is imperative to study the effect of buildings and vegetation on direct solar radiation.

Since, the temperature ranges between 22 °C to 41 °C as measured in the street of Lumbini Sanskritik Municpality of Nepal, it is difficult to carry out outdoor activities during the sunny day. People tend to shift their outgoing time to only in the early morning or late evening due to scorching solar radiation during the daytime. In the context of Nepal, there is not much research carried out that provides ideas to reduce direct solar radiation in the street. This research examines the effect of buildings and vegetation on solar radiation in a street of Lumbini Sanskritik Municipality connecting Majhediya to Mahilwaar for pedestrian comfort.

1.1 Outdoor Thermal Comfort

Outdoor thermal comfort is an indicator that cannot be quantified easily. However, it can be described as the range of climatic conditions where most of the people feel comfortable [8]. Outdoor thermal comfort is dependent on different climatic variables along with other parameters such as psychological and physiological. The major climatic variables that affect outdoor thermal comfort are air temperature, mean radiant temperature, humidity, and air speed. If all these parameters are in balanced condition with the heat energy balance of human body, then thermal comfort can be achieved.

Psychological and physiological parameters also affect thermal comfort in outdoor conditions. Physiological parameters including skin and core temperatures, as well as perspiration rate and psychological factors like behavior, culture, alliesthesia, etc. are useful indicators of outdoor thermal comfort [9]. Out of all these parameters and factors, the most significant factor that affects heat gain and loss is solar radiation [10]. Hence, the arrangement of buildings and vegetation that provide shading to the street is an important aspect to look at so as to reduce the direct solar radiation in the street and to improve the thermal comfort in outdoor conditions.

1.2 Solar radiation access in the street

Solar radiation has a significant impact on many elements of urban life, including street temperature climate, day illumination, solar energy use such as photovoltaic cells, and the well-being of living creatures[11] [12]. Solar access and shading conditions have a significant impact on the street micro climate. The geometry of buildings, street orientation, and availability of vegetation determine the access of solar radiation incidents to the street. Shade surfaces in urban settings, such as streets, seating spaces, building facades, and roofs, limit direct sun radiation and so efficiently keep the temperature low [13].

In a study carried out at a university campus in Central Taiwan, it was found that suitable shading is required in outdoor spaces to ensure thermal comfort either by buildings or vegetation [14]. Another study concluded that shaded spaces provided more thermally comfortable conditions than unshaded areas since the shaded areas have a longer period of acceptable temperature range [15]. It was discovered that increasing the roadway width from 15 m to 20 m enhanced sun radiation by (17-20 percent)[16].

The exposure of direct solar radiation in the street is a critical parameter for pedestrian thermal comfort. The incident radiation during the daytime makes the street thermally uncomfortable, especially in a hot and humid region. The streets become thermally uncomfortable if no shadings are provided due to high-intensity solar radiation incident to the region. It is very difficult to walk during the daytime, especially during the summer season. Hence, streets should be designed in a way to utilize solar access to improve urban micro climate and pedestrian thermal comfort.

The shading can be done either from buildings or vegetation or artificial shading devices. The street surfaces receive the highest solar radiation when the aspect ratio is low [17]. The aspect ratio and orientation determine the quantity of solar radiation incident and also affect the ambient surface temperature of the street [18]. The increase in height of a building or decrease in width of the road increases the shading which decreases the air temperature and physiologically equivalent temperature, thereby improving the thermal comfort at the pedestrian level especially in the summer [19].

2. Methodology

The study used a mixed-method approach to investigate the influence of buildings and vegetation on pedestrian thermal comfort due to shading. Using Kobo Collect, a structured questionnaire was utilized to examine pedestrian perceptions of the shaded and unshaded outdoor environments. During the sunny outside settings, 15 samples were randomly selected under non probability survey. Sketchup was used to model a 100 m street as a reference for the solar analysis as maximum number of buildings were present in that 100m section.

3. Study Area

3.1 Lumbini Sanskritik Municipality

The study area was chosen in Nepal's Lumbini Province, Rupandehi District, which is located in the Hot and Humid Climatic Zone. The research is carried out in a street of Lumbini Sanskritik Municipality which begins from gate number 5 to villages like Madhubani, Mahilwar, etc. The street near the Lumbini master plan consists of hotels and lodges with very few residences. The width of the street is 13 m (42.6'), with a 2 m (6.5') pedestrian sidewalk, while the surrounding buildings have 1 to 5 stories. Only two mango trees were found to be present in this road section.

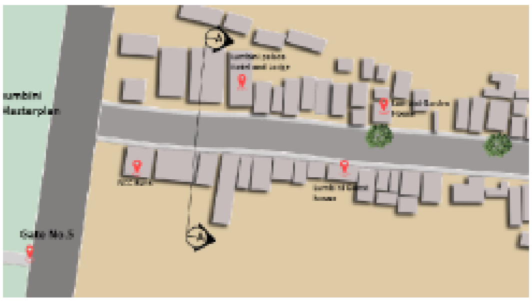

Figure 1: Site Selection Top View of Lumbini Sanskritik Municipality(Google Earth)

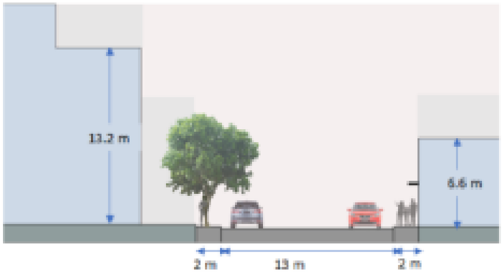

Figure 2: Site Section View of the Majhediya to Mahilwaar Road

4. Findings and Discussion

The data collected from the field visit was used to model the buildings in SketchUp for solar analysis. This resulted in the presence of variations in building heights in the base case. It was observed that a few buildings on the western side of the south section of the road possessed cantilever slabs of 800 mm which acted as shading devices for the pedestrian walkway. Figure 3 depicts the variation of heights available in the study area.

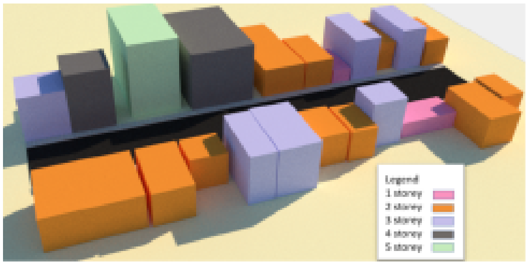

Figure 3: Building Heights in the selected site

4.1 Questionnaire Survey

The questionnaire survey was carried out on July 22. Thermal conditions before 8 am were determined to be tolerable by 6 interviewees, whereas temperatures between 9 am and 10 am were found to be suitable for 2 people and unacceptable for 1 person . The thermal conditions in the afternoon were found to be unacceptably hot for 3 people, however, the thermal conditions in the evening after 4 p.m. were determined to be rather pleasant for 2 people .

Most of the people (11 people) prefer moving to the shaded area rather than using umbrellas(1 person) to reduce clothing as seen in figure 5.

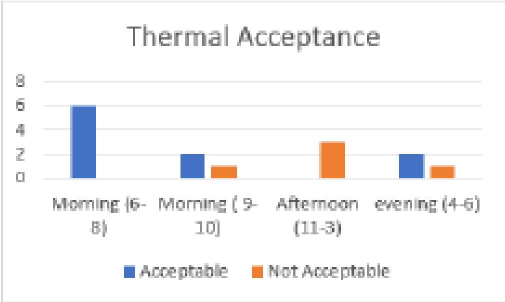

Figure 4: Thermal Acceptance

Figure 6: Monthly solar analysis of selected site

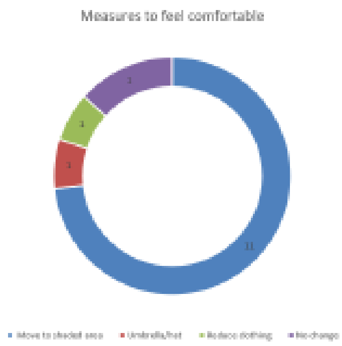

Figure 5: Measure to feel comfortable

4.2 Solar Analysis

From figure 6, it can be seen that the southern buildings cast a shadow on the southern pedestrian walkways while northern pedestrian walkways are illuminated all along the year in East-West oriented streets. The buildings of different heights cast shadows differently as seen in the figure. The tree casts a shadow around it making the pedestrian walkway around the tree thermally comfortable.

For the months from November to February, being winter season, the buildings in the southern section of the road are efficient enough in shading the southern walkway while the northern walkway fails to be shaded. Only the part with the vegetation was found to be somewhat shaded. For the month of March, it was observed that the present buildings were somewhat feasible in terms of walkway shading but in the case of April and May, only the tall buildings (more than two storey) were able to provide shade to their walkway whereas short buildings (less than two storey) with protruding cantilever slabs were also actively involved in shading the walkway. For the month of June, no shading on the walkway was observed at all by the buildings whereas slight shading of the walkway begins from the month of July by only the tall buildings. Beyond august, the walkways are either partially or fully shaded by the present buildings during the peak time of 2 pm. Like in the winter months, September and October the current buildings were successful in providing complete shade to the walkways.

Thus, the pedestrian walkway towards the southern side is completely in shade from September to March. When the sun comes towards the zenith, the shaded portion begins to decrease as seen from the figure. Due to the low position of the sun during the winters, the present buildings were efficient enough to provide complete shading to the southern side of the road whereas in the summer due to the high position of the sun, the same buildings fail to provide enough shading to the same road section which is undesirable.

From 7 a.m. to 8 a.m., the northern half of the

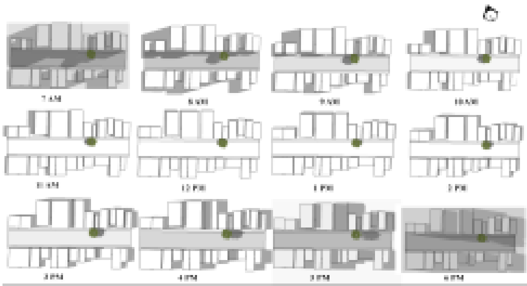

Figure 7: Hourly solar analysis on July 22nd

roadway is entirely shadowed by the northern buildings, with some shading at 9 a.m. The streets are entirely lighted after 9 a.m., with shade around the tree only until 12 p.m. After 12 p.m., the sun position

shifts as the street's southern walkway begins to be shadowed. The buildings over three stories shade the southern walkway, however, the street is thermally unpleasant due to the height range of the buildings and the shaded walkway. The street is thermally uncomfortable 9 a.m. to 5 p.m. in the month of July.
From the monthly and hourly solar analysis, it was observed that the pedestrian walkways were shaded better by the buildings more than three stories all over the year but it is not enough to completely shade the entire walkway to the extent of improving pedestrian thermal comfort. The solar analysis as well as field survey proves that the current street is still not comfortable enough to the pedestrians to continuously interact with the public spaces present there.

5. Conclusion and Recommendation

The present building layout in the road section oriented at the E-W direction is not very efficient in shading every part of the walkway throughout the year as found by solar analysis in figure 6, which makes it more difficult for pedestrians to commute through this road. While it has been found that the same building section is shading the walkways during winter as per figure 6, it was found to be lacking during the summer when it is more desirable. The presence of vegetation also helped to shade the area around it which is quite encouraging in terms of pedestrian comfort as well as the street aesthetics. So, for complete shading of the walkway in the E-W oriented road sections, buildings of more than two storeys are recommended for the southern section of the road while plantation of local trees is strongly suggested to improve the shading of the northern section of the road. Thus, this study concludes that southern buildings over three storeys provide shading most of the time in the southern walkway however, trees can provide shading around it all over the year regardless of the direction of the streets.

6. Limitations

The study focuses on the current situation as it is, with no additional intervention. This study concentrates solely on the solar analysis of the first row of buildings on each side of the road and avoids the idea of the light plane altogether. To facilitate the study, homogeneous box models were utilized in place of the real building structures, with the height remaining constant. Only 100m of the road was chosen for analysis, which does not represent the entire situation of the Mahilwaar to Majhediya road. Hence, further study can be conducted with interventions in building height and the positioning of vegetation that can provide improved shade. The influence of building shadowing on other rows of urban arrangement may also be explored.

Acknowledgments

The authors would like to express their thanks to the Department of Architecture for permission to prepare and publish this paper.

References

[1] Steemers Nikolopolou, Baker. Thermal comfort in outdoor urban spaces: Understanding the human parameter. 70:227–235, 2001.

[2] ASHRAE ANSHI. Thermal environmental conditions for human occupancy. [Online; accessed 2022-08-16].

[3] Maricopa Association of Governments. Shade and thermal comfort.

[4] Khodakarami Taleghani Nasrollahi, Ghosouri. Heat mitigation strategies to improve pedestrian thermal comfort in urban environments: A review. *Sustainability*, 2020.

[5] Matzarakis Rodriguez-Algericas, Tablada. Effect of asymmetrical street canyons on pedestrian thermal comfort in warm-humid climate of cuba. *Theor Appl Climatol*, 133:663–679, 2018.

[6] Koen Nikolopolou. Thermal comfort and psychological adaptation as a guide for designing urban spaces. 35:95–101, 2003.

[7] Ahmed. Comfort in urban spaces: defining the boundaries of outdoor thermal comfort for the tropical urban environments. *Energy and Buildings*, 35(1):103–110, 2017.

[8] Pierantozzi Grifoni, Passerini. Assessment of outdoor thermal comfort and its relation to urban geometry. *Sustainable Development and Planning VI*, 173, 2013.

[9] Liu Guo Liu Liu Chen Lai, Lian. A comprehensive review of thermal comfort studies in urban open spaces. *Science of The Total Environment*, (742), 2020.

[10] Mahmoud Kenawy, Afifi. The effect of planning design on thermal comfort in outdoor spaces. *First International Conference of Sustainability the Future.*, 2010.

[11] Kunckler Upadhyay Kämpf Scartezzini Mohajeri, Gudmundsson. How street-canyon configurations affect the potential of solar energy. los angeles: Passive and low energy architecture. *Elsevier*, 2016.

[12] Yan Du, Ning. How long is the sun duration in a street canyon? —— analysis of the view factors of street canyons. *Building and Environment*, (172), 2020.

[13] Kalogirou Vartholomaios. Optimisation of outdoor shading devices with thermal comfort criteria: The case of the venetian port of chania. *Earth and Environmental Science*, 2020.

[14] Hwang Lin, Matzarakis. Shading effect on long-term outdoor thermal comfort. *Building and Environment*, 45(1):213–221, 2010.

[15] Jaafar GhaffarianHoseini Makaremi, Salleh. Thermal comfort conditions of shaded outdoor spaces in hot and humid climate of malaysia. *Building and Environment*, 48:7–14, 2012.

[16] Shishegar. Street design and urban micro climate: Analyzing the effects of street geometry and orientation on airflow and solar access in urban canyons. *Journal of Clean Energy Technologies*, 2013.

[17] Kunckler Upadhyay Assouline Kämpf Scartezzini Mohajeri, Gudmunsson. A solar-based sustainable urban design: The effects of city-scale street-canyon geometry on solar access in geneva, switzerland. *Applied Energy*, (240):173–190, 2019.

[18] Chang Akarman. The influence of height/width ratio on urban heat island in hot-arid climates. *Procedia Engineering*, (118):101–108, 2015.

[19] Carvalho Mota Muniz-Gäal, Pezzuto. Urban geometry and the microclimate of street canyons in tropical climate. *Building and Environment*, (169), 2020.

ANNEX 4- IOE GC Acceptance Letter

त्रिभुवन विश्वविद्यालय
Tribhuvan University
इन्जिनियरिङ अध्ययन संस्थान
Institute of Engineering
डीनको कार्यालय
OFFICE OF THE DEAN

GPO box- 1915, Pulchowk, Lalitpur
Tel: 977-5-521531, Fax: 977-5-525830
dean@ioe.edu.np, www.ioe.edu.np
गोश्वारा पो.ब. नं- १९१५, पुल्चोक, ललितपुर
फोन- ५५२१५३१, फ्याक्स- ५५२५८३०

Date: September 25, 2022

To Whom It May Concern

This is to confirm that the paper titled "*Analysis of Solar Radiation for Pedestrian comfort in the streets of hot and humid climate, A case of Lumbini, Nepal*" submitted by **Apekshya Ghimire** with Conference ID **12158** has been accepted for presentation at the 12th IOE Graduate Conference being held in October 19 – 22, 2022 at Thapathali Campus, Kathmandu.

Khem Gyanwali, PhD
Convener,
12th IOE Graduate Conference